MSc thesis

REINFORCED HYBRID CONCRETE BEAMS WITH A U-SHAPED SHCC MOULD

DEVELOPING THE SYSTEM AND EXTENDING THE MULTI-LAYER MODEL TO PREDICT ITS BENDING BEHAVIOUR

TU Delft

Ammar Yassiri

Cover photos: designed by Tirachard / Freepik & kjpargeter / Freepik

MASTER THESIS

REINFORCED HYBRID CONCRETE BEAMS WITH A U-SHAPED SHCC MOULD

Developing the system and extending the multi-layer model to predict its bending behaviour

by

Ammar Yassiri

To obtain the degree of Master of Science
in Structural Engineering
at the Delft University of Technology

To be defended publicly
on the 31st of August, 2020 at 09:00

Student number: 4437675

Project duration: November 2019 – August 2020

Thesis committee:

Dr. M. Luković (chair + daily supervisor)	TU Delft – Concrete Structures
Dr. M. Pavlović	TU Delft – Steel and Composite Structures
Dr. B. Šavija	TU Delft – Materials and Environment
ir. S.A. Sligman	Van der Vorm Engineering

Acknowledgements

Pelé once said: “Success is no accident. It is hard work, perseverance, learning, studying, sacrifice and most of all, love of what you are doing or learning to do”. I couldn’t say it any better. Hard work really pays off. And to stay in the world of football (Pelé was a great football player), that is what made me a big fan of Cristiano Ronaldo. He really inspired me to always work hard, whether it is in sport or study. Although our achievements cannot be compared in any way, I can definitely say that like him, I also achieved something great.

I would like to thank many people for this great achievement. Without you all, it would only be ‘an’ achievement, not a great one. First of all, I want to thank my daily supervisor, Mladena. The best thing I can say about Mladena is that, if I could turn back time, I would not hesitate to ask Mladena again to be my supervisor. I honestly could fill this page thanking her. She was always ready (like really always; from Sundays to after midnight) to help me if I needed it. I never have seen anyone so passionate about his/her job.

Next, I want to thank my three other committee members. First of all, Marko, who was the first person that inspired me about fibre reinforced structures during his lectures, and ultimately leading to me investigating hybrid structures. Secondly, Branko, who I sincerely want to thank for how interested he always was in my subject and explanations. Although we did not have many interactions, it always felt good speaking to you. Finally, Sjors, who is the director of the engineering firm where my first structural engineering job will be. He was a very valuable addition to the committee as he always challenged me with practical questions about my theoretical model. See you soon in the company!

I also want to thank everyone that contributed to making me succeed in my research. Ajlal, my new friend, thank you for helping me in the lab (physically and mentally) and your AutoCAD skills! Dawei, thank you for the discussions we had about how to calculate deflections and comparing our codes! Ton and Maiko, you are really the best what can happen in the lab! Really the funniest people (in a very positive way of course) of the TU Delft. Shozab, thank you for providing me feedback on my report; I hope that the results will also be useful for your research. I also want to thank Nikhil, who provided essential data to use for the drying shrinkage calculations that I used in the report. We have never met, but thank you!

Finally, I want to thank my family, especially my mother, father and my sister (who soon will also go through the process of studying at university; so okhti: be ready!). My mother once started studying Civil Engineering, but she couldn’t finish it due to circumstances that were not in her control. So: “mama, this is for you!”. I really hope my parents are proud of me, after raising and supporting me from 1997 until this moment.

Ammar Yassiri

Maassluis, August 2020

Content

List of abbreviations/symbols

ABBREVIATION	EXPANSION
c	Concrete cover
δ	Deflection
DIC	Digital Image Correlation
ε	Strain
FEM	Finite Element Method
ϕ	Reinforcement bar diameter
HSC	High strength concrete
HSFRC	High strength fibre reinforced concrete
κ	Curvature
L	Span of the beam
L_1	Distance between the support and the force
L_2	Length of the constant bending moment region
l_{inf}	Influence length
MLM	Multi-layer model
n.a.	Neutral axis
NSC	Normal strength concrete
RC	Reinforced concrete
SHCC	Strain hardening cementitious composite
SLS	Serviceability limit state
t_{bot}	Thickness of bottom layer
t_{top}	Thickness of top layer
t_{web}	Web thickness (U-shape)
ULS	Ultimate limit state
w	Crack opening displacement
w_{max}	Crack width
#	Number of layers
Δh	Neutral axis steps

Abstract

Hybrid concrete-SHCC beams are a new development in construction techniques. SHCC stands for **S**train **H**ardening **C**ementitious **C**omposite. In such beams, the tension zone could for example consist, next to the traditional reinforcement, of a material that shows strain hardening behaviour. That helps with controlling the crack width. In traditional (non-hybrid) beams, the steel reinforcement would have to control the crack width on its own. This means that there are situations that the steel reinforcement fulfills the strength requirements, but additional steel reinforcement is needed to limit the crack width. Therefore, a certain amount of steel reinforcement is needed for meeting the SLS (**S**erviceability **L**imit **S**tate) requirements, while it is not used for the ULS (**U**ltimate **L**imit **S**tate) requirements. The use of hybrid beams consisting of an SHCC layer applied in the tension zone in which the reinforcement is embedded, solves this problem. This was shown in previous MSc studies by Huang and Singh.

In this study, the concept of the hybrid beam is extended. A design was made of a reinforced U-shaped SHCC mould, to be used for casting a hybrid beam. In that way, a reinforced hybrid concrete beam is created, in which the webs of the U-shape prevent the need of temporary moulds at the side of the beam, which reduces costs. A complete design is presented which is ready for further research.

In this research, it is investigated how the bending behaviour of the extended concept of the hybrid beams can be modelled. A model, that has been initially proposed by Hordijk in 1991, and is called the multi-layer model, is suitable for this purpose. It enables modelling the non-linear behaviour, which is exactly what is needed to be able to model the bending behaviour of hybrid beams. The initial version of the multi-layer model has been developed with monolithic concrete beams in mind. In other words, the model was applied for beams that consisted of one material. Using the same principles of the initial version of the multi-layer model, the model is extended in this research to be suitable for reinforced hybrid concrete beams containing a U-shaped SHCC layer. The model was built using VBA (**V**isual **B**asic for **A**pplications) in Microsoft Excel, and is suitable for extension in future research. Different from the previous built models, the model proposed in this thesis includes additional aspects, such as imposed deformations caused by drying shrinkage, and the possibility to model hybrid beams (with a U-shape). The imposed deformations were investigated, as the different materials in a hybrid section can shrink very differently, which could have an effect on the resistance of a hybrid beam.

The essential assumption of the extended model is that a perfect bond exists between the two layers (or, in a more general sense, two materials). In other words, no slipping occurs between the two materials in the beam. This lead to the conclusion that the effects of drying shrinkage in hybrid beams can not be simulated, as the main effect of drying shrinkage in such beams is on the interface between the two materials (the forces due to drying shrinkage have to be transferred through the interface). Nevertheless, the drying shrinkage calculations can be applied on monolithic beams.

Slipping between the steel reinforcement and the concrete is taken into account in the extended model in order to calculate the crack width. The model is suitable for simulating the deflection of a 3-point or 4-point bending test in which only a bending moment is applied in such a way that tension occurs at the bottom, and compression at the top (no normal force is applied). The bending resistance of the cross-section is also calculated. In order for the multi-layer model to work, it requires stress-strain input (tension and compression) for the material(s) that need(s) to be investigated. In return, the moment-to-curvature, force-to-deflection, moment-to-deflection, stress-to-deflection, load-to-crack opening displacement and crack width-to-force diagrams are found.

The model has been verified in four steps. In general, the experimental results from previous studies were compared to the results that follow from the model. In the first step, the results of the extended multi-layer model were compared with two previous studies in which a monolithic beam was investigated, and in which the multi-layer model also was used in one of the studies. In the second step, a comparison was made with research in which traditionally reinforced beams were tested. In this way, the second step consisted of an added element (compared to the first step), namely the addition of steel reinforcement. In the third step, one more addition was taken into account, namely that of a second layer/material in the beam. In the fourth and last step, the proposed experimental setup of a hybrid beam containing a U-shape was modelled. However, as this experiment has never been performed before, there were no experimental results to verify the model. Therefore, the results for this setup are to be compared with the results that follow after experimenting with the presented design of the beam. Comparing the force-to-displacement curves for the first three steps showed that the end-resistance of the beams is predicted well, and that generally the same trend of the curve is followed by the extended multi-layer model.

The other aspect that has been verified was the inclusion of the effect of drying shrinkage. It was verified what the effect of drying periods would be on the flexural strength of two different materials: NSC (**N**ormal **S**trength **C**oncrete) and HSC (**H**igh **S**trength **C**oncrete). This was done by comparing with previous obtained results in the MSc study of Awasthy. This verification showed that the trend of the curve that is predicted by the FEM-model FEMMASSE is predicted well by the extended multi-layer model. In FEMMASSE, it is possible to model the stresses due to drying shrinkage.

It is recommended to further expand the proposed model in future research. One of the possible expansions is the inclusion of the bond between the two materials (and between the bottom layer and the reinforcement) in a hybrid beam in terms of crack width. This could make the proposed model more powerful, as it would then be possible to optimize beam configurations in terms of crack width control. Such optimizations can currently be performed for traditionally reinforced beams in the model. Next to that, it is recommended to investigate how the longitudinal shear stress can be calculated for hybrid beams containing a U-shape.

1. Introduction

1.1. Background information

Concrete has the generally known property that it is strong in compression, but not in tension. In order to compensate this weakness, steel reinforcement is applied. Next to taking up the tensile forces, steel reinforcement also contributes to limiting the maximum crack width. Taking up the tensile forces prevents the construction from failing, which is achieved by meeting ultimate limit state (ULS) criteria. Limiting the crack width, or limiting the deflection is something that is achieved by meeting serviceability limit state (SLS) criteria. The term 'serviceability' indicates that failing to meet those requirement will not lead to structural failure. For example, too large deflections will not cause structural failure, but will cause discomfort for users. Sometimes there is the situation that an element fulfills the ULS requirements, but not the SLS requirements (for example because of too large crack widths). That makes that additional steel reinforcement is needed, which is not an optimal situation as that additional reinforcement is not needed from the ULS criteria.

Applying materials with strain hardening properties, such as SHCC (which is the abbreviation of **S**train **H**ardening **C**ementitious **C**omposites), is another way to limit the crack width. The characteristic of this material is that many microcracks occur instead of a few large cracks. This is due to the (metal-like) strain hardening behaviour of SHCC, which is illustrated in (Zhou, et al., 2010). SHCC is, as the name also suggests, a composite. Synthetic fibers are added to the 'concrete' mixture. Those fibers are what results in crack width limitation, as the fibers cross the crack openings and transfer stresses. This type of 'concrete' is also called Engineered Cementitious Composite (ECC). By applying this concept, the amount of needed steel reinforcement can be reduced, as this mixture is contributing in controlling the crack width.

A disadvantage is however that this mixture is rather expensive due to the lack of coarse aggregates (that are very cheap). So it is not an economic option to only use SHCC in the cross section. By combining regular concrete with SHCC, the disadvantages of both can be addressed. In that way, the so called 'hybrid' beam is created. By applying the SHCC layer in the tension zone, the concrete does not have to perform in tension, and by applying concrete in the compression zone, savings can be made on the amount of SHCC.

This hybrid beam concept has been tested before by (Huang, 2017). In his research, it was proven that an addition of an SHCC layer of 70 mm in a beam with a height of 200 mm resulted in better controlled cracks. For illustration, a comparison made in the research of (Huang, 2017) is used. First of all, it is shown in Figure 1-1 how the results of the crack pattern are presented.

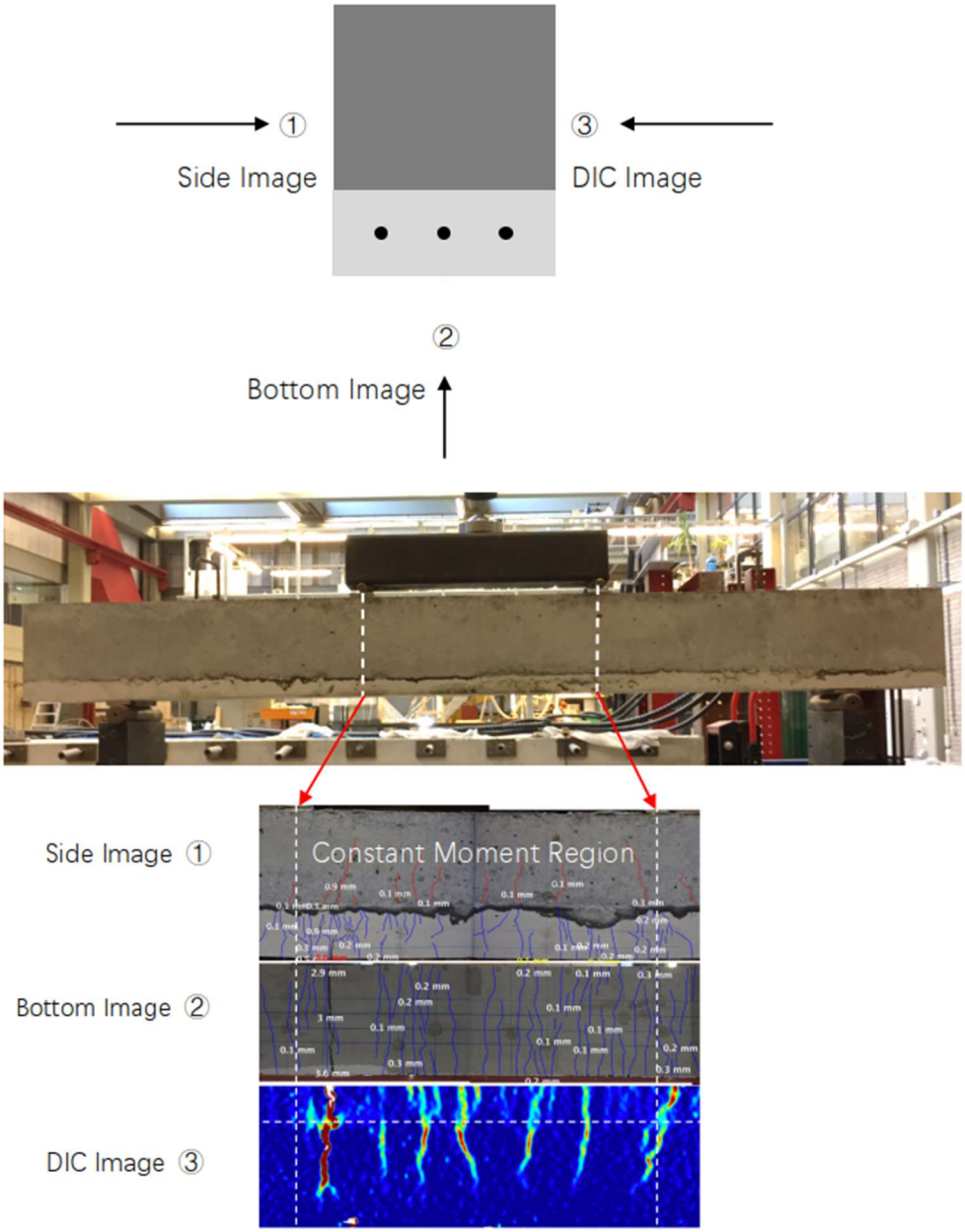

Figure 1-1: illustration of how the cracking pattern results are presented (Huang, 2017)

In Figure 1-2 and Figure 1-3, two different cases are presented. The beam in Figure 1-2 is a traditionally reinforced beam; the beam in Figure 1-3 is a hybrid beam (SHCC + traditional concrete). The blue images in Figure 1-2 and Figure 1-3 are, as is shown in Figure 1-1, the DIC (**D**igital **I**mage **C**orrelation) images. In this images, all colors except blue show the strains that lead to cracks. The green colour indicates small strains, while the red colour indicates large strains. So the larger the strains, the more visible the cracks are. Note that those images are flipped upside down (so the cracks at the top are in reality the cracks at the bottom).

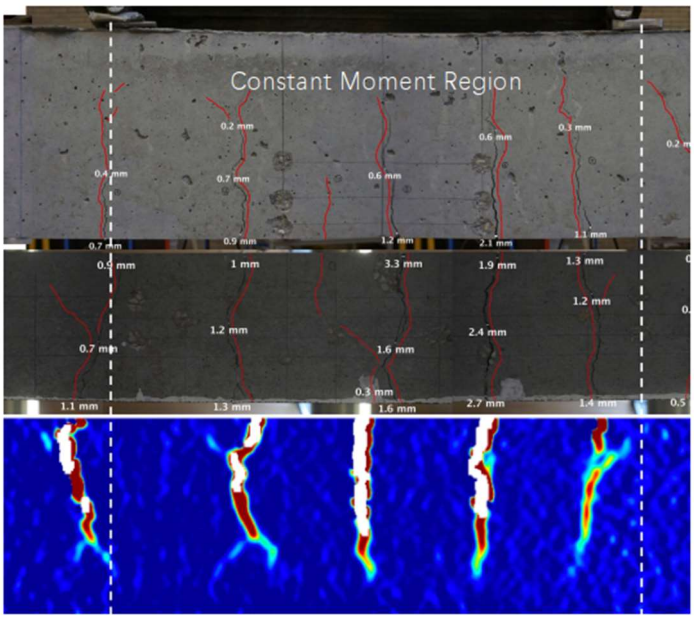

Figure 1-2: crack pattern of a traditionally reinforced concrete beam (Huang, 2017)

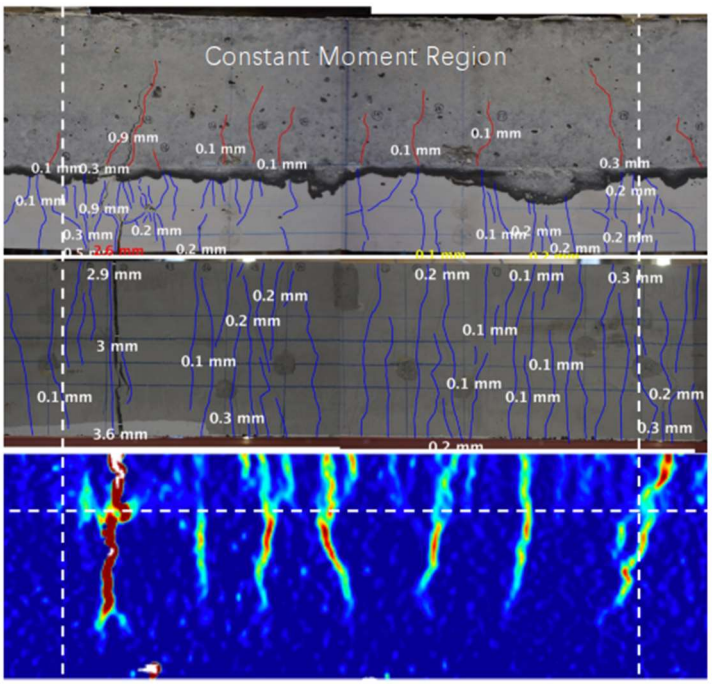

Figure 1-3: crack pattern of a hybrid reinforced concrete beam (Huang, 2017)

Not only the crack width is limited; it was shown that the cracks localize later for beams that contain SHCC (Luković, Hordijk, Huang, & Schlangen, 2019). This is illustrated in Figure 1-4, in which can be seen that the large crack width increase happens earlier for the reference beam (traditionally reinforced concrete) compared to the beam containing an SHCC layer.

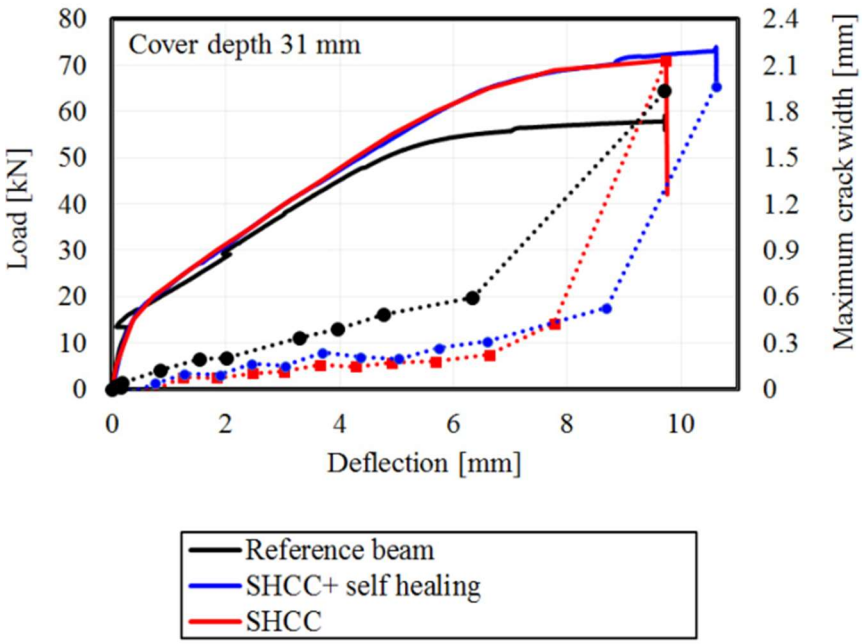

Figure 1-4: load-to-deflection and load-to-crack width diagrams; reference beam=traditionally reinforced concrete, SHCC=70mm layer over 200 mm height (Luković, Hordijk, Huang, & Schlangen, 2019)

In the study of (Huang, 2017), it was recommended to further research the U-shaped moulds made of SHCC. In this research, it will be investigated how this mould can be made. An earlier concept as was proposed by (Huang, 2017) is shown in Figure 1-5. However, in this thesis, another concept is investigated and proposed. The main reason for that is that the proposed method by (Huang, 2017) is only suitable for small scale experiments, as the sides of the U-shape have to be manually held in place for some time during casting (the sides are casted on a horizontal surface and then flipped 90 degrees to form a U-shape). For small U-shaped, this is feasible, but not if ultimately the same beams as in (Huang, 2017) are to be tested (which have a length of 1900 mm).

Figure 1-5: concept of a U-shaped SHCC mould as proposed by (Huang, 2017)

The strain hardening effect appears after the linear elastic stage. Modelling the non-linear stage is not possible by using analytical expressions such as in the linear elastic stage. To solve that, a model was proposed by (Hordijk, 1991), called the 'multi-layer model'. This model divides the cross section of a beam into multiple layers. When the beam is loaded in bending, a curvature is applied which leads to a strain diagram. Then, a strain can be assigned to each layer. By using the stress-to-strain material input, the corresponding stress for each layer can be found. As each layer has an area, the stress can be translated to the force by multiplying with the area. By achieving horizontal equilibrium of the forces in the cross-section, the bending resistance of the beam can be calculated by multiplying each force with its distance to the neutral axis. By doing that, the bending moment corresponding to the considered curvature is found. Doing this for multiple curvatures leads to a moment-to-curvature diagram, in which the resistance in the non-linear stage can be found. This is one of the possible output diagrams.

In this thesis, the multi-layer model will be extended. The most noticeable extension is the implementation of hybrid beams, in order to be able to model the reinforced hybrid concrete beam with a U-shaped mould that will be proposed in this research. If the basic case, which is used in the initial multi-layer model, is an SHCC beam, the following extensions are made in this research: first of all, steel reinforcement is included. Secondly, a layer of concrete is included on top of the SHCC, by which the beam becomes a hybrid beam. Finally, along the height of the concrete layer, SHCC webs are added. This makes that the proposed multi-layer can handle reinforced hybrid concrete beams containing a U-shape.

Next to those inclusions, the effect of drying shrinkage is considered, and an attempt is made to implement it in the multi-layer model for hybrid beams. The inclusion of drying shrinkage effects is of importance in hybrid beams. Normally, SHCC will shrink much more than concrete if both are considered separately. This difference is illustrated in Figure 1-6 for a repair material instead of regular concrete; for regular concrete the difference is even larger.

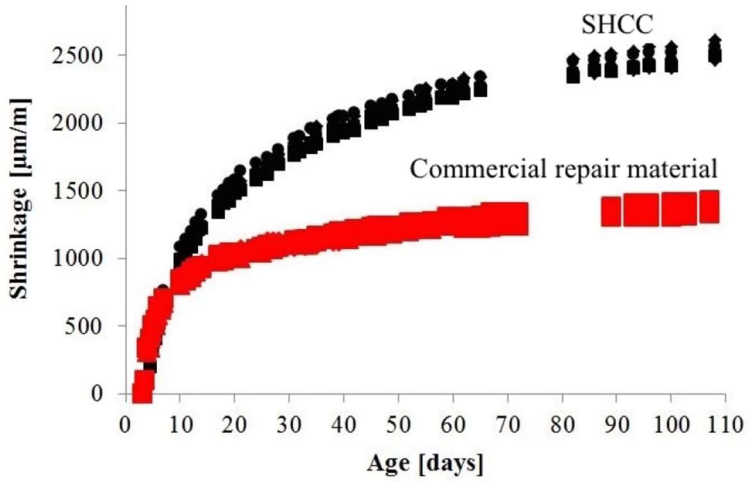

Figure 1-6: free shrinkage measurements of SHCC and commercial repair material (Luković, 2016)

In a hybrid beam, the concrete will be casted after the SHCC. But because the SHCC shrinks much more than regular concrete, the SHCC will, although it is casted earlier, shrink more than the concrete. This can have an effect on the resistance of the considered beam.

In the research of (Awasthy, 2019), it was measured how some mechanical properties of concrete, like the Young's modulus and the compressive strength, are affected by eigenstresses due to drying shrinkage over time. The way drying shrinkage occurs, which will be further investigated in this report, is the case in which a specimen is exposed to a dry environment after curing. When exposed to a dry environment, the specimen loses water due to evaporation, as it contains more water than the environment (equilibrium needs to be achieved with the environment). At some point, water from the small capillary pores of the concrete is lost, which generates an under-pressure in the pore system (Awasthy, 2019). This leads to compressive (eigen)stresses. These stresses are compensated with the tensile eigenstresses that occur at the surface, which could lead to cracks if the tensile strength of the concrete is exceeded (Moris & Dux, 2003). An example of the appearance of those cracks is shown in Figure 1-7.

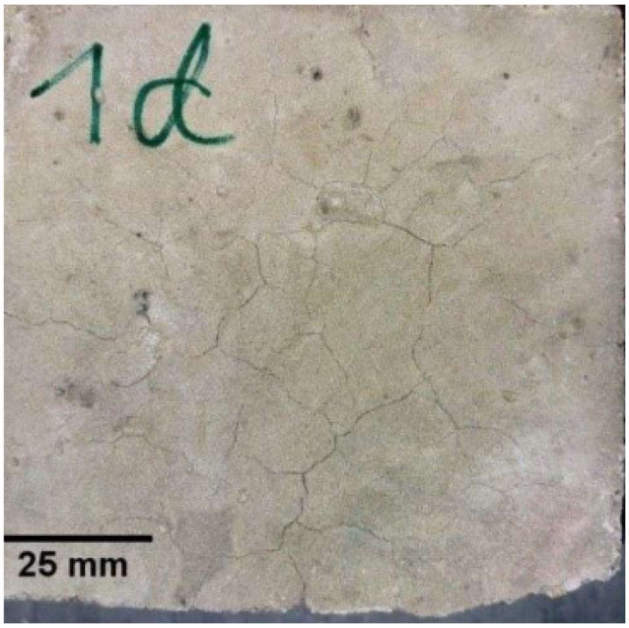

Figure 1-7: example of drying shrinkage cracks (Awasthy, 2019)

1.2. Research question(s)

The ultimate goal of this research is to build a reliable model that predicts the bending behaviour of reinforced hybrid concrete beams with a U-shaped (SHCC) mould, and to consider the eigen-strains due to drying shrinkage in the same hybrid beams. To make sure it is a reliable model, it needs to be verified. To reach this goal, the following three questions are addressed in this research:

- How can a reinforced U-shaped mould be made to be used in a reinforced hybrid concrete beam?
- How can the principles of the multi-layer model be used to model reinforced hybrid concrete beams with a U-shaped mould?
- How can the eigenstresses due to drying shrinkage be implemented in the multi-layer model?

In order to be able to answer the second and third question, the process that is illustrated in Figure 1-8 is followed.

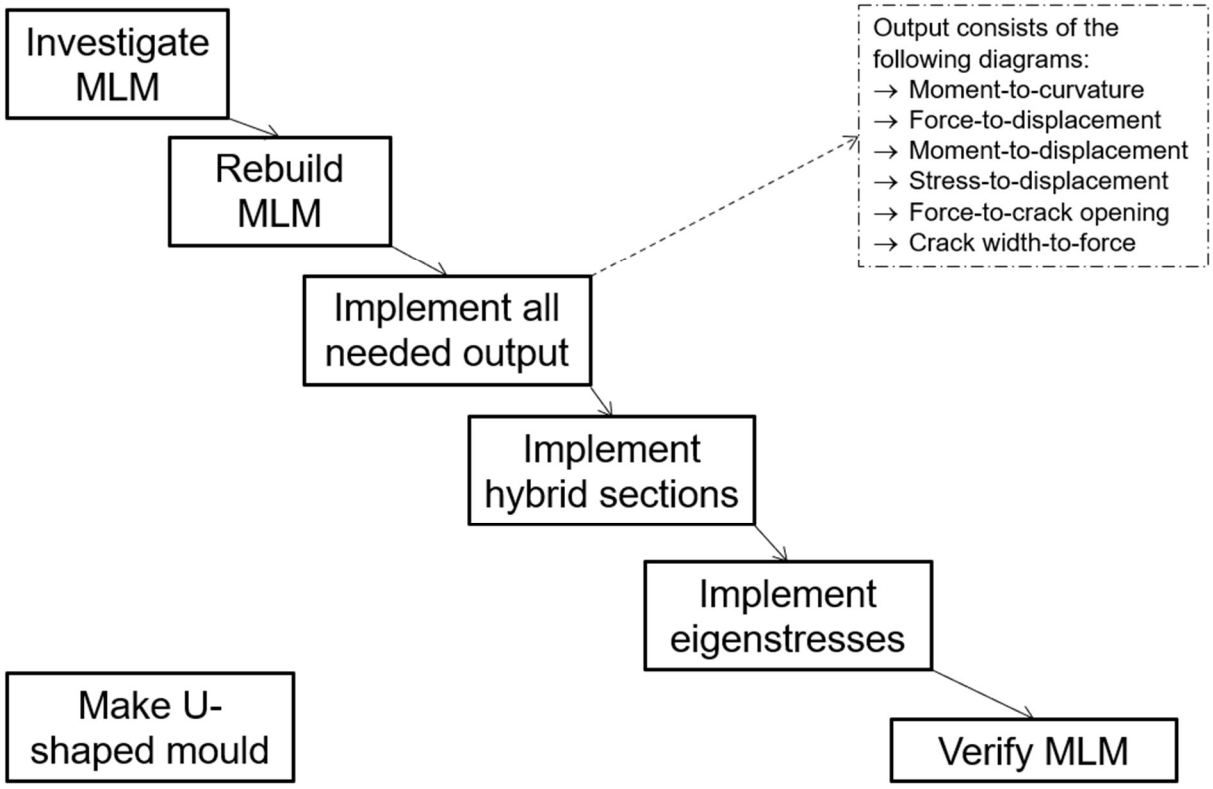

Figure 1-8: flow-chart of the process that is to be followed concerning the multi-layer model

In this research, a procedure is developed of producing a reinforced hybrid concrete beam with a U-shaped SHCC mould. This is an essential step, as there has never been any experiments done with such beams. And in order to be able to verify the proposed model that predicts the behaviour of such beams, experiments have to be performed on them.

1.3. Problem statement

Currently, there are no analytical expressions that address the bending behaviour of hybrid beams. As hybrid beams partly consist of a material that shows strain hardening behaviour, it is of importance to be able to model the behaviour of such beams in the non-linear stage. In 1991, the multi-layer model was proposed by (Hordijk, 1991) to model the non-linear behaviour of materials. The model was developed for monolithic (unreinforced) concrete beams. In this research, its suitability is extended to modelling reinforced hybrid concrete beams with a U-shaped mould. After this extension, the model needs to be verified. The most advanced available experimental results that can be used for verification are in the research of (Huang, 2017), in which he experimented with reinforced hybrid concrete beams. However, as there are no experiments that are performed with reinforced hybrid concrete beams with a U-shaped mould, the procedure of making this U-shaped mould needs to be developed. After that, experiments can be performed to verify the results that follow from the proposed model.

1.4. Research outline

Besides this introduction, the report is divided into six chapters. In chapter 2, the U-shaped SHCC mould is analyzed, and a proposal is made for an experimental setup. Chapter 3 explains the multi-layer model, which will be extended to be able to model hybrid structures such as the system that will be proposed in chapter 2. Next, the extended multi-layer model is verified in chapter 4 by comparing to previous research and previously made models. In the same chapter, an experimental setup with predicted results is presented for the part that cannot be verified in this research, namely the reinforced hybrid concrete beam with a U-shaped mould. This can be verified in the future by using the experimental procedure that is presented in this research. After that, the results are discussed and the limitations of the proposed MLM are analyzed in chapter 5. Subsequently, the conclusions of this research are presented in chapter 6. Last but not least, recommendations of future research are made in chapter 7.

2. U-shaped SHCC mould

This chapter is about the design of a U-shaped SHCC mould, which can ultimately be used in a system of a reinforced hybrid concrete beam. Next to that, the advantages of having a U-shaped mould are discussed. The procedure of making a U-shaped mould was a result of multiple stages, setbacks and successes in the process. However, only the final result is presented in this chapter. The rest is described in Appendix F.

2.1. Inspiration

In the study of (Huang, 2017), it was proven that a 70 mm layer of SHCC in a reinforced hybrid concrete beam helped limiting the occurring crack widths. In this chapter, a next step is presented to expand the concept. The cross-section of the 'ideal' beam that controlled the crack widths best, as was found by (Huang, 2017), is shown in Figure 2-1.

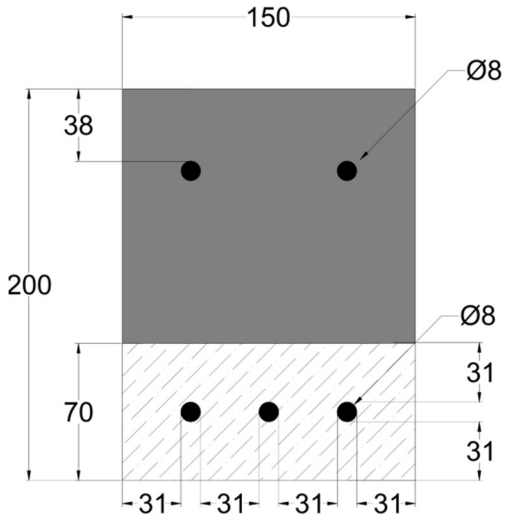

Figure 2-1: cross-section of a reinforced hybrid beam containing an SHCC layer (Huang, 2017)

The beam was tested in a 4-point bending test, according to the setup that is shown in Figure 2-2.

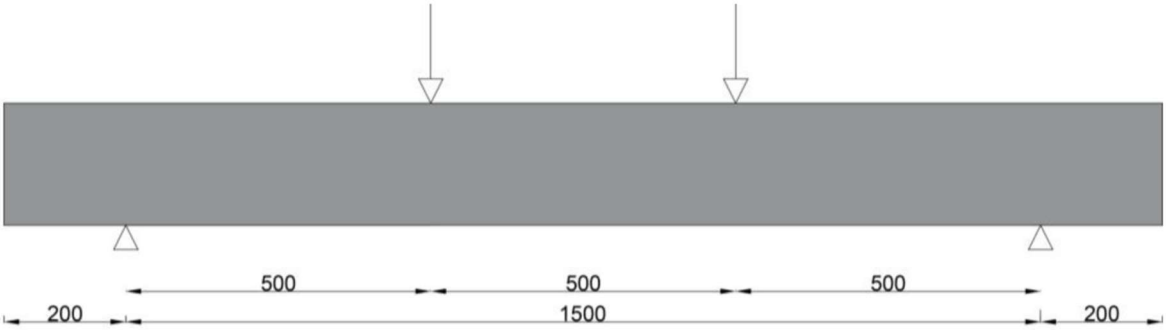

Figure 2-2: 4-point bending test setup in which the reinforced hybrid concrete beam was tested (Huang, 2017)

In this chapter, it is proposed to use the same setup, but only add the U-shaped webs to the beam. However, the casting process drastically changes with this small addition. The reinforced SHCC layer will now not only be casted as a layer; it will be casted as a reinforced U-shaped mould in which the concrete can be poured.

2.2. Advantages

Applying SHCC, in general, has numerous advantages. As was explained before, the crack width is limited when SHCC is applied. This is due to the strain hardening property and the occurring microcracks. This property can be recognized from the stress-to-strain diagram that follows from a direct tensile test. An example is shown in Figure 2-3.

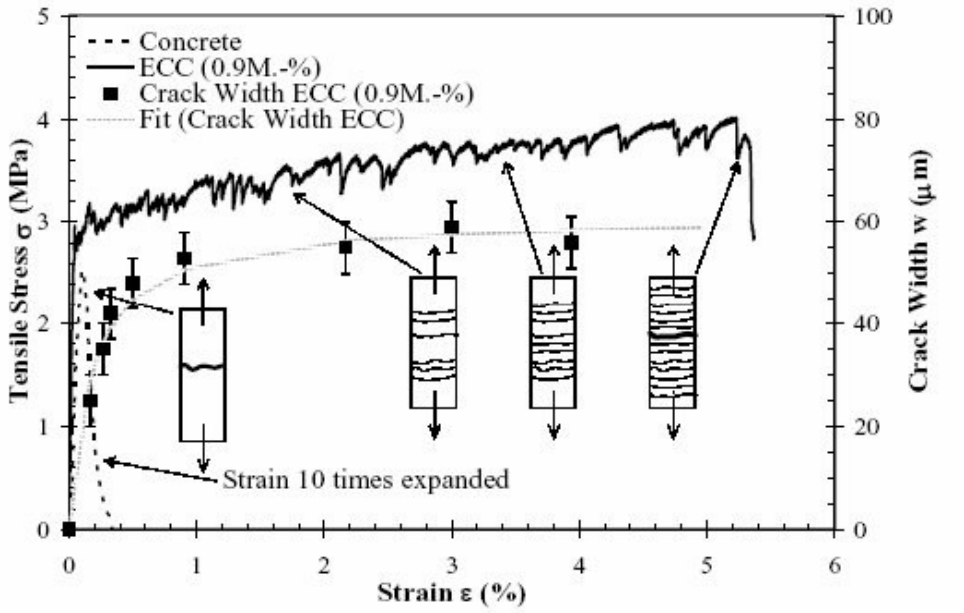

Figure 2-3: strain hardening of SHCC during a direct tensile test (Li & Li, 2011)

Next to that, the reduced crack widths mean that penetration of water and aggressive ions (such as chloride and CO_2) into the concrete is more difficult. Durability of the concrete is therefore

improved, as there will be less corrosion; freezing damage is also reduced (Paul & Babafemi, 2017). If a prefabricated SHCC layer is to be used, also savings can be made on formwork (and labor costs of setting it up).

In this chapter, it is proposed to combine all advantages of applying SHCC and include the advantage of a U-shape, namely the further savings on formwork. Previously, formwork was needed at the sides; that is no longer the case if a U-shaped SHCC mould is chosen. In that way, not only formwork costs are saved, but also the labor costs of setting those up. A possible advantage is that the moulds, that will be used to produce the U-shape, are reusable. Next to the practical advantages, the SHCC webs of the U-shape could contribute to the bending resistance of the beam that is considered.

2.3. Production

The way to make a U-shape is by having two moulds. One outside mould, and one inside mould. By placing the inside mould inside the outside mould, an inversed U-shape is created after casting. This is shown in Figure 2-4 and Figure 2-5.

Figure 2-4: inside and outside moulds for casting a U-shaped mould

Figure 2-5: inverse U-shape after casting

The most desirable results were obtained when the outside mould was made out of steel and the inside mould out of high-quality Styrofoam that is wrapped with tape. Vaseline needs to be applied to the surface of both moulds. During demoulding, the result in Figure 2-6 can then be obtained (after detaching the SHCC + the Styrofoam in it from the outside mould and flipping it upside down):

Figure 2-6: demoulding of the SHCC U-shape

If the procedure in Figure 2-6 is done very carefully, there is a possibility that the Styrofoam inside mould stays intact and can be reused.

The U-shaped mould is not meant to only consist of SHCC. An addition is to include steel reinforcement. If shear failure is to be prevented, to force bending failure, also shear reinforcement can be added. In order to include the reinforcement, first the reinforcement cage has to be completely prepared. The challenge is to place the reinforcement in a way that the stirrups would stick out of the SHCC. That was done as is shown in Figure 2-7. To get the concrete cover correctly, timber pieces of the required height were placed inside the slots, so that the stirrups would rest on them. In that way, traditional spacers that mix with the SHCC after casting are prevented.

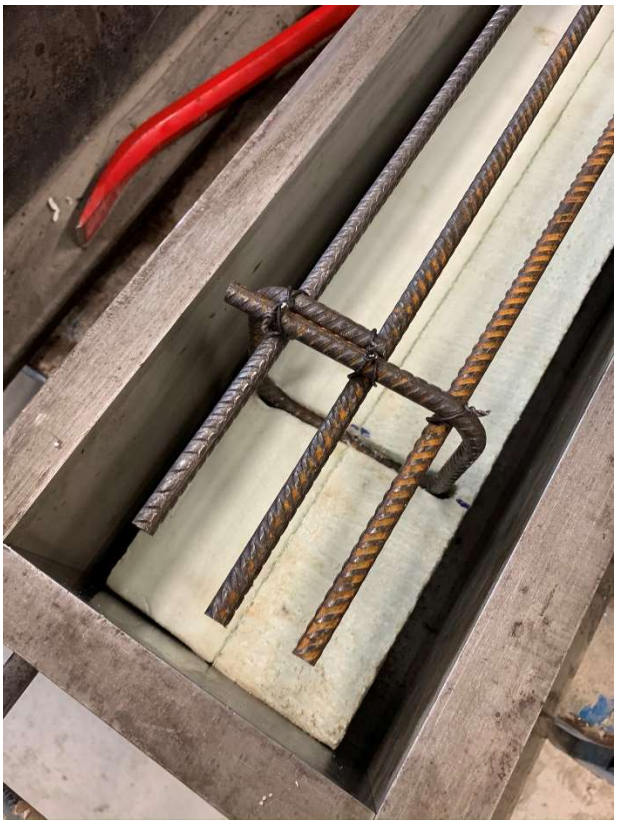

Figure 2-7: slots in the Styrofoam inside mould to place the stirrups in

To prevent leakage inside those slots, the slots were covered with tape. At the end, this was the way to produce the U-shape with reinforcement in it (see Figure 2-8):

Figure 2-8: preparation of a U-shaped SHCC mould with steel reinforcement in it

This procedure should lead to the 'reinforced U-shaped mould' that is shown in Figure 2-9.

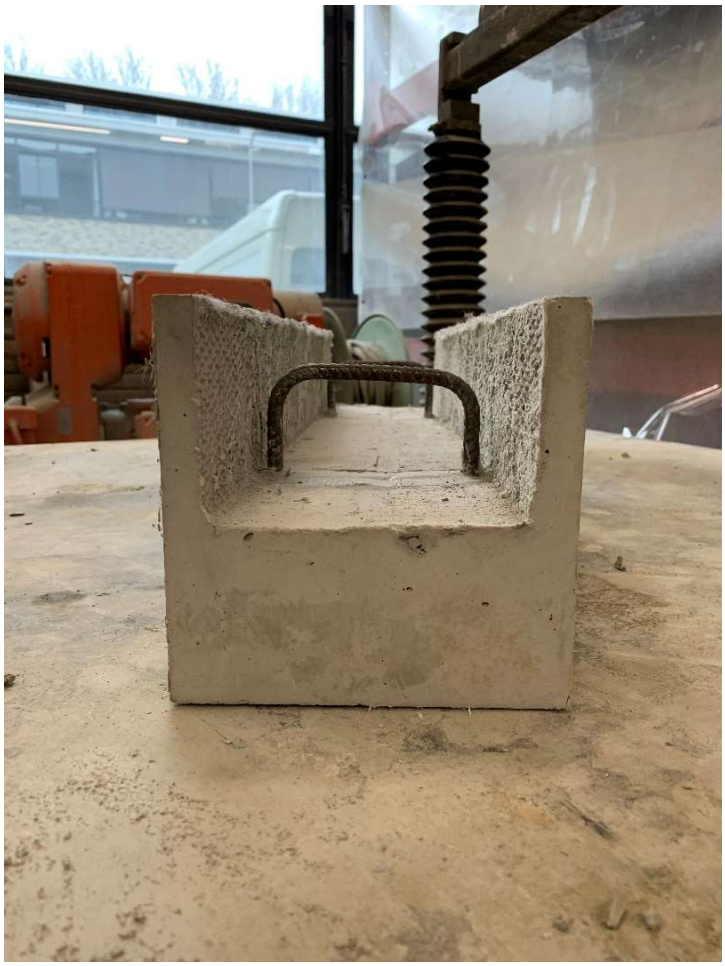

Figure 2-9: end result after demoulding a reinforced U-shaped SHCC mould

2.4. Experimental setup

The mixture that was used to produce the U-shaped mould is shown in Table 2-1, and is the same mixture as was used in (Huang, 2017).

Ingredient	Used amount [kg/m^3]
Portland cement CEM III/B 42,5	790
Limestone powder	790
Water	410
Superplasticizer	2.13
PVA-fibres	26
TOTAL	**2018.13**

Table 2-1: used SHCC mixture during production of U-shaped mould

As was explained before, the same setup, apart from the webs of the U-shape, as in (Huang, 2017) is proposed. For the webs, a thickness of 15 mm is chosen. The web thickness is checked on its resistance to the load that follows during casting, as it is acting as a wall that is under

pressure. A thickness of 15 mm is safe. The check is shown in Appendix F. The dimensions of the proposed experiment are shown in Table 2-2:

Part	**Dimension [mm]**
Outside mould	1900x150x2000
Inside mould	1900x120x130
Web thickness	15
SHCC bottom layer	70

Table 2-2: recommended dimensions for system of hybrid beam containing a U-shape

The dimensions of the moulds are chosen to produce beams that are comparable with the previously explained 'ideal' beam as was found in (Huang, 2017).

As for the reinforcement design, it is shown in Figure 2-10. Note that the top reinforcement is not included in the reinforcement cage, as it cannot be put into the inside mould (see Figure 2-7). Therefore, it has to be mounted afterwards.

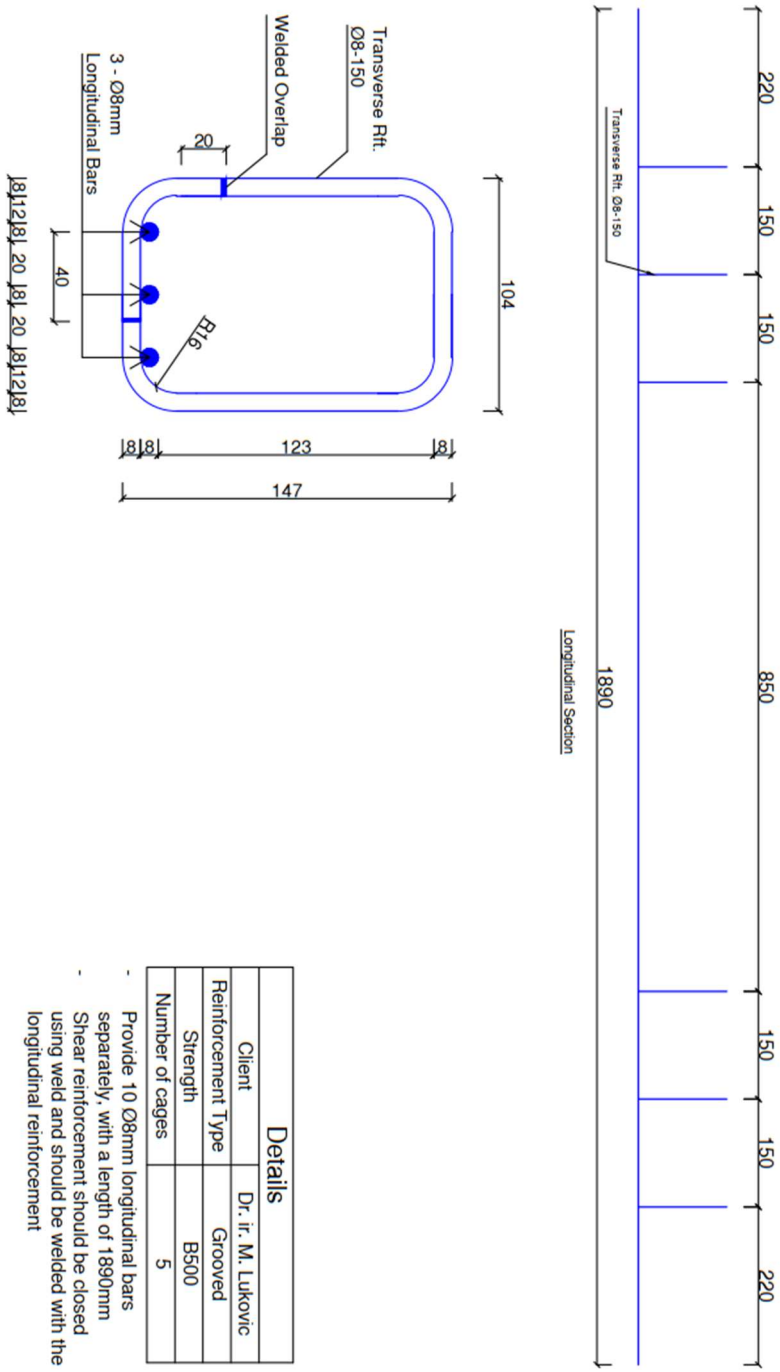

Figure 2-10: reinforcement design of large scale experiment hybrid beam containing a U-shape

The reinforcement design was such that shear failure is prevented. The stirrups are placed as was done in (Huang, 2017), where shear failure was also prevented. This is shown in Figure 2-11.

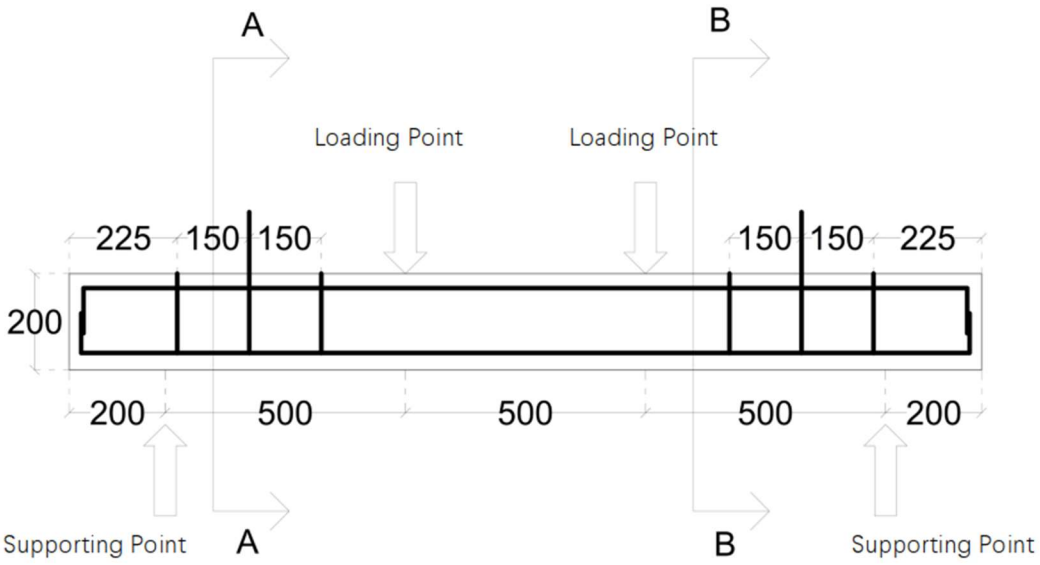

Figure 2-11: shear reinforcement placing to prevent shear failure (Huang, 2017)

In subchapter 4.4, the bending resistance of the proposed experimental setup is modelled and shown using the (extended) multi-layer model.

3. Multi-layer model

In this chapter, the originally proposed multi-layer model will be investigated. In this same chapter, the inclusions to the model are introduced, which are used to expand the multi-layer to be able to model the bending resistance of the experimental setup that was proposed in the previous chapter. Ultimately, the multi-layer can be used to model any hybrid beam, as long as the material input, that will be shown in this chapter, is available.

3.1. Principles and goal

The multi-layer model (also noted as MLM in this thesis) was first proposed by (Hordijk, 1991). The theory on which this model is based on, is to divide the cross section of a beam, at the location of (expected) fracture, into multiple layers that are schematized as springs. In this way, the beam is divided into two section of equal length, that are connected by those springs. The behaviour of each layer is represented by its corresponding spring.

This model is used because the post-linear stage can be analyzed quite accurately. Normally, analytical expressions can be used to calculate the resistance of every beam in the linear elastic stage. For example, if a simply supported plain concrete beam is considered, the moment resistance of the beam can be found using Eq. (3.1):

$$\sigma = \frac{M}{W} \rightarrow \sigma = f_{ct} \rightarrow M = f_{ct} * \frac{1}{6} * b * h^2 \qquad \textit{Eq. (3.1)}$$

As concrete is weaker in tension than in compression, the tensile stress is governing for the linear elastic stage. The strain diagram in Figure 3-1 occurs, and it is assumed that the (plain) concrete beam fails.

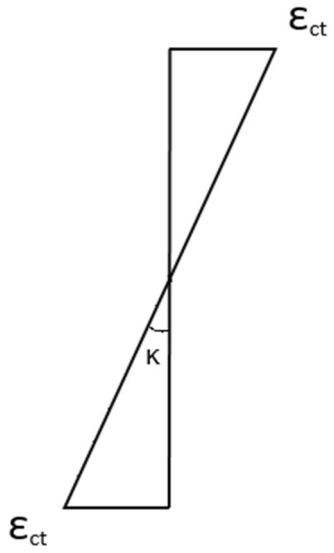

Figure 3-1: strain diagram at failure for a plain concrete beam

The strain diagram in Figure 3-1 can only be linear if the considered beam acts according to the Bernoulli hypothesis; if the beam would consist of longitudinal fibres, each cross-section that is made should stay straight during bending. The fibres and the cross-sections are illustrated in Figure 3-2. It is **assumed** that the Bernoulli hypothesis always applies in this research.

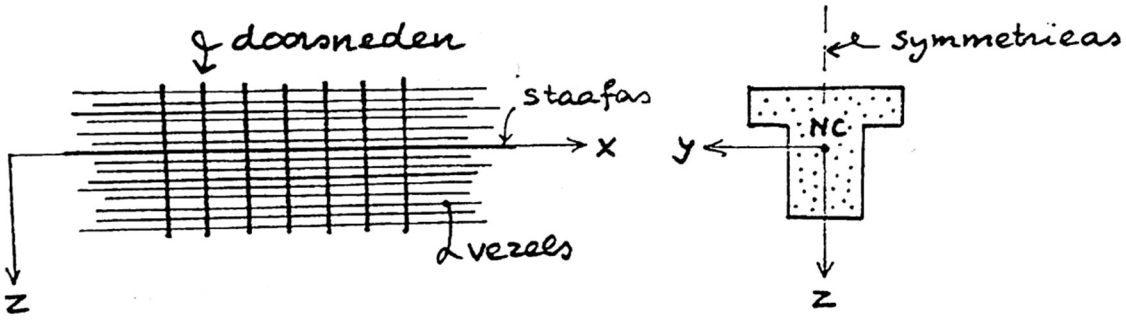

Figure 3-2: Bernoulli hypothesis as is explained by (Hartsuijker, 2001)

If reinforced beams are considered, more expressions can be used to model the resistance of the beam, such as at failure. Then, next to the end of the linear elastic stage that is known, the moment of failure will also for example be known. This is illustrated in Figure 3-3. In this figure, an example of a moment-to-curvature diagram is shown. The datapoints that can be determined using analytical expressions are marked in red.

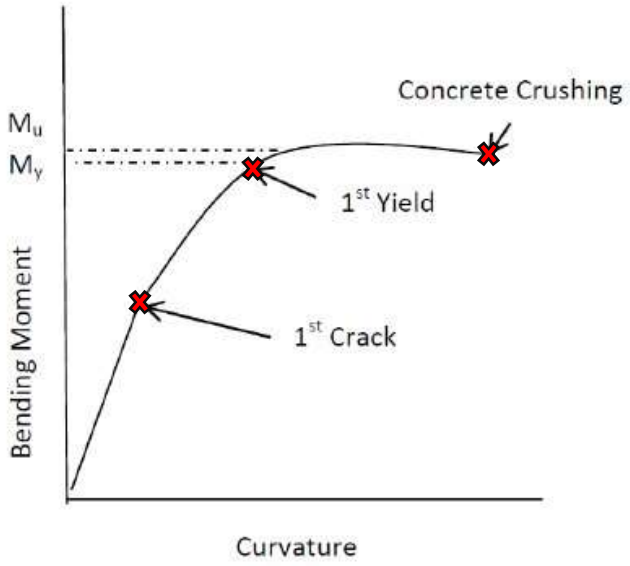

Figure 3-3: example of a moment-to-curvature diagram (Hajializadeh, Eugene, Enright, & Schiels, 2012); edited

Between zero and the first red marking in Figure 3-3, the behaviour is linear. However, there are no (exact) expressions that result in output for the steps in **between** the red markings. This is where the multi-layer model is usable. (Hordijk, 1991) used it for modelling the behaviour of plain concrete, while (Kooiman, 2000) used it for fibre-reinforced concrete. As the strain hardening behaviour is expressed in the non-linear stage, and as hybrid beams are investigated (which contain a material that shows strain hardening behaviour) in this research, the multi-layer model is the ideal theory to use for modelling the bending behaviour.

In this research, the goal by using this model is to model every step after the linear elastic stage and extract datapoints for the following diagrams: the moment-to-curvature, force-to-deflection, stress-to-deflection, moment-to-deflection, load-to-crack opening and crack width-to-force diagrams. How this is done and which limitations there are, is discussed in subchapter 3.4.

3.1.1. Bending moment resistance

The procedure in which the bending moment resistance is calculated, is the essential part of the MLM, which also shows all the principles of the model. All possible output of the MLM is based on this calculation.

As is explained, the multi-layer model is about dividing the cross section of a beam into multiple layers that are schematized as springs. In order to know the resistance of the beam that is considered, the springs should be located where failure is expected to occur. This is shown in Figure 3-4, in which a 4-point bending test is schematized. Failure is **assumed** to always occur at midspan. This will also be assumed for the 3-point bending test.

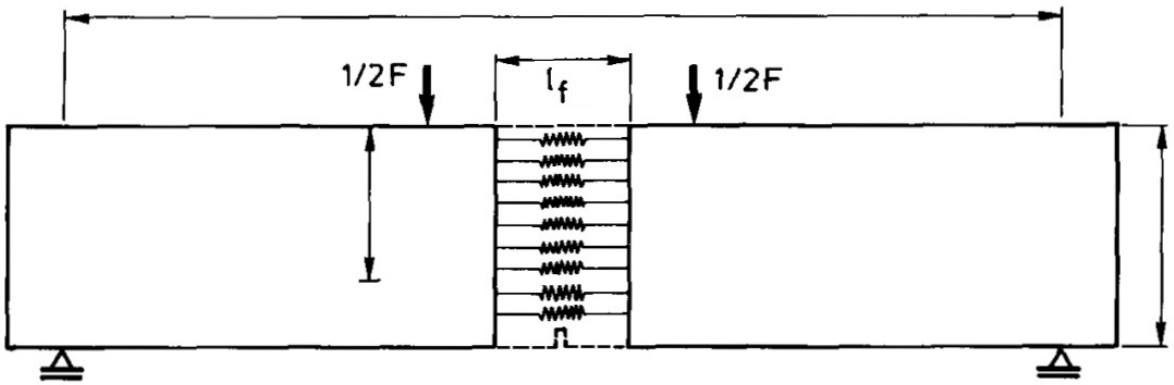

Figure 3-4: springs at the fracture zone to schematize the layers that are used in the MLM (Hordijk, 1991); edited

An example of how the cross-section is divided into layers is shown in Figure 3-5. Each of the layers in that figure represents a spring as is schematized in Figure 3-4.

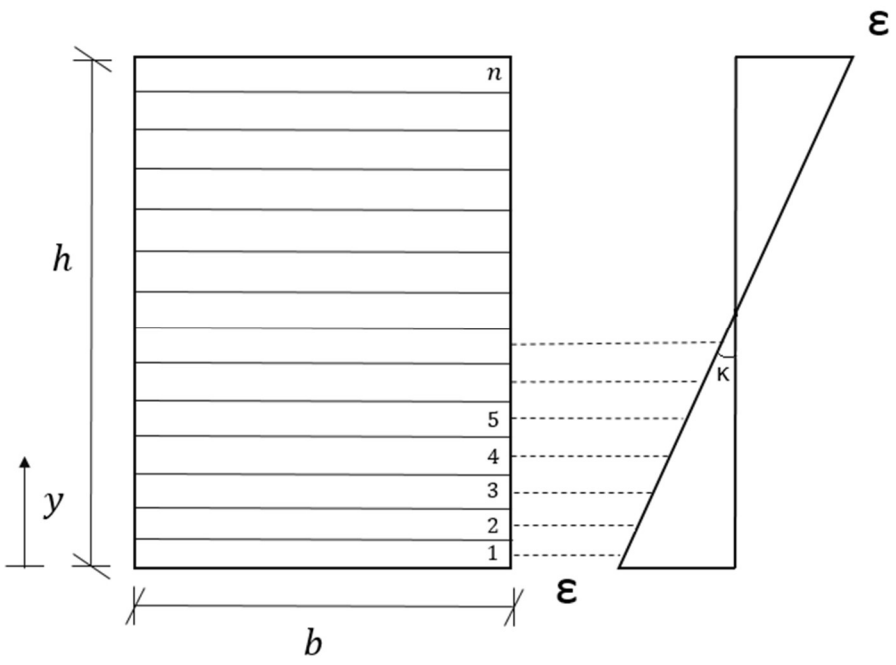

Figure 3-5: numbering of layers in a cross-section + reference y-axis

The strain at the centerline of each layer determines the force in the 'spring'. Normally, a force can be found using Eq. (3.2):

$$\sigma = \frac{N}{A} \rightarrow N = \sigma A \qquad \textit{Eq. (3.2)}$$

For the linear elastic stage, the stress is found using Hooke's law. This is shown in Eq. (3.3). Here, the relationship between the strain and the force can be recognized, as the stress (that is dependent of the strain in the linear elastic stage) is used in Eq. (3.2) to determine the force.

$$\sigma = E * \varepsilon \qquad \textit{Eq. (3.3)}$$

The area in Eq. (3.2) is equal to the area of the layer. Rewriting Eq. (3.2) gives the result in Eq. (3.4):

$$N = \frac{h}{n} * b * \sigma \qquad \textit{Eq. (3.4)}$$

In Eq. (3.4), 'h' is the total height of the beam, 'b' is the width of the beam, 'n' is the number of layers and 'σ' is the stress according to the 'centerline strain'.

Normally, the material properties are affected by size effects, which result in a lower bending moment resistance for increasing sizes. There are two size effects: statistical size effects, which are characterized by the randomness of the material properties that are considered, and

the deterministic size effects, which is partly related to fracture energy and crack localization (Kapteijn, 2020). For example, the stress 'σ' that should be inserted in Eq. (3.4), can be smaller for larger specimens than the input that is assumed. However, those effects are not considered in this research; it is **assumed** that the material properties are not affected by size effects.

3.1.1.1 Linear elastic stage

Using Eq. (3.3), the force in the spring can be calculated with Eq. (3.5). As can be seen, there is a direct relation between the strain and the force in the spring.

$$N = \frac{h}{n} * b * E * \varepsilon \qquad \textit{Eq. (3.5)}$$

For each spring, all parameters except the strain will be the same (in case the same cross-section as in Figure 3-5 is considered). So the force in each spring will be different. The main condition that holds for the MLM, is that horizontal equilibrium should be achieved while the beam bends according to the Bernoulli hypothesis. So the summation of all forces in the springs should be equal to zero. As the force in each layer only differs because of the strain, and as the strain diagram that is shown in Figure 3-5 is symmetric (linear elastic stage), this requirement is fulfilled. The requirement of horizontal equilibrium of the forces in the springs is only valid if no external normal force is applied; so one important **assumption** is that the beam is only loaded in bending, and not by a normal force.

When this condition is met, the next step can be made, namely that of calculating the bending moment. The ultimate desire is to obtain the bending moment and the curvature; the curvature is already known, as it is the slope of the strain diagram. The bending moment can be determined as follows: as can be seen in Figure 3-5, the neutral axis is located in the middle. For each force (in each spring), its magnitude times its distance to the neutral axis is equal to a bending moment. Summing this up, for all layers, the internal bending moment is found. It is **assumed** that there is no normal force acting on the beam (which could introduce additional bending moments due to possible eccentricity), so this internal bending moment is equal to the external (applied) bending moment.

In the linear elastic stage, there is a linear relation between the start and end of it. Therefore, it is only necessary to determine the bending moment of the first point (zero) and of the last point (end of the linear stage). A line between those two points can be drawn to find how the bending moment develops in the linear elastic stage.

3.1.1.2 Non-linear stage

For the non-linear stage, the situation becomes different. It was earlier mentioned that the stress could be determined according to Eq. (3.3). This expression is however not valid for the non-linear stage. Before explaining how the stress is determined for the non-linear stage, the previously described procedure of determining the stress in the linear elastic stage is explained

in a different way. The bottom layer of Figure 3-5 is now considered separately. This is shown in Figure 3-6.

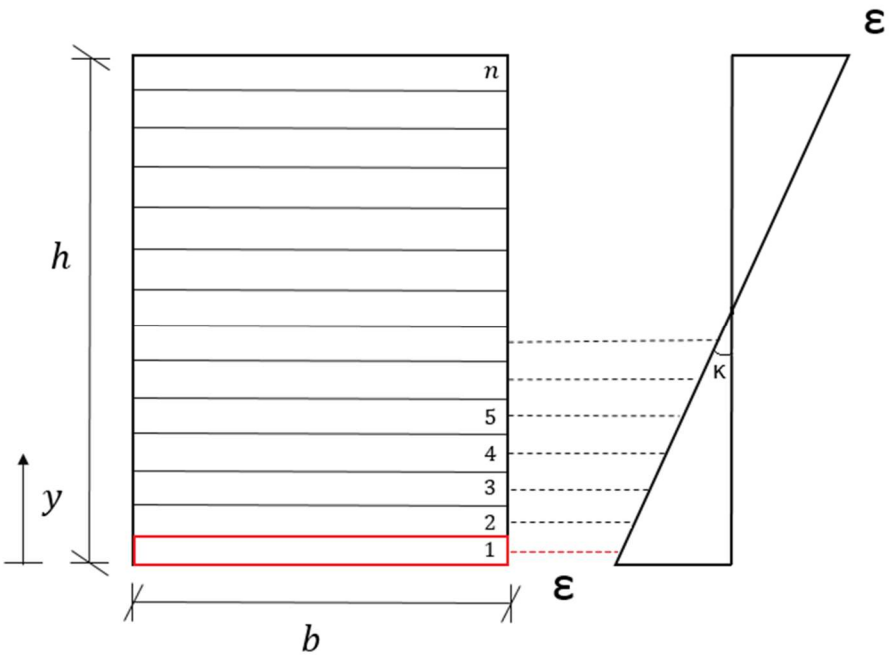

Figure 3-6: bottom layer of a cross-section marked in red

The strain at the centerline of the layer is taken. To know the stress, the stress-to-strain diagram of the material can be used. An example is shown in Figure 3-7.

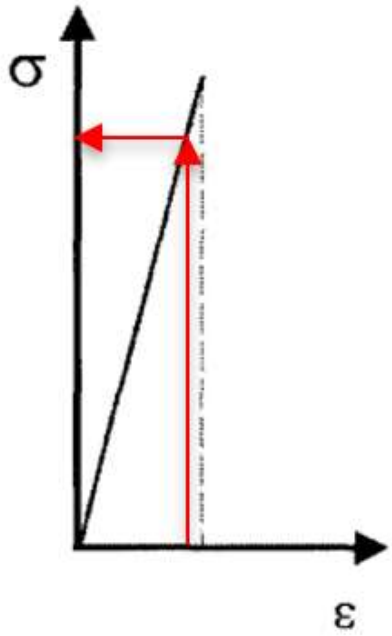

Figure 3-7: matching the strain with its corresponding stress in a linear stress-to-strain diagram

Reading the stress from Figure 3-7, and multiplying with the area of the layer gives the force in the spring. Doing that for all layers, and following the same procedure as was explained in subchapter 3.1.1.1 after that, leads to finding the bending moment resistance.

Now, the next step, which is the non-linear stage, can be considered. **Only** the curvature is increased with a (very) small step, which gives the situation in Figure 3-8 compared to the linear elastic stage. The red line represents the first step after the linear elastic stage.

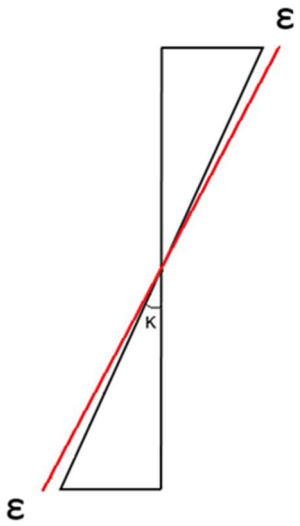

Figure 3-8: first step of the non-linear stage, in which the strain diagram is given by the red line

To determine the stresses corresponding to the occurring strains, a stress-to-strain diagram is needed. In order to illustrate the calculation procedure, a hypothetical stress-to-strain diagram of concrete is presented. It is shown in Figure 3-9.

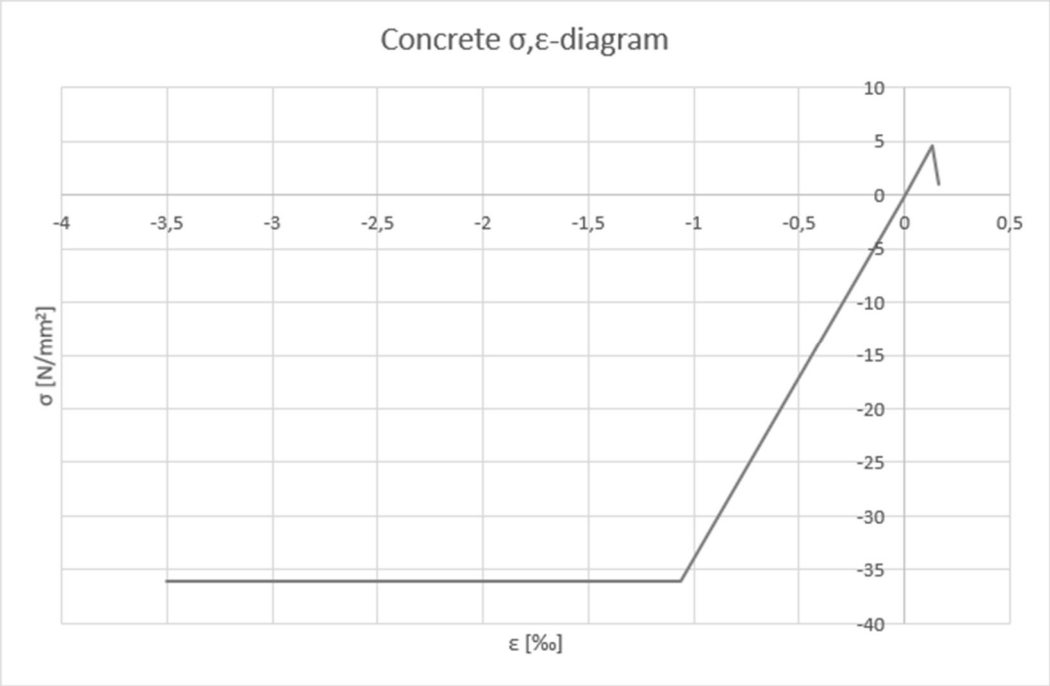

Figure 3-9: assumed stress-to-strain diagram of concrete

What can be read from Figure 3-9, is that the concrete has more resistance in compression than in tension. Next to that, the concrete acts linearly to a much higher stress in compression in comparison to tension. To be able to show the important details, a zoomed-in version of the stress-to-strain diagram is shown in Figure 3-10.

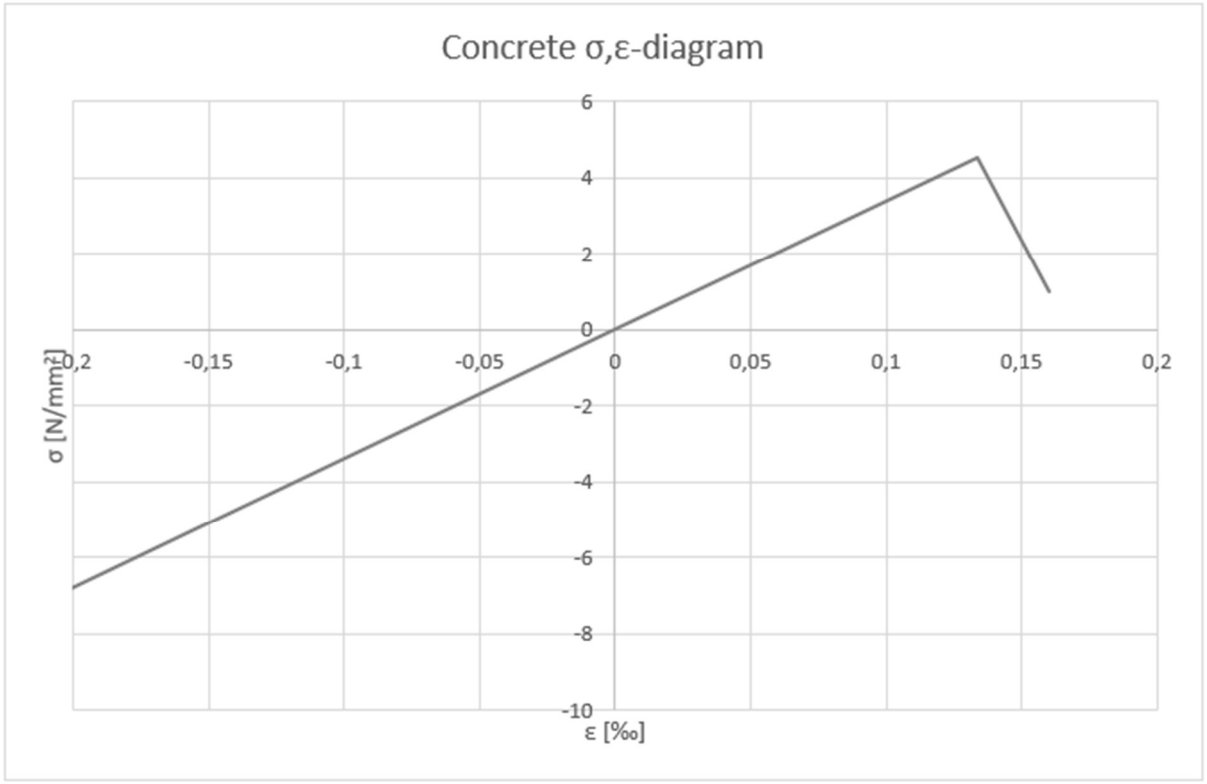

Figure 3-10: zoomed-in version of the assumed stress-to-strain diagram of concrete

Now, the bottom and top layer of the cross-section are considered. This is shown in Figure 3-11.

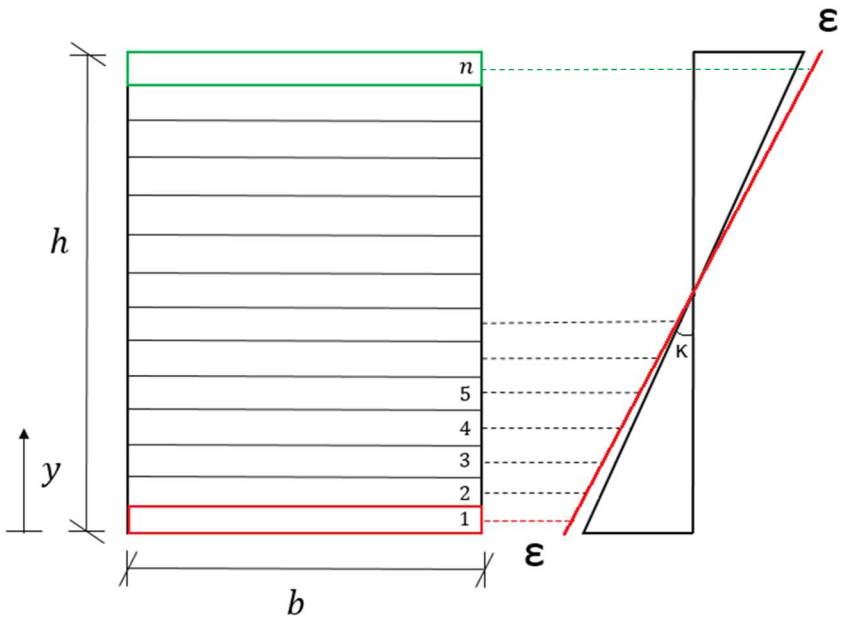

Figure 3-11: bottom layer of a cross-section marked in red and the top layer marked in green

Reading the corresponding strains and inserting them to the stress-to-strain diagram gives the results in Figure 3-12.

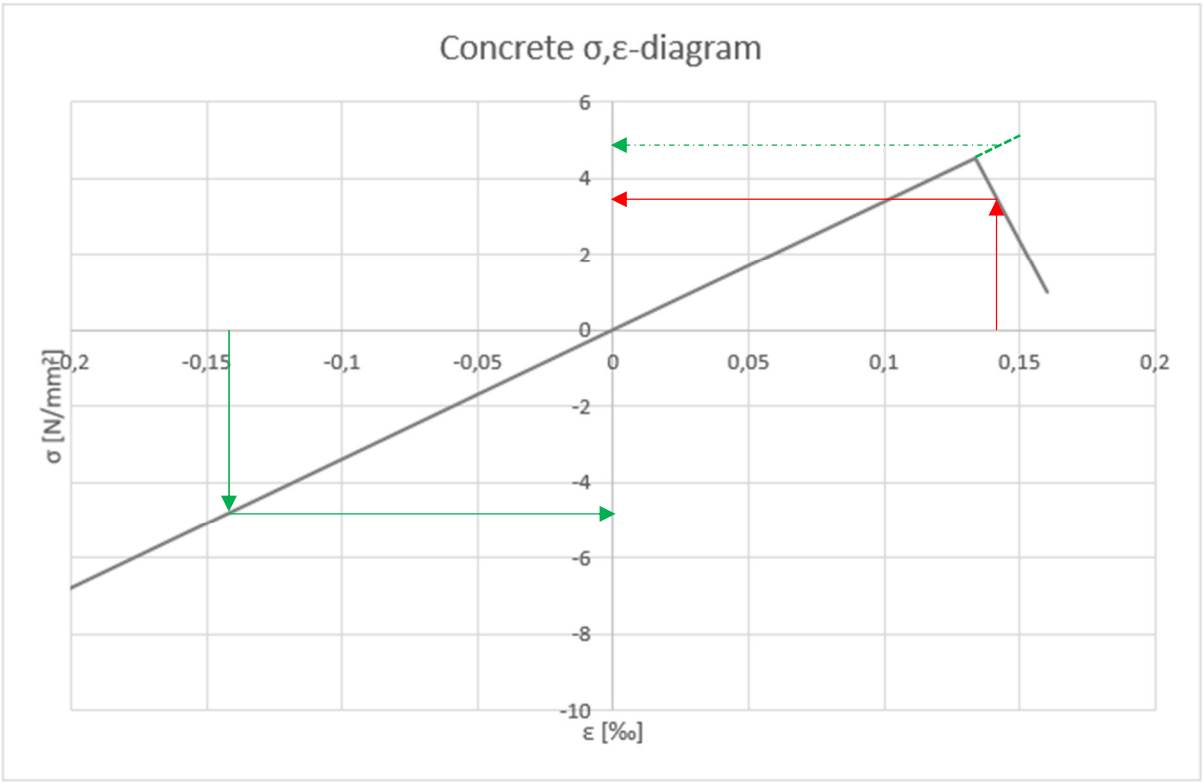

Figure 3-12: difference of stress between top (green) and bottom layer (red) after the linear elastic stage

As can be seen in Figure 3-12, the resistance in compression is higher than in tension. This is due to the fact that after the linear elastic stage in tension, there is a decrease in stress. The green stippled line indicates what would have been the stress if the material still behaved linearly, and it is exactly the same stress that is occurring in compression, as the material is still behaving linearly in compression.

As the neutral axis is still located in the middle of the cross-section, no horizontal equilibrium will be achieved if the forces in each spring were calculated. If the neutral axis is located in the middle, each spring has to carry the same force as its 'mirror spring' (the first layer at the top mirrors with the first layer at the bottom etc.). This is clearly not the case. Therefore, something has to change besides the curvature. What needs to change is the location of the neutral axis position. Note however that the curvature stays the same. What needs to be done is that, at each curvature, the neutral axis is moved upwards in small steps until there is horizontal equilibrium. An example of such an end result is shown in Figure 3-13.

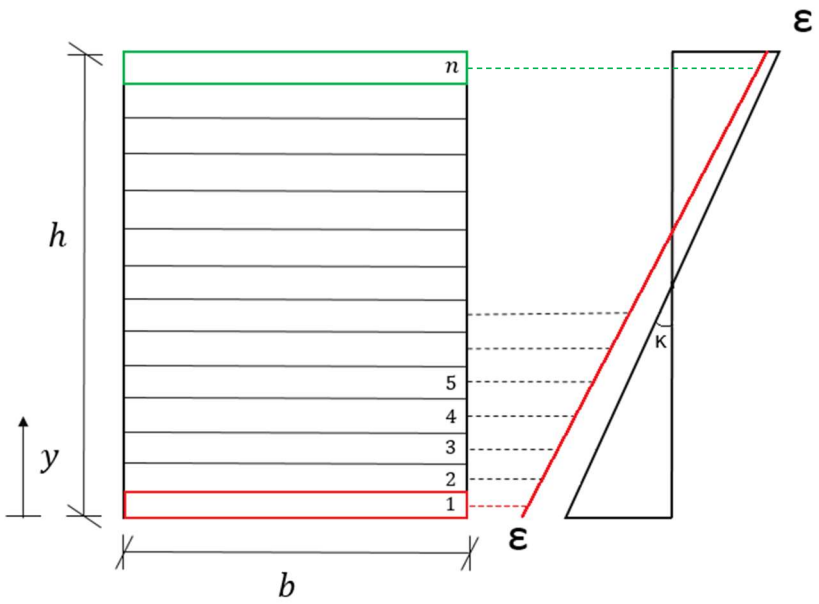

Figure 3-13: neutral axis position moved upwards to achieve horizontal equilibrium in the cross-section

By doing this, a stress diagram as is shown in Figure 3-14 can be achieved, which results in horizontal equilibrium. Note that this is only an example to illustrate the effects.

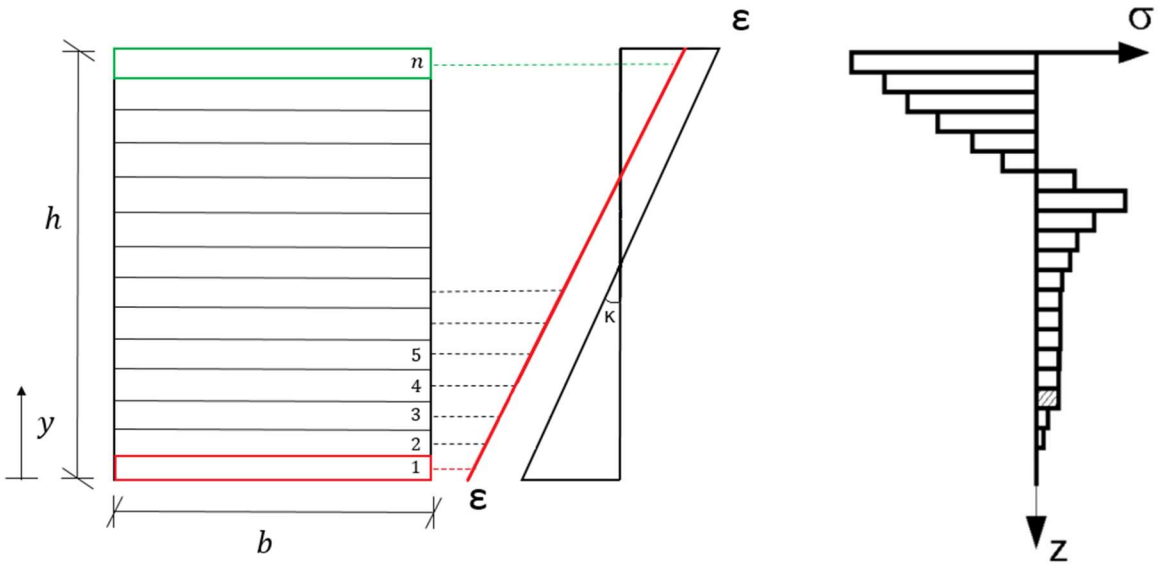

Figure 3-14: example of a stress diagram corresponding to a neutral axis position that has moved upwards

After the stresses are found, the same procedure as was explained before to find the bending moment resistance can be used (multiplying of all forces by their distances to the neutral axis). After the bending moment resistance is found, a new datapoint is achieved. The next step is then to increase the curvature again by a small step and to repeatedly go through the same process. To make the calculation method clear, all steps needed to draw the final moment-to-curvature diagram are shown in Figure 3-15.

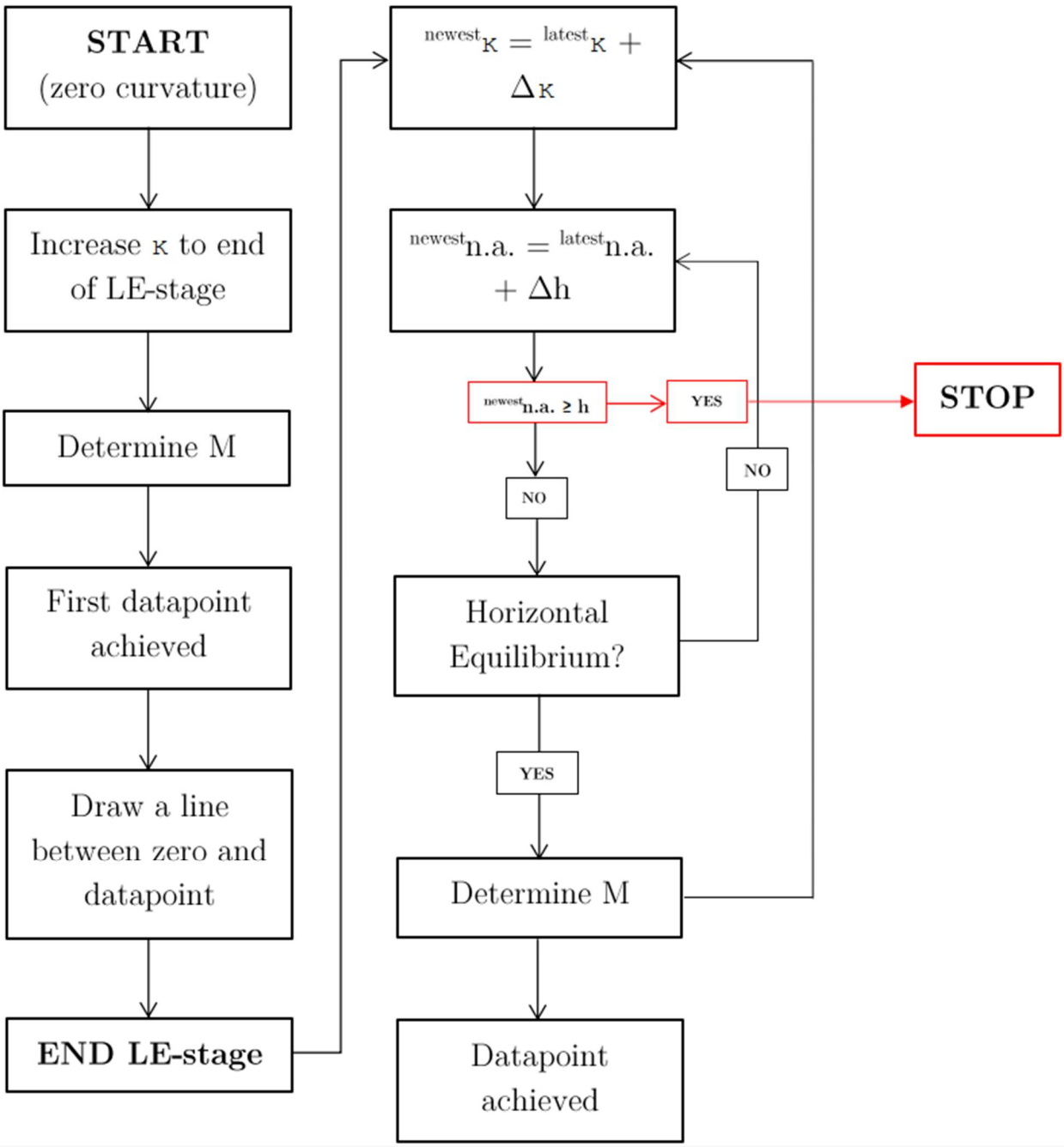

Figure 3-15: flowchart of the multi-layer model procedure

The essence of the process is that there has to be equilibrium for each curvature that is applied. If that is not the case, the location of the neutral axis will keep going upwards until it is physically impossible; the height of the beam is reached. When this happens, the specimen fails. With that, the process in Figure 3-15 ends.

One of the differences with the linear elastic stage is, that an iterative procedure is needed to obtain the datapoints. The bottom part of the concrete will have decreased resistance, so the neutral axis has to shift up. Doing this by small steps until equilibrium is found is the essence of the iterative procedure.

To summarize the calculation procedure: first, the cross section of the beam is divided into multiple layers over its height. After that, the curvature is increased until the end of the linear elastic stage is reached. For each layer, the strain at its centerline is taken. From the stress-to-strain input, the corresponding stress can be read. This stress times the area of the layer gives a force. And if the forces of all layers are summed up, there should be horizontal equilibrium. This is the check that a correct result is found. After this, the non-linear stage is entered. To find a new datapoint, the curvature is repeatedly increased by a small step. The neutral axis moves up until there is horizontal equilibrium of forces (for each curvature). If at some point (for a certain curvature) this equilibrium requirement cannot be met by moving up the neutral axis (because it reaches the top of the specimen), it means that the beam has failed. The datapoints that are found until failure lead to a moment-to-curvature diagram.

3.1.1.3 Effects of hybrid section

The calculation process for a hybrid beam is almost the same as was described in the previous subchapters. There is however one big difference, which becomes clear in Figure 3-16. A hybrid beam is shown with a height of 100 mm. The beam is divided into 10 layers; each layer has therefore a thickness of 10 mm.

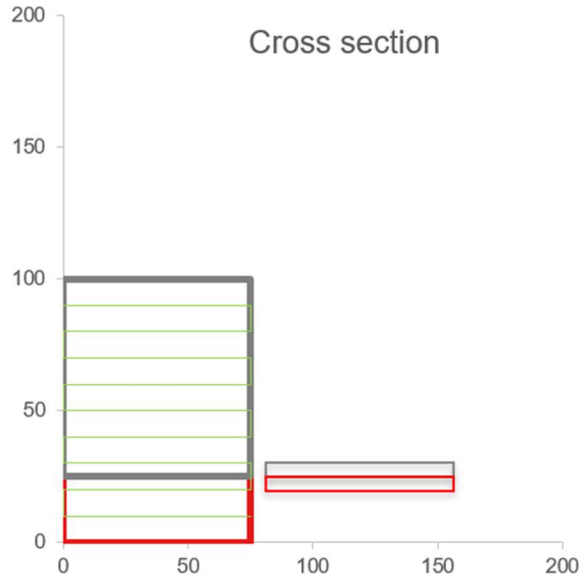

Figure 3-16: possible sublayers in the MLM for hybrid sections; dimensions in [mm[

The grey colour in Figure 3-16 indicates the presence of concrete, while the red colour belongs to the other material (SHCC for example). In green, the layers are viewed (in Figure 3-16). What can be noticed is, that the interface between the two materials is exactly at the middle of one of the layers. To be precise, it is at 25 mm height. This means that the third layer from the bottom contains 5 mm of SHCC, and 5 mm of concrete. And as both materials have different properties, the strain at the centerline cannot be translated to the right stress. This problem occurs when the thickness of one of the materials is not equal to an integer multiplier of the layer thickness. In this case, the thickness of the concrete was 75 mm, and that is 7.5 times the layer thickness (and 7.5 is not an integer). In this case, the problem could have been solved by using 20 layers. The layer thickness would then be 5 mm, and the concrete thickness would be a multiplier of 5. However, this problem cannot always be easily solved as in this example.

The solution to this problem is to isolate the layer in which the problem occurs, and to divide it into two sublayers with the corresponding thickness that is needed. If the concrete layer had a thickness of 78 mm for example, the sublayers would be 8 mm of concrete, and 2 mm of SHCC. The centerline of those two sublayers can then be taken, and the strain can again be translated to a stress by using the corresponding material input. After that, the same procedure can be followed as was described before to find the desired output. In the proposed MLM, this will be called the 'advanced method', while the previous method without the sublayers will be called the 'simple method'. Depending on the situation, the corresponding method automatically is used.

Another effect that appears when modelling hybrid sections, is if it is desired to model a U-shape. An example of this situation is shown in Figure 3-17.

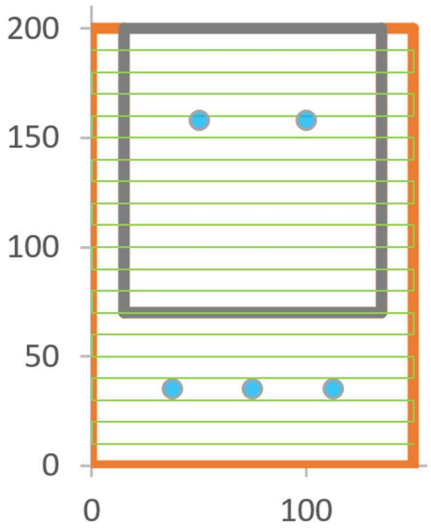

Figure 3-17: example of a U-shape in a hybrid beam; dimensions in [mm]

If the layer between 190 and 200 mm is considered in Figure 3-17, it can be seen that the layer contains two materials (concrete in grey, and SHCC in orange). This means that it is not possible to follow the same approach as was explained in subchapter 3.1.1. When the strain is known at

the centerline of this layer, the strain cannot be coupled to a stress using the stress-to-strain diagram, as there are two different materials in the same layer. This is tackled as follows. The strain at the centerline of the layer is taken. For both materials, the stress is determined that corresponds to this strain. After that, a weighted average is searched for to determine the stress that corresponds to the layer. In Figure 3-17, the width is equal to 150 mm. The webs of the U-shape each have a thickness of 15 mm, which means that the concrete has a width of 150-2*15= 120 mm. So, the webs contain 30/150*100= 20% of the layer, while the concrete contains 80%. For this example, it means that the (weighted) stress in this layer becomes equal to:

$$\sigma_{layer} = 0.2\sigma_{web} + 0.8\sigma_{concrete} \qquad \textit{Eq. (3.6)}$$

Or in general, using the MLM terms:

$$\sigma_{layer} = \frac{2t_{web}}{b}\sigma_{web} + \frac{b - 2t_{web}}{b}\sigma_{concrete} \qquad \textit{Eq. (3.7)}$$

3.2. Possibilities and limitations

Many researchers have used the multi-layer model after (Hordijk, 1991) proposed it. Examples are in the research of (Kooiman, 2000), (Grünewald, 2004), (Lappa, 2007) and (Schumacher, 2006). However, in those studies, the model was only used for monolithic specimens. In this research, the multi-layer model is further developed. Table 3-1 describes the limitations of the previously developed version of the MLM and briefly introduces the new developments of the MLM within the context of the present thesis.

	Previous MLM's	**Proposed MLM**
Simply supported beams	✓	✓
3-point bending test	✓	✓
4-point bending test	✓	✓
Monolithic beams	✓	✓
Monolithic beams + traditional reinforcement	✗	✓
Hybrid beams	✗	✓
Crack opening input	✓	✓
Effect of eigenstresses due to drying shrinkage	✗	✓

Table 3-1: comparison of MLM's; red=not implemented, orange=limited implementation, green=fully implemented

As can be seen in Table 3-1, one of the check marks is coloured orange instead of green. This means that although the property is present, it is limited. The effect of eigenstresses due to drying shrinkage is implemented in the proposed MLM, but it is only applicable for monolithic beams (which will be explained in subchapter 3.4.5.2).

One of the strengths of the multi-layer model is that parametric input is used. In this way, the thickness of an SHCC layer in a hybrid beam can for example be optimized by modelling with different input.

3.3. Input parameters

There are multiple input options in the MLM that is proposed in this thesis. The input parameters are listed in Figure 3-18.

BEAM INPUT
Δh
L
L_1
L_2
h
n
t
b
$\Delta\kappa$
n.a.

MATERIALS
E
f_1
ε_1
f_2
ε_2
f_3
ε_3
ρ

DEFLECTION
Test type
$\#_{seg}$
b_{seg}

LAYER SPECS
Top layer
Bottom layer
Web
t
E
ρ

CRACK INPUT
L_{inf}
$w_{c,2}$
f_2
ε_2
$w_{c,3(END)}$
$f_{3(END)}$
$\varepsilon_{3(END)}$

REINFORCEMENT
ϕ
c
#
y

Figure 3-18: MLM input parameters

The MLM parameters are divided into eight sections: 'beam input', 'materials', 'layer specs', 'reinforcement', 'points', 'drying shrinkage', 'crack input' and finally 'deflection'. All sections and their corresponding parameters are explained in Appendix B. In Figure 3-18, two sections and their parameters are not shown, namely the 'points' and the 'drying shrinkage' sections. The reason for this is that both sections only contain one type of input, which is not in 'symbol' format. In Appendix B, those are explained further.

The two parameters, that distinguish the MLM, are the 'number of layers' and the 'influence length'. The first parameter determines by how many 'springs' the cross-section is represented. The second parameter needs more explanation. The 'influence length' parameter was first introduced by (Hordijk, 1991) as the 'fracture zone length' (given by 'l_f'). It was mentioned before that the multi-layer model is about dividing the cross-section into layers that are represented by springs. The length over which that happens is this fracture zone length. This is visualized in Figure 3-4.

The length of this fracture zone is approximated to be equal to half the effective height of the beam (Lappa, 2007). However, this is not a fixed value, so other values can be chosen. Other researchers called this length the 'influence length' (Kooiman, 2000), as it greatly **influences** the results that follow from the MLM. The results are affected because the crack input parameters in tension are affected by the influence length (which leads to different behaviour in tension). Therefore, the results are only affected when crack input is available. In the study of (Kooiman, 2000), the influence of this parameter was illustrated. Using the input material relations that are shown in Figure 3-19, the load-to-displacement curve was determined.

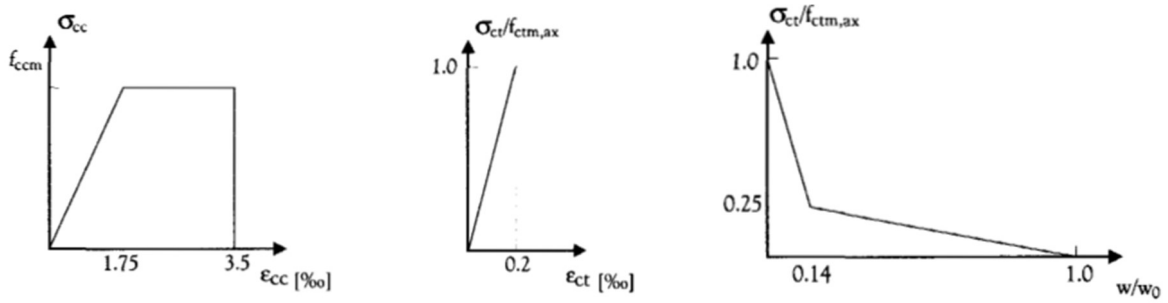

(a) assumed stress-strain diagram in compression *(b) assumed stress-strain diagram in tension* *(c) assumed tensile stress-crack opening diagram (softening)*

Figure 3-19: assumed input material relations by (Kooiman, 2000)

A plain concrete beam of 150x150x600 [mm] was considered, which lead to the load-to-displacement curves in Figure 3-20.

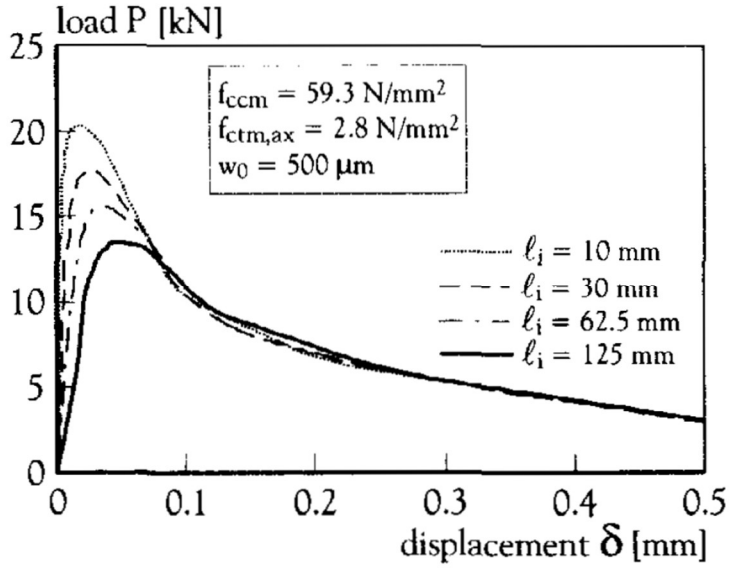

Figure 3-20: effect of the influence length for plain concrete on the force-to-displacement curve

If the material input only consists of stress-strain 'couples' in tension, which directly lead to a stress-to-strain diagram, the influence length is not used at all. When there is crack input

available for a material, the influence length is used in accordance with Eq. (3.8) to find the strain (Kooiman, 2000):

$$l_{inf} = w_{crack} * \epsilon \qquad \textit{Eq. (3.8)}$$

Here, 'l_{inf}' is the influence length [mm], 'ε' the strain [-], and w_{crack} the crack opening displacement [mm]. Rewriting Eq. (3.8) gives Eq. (3.9):

$$\epsilon = \frac{w_{crack}}{l_{inf}} \qquad \textit{Eq. (3.9)}$$

From the crack input of the considered material (which is a fixed value), the strain can be found using the influence length (which is chosen). So the influence length determines what the strain will be equal to. After the strain is calculated, a stress-to-strain diagram is achieved, as the stress that corresponds to the strain is also part of the input.

3.4. Output

In this subchapter, all available output in the proposed MLM, next to the bending moment resistance, is discussed in detail.

3.4.1. Applied force

The applied force can directly be determined using the calculated bending moment resistance (for each step). In the proposed MLM, there are two options: a 4-point bending test and a 3-point bending test. In Figure 3-21, the 4-point bending test scheme is shown with its corresponding parameters that are used in the MLM.

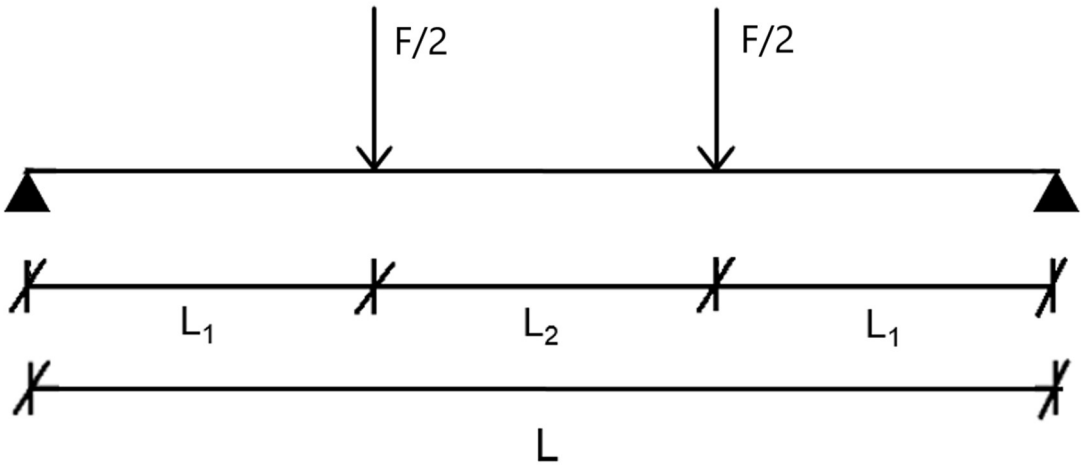

Figure 3-21: 4-point bending test scheme

The bending moment at midspan is equal to:

$$M = \frac{F}{2} L_1 \qquad \textit{Eq. (3.10)}$$

Rewriting Eq. (3.10) gives Eq. (3.11):

$$F = \frac{2M}{L_1} \qquad \textit{Eq. (3.11)}$$

For a 3-point bending test, Eq. (3.11) can also be used, as the only difference between the 3-point and the 4-point bending test is the 'L_2', which is not present for the 3-point bending test. However, that has no influence on the bending moment at midspan and its conversion to the applied force.

3.4.2. Deflection

The deflection of a beam can be predicted by the MLM. In this subchapter, it is explained how this deflection is obtained. In the previous subchapter, it was shown that the moment-to-curvature relationship was the same for 3- and 4-point bending tests. However, this is not the case for the deflection. The calculation of the deflection can be performed based on four different methods:

- Method 1: a method based on constant curvature is presented, which provides underestimated results. This method is only suitable for 4-point bending tests.
- Method 2: the deflection is calculated using the 'momentvlakstellingen' theory based on (Hartsuijker, 2001). This method is suitable for both bending tests.
- Method 3: a method based on the 'forget-me-nots'. This method is suitable for both bending tests, and provides an overestimated deflection.
- Method 4: a method based on small scale geometry. This method provides similar results to method 2. It will not be used in this MLM, as for the same input parameters, method 2 provides more accurate results. The cause for this and the theory itself are presented in Appendix D.

3.4.2.1 Method 1: constant curvature

The first method is the constant curvature method. It is only suitable for the 4-point bending test, as the 3-point bending test does not contain a constant curvature region. The bending moment diagram of a 4-point bending test is given in Figure 3-22.

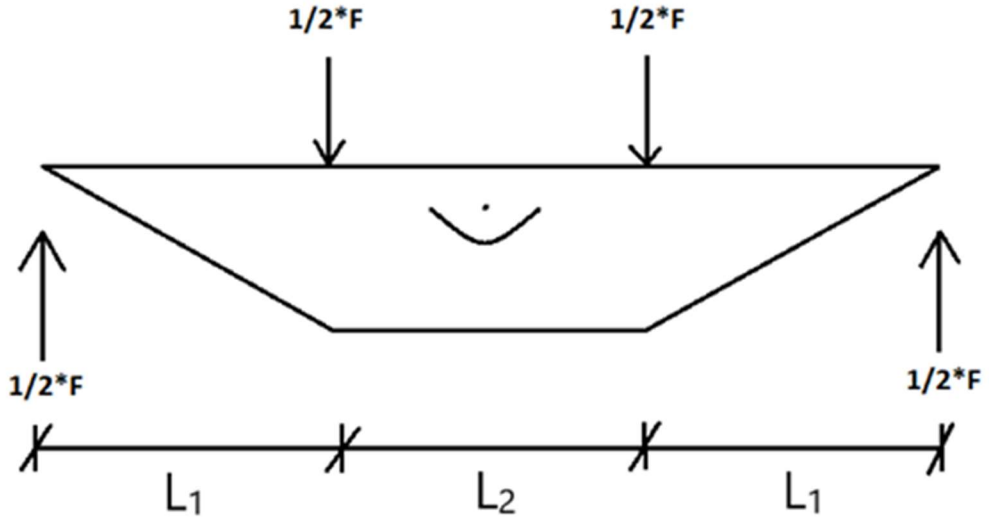

Figure 3-22: bending moment diagram of a 4-point bending test

As can be seen in Figure 3-22, the bending moment is constant in the middle region. The bending stiffness is constant for a given bending moment; so that means that if the moment is constant, the curvature 'κ' is also constant. To turn this information into an occurring deflection, the curvature is translated into a radius of curvature. That is done by the known expression in Eq. (3.12):

$$R = \frac{1}{\kappa} \qquad \textit{Eq. (3.12)}$$

Using this relationship, the geometrical situation in Figure 3-23 can be constructed:

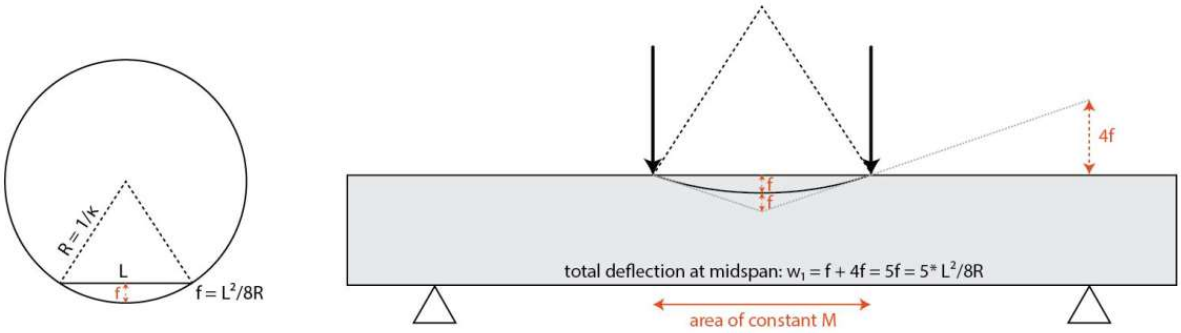

Figure 3-23: calculating the deflection at midspan using the curvature in the constant bending region (Prinsse, 2017)

Using the relationships in Figure 3-23, the deflection at midspan is equal to:

$$\boldsymbol{w_1 = \frac{5}{72}\frac{L^2}{R}} \qquad \textit{Eq. (3.13)}$$

Note that this expression is different from Figure 3-23, in which the 'L' is the length of the constant bending moment region (or the 'L_2' in Figure 3-22). That distance is equal to the total span divided by three in normal cases. To avoid any misconceptions, 'L' in this thesis is always the total span. Eq. (3.13) is however only valid for a typical 4-point bending tests, in which all three spans are equal. A generical expression for the deflection is:

$$\boldsymbol{w_1 = \frac{L_2}{2R}\left(\frac{L_2}{4} + L_1\right)} \qquad \textit{Eq. (3.14)}$$

In Eq. (3.14), the 'L_2' is the length of the constant bending moment region. The derivation of Eq. (3.14) is shown in Appendix D.

A crucial assumption in this method is that only the constant bending moment region provides the curvature that contributes to the deflection. In other words, it is assumed that there is no bending moment between the force and the support. In reality, that is not the case as the bending moment decreases linearly from the location of the application of the force to the support (see Figure 3-22). As this bending moment is not taken into consideration in this method, it means that the found deflection is lower than the real deflection; the obtained/calculated deflection based on the constant curvature is therefore **underestimated**.

3.4.2.2 Method 2: momentvlakstellingen

The 'momentvlakstellingen' theory will be applied in this subchapter. First, it is applied for the linear elastic stage. After that, the changes in the non-linear stage are explained. For both stages, the bending moment line has exactly the same shape. However, the 'reduced' moment line, which is the bending moment distribution that is scaled by the stiffness, is different. To explain the 'momentvlakstellingen' theory in short: the reduced moment line is needed to determine the rotation angels, which are given by the area under the reduced moment line. Those rotation angles are needed to calculate the deflection, as the deflection is equal to the rotation angle times its corresponding distance to the point of which the deflection is calculated. This theory is explained in detail in Appendix D.

3.4.2.2.1 Linear elastic stage

In Figure 3-22, the bending moment diagram is shown for a 4-point bending test. In order to 'reduce' this diagram into the reduced moment diagram, it has to be scaled by the stiffness 'EI'. In the linear elastic stage, the stiffness is constant for the whole beam. This leads to a reduced moment diagram that has exactly the same shape as the original bending moment diagram. This is shown in Figure 3-24.

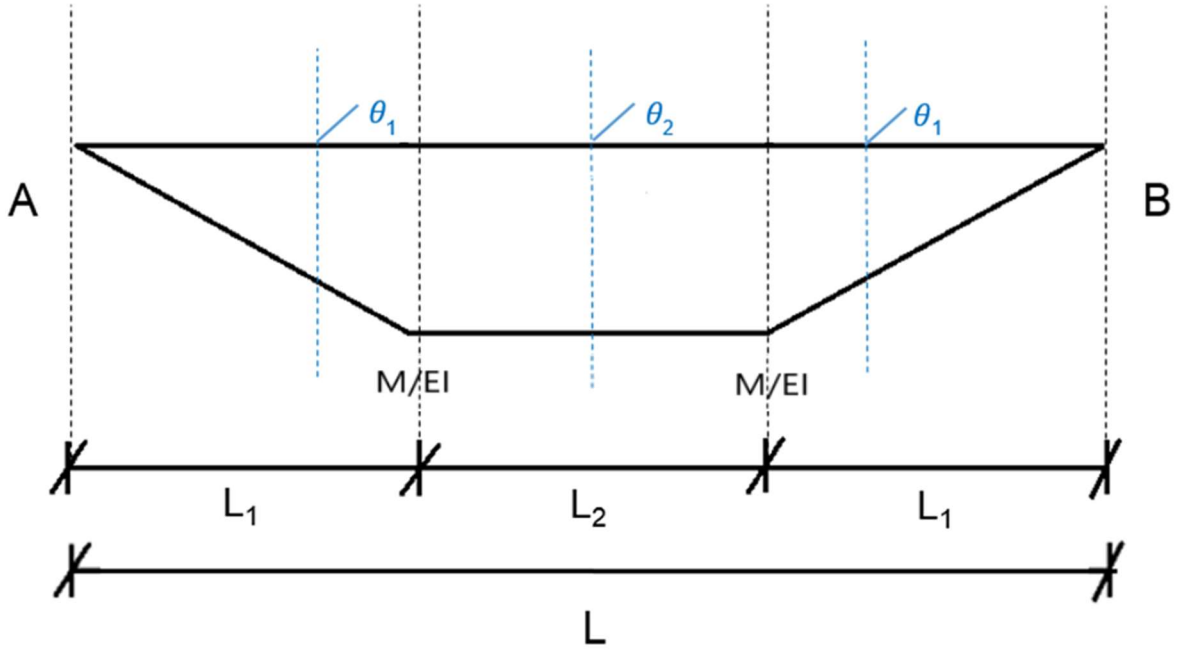

Figure 3-24: the reduced bending moment diagram for a 4-point bending test

Applying the momentvlakstellingen theory, the diagram in Figure 3-24 is split into straightforward geometrical parts. In this case, the diagram is split into two triangles and a rectangle. Those lead to the 'θ_1', 'θ_2' and 'θ_3' that are shown in Figure 3-24. As the two triangles have exactly the same area, $\theta_1 = \theta_3$. The location of each angle is at the 'projected center of gravity' of the geometrical shape. So for the triangles, it is at one-third of the width of the triangle from the highest point of the triangle; for the rectangle it is in the middle.

The deflection that is looked for when doing bending tests, is the deflection at midspan. However, finding this deflection is not straightforward. The deflection is by definition the angle times the distance to the point of deflection. However, from Figure 3-24 it is clear that if this is applied for point B (which is a support), there would be a deflection. This cannot be the case. Therefore, there has to be a rotation that mitigates this deflection. This rotation is located at point A (the first support). This is shown in Figure 3-25.

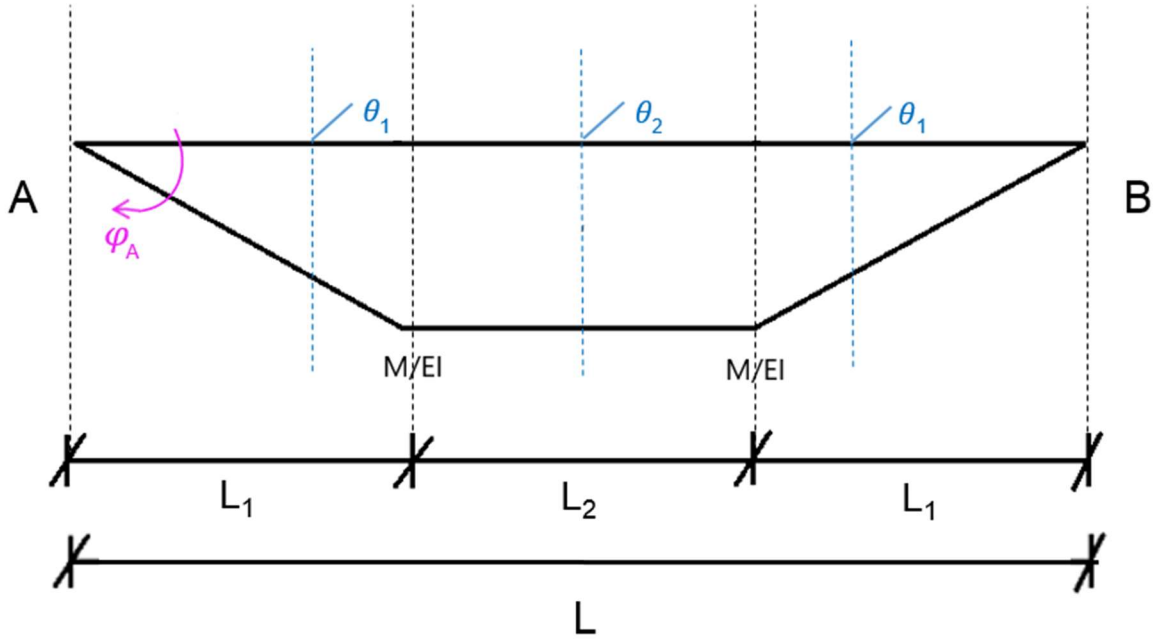

Figure 3-25: rotation φ_A at point A to compensate for the imaginary displacement at support B

The equation in this case (with respect to point B) becomes:

$$\varphi_A L = \theta_1 \left(L - \frac{2}{3} L_1 \right) + \theta_2 \frac{L}{2} + \theta_3 \frac{2}{3} L_1 \qquad \textit{Eq. (3.15)}$$

In other words, the displacement at B caused by the rotations due to the reduced bending moment line has to be compensated by a rotation at the other support.

After this is found, and after it is known that the deflection at midspan is desired, the reduced bending moment diagram can be split in half. This is shown in Figure 3-26. Note that the diagram in Figure 3-25 is in theory also suitable to calculate the deflection at midspan. However, everything that is at the right of the midspan location cannot be taken into account. So 'θ_3' has to be excluded. Not only that: the 'θ_2' also contains the area to the right of the midspan location, so it has to be altered. That is why the diagram in Figure 3-26 is introduced.

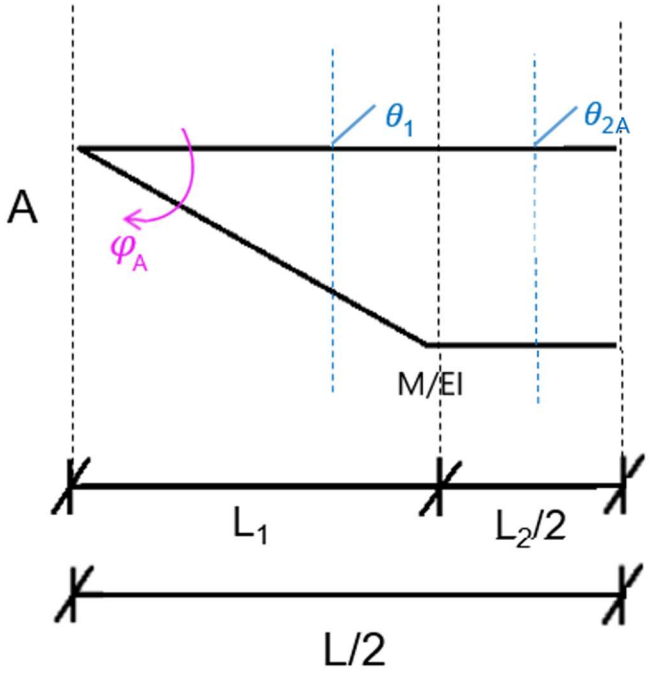

Figure 3-26: part of the reduced moment diagram that is needed for finding the deflection at midspan

As can be seen in Figure 3-26, a new angle is introduced, namely 'θ_{2A}', which is the angle along $L_2/2$. Its distance from midspan is now $\frac{1}{2} * \frac{L_2}{2} = L_2/4$. Now the deflection is equal to:

$$w_{midspan} = \varphi_A \frac{L}{2} - \theta_1 \left(\frac{L}{2} - \frac{2}{3} L_1\right) - \theta_{2A} \frac{L_2}{4} \qquad \textit{Eq. (3.16)}$$

Note the minus signs because of the different directions of the rotations.

3.4.2.2.2 Non-linear stage

After the linear elastic stage is passed, there is an important change. The scaling of the bending moment diagram becomes now very difficult, as the stiffness 'EI' is not a constant anymore. For every location of the beam, the stiffness is different. As the moment and the curvature are related by the stiffness, one way to work around this problem is to couple those two values. In this way, a reduced bending moment diagram can be found. What is done, is that the values from the bending moment diagram are coupled with the corresponding curvature values that are traced from the moment-to-curvature diagram. All found curvatures can then be put into a diagram, which is in fact the reduced bending moment diagram.

If the bending moment diagram for a 4-point bending test is taken into account again, it can be split into three regions that are shown in Figure 3-27.

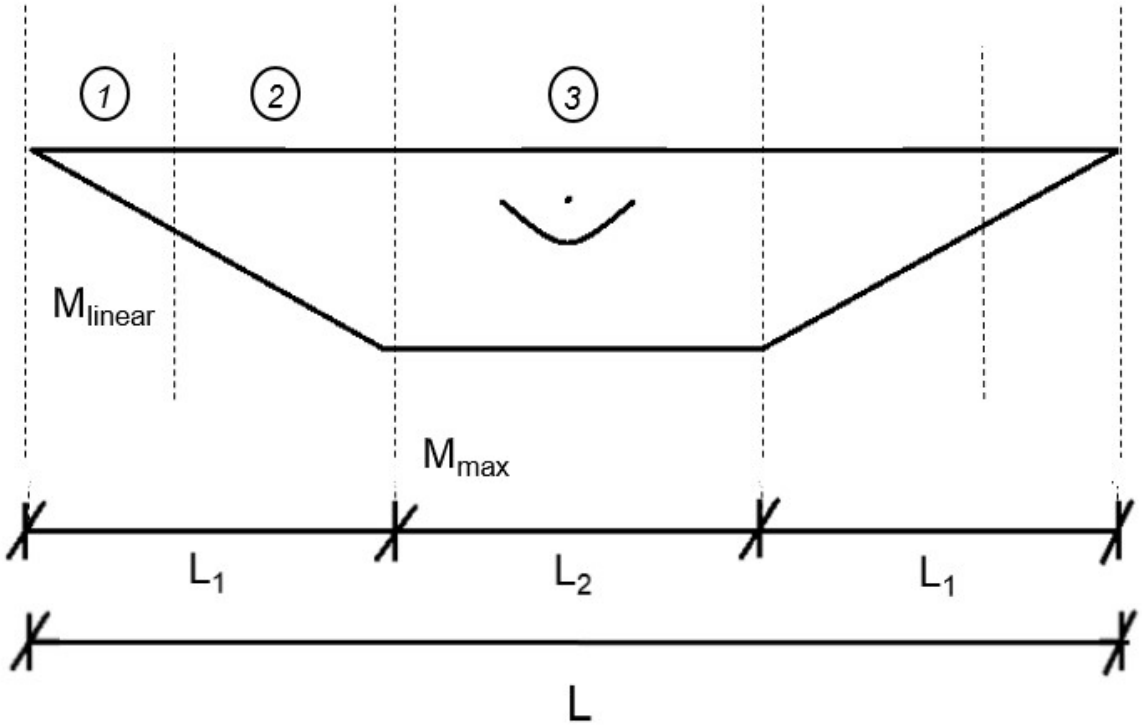

Figure 3-27: three bending moment diagram regions in the non-linear stage for a 4-point bending test

Those three regions can be explained as follows:

→ *Region 1*: linear elastic region. In this region, the undamaged material is taken into consideration. The same principle as in subchapter 3.4.2.2.1 is used, as the material is acting linearly. The geometrical figure that results in the reduced bending moment diagram is a triangle near the support.

→ *Region 2*: non-linear segments region. Between the location of the end of the undamaged material and the location of the applied force, the bending moment varies. Therefore, this region has to be split into multiple segments, that have the shape of a rectangle. The bending moment at the centerline of each segment is coupled with the corresponding curvature. For a large amount of segments, the approximation becomes accurate.

→ *Region 3*: non-linear constant region. This region contains a constant bending moment value, and therefore a constant corresponding curvature value.

This is all summarized in Figure 3-28. A sketch is shown of a possible configuration.

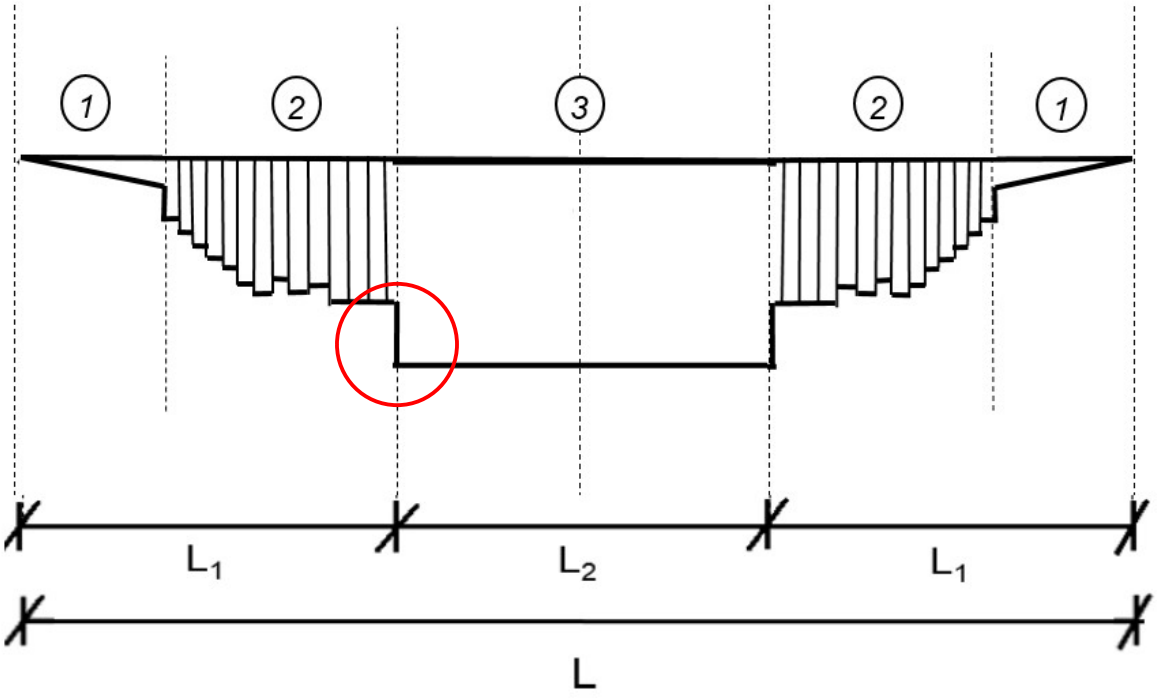

Figure 3-28: a 'jump' in the transition between regions 2 and 3 marked in red in the non-linear stage

As can be seen in Figure 3-28, region two is not a straight line between region 1 and region 3. Next to that, region 1 has a very shallow slope. Both observations can be explained. First of all, region 1 has a very shallow slope because the stiffness 'EI' of a non-damaged part is much higher than a cracked part. As region 1 is still in the linear elastic stage, the material is undamaged. And as the bending moment diagram is scaled by the stiffness, region 1 results in lower values for the reduced bending moment diagram (as it is scaled by a larger stiffness). Therefore, the slope of this region is also very shallow.

As for region 2, it was explained earlier that for every bending moment value, the corresponding curvature is coupled with it. For example, a jump can be seen near the location of the applied force. It is marked in red in Figure 3-28. This can be the case if the maximum bending moment is at the end of a horizontal plateau. This is illustrated in Figure 3-29.

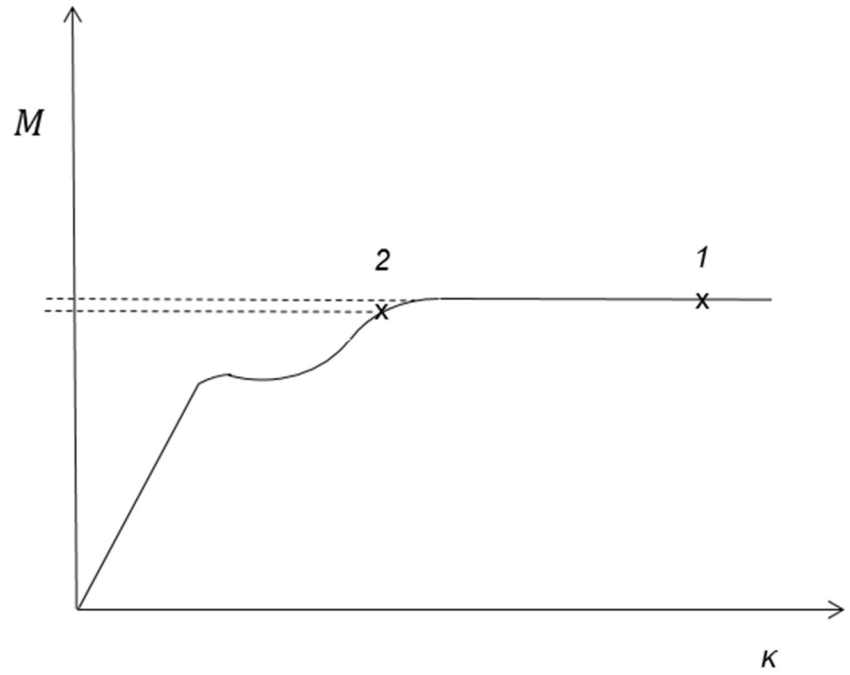

Figure 3-29: cause of a jump in the reduced bending moment diagram in the non-linear stage

As can be seen in Figure 3-29, point 1 marks the maximum bending moment. Suppose that this bending moment is the bending moment at region 3 of Figure 3-28. Point 2 marks a slightly lower bending moment value. Consider this as the bending moment directly next to region 3 (so the start of region 2). Although the bending moment values do not differ by much, the curvature that corresponds to point 2 is much lower than the curvature that corresponds to point 1. And as the curvature is shown in the reduced bending moment diagram, there will be a jump in the diagram.

This is one of the many possibilities. Not all of them can be taken into account in this research, but at least it is clear that the segments at region 2 will vary much in (curvature) value and will not be a linear interpolation between region 1 and region 3.

In order to find the deflection at midspan, all areas that are shown in Figure 3-28 have to be found and multiplied with their distance to support B in order to find the rotation at support A. After that, the reduced bending moment diagram can be split into two, and all the areas including the rotation at support A have to be multiplied with their distance to midspan.

Calculating the deflection for a 3-point bending test is done in the same way as for the 4-point bending test, apart from the geometrical differences between the two tests. The same procedure that is explained for the 4-point bending test is explained for the 3-point bending test in Appendix D.

3.4.2.3 Method 3: forget-me-nots

The third method is based on the forget-me-nots. In this subchapter, the application for both the 3-point and 4-point bending test is presented. The assumption that is of most importance in this method is that the bending stiffness ‘EI’ is equal for the whole beam. This is true in the

linear elastic stage, but not after that. The bending stiffness that is used in the expression of the displacement is found by rewriting the known expression for the bending moment:

$$M = EI\kappa \rightarrow EI = \frac{M}{\kappa} \qquad \textit{Eq. (3.17)}$$

In a moment-to-curvature diagram, that is equal to the slope at each point. This slope changes for each datapoint. In case of a material with strain hardening properties, the bending stiffness keeps decreasing after the linear elastic stage. Therefore, the bending stiffness after the linear stage, which is assumed to act over the whole beam, is lower than the real bending stiffness at each location between the location of the force and the support. This means that the deflection that is found, is higher than the real deflection, as the bending stiffness near the support is for example higher than at the constant bending moment region (in which cracks have occurred). This all is because the bending stiffness is in the nominator of the expression that calculates the deflection. As a result, this method results in a deflection that is **overestimated**.

3.4.2.3.1 4-point bending test

The mechanical scheme that corresponds to the forget-me-not of a 4-point bending test is shown in Figure 3-30.

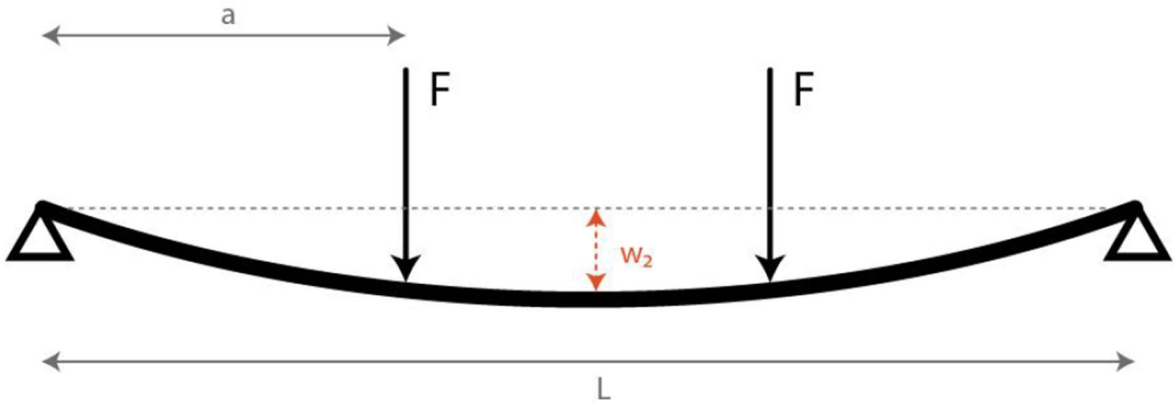

Figure 3-30: mechanical scheme for determining the deflection at midspan using the forget-me-nots (Prinsse, 2017)

The deflection that follows from the forget-me-not is equal to (Prinsse, 2017):

$$w_2 = \frac{ML^2}{24EI} * \left(3 - 4 * \frac{a^2}{L^2}\right) \qquad \textit{Eq. (3.18)}$$

In which 'M' is the maximum bending moment, 'L' the total span of the beam and 'a' the distance between the support and the applied force (equal for both sides). Using the earlier found relationship between the curvature and the moment in Eq. (3.17), the forget-me-not can be rewritten into:

$$w_2 = \frac{23}{216}\frac{L^2}{R} \qquad \textit{Eq. (3.19)}$$

Eq. (3.19) is however only valid for the typical 4-point bending tests, in which all three spans are equal. A generical expression for the deflection is:

$$w_2 = \frac{1}{2R}\left(\frac{L^2}{4} - \frac{L_1^2}{3}\right) \qquad \textit{Eq. (3.20)}$$

In which the 'L_1' is the distance between the support and the force. The derivation of Eq. (3.19) and Eq. (3.20) is shown in Appendix D.

3.4.2.3.2 3-point bending test

The forget-me-not for a 3-point bending test setup is show in Figure 3-31.

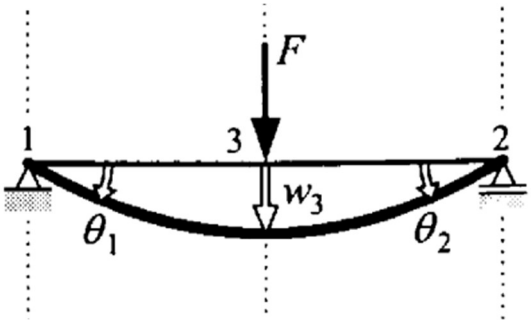

$$w_3 = \frac{1}{48}\frac{F\ell^3}{EI}$$

Figure 3-31: forget-me-not to find the midspan deflection in a 3-point bending test (Hartsuijker & Welleman, 2013)

Using the earlier found relationship between the curvature and the moment in Eq. (3.17), and using the maximum bending moment that was already shown in Eq. (3.10), the forget-me-not can be rewritten into:

$$w_3 = \frac{1}{24}\frac{L^3}{L_1 R} \qquad \textit{Eq. (3.21)}$$

As the 'L_1' parameter is always half of the total span for a 3-point bending test, Eq. (3.21) can be rewritten to:

$$w_3 = \frac{1}{12}\frac{L^2}{R} \qquad \textit{Eq. (3.22)}$$

The derivation of Eq. (3.21) is shown in Appendix D.

3.4.2.4 Comparison of methods

Ultimately, the 'momentvlakstellingen' method will be used in the MLM to calculate the deflections. As a result, this method is used in the verification of earlier experimental results in chapter 4. However, to make sure that the deflections that follow from this method are 'logical', they will be compared to the under- and the overestimated deflections that follow from the first method (constant curvature) and the third method (forget-me-nots). If the result from the 'momentvlakstellingen' method lies in between the under- and overestimated deflections, it can be concluded that the acquired deflection is logical. For the 3-point bending test, the results can only be compared to the overestimated deflection, as the first method (constant curvature) is not suitable for calculating an underestimated deflection of a 3-point bending test.

3.4.3. Crack width

The crack width at midspan of a beam can be calculated using the expressions from the Eurocode. Note that these expressions only apply for traditionally reinforced concrete beams (or in other words: non-hybrid concrete beams with steel reinforcement in the tension zone). Therefore, the method that is applied in the proposed MLM will also only be applicable for those beams.

In a traditionally reinforced concrete beam, steel reinforcement is placed in the tension zone. For a specimen that is purely loaded in tension, as is shown in Figure 3-32, the reinforcement is placed in the middle of the cross-section.

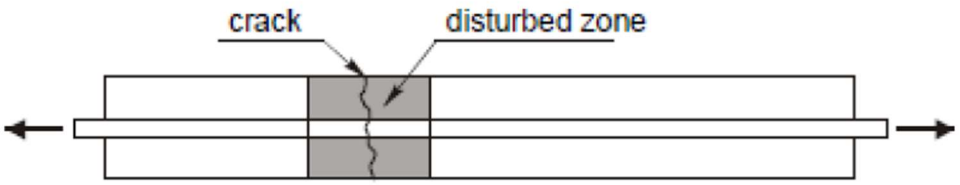

Figure 3-32: reinforced concrete bar subject to a tensile force (Luković & van der Ham, 2020)

As the tensile load increases, the connection between the steel and the concrete gets loaded heavier and heavier. At some point, it will slip. In that case, one of the materials will elongate more than the other. The difference between those two elongations is the crack width 'w', which is illustrated in Figure 3-33.

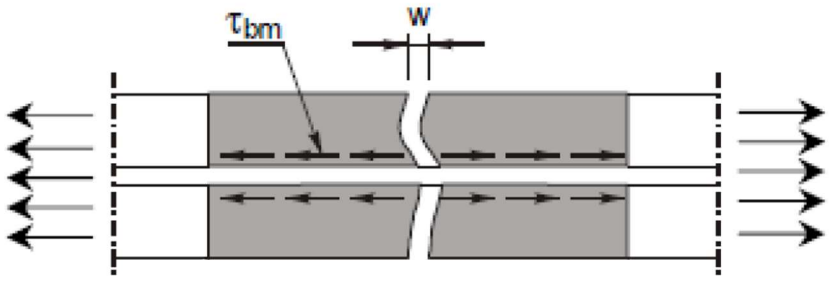

Figure 3-33: definition of crack width due to slip between concrete and steel (Luković & van der Ham, 2020)

The crack width in a traditionally reinforced concrete beam can be calculated according to the Eurocode. The expression is (NEN, 2011):

$$w_{max} = \frac{1}{2}\frac{f_{ctm}}{\tau_{bm}}\frac{\phi}{\rho_{eff}}\frac{1}{E_s}(\sigma_s - \alpha\sigma_{sr} + \beta\epsilon_{cs}E_s) \qquad \textit{Eq. (3.23)}$$

Before explaining the parameters, some parameters will be discussed that result in rewriting this expression. First, the 'τ_{bm}' parameter. If a ribbed steel reinforcement bar is chosen, this parameter is equal to '$2f_{ctm}$'. Because this parameter only contributes to the rewriting of the expression, it will not further be explained. For different types of reinforcement bars this value can be different. However, for now it is **assumed** that we are only dealing with ribbed bars. Implementing this into Eq. (3.23) results in Eq. (3.24):

$$w_{max} = \frac{1}{4}\frac{\phi}{\rho_{eff}}\frac{1}{E_s}(\sigma_s - \alpha\sigma_{sr} + \beta\epsilon_{cs}E_s) \qquad \textit{Eq. (3.24)}$$

The other two parameters that will result in a different expression are the 'α' and the 'β' parameters. Their values are given in Figure 3-34.

	crack formation stage	stabilized cracking stage
Short term loading	α = 0,5 (0,6) β = 0 $\tau_{bm} = 2{,}0\, f_{ctm}$	α = 0,5(0,6) β = 0 $\tau_{bm} = 2{,}0\, f_{ctm}$
long term or dynamic loading	α = 0,5 (0,6) β = 0 $\tau_{bm} = 1{,}6\, f_{ctm}$	α = 0,3 (0,4) β = 1 $\tau_{bm} = 2{,}0\, f_{ctm}$

Figure 3-34: values for the 'α' and 'β' parameters in the crack width equation (Luković & van der Ham, 2020)

In the MLM that is proposed in this report, only short term loading is considered (regular 3-point or 4-point bending test). Therefore, 'α' becomes equal to 0.5, and 'β' becomes equal to zero. Inserting those values in Eq. (3.24) results in Eq. (3.25):

$$w_{max} = \frac{1}{4}\frac{\phi}{\rho_{eff}}\frac{1}{E_s}(\sigma_s - 0.5\sigma_{sr}) \qquad \textit{Eq. (3.25)}$$

The parameters in Eq. (3.25) are explained in Appendix G.

3.4.4. Crack opening displacement

In Figure 3-36, the crack opening displacement is illustrated. In this figure, a beam that is deflecting is shown, with the 'crack' occurring in the tension zone at midspan. As the beam deflects more, the crack opening displacement 'w' becomes larger.

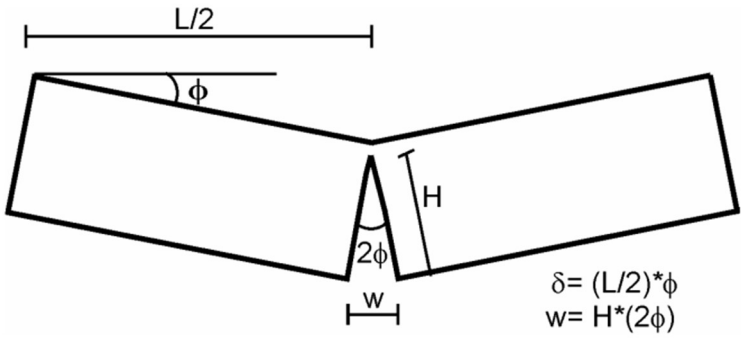

Figure 3-35: definition of crack opening displacement 'w' (Lappa, 2007)

Eq. (3.8) is ultimately used for finding the crack opening displacement. Rewriting this equation gives Eq. (3.26):

$$w_{crack} = \frac{l_{inf}}{\epsilon} \qquad \textit{Eq. (3.26)}$$

The influence length 'l_{inf}' is used as input, while the strain can be found from the output at each step. The way the strain is found is shown in Figure 3-36. It is an arbitrary strain diagram over the height of the cross-section.

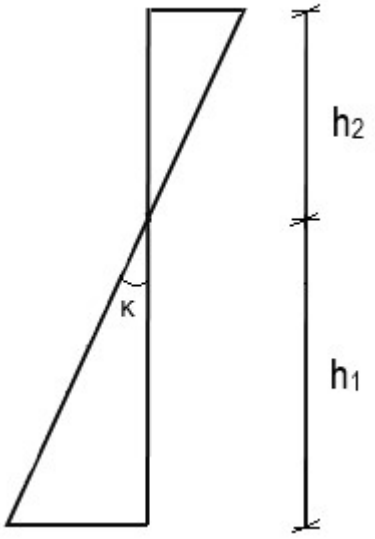

Figure 3-36: strain diagram for finding the strain at the bottom of the cross-section

The two parameters that are needed here are the curvature 'κ' and the height from the bottom to the neutral axis 'h_1'. As the neutral axis position that is calculated in the MLM is calculated from the bottom, h_1 is equal to the neutral axis position that is already calculated in the MLM for each step/datapoint. What now rests is finding the strain at the bottom; this is strain is found by multiplying the curvature with the neutral axis position. Or in the MLM terms:

$$\epsilon_{bot} = \kappa * n.a. \qquad \textit{Eq. (3.27)}$$

With this, the crack opening displacement for each step/datapoint becomes equal to:

$$w_{crack} = \frac{l_{inf}}{\kappa * n.a.} \qquad \textit{Eq. (3.28)}$$

It is assumed that this calculation method holds for all types of cross-sections as long as there is no reinforcement involved that has effect on limiting the crack opening displacement, such as steel reinforcement in a concrete beam. At the same time, it is assumed that it holds for hybrid sections without any additional reinforcement (SHCC + concrete without steel reinforcement for example).

3.4.5. Drying shrinkage

In this subchapter, more information on the drying shrinkage process is presented in the form of calculations. First, the previous research is shown on which the proposed MLM relies in terms of implementation of the drying shrinkage. After that, it is shown how the results of previous research are implemented in the MLM. Last but not least, the effects of a hybrid section on all presented information is investigated.

3.4.5.1 Background information

As was explained before, the drying shrinkage process occurs when a specimen is exposed to an environment that contains less water than the specimen itself. This process introduces compressive and tensile stresses. However, these compressive and tensile stresses only occur if there is any form of restraint. If the specimen is unrestrained, no problems occurs. The restraint that occurs in the specimen, which will result in the drying shrinkage stresses, is the difference in the moisture gradient. As is mentioned in (van Breugel, 2011), the drying shrinkage of a (thick) specimen is not uniform. There is more drying at the surface. Following the earlier described process of water loss in the small capillary pores, the stresses are initiated. An example of the moisture gradient is shown in Figure 3-37, in which a cube of 150 mm is modelled using a finite-element program called FEMMASSE. The result after 28 days of drying is shown. The legend of Figure 3-37 shows the relative humidity of the specimen; a relative humidity of one (red colour) means that the specimen is saturated.

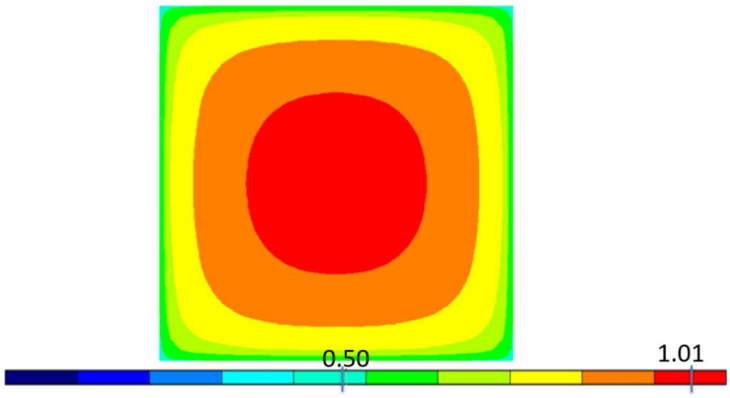

Figure 3-37: relative humidity profile for a cube of 150 mm after 28 days of drying;1=red=saturated (Awasthy, 2019)

While tensile stresses act at outer parts of the specimen, compression stresses occur inside the concrete. This is due to the need of horizontal equilibrium of the so called 'eigenstresses'.

In the research of (Awasthy, 2019), an attempt was made to model those stresses that occur after curing of the specimen. This was done by using a method from (van Breugel, 2011), which originally was meant to deal with temperature loads. But like temperature loads, drying shrinkage is also a form of an imposed deformation. Therefore, the method could also be used for drying shrinkage. The method is shown in Figure 3-38.

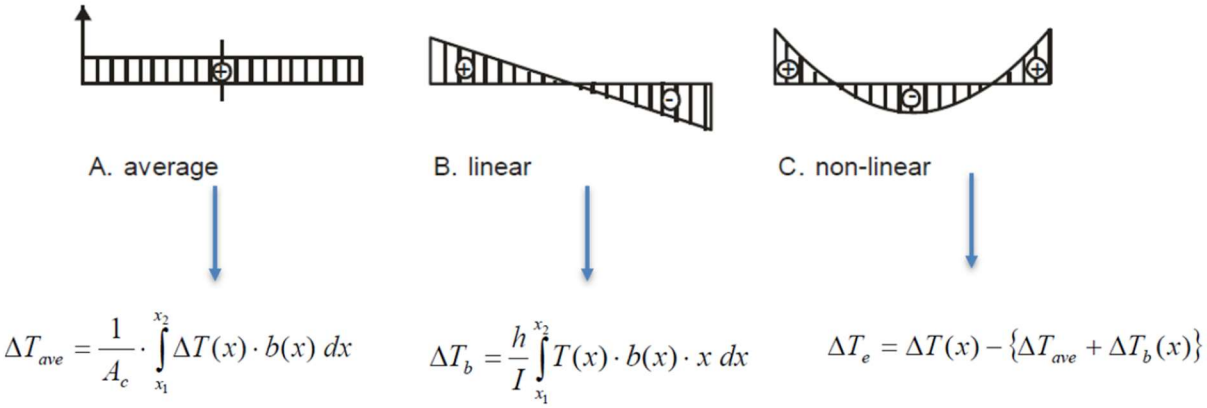

Figure 3-38: subdividing each shrinkage profile into three sub-profiles and the corresponding calculation: average, linear and non-linear (Awasthy, 2019)

The goal is to find the 'non-linear' component that is shown in Figure 3-38, that represents the eigen-strains that occur in the cross-section and are used to find the eigen stresses (which should lead to equilibrium). Those are the stresses that occur due to the drying shrinkage, and are used in the calculation of the MLM.

For the relative humidities that are shown in Appendix E, which are all symmetric with respect to the middle of the cross-section, the 'linear' component in Figure 3-38 is equal to zero. Proof of that is shown in Appendix E. The 'eigen-strains' therefore become (using the same notation as in Figure 3-38):

$$\Delta T_e = \Delta T(x) - \Delta T_{ave} \qquad \textit{Eq. (3.29)}$$

However, this results in compression stresses at the surface, and tensional stresses in the core. As it is known that exactly the opposite is the case, Eq. (3.29) is rewritten to:

$$\Delta T_e = \Delta T_{ave} - \Delta T(x) \qquad \textit{Eq. (3.30)}$$

The 'ΔT_{ave}' is the average humidity along the height. In Appendix E, it is shown for a drying period of 28 days how this is formally calculated. Therefore, the drying strain at each location along the height is equal to the average humidity minus the actual occurring humidity at the same location. In the MLM that is proposed in this thesis, the strains will be used in the calculation, and not the stresses directly. The strains will be considered as 'initial strains', that are present in the layers of the MLM before an external load is applied to the beam.

Performing the calculations as was proposed by (Awasthy, 2019) leads to the results in Figure 3-39 for different drying periods. The drying periods are after 28 days of curing in controlled conditions.

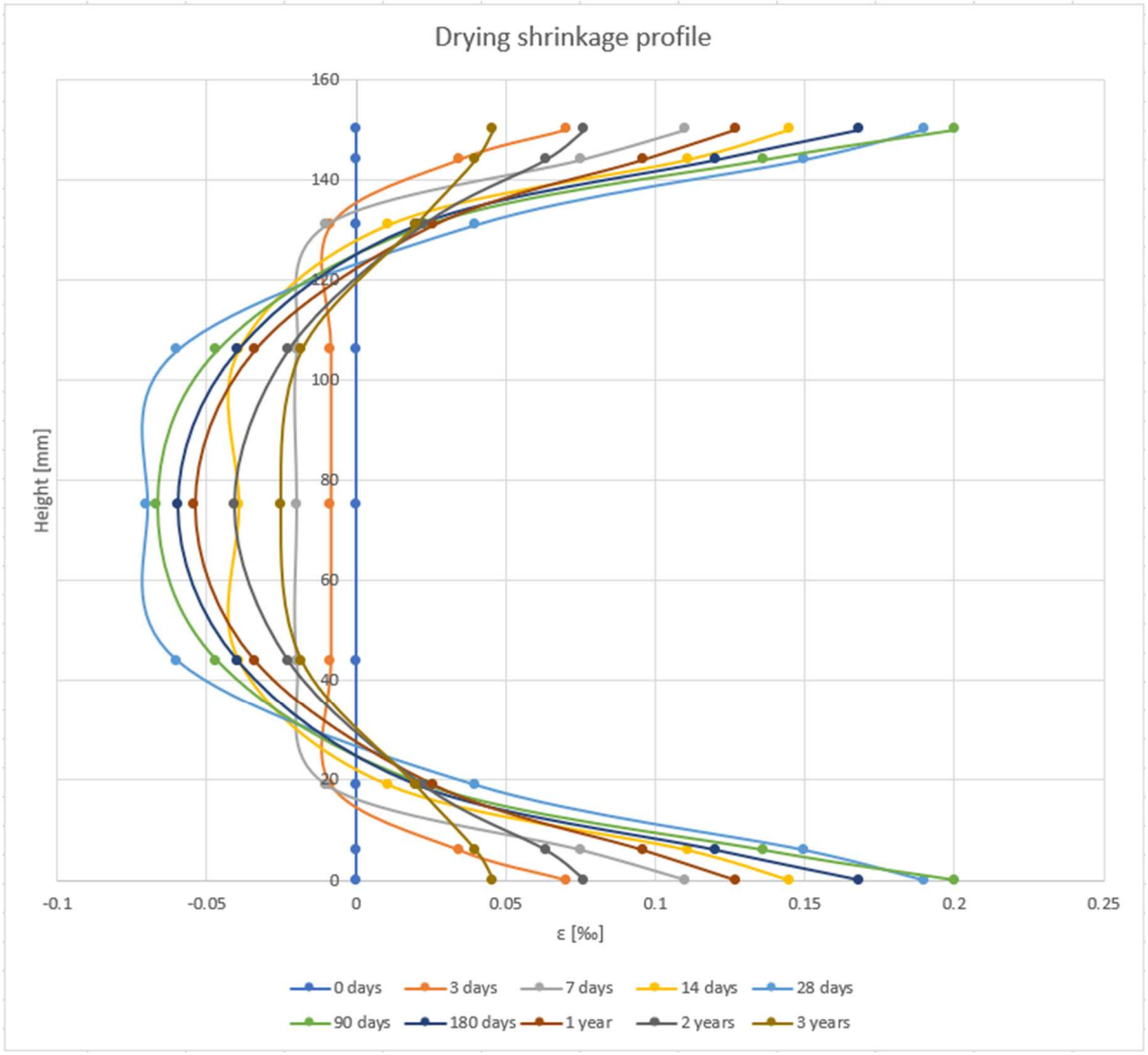

Figure 3-39: profile of eigen-strains due to drying shrinkage for different drying periods

The data that is shown in Figure 3-39 is related to a specimen of 150 mm height. As the relative humidity profile depends on the specimen size (Awasthy, 2019), this data can only be used for this size. So if a calculation needs to be performed of a different specimen size, external input is needed of the relative humidity profile (for different drying periods). Another option is to use the eigen-strains directly as input.

The drying shrinkage strains that follow from Figure 3-39 are implemented in the MLM as follows. First, the strain at the centerline of each layer of the MLM is calculated. This is done by **assuming** a linear relation between the known datapoints in Figure 3-39. For example, at 90 days of drying, it is shown in Figure 3-40 what this results in.

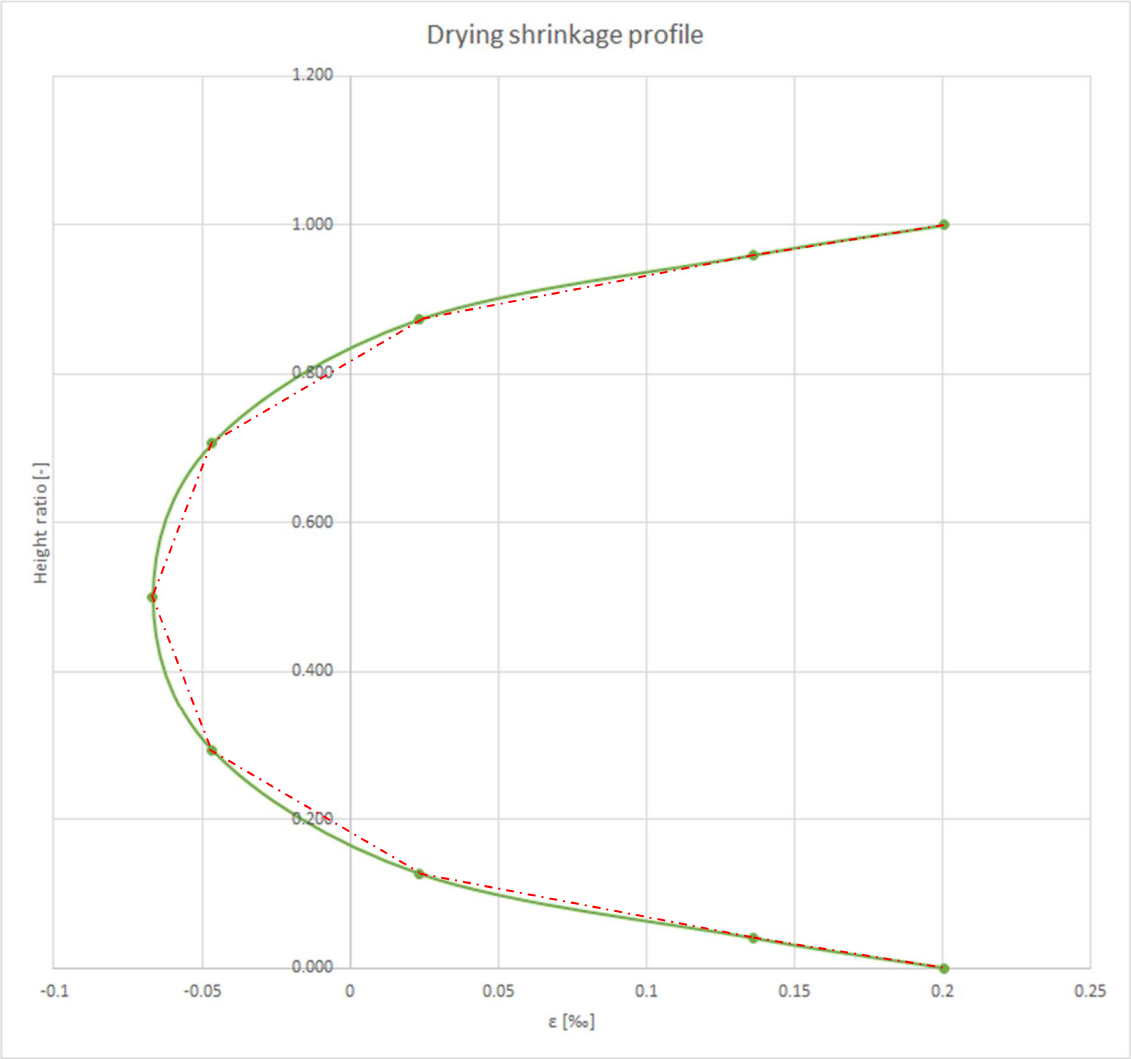

Figure 3-40: interpolation between known datapoints of drying shrinkage eigen-strains for 90 days of drying

Although the results are not precise, they are acceptable. At the surface, the results are accurate, but the more the core is approached, the less accurate the results become. One could argue that a parabola is an obvious better option, but as can be seen in Figure 3-39, many of the drying shrinkage profiles can certainly not be modelled accurately using a parabola.

The strains that are found at each layer are considered the 'initial strains', that are present before the 3-point or 4-point bending test is performed. The first effect on the calculation is that the linear elastic stage will be reached earlier than if there was no drying shrinkage. As there is already a tensional stress at both surfaces (and thus also at the tension zone of the beam), the tension that is needed to reach the end of the linear elastic stage is lower. In other words, a lower load in the bending test will be needed to reach the end of the linear stage. The initial strains are visualized in Figure 3-41. The strain diagram at the left is the strain diagram due to loading; the strain diagram at the right is a hypothetical strain diagram due to drying shrinkage. The strain diagram due to drying shrinkage is always present, and the strains due to loading are added to those strains.

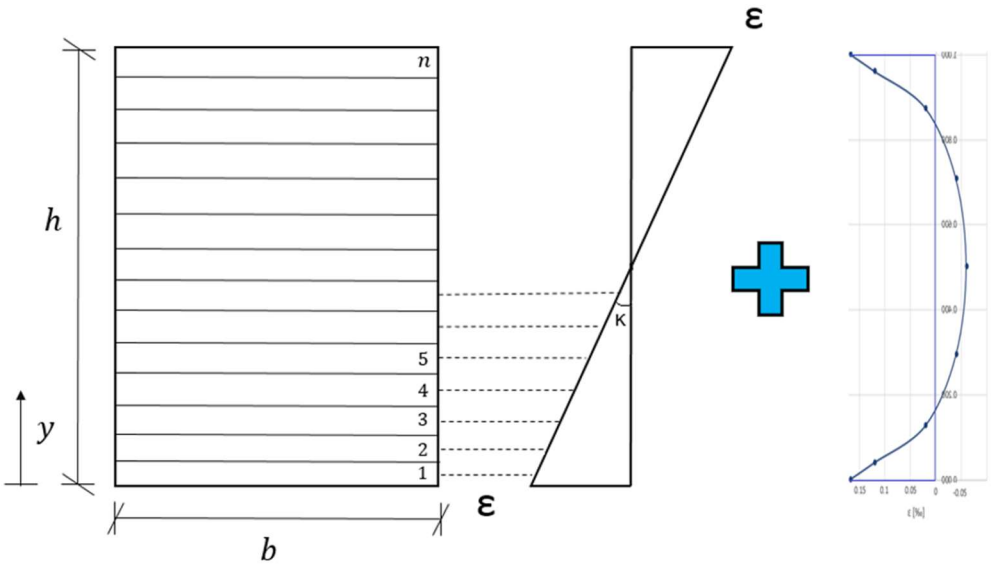

Figure 3-41: superposition of strain due to loading and initial strains due to drying shrinkage

After the end of the linear elastic stage is found, the same process as was described before is followed. The curvature increases with a little step, the neutral axis position that results in horizontal equilibrium is searched for, and finally the bending moment resistance is found. Repeating that until failure leads to the desired output.

The second effect that appears due to the drying shrinkage, is a decrease of (general) resistance; for the same curvature/displacement, generally a lower force is needed. The most extreme situation is illustrated: for plain concrete, the maximum resistance is reached at the end of the linear elastic stage; after that, the concrete cracks and the resistance decreases. If the tensile strength of a concrete specimen would be 3 N/mm^2 with a Young's modulus of 30 GPa, the end of the linear elastic stage would be at 0.1‰ if Eq. (3.3) is used. In bending, the maximum tensile stress is reached at the bottom. At this position (for a specimen of 150 mm height), using Figure 3-40 for example, the tensile strain due to drying shrinkage is equal to 0.2‰. This means that the linear elastic stage is already exceeded without external loading, which means that the resistance of plain concrete would be negligible compared to if there was no drying.

Another example is shown to illustrate the effect of drying shrinkage. An SHCC cross-section of 150x150 mm is considered. Two beams are simulated, with one beam exposed to 28 days of drying, and the other not (so no drying). A 4-point bending test is used with equal spans of 500 mm; so the total span is equal to 1500 mm. In Figure 3-42, the modelled results are shown. The input that is used for this specimen for 28 days of drying is shown in Appendix E.

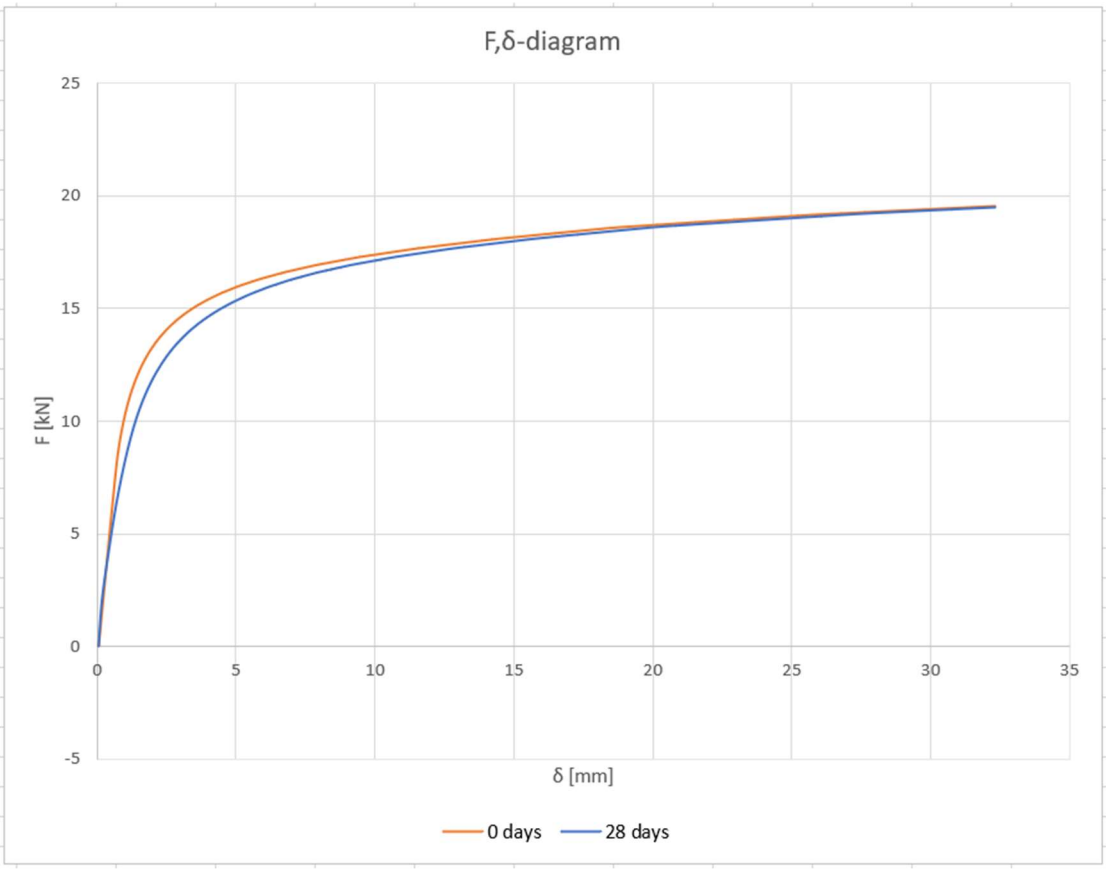

Figure 3-42: no drying vs. 28 days of drying after 28 days of curing; effects on the force-to-displacement curve

As can be seen, the force that is required for the same displacement is higher if there is no drying (so there is more resistance). For example, when a force of 13.5 kN is applied, the deflection is equal to 2.09 mm for the beam that was not exposed to drying. The other beam deflects 2.90 mm. That is an increase of 38.8% in this example. The maximum force that can be applied on the beam also decreases if there is drying. However, it is around 2.4‰ in this example, which is negligible. However, this depends on the experimental setup.

The described method in this subchapter is suitable for beams consisting of a single material. Eigen-strains can directly be used as input, or the relative humidity profile can be used to calculate the eigen-strains.

3.4.5.2 Applicability for hybrid beams

When a hybrid beam is considered, a material with strain hardening properties is used in the tension zone. The behaviour that was shown in Figure 2-3 is of importance to explain the applicability of the drying shrinkage calculation for such beams. In this subchapter, SHCC is considered as the material that is applied in the tension zone, in accordance with the proposed system in chapter 2.

Normally, the SHCC layer will be casted before the concrete layer. As was shown in Figure 1-6, SHCC can shrink up to approximately 2500 μm/m, which is equal to 2.5‰. In order to illustrate what happens, the worst-case scenario is assumed in which the SHCC shrinks, while the concrete is not. This is illustrated in Figure 3-43. The SHCC layer is shown in orange, while the concrete layer is shown in grey.

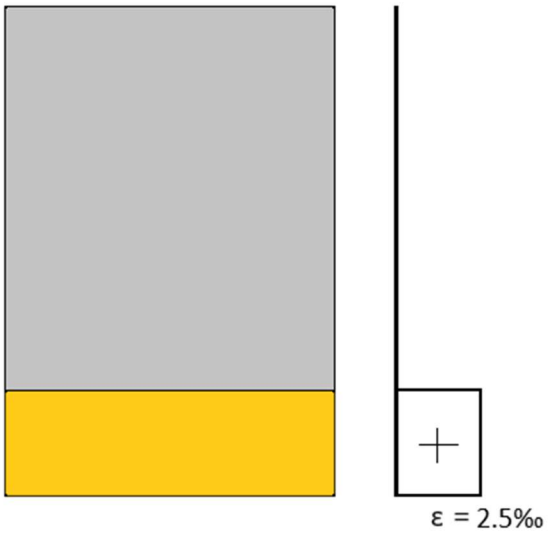

Figure 3-43: hypothetical situation in which only the SHCC shrinks due to drying

As can be seen in Figure 2-3, the resistance of SHCC in tension keeps increasing until approximately 5% = 50‰ (for this particular example). The 2.5‰ that is added due to drying shrinkage will not affect the SHCC by much. In fact, due to the increasing resistance in tension, the drying shrinkage will cause an increase in resistance (as long as the 50‰ strain is not governing for failure, and as long as a perfect bond is assumed). Therefore, the effect on the bending resistance will not be noticeable, which makes the calculation method **not** suitable for hybrid beams. However, the challenge of drying shrinkage in this case is to transfer the force that occurs due to the drying shrinkage from the SHCC to the concrete. This could have a big effect on the interface between the two materials. The force due to drying shrinkage could be such that it influences the resistance of the beam because the interface cannot (fully) transfer this force. But, in the proposed MLM, a perfect bond between the two materials is assumed (in all cases), which means that this effect is not considered/modelled.

3.4.6. Flexural stress

As the MLM that is proposed in this report only considers tension at the bottom of the beam, the flexural stress that will be searched for will automatically also be the stress at the bottom of the beam. The method that will be presented in this subchapter will sound counter-intuitive, and it will be explained why that is the case and why it does not form a problem.

The calculation of the flexural stress will purely be a linear elastic calculation. In case a fully symmetric beam is considered, Eq. (3.1) can be used for finding the flexural stress. However, this is not a general expression as it is only applicable for fully symmetric beams. The general expression is:

$$\sigma = \frac{Mz}{I} \qquad \textit{Eq. (3.31)}$$

Here, 'M' is the occurring bending moment, 'z' is the distance from the neutral axis to the bottom fibre and 'I' is the known '$\frac{1}{12}bh^3$' value.

As was mentioned before, the calculation will be purely linear elastic. This means that the position of the neutral axis is fixed. Because as was shown before, the neutral axis moves upwards in the non-linear stage. This is the first part that feels counter-intuitive, as it is **assumed** that the position of the neutral axis is fixed, while in reality this is not the case.

The same issue occurs when calculating the second moment of area 'I'. The general expression is '$\frac{1}{12}bh^3 + d^2A$', in which 'd' is the distance from the center of mass the cross section to the neutral axis. In the linear elastic stage, this distance is equal to zero, which is why the '$\frac{1}{12}bh^3$' is directly used. However, in the non-linear stage, the neutral axis position will move, which means that there will be a contribution from the 'd^2A' part. However, it is **assumed** that the neutral axis position is fixed, as was mentioned before. Therefore, only the '$\frac{1}{12}bh^3$' is used.

The reason that a purely linear elastic calculation is used, is to be able to compare with other regular tests. Traditionally, the non-linear stage is not considered when testing concrete specimens, as they show no strain hardening behaviour. The strain hardening behaviour of cementitious materials is a rather new development. Therefore, to be able to compare with traditional tests, the same calculation model needs to be followed.

3.4.7. Longitudinal shear

The main **assumption** related to the longitudinal shear in the proposed MLM is that a perfect bond exists between the two materials of the hybrid section. This is not the case for the bond between the steel reinforcement and the concrete, as was explained in subchapter 3.4.3. Therefore, slip can occur between steel reinforcement and the concrete, which translates back to a crack width. So, a calculation of the longitudinal shear can only be made if a hybrid section is investigated. Therefore, this subchapter is only applicable for hybrid sections.

It is found that the longitudinal shear stress is equal to the vertical shear stress. In other words, the expressions for the vertical shear stress can be used to find the shear stress at the interface between the two materials; the longitudinal shear stress is then equal to it. Proof of that is shown in Appendix H.

The vertical shear stress (which is equal to the longitudinal shear stress) is calculated using Eq. (3.32). This shear stress is given in [N/mm^2]. To translate it to a force per unit length (of the beam), it can be multiplied with the length of the interface, which is the width of the beam.

$$\tau = \frac{VS}{bI} \qquad \textit{Eq. (3.32)}$$

In which 'V' is the shear force. As can be seen in Figure 3-44, the maximum shear force for a 4-point bending test is between the support and the location of the force. It is equal to half of the applied force.

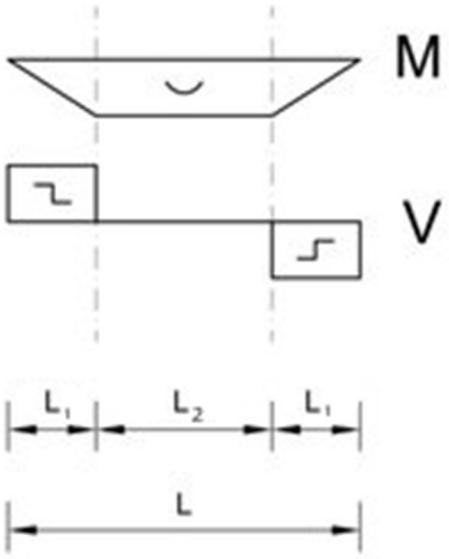

Figure 3-44: shear force diagram for a 4-point bending test (Huijben, van Herweijnen, & Nijsse, 2010)

For a 3-point bending test, the maximum shear force is the same as for the 4-point bending test. The only difference is that there is no constant bending moment region in which the shear force is equal to zero. So in the proposed MLM, the maximum shear force can always be taken as half of the applied force.

The parameter 'b' is the width of the interface. In a hybrid section, it is equal to the width of the beam itself. An example of this is shown in Figure 3-45.

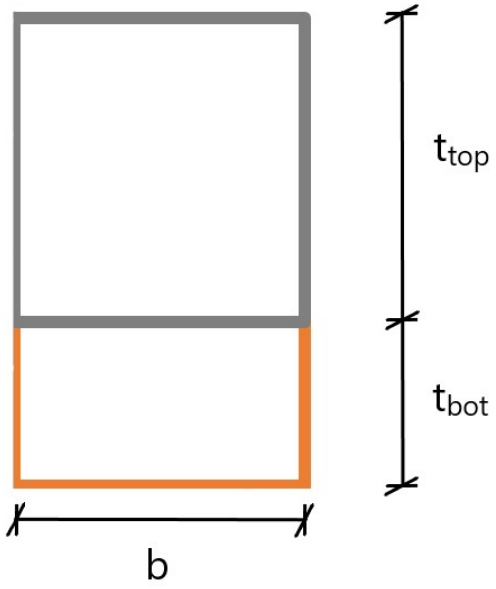

Figure 3-45: example of the cross-section of a hybrid beam

The 'I' parameter is again the known '$\frac{1}{12}bh^3$' value. The last parameter that needs some explanation is the 'S' parameter, which represents the first moment of area [mm^3]. It is calculated with respect to the interface, as that is the location of interest. As a cut is made at the interface, the beam is divided into two sections: the concrete (top layer) and the other material (bottom layer). One of the areas needs to be chosen to determine the first moment of area of it. It does not matter which area is chosen. In the MLM that is proposed in this thesis, the bottom area is taken. That is indicated in Figure 3-46.

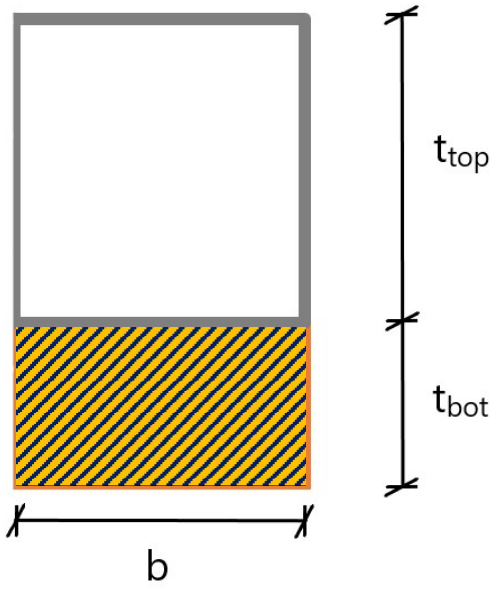

Figure 3-46: determining the first moment of area of the bottom area in a hybrid beam with respect to the n.a.

Determining the first moment of area goes as follows: first, the area of the bottom layer in Figure 3-46 is calculated. It is equal to 'b*t_{bot}'. After that, this area is multiplied with the distance from the center of the area to the location of the neutral axis. This is shown in Figure 3-47.

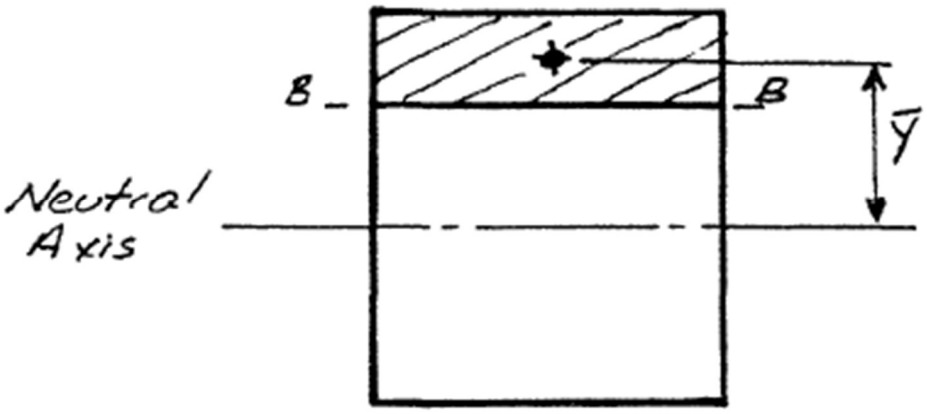

Figure 3-47: distance from the center of the area that is cut to the neutral axis position (Learneasy, 2020)

In this case, this distance is, using the MLM parameters, equal to 'n.a. - $t_{bot}/2$'. As a result, a first moment of area of 'b*t_{bot}*(n.a. – $t_{bot}/2$)' is found. Gathering all information that is found, the shear stress becomes equal to (again using the same parameters as in the MLM):

$$\tau = \frac{6F * t_{bot}\left(n.a. - \frac{t_{bot}}{2}\right)}{bh^3} \qquad \textit{Eq. (3.33)}$$

Note that the neutral axis position is **not** the initial neutral axis position, but the position at each iteration.

This calculation is however not suitable if U-shapes are used in the MLM as the interface between the SHCC (for example) and the concrete is much larger and much different. The shear stress is not only calculated for a certain position over the width, but also along the height. This can in the future be implemented in the MLM.

4. Verification of multi-layer model

In order to use the multi-layer model for further research, it first has to be verified. That will be done in this chapter. Two verifications 'groups' are considered. One group has the effect of drying shrinkage included, while the other group has not.

The verification of the group that does not contain the drying shrinkage effect is done in four phases. The phases are related to the complexness of the verification. In the first phase, two previous studies will be used for comparison, in which a beam consisting of a single material is considered. In the first research, a previous version of the multi-layer model was used by (Lappa, 2007). The advantage is that there are both experimental and modelled results to compare with. The other study only contains experimental results. In the second phase, a comparable approach will be used. Again, both experimental and modelled results are available. Next to that, an addition will be in place in the form of steel reinforcement. So although again a single material beam is considered, it now also contains reinforcement. In the third phase, a research with hybrid (concrete + SHCC + reinforcement) experiments will be used for verification. The added difficulty in this phase will be the addition of a material to the model and the verification. Here, also modelled results are available. In the last phase, the added difficulty will be the addition of the webs of U-shape to the reinforced hybrid beam. As this type of experiment has never been performed before, only the modelled results using the MLM will be presented. The same experimental setup as in the third phase, apart from the webs of the U-shape, will be used. These results can be verified in the future by experiments.

The other group, that contains the drying shrinkage effect, is verified by comparing results from (Awasthy, 2019), in which the effect of drying periods on the flexural strength of NSC (**N**ormal **S**trength **C**oncrete) and HSC (**H**igh **S**trength **C**oncrete) was investigated. Next to that, a verification from the research of (Awasthy, 2019) is shown.

4.1. Phase 1: non-hybrid section

4.1.1. HSFRC

Firstly, the multi-layer model will be compared with previous research (Lappa, 2007). One of the materials that was investigated in this research, is HSFRC, which stands for **H**igh **S**trength **F**ibre **R**einforced **C**oncrete. This material also shows strain hardening behaviour. Multiple sorts of experiments were performed using this material. The type that is of importance in this thesis, is the unnotched 4-point bending test on a beam of the following dimensions: 1000x125x125 [mm]. The span was equal to 750 mm. For this beam, experimental results were provided that were compared with modelled results (also by the multi-layer model).

In order to model this beam, the input parameters as in Table 4-1 were used by (Lappa, 2007). Exactly the same input is used for the verification by the proposed MLM.

General model parameters	
Number of layers	500
Influence length, 0.5*hlig [mm]	52.5
Compression	
Bi-linear compressive relation	
Compressive strength [MPa]	120
Linear elastic strain limit [promille]	3
E-Modulus [GPa]	40
Ultimate limit strain [promille]	8
Tension	
Strain hardening and linear descending branch	
Linear elastic tensile strength [MPa]	8.5
Linear elastic tensile strain [promille]	0.2
Hardening strength [MPa]	9
Hardening strain [promille]	8
Ultimate crack width [mm] = L_f /4	3.25

Table 4-1: assumed HSFRC input parameters that was used in the Lappa MLM (Lappa, 2007)

Note however that the influence length that was used in Table 4-1 was for a notched beam. For the unnotched beam, half the height is 0.5*125= 62.5 mm; so that influence length will be used in the verification. The compressive input parameters that are listed in Table 4-1 are visualized in Figure 4-1.

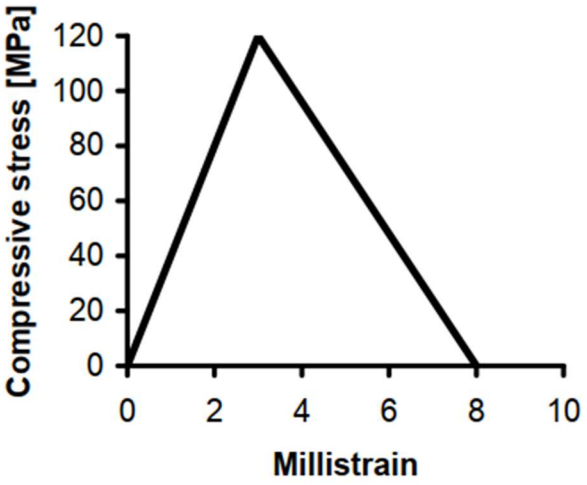

Figure 4-1: compressive stress-to-strain relation for HSFRC that was used in the Lappa MLM (Lappa, 2007)

The tension input parameters are shown in Figure 4-2. The orange line is the line that considers a critical crack width of 3.25 mm. This line is drawn in the original figure from (Lappa, 2007). As was explained before, and as can be seen in Eq. (3.8), the strain is calculated as the crack opening displacement divided by the influence length.

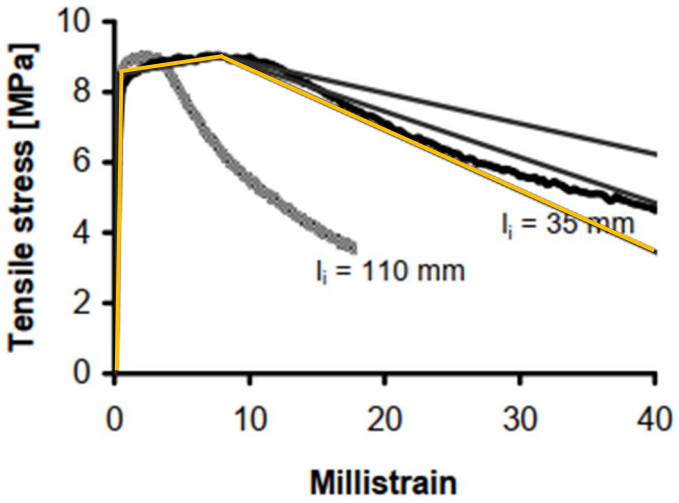

Figure 4-2: modified tensile input for HSFRC that was used in the Lappa MLM (Lappa, 2007); edited

Using all the input in the MLM, it results in the input parameters shown in Figure 4-3.

BEAM INPUT		
Δh	0.05	mm
L	750	mm
L_1	250	mm
L_2	250	mm
h	125	mm
n	500	[-]
t	0.25	mm
b	125	mm
$\Delta\kappa$	1E-5	mm^{-1}
n.a.	62.5	mm

MATERIALS		
E	40,000	N/mm^2
ρ	2390.9	Kg/m^3
Tension:		
f_1	8.5	N/mm^2
ε_1	2.13E-4	[-]
f_2	9	N/mm^2
ε_2	8E-3	[-]
Compression:		
f_1	120	N/mm^2
ε_1	3E-3	[-]
f_2	0	N/mm^2
ε_2	8E-3	[-]

LAYER SPECS		
Top layer	×	
Bottom layer	✓	
Web	×	
t	125	mm

DEFLECTION		
Test type	4-point	
$\#_{seg}$	500	[-]
b_{seg}	< 0.5	mm

POINTS
90

CRACK INPUT		
L_{inf}	62.5	mm
$w_{c,2}$	-	
f_2	-	
ε_2	-	
$w_{c,3(END)}$	3.25	mm
$f_{3(END)}$	0	N/mm^2
$\varepsilon_{3(END)}$	0.06	[-]

Figure 4-3: input parameters used in the MLM to verify the results from (Lappa, 2007)

This results in the stress-to-strain diagram in Figure 4-4:

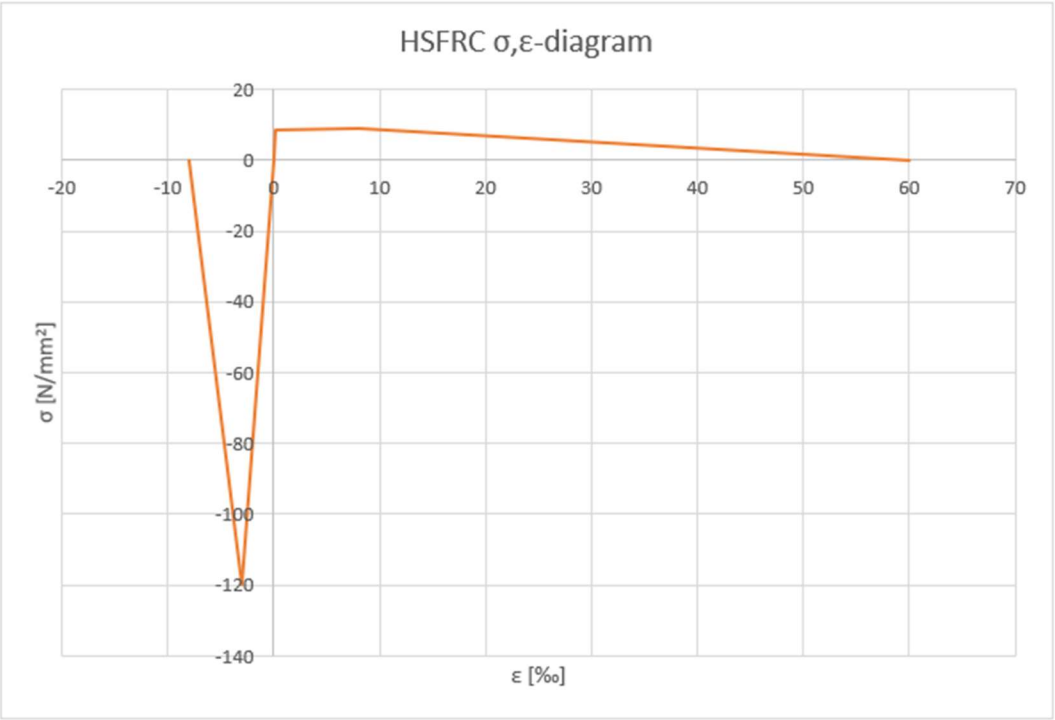

Figure 4-4: HSFRC stress-to-strain input to use in the MLM

Comparing the force-to-displacement diagram that follows from the developed MLM with the results from (Lappa, 2007) leads to the comparison in Figure 4-5.

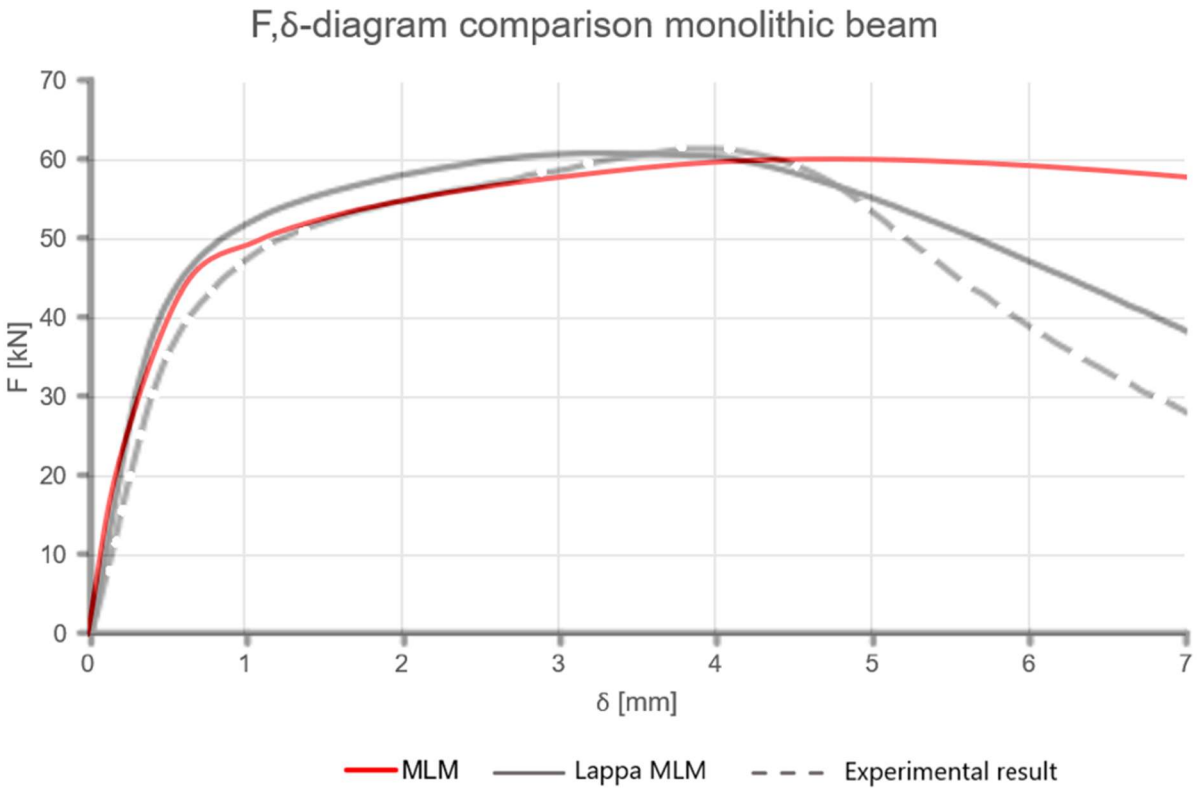

Figure 4-5: verification HSFRC force-to-displacement curve by comparing with (Lappa, 2007)

As can be seen in Figure 4-5, the behaviour is quite the same in the beginning stages. Up until a deflection of approximately 3.2 mm, the behaviour of the proposed MLM is more in line with the experiment than the 'old' MLM. However, the drop (more displacement with a decreasing force) is not present in the shown range. The drop happens later (as can be seen in Appendix C). This is not in line with the experiment. However, one of the positives is that nearly the same maximum force is achieved, which means that the end resistance is predicted well. Next to that, the non-linear part is partly predicted well. A possibility that the 'drop' happens earlier in the experiment, could be that the casted specimen had certain imperfections, which resulted in earlier failure. A parameter that greatly influences the results, is the influence length. If a higher value is chosen than half the height, the drop happens earlier. As was explained before, the strain is equal to the crack width divided by the influence length. If a larger influence length is chosen, the strain in the stress-to-strain diagram will decrease, which means that the considered material has less strength. This leads to an earlier drop. In the verification, half the height was chosen as the influence length to have exactly the same parameters as was used in (Lappa, 2007). So although the results did not match completely with the experimental results, improvements can be made if the influence length is changed. However, for the same influence length, the 'Lappa MLM' performed better for this curve.

The other diagram from the research of (Lappa, 2007) that is used to verify the MLM, is the force-to-crack opening displacement diagram. Using the same input, the comparison in Figure 4-6 is found.

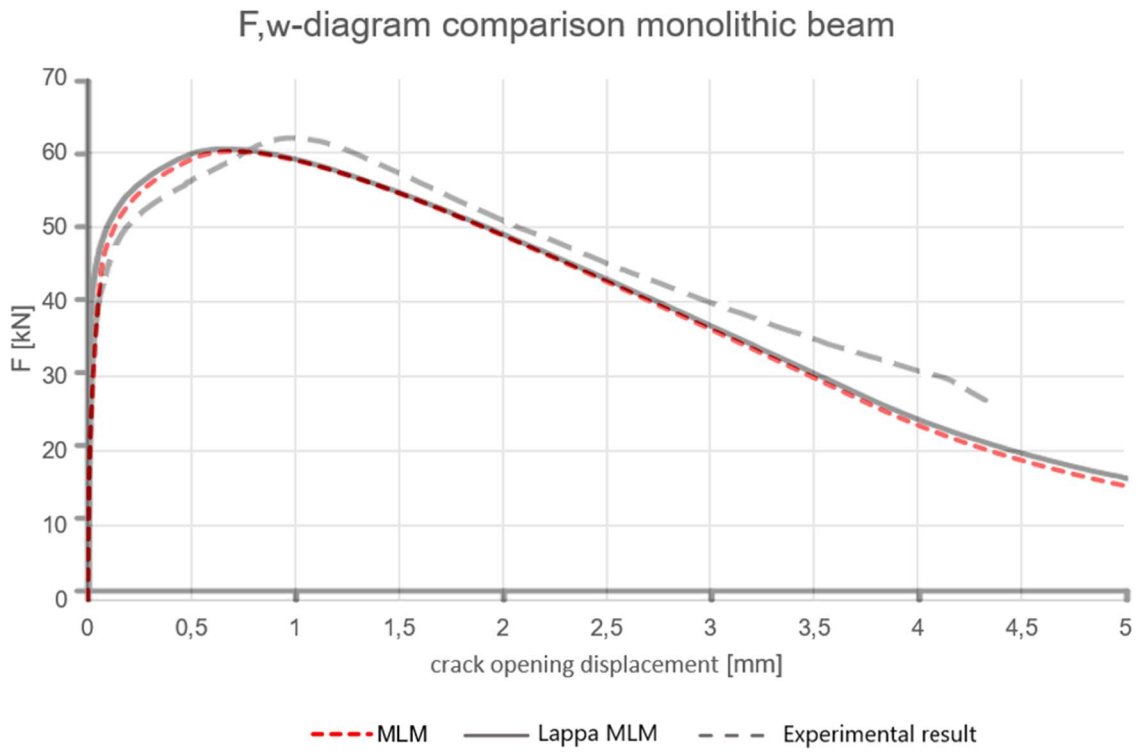

Figure 4-6: verification HSFRC force-to-crack opening displacement curve by comparing with (Lappa, 2007)

As can be seen in Figure 4-6, the results are much more in line with the experiment compared to the force-to-displacement curve. Next to that, the same trend as before is noted; the proposed MLM is more in line with the experimental results in the beginning stages. In fact, it is more in line than the 'Lappa MLM' overall. This was different for the force-to-displacement diagram.

The most positive conclusion from this verification is that the new and old MLM almost overlap for the force-to-crack opening displacement diagram, which clearly indicates that the same calculation process is behind it (which is the purpose of the verification).

The input parameters that are used in this subchapter have already been shown in Figure 4-3. A screenshot of the input and output of the developed MLM for this verification is shown in Appendix C.

4.1.2. SHCC

In the paper of (Zhou, et al., 2010), SHCC specimens were tested in a flexural test, which lead to a stress-to-deflection diagram. Next to that, a direct tension test was performed. The output of that test was used as input in the proposed MLM. The direct tension test results are shown in Figure 4-7.

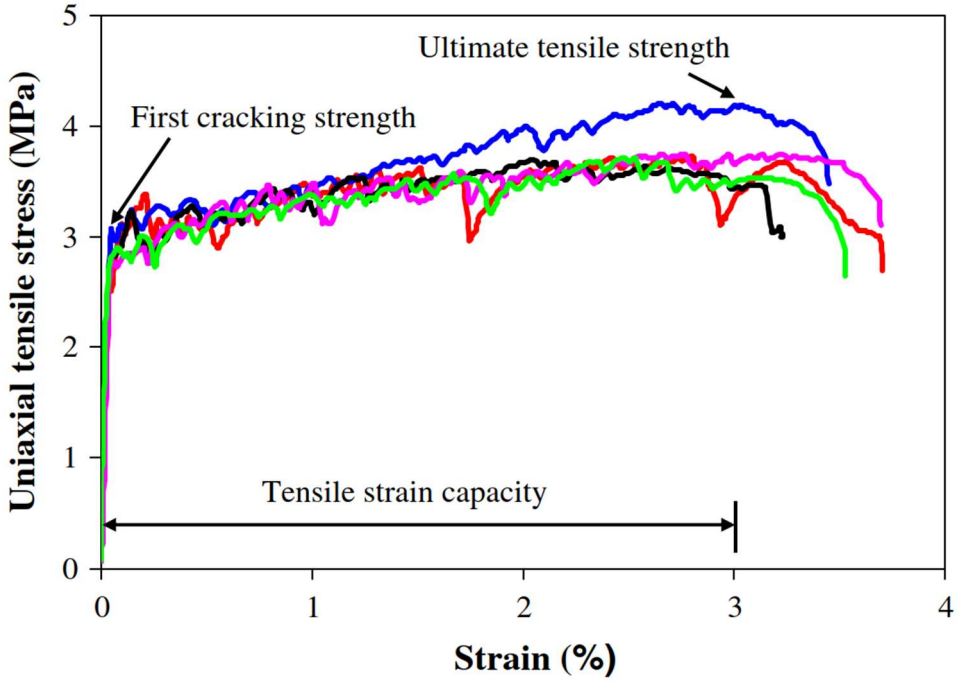

Figure 4-7: stress-to-strain relation for SHCC according to a direct tensile test (Zhou, et al., 2010)

Based on this input from the direct tension test, the output from the MLM will be compared with the experimental results of the flexural test, as obtained by (Zhou, et al., 2010). In this subchapter, the red line in Figure 4-7 will be used for the verification. The compressive input is **assumed** to be equal to conventional concrete. Using all the input in the MLM, it results in the input parameters shown in Figure 4-8.

BEAM INPUT		
Δh	0.05	mm
L	110	mm
L_1	40	mm
L_2	30	mm
h	10	mm
n	100	[-]
t	0.1	mm
b	30	mm
$\Delta\kappa$	1E-4	mm^{-1}
n.a.	5	mm

MATERIALS		
E	18,000	N/mm^2
ρ	2000	Kg/m^3
Tension:		
f_1	3	N/mm^2
ε_1	1.7E-4	[-]
f_2	3.4	N/mm^2
ε_2	0.015	[-]
Compression:		
f_1	36	N/mm^2
ε_1	2E-3	[-]
f_2	36	N/mm^2
ε_2	3.5E-3	[-]

LAYER SPECS		
Top layer	×	
Bottom layer	✓	
Web	×	
t	10	mm

DEFLECTION		
Test type	4-point	
$\#_{seg}$	500	[-]
b_{seg}	< 0.08	mm

POINTS
160

CRACK INPUT		
L_{inf}	5	mm
$w_{c,2}$	0.09	mm
f_2	3.4	N/mm^2
ε_2	0.033	[-]
$w_{c,3(END)}$	0.11	mm
$f_{3(END)}$	2.8	N/mm^2
$\varepsilon_{3(END)}$	0.037	[-]

Figure 4-8: input parameters used in the MLM to verify the results from (Zhou, et al., 2010)

Here, three notes need to be made. First of all, the density of SHCC is assumed to be equal to 2000 kg/m^3. As the goal of this verification is not to reach failure, the density value that is used has a negligible effect on the results. Secondly, as can be seen in Figure 4-8, there is crack input that is used. The reason that this is done, is to be able to have the maximum of four datapoints in the material stress-to-strain diagram in tension (shown in Figure 4-10), in order to approximate the direct tension results as good as possible. Finally, the Young's modulus data was not available and therefore assumed to be equal to 18,000 N/mm^2. This is based on the assumption in (Huang, 2017).

This used input in the MLM leads to the stress-to-strain diagrams that are shown in Figure 4-9 and Figure 4-10.

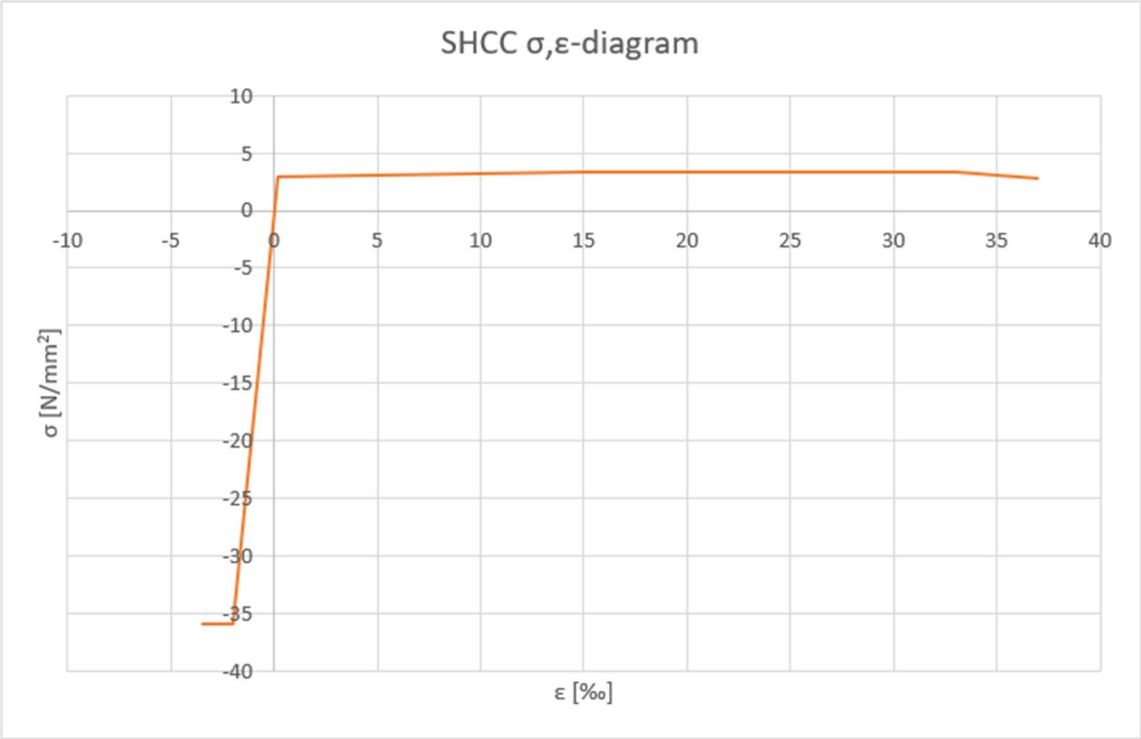

Figure 4-9: SHCC stress-to-strain input to use in the MLM

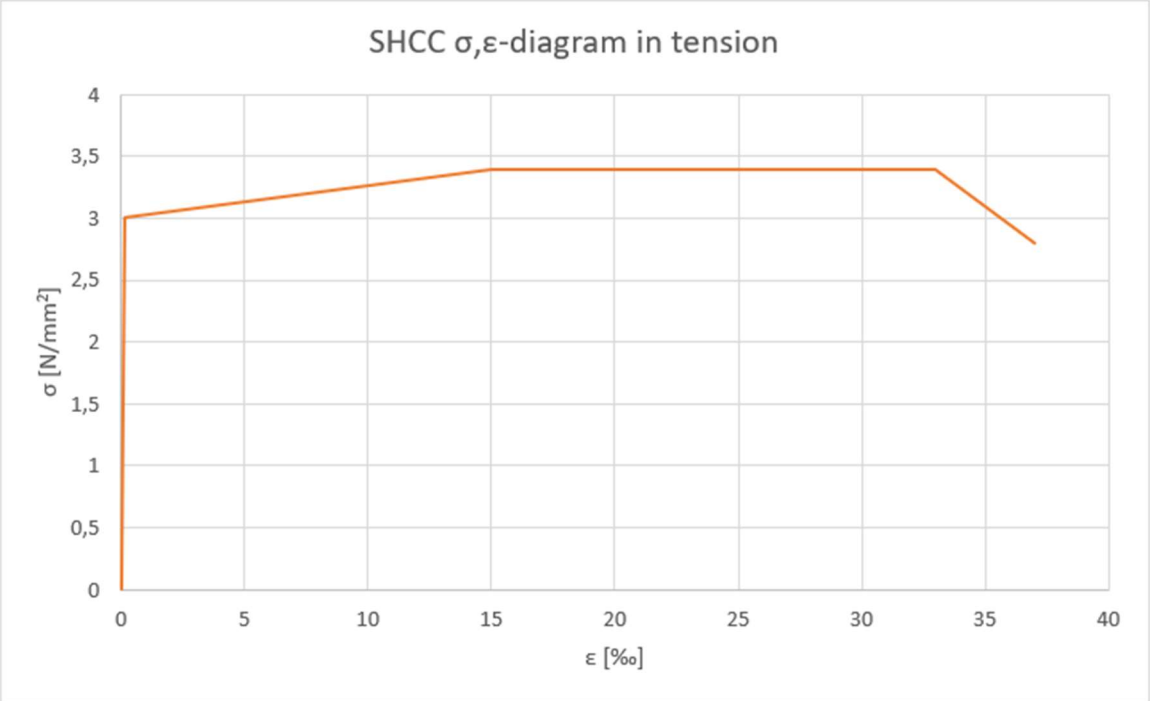

Figure 4-10: SHCC stress-to-strain input in tension to use in the MLM

The experiment that was performed is an unnotched 4-point bending test on a beam of the following dimensions: 120x30x10 [mm]. The span was equal to 110 mm.

Comparing the stress-to-displacement diagram that follows from the proposed MLM with the results from (Zhou, et al., 2010) results in the graph that is shown in Figure 4-11.

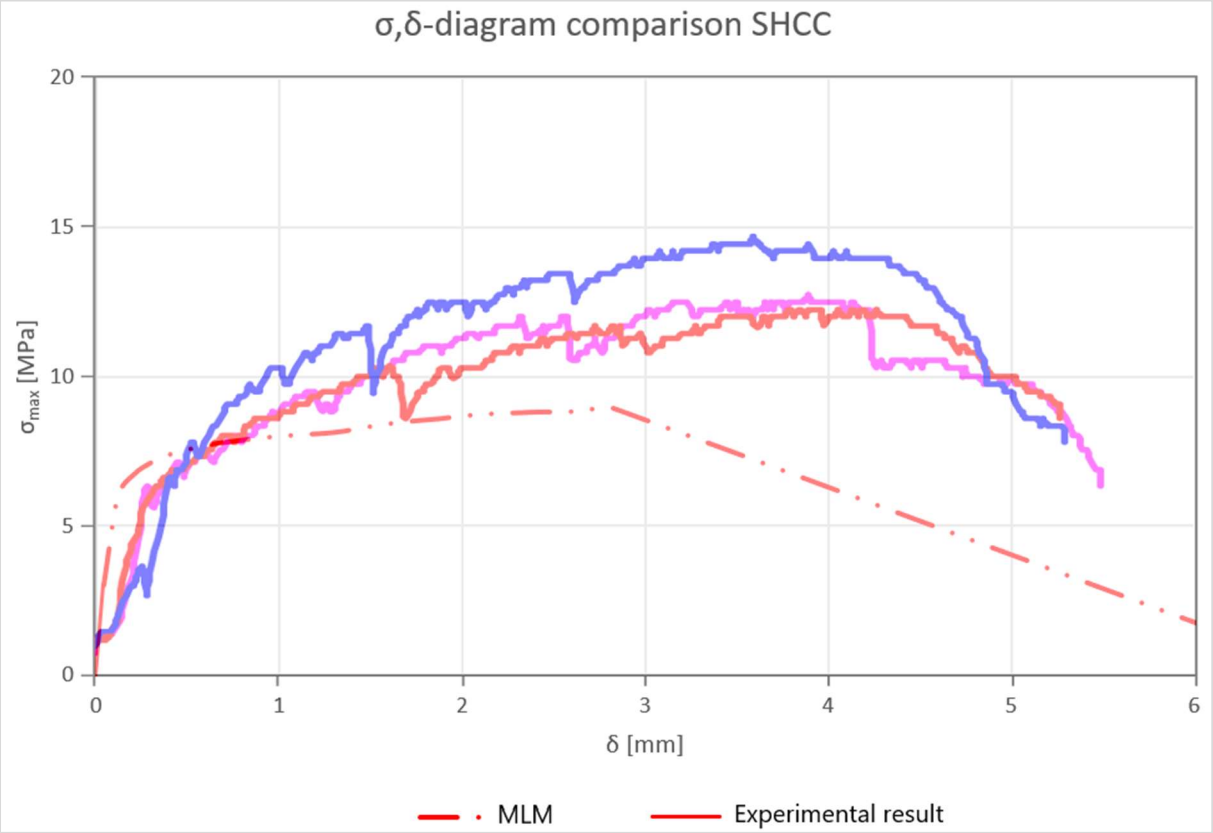

Figure 4-11: verification SHCC stress-to-displacement curve by comparing with (Zhou, et al., 2010)

As can be seen in Figure 4-11, the results do not overlap at all. The ultimate stress is underestimated (12.5 MPa vs. 9 MPa). There is only one stage in which the results completely overlap: the very start of the experiment. As can be seen, a very small part near a deflection of zero is equal. Or in other words, the initial stiffness is equal. This means that the assumed Young's modulus was accurate. However, the linear elastic stage ends very quickly for the experiment. At a deflection of 0.1 mm, the non-linear stage is already reached. This does not seem logical, so it could be that there was a problem with the experiment. The lack of match concerning the ultimate stress (12.5 MPa vs. 9 MPa) could be explained as follows: as the width of the considered beam is three times the height (30 mm width and 10 mm height), the specimen is more behaving like a slab. Due to the larger width, there is also some resistance in the other direction than in which it is loaded. This is illustrated in Figure 4-12. This behaviour is not implemented in the MLM.

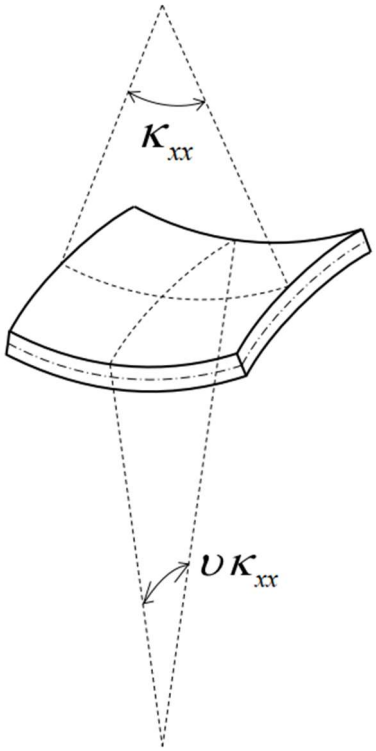

Figure 4-12: slab like behaviour in which there is additional resistance from the secondary direction (Hendriks, 2018)

In the MLM, the specimen ultimately fails in compression (crushing). This could mean that the compressive strength is underestimated; an increase in compressive strength would increase the bending moment resistance which would lead to a higher flexural strength.

Another reason could be that the tensional input that is assumed is underestimated. To obtain the tensional input, the uniaxial test was performed. However, the size of the specimen that was used for this test is larger than the specimen that was used for the 4-point bending test. This could mean that there were more weak points in the larger specimen, which resulted in decreased (assumed) resistance.

Next to that, there is also a mismatch in the trend that each line follows in Figure 4-11. As can be seen in that figure, the experimental results show small drops with increasing deflections. This is due to the strain hardening effect, which can be seen in the direct tension test example in Figure 2-3. As the microcracks appear, a small drop in resistance can be seen. This behaviour cannot be seen in the modelled results, as the proposed MLM does not take into account these microcracks.

The input parameters have already been shown in Figure 4-8. A screenshot of all the input and output of the developed MLM for this verification is shown in Appendix C.

4.2. Phase 2: reinforced non-hybrid section

In the second and third phase, the multi-layer model will be compared with the same research performed by (Huang, 2017). The reason that this is done, is to have a reference about how

comparable the results are for non-hybrid and hybrid sections. As both experiments are performed by the same researcher, the way of casting, experimenting, placing reinforcement etc. is equal for both experiments. This means that if the results of the non-hybrid experiment, that is discussed in this subchapter, are similar to the results of the proposed MLM, the same similarity should be expected when comparing with the hybrid sections. If the hybrid section would be investigated on its own, it could have been the case that possible differences in results become unexplainable. Now, this problem is solved by having both experiments performed by the same researcher under the same conditions.
Additionally, both phases will have another comparison included, namely the modelled results of (Jayananda, 2017). In his research, the FEA-program ATENA was used to model the bending resistance of the same beams that (Huang, 2017) experimented with.

The non-hybrid section is a traditionally reinforced concrete beam of the following dimensions: 1900x150x200 [mm]. The total span is equal to 1500 mm (which is used as input in the MLM). The cross-section is shown in Figure 4-13.

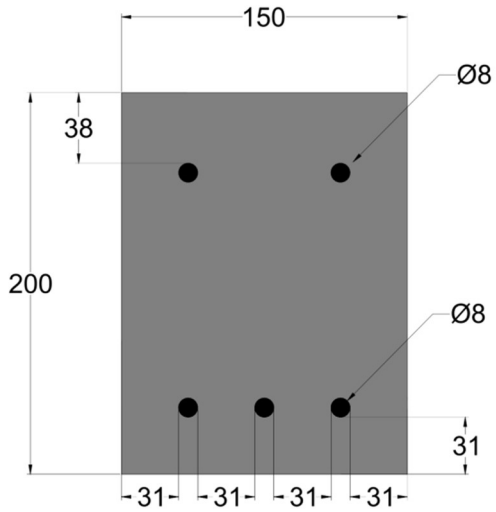

Figure 4-13: traditionally reinforced concrete beam setup (Huang, 2017)

A 4-point bending test was performed; the location of the application of the forces was such that three equal spans of 500 mm occurred. The experimental setup was shown before in Figure 2-2. For this beam, only the experimental results are available for comparison with the proposed MLM. What will be compared in this subchapter are the force-to-displacement and crack width-to-force curves.

In order to model this beam, the input parameters are chosen in accordance to what was assumed in the research of (Huang, 2017). The compressive input parameters that are assumed by (Huang, 2017) for concrete are visualized in Figure 4-14a; the tensional input parameters that are assumed by (Huang, 2017) for steel (to model the steel reinforcement bars) are visualized in Figure 4-14b.

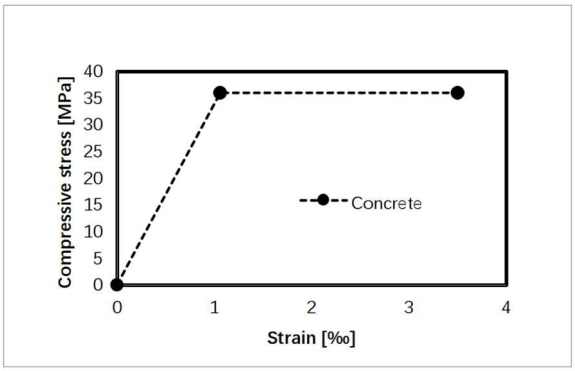

(a) assumed concrete compressive input

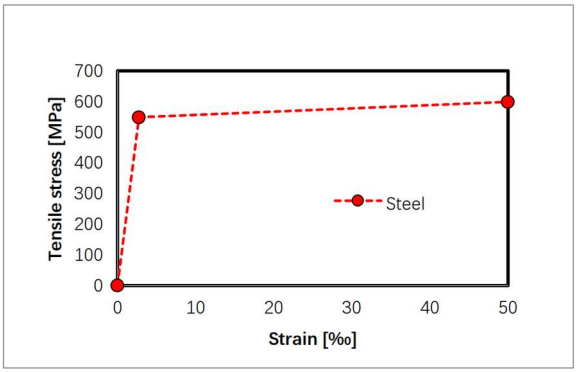

(b) assumed steel tensile input

Figure 4-14: assumed material properties for concrete and steel (Huang, 2017)

The tensional input parameter for concrete is a single datapoint, which corresponds to the cracking stress and the cracking strain. The cracking stress is assumed to be 4.536 N/mm^2, while the strain that corresponds to it is assumed to be equal to 0.106 ‰ (which corresponds to a Young's modulus of 34,000 N/mm^2). It is **assumed** that for compression, the same input as in tension can be used for the steel reinforcement. However, steel reinforcement will not be governing in compression in the setups that are discussed, so this assumption will not influence the results at all. Using all the input in the MLM, it results in the input parameters shown in Figure 4-15.

BEAM INPUT		
Δh	0.05	mm
L	1500	mm
L_1	500	mm
L_2	500	mm
h	200	mm
n	200	[-]
t	1	mm
b	150	mm
$\Delta\kappa$	1E-6	mm^{-1}
n.a.	99.26	mm

LAYER SPECS		
Top layer	✓	
Bottom layer	×	
Web	×	
t	200	mm

POINTS
60

MATERIALS			
	Concrete	Steel	
E	34,000	200,000	N/mm^2
ρ	2000	7850	Kg/m^3
Tension:			
f_1	4.536	550	N/mm^2
ε_1	1.33E-4	2.75E-3	[-]
f_2	-	600	N/mm^2
ε_2	-	0.05	[-]
Compression:			
f_1	36	550	N/mm^2
ε_1	1.06E-3	2.75E-3	[-]
f_2	36	600	N/mm^2
ε_2	3.5E-3	0.05	[-]

DEFLECTION		
Test type	4-point	
$\#_{seg}$	500	[-]
b_{seg}	< 1	mm

REINFORCEMENT		
Top:		
φ	8	mm
c	31	mm
#	3	[-]
y	35	mm
Bottom:		
φ	8	mm
c	38	mm
#	2	[-]
y	158	mm

CRACK INPUT		
L_{inf}	5	mm
$w_{c,2}$	0.09	mm
f_2	3.4	N/mm^2
ε_2	0.033	[-]
$w_{c,3(END)}$	0.11	mm
$f_{3(END)}$	2.8	N/mm^2
$\varepsilon_{3(END)}$	0.037	[-]

Figure 4-15: input parameters used in the MLM to verify the results from (Huang, 2017)

This used input in the MLM results in the stress-to-strain diagrams that are shown in Figure 4-16, and Figure 4-17:

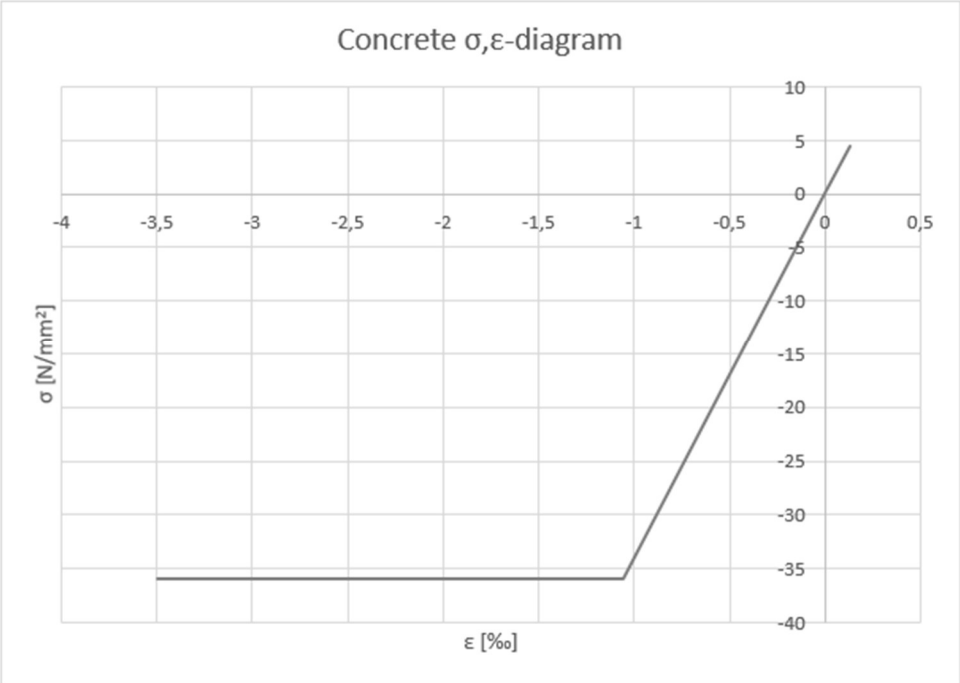

Figure 4-16: assumed concrete stress-to-strain input to use in the MLM

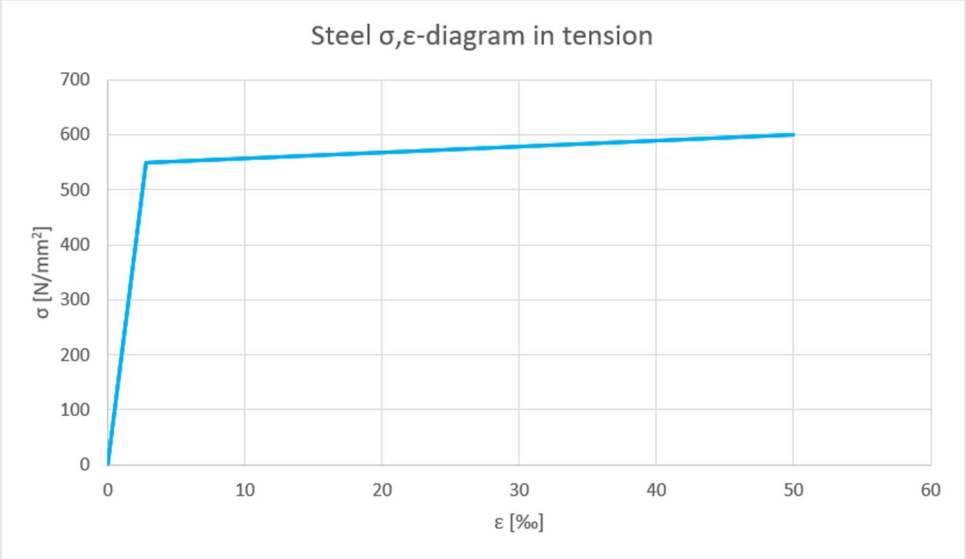

Figure 4-17: assumed steel stress-to-strain input in tension to use in the MLM

A comparison between the force-to-displacement diagram that follows from the proposed MLM, the modelled results with ATENA that follow from (Jayananda, 2017) and the experimental result that follows from the research of (Huang, 2017) is shown in Figure 4-18. The recorded deflections during the experiment were limited to around 10 mm; this is also the chosen limit in the calculations of the MLM.

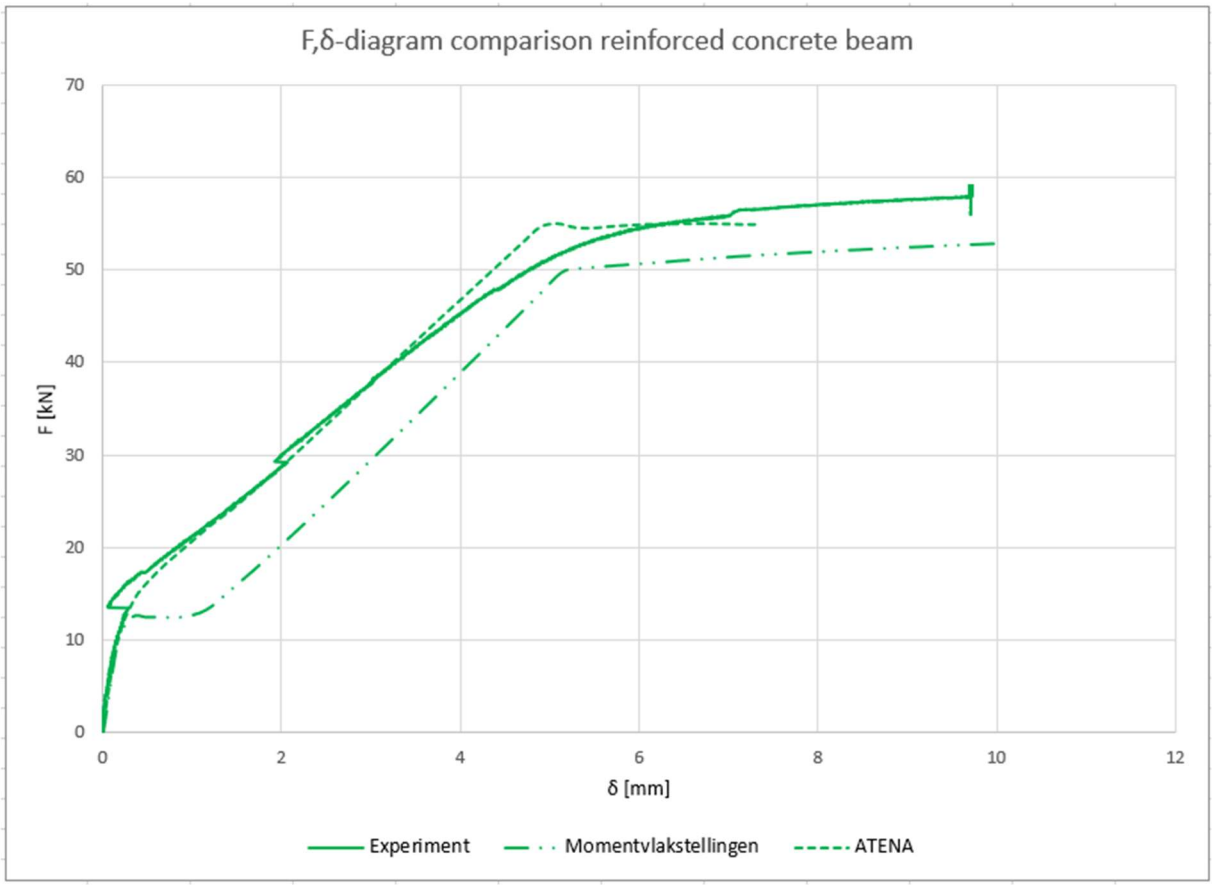

Figure 4-18: verification force-to-displacement curve of reinforced non-hybrid beam by comparing with (Huang, 2017) and (Jayananda, 2017)

Before drawing conclusions about the comparison, a check is presented to verify if the previously shown curves in Figure 4-18 are logical. As was presented in subchapters 3.4.2.1 and 3.4.2.3, the under- and overestimated deflection can be calculated to check if the modelled deflection lies in between those two 'boundaries'. The underestimated deflection was calculated using the 'constant curvature' method, while the overestimated deflection was calculated using the 'forget-me-nots'. The first check is performed for the deflection curve that is found using the momentvlakstellingen method. This is presented in Figure 4-19.

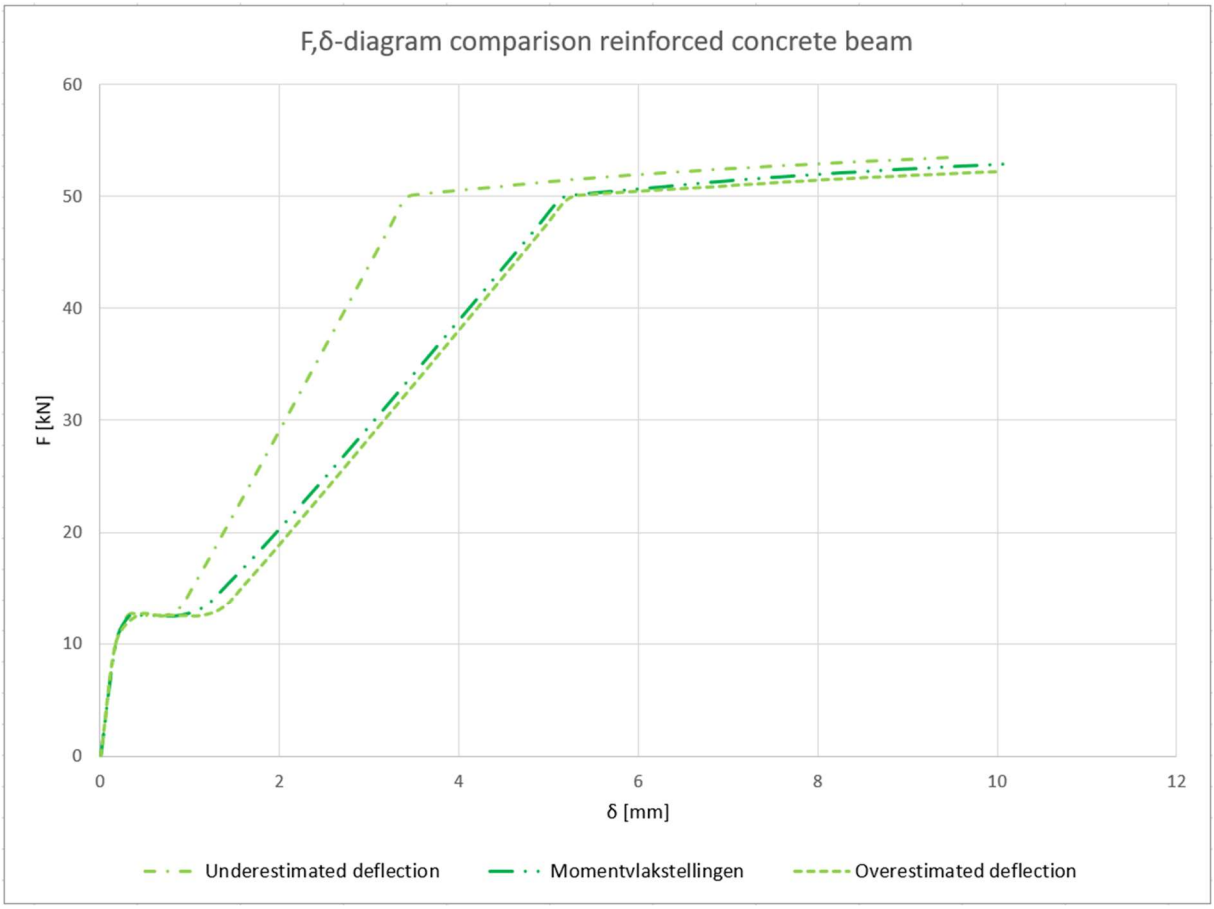

Figure 4-19: comparison of calculated MLM deflection with under- and overestimated deflections

As can be seen in Figure 4-19, the deflection curve that follows from the momentvlakstellingen method is always in between the under- and overestimated deflection. This indicates that the deflection that is found is 'logical'. The calculated deflection is very close to the overestimated deflection. The overestimated deflection is based on the assumption that the bending stiffness of the whole beam is equal to the bending stiffness at the constant bending moment region. From a deflection of 2 mm and onwards, this could mean that, if the bending stiffness between the location of the force and the support is calculated, there is not much difference with the bending stiffness in the constant bending moment region. Therefore, it becomes almost equal to the calculated overestimated deflection.

In Figure 4-19, the calculated deflection becomes more and more in line with the overestimated deflection towards the end stage. This should happen as the 'undamaged' part of the beam (between the support and the application of the force), with a high bending stiffness, becomes smaller with an increasing load. So towards the end, most of the beam will be damaged, and have a small bending stiffness, equal to the bending stiffness in the constant bending moment region.

If the same comparison is made with the experimental result, it results in the curves that are shown in Figure 4-20.

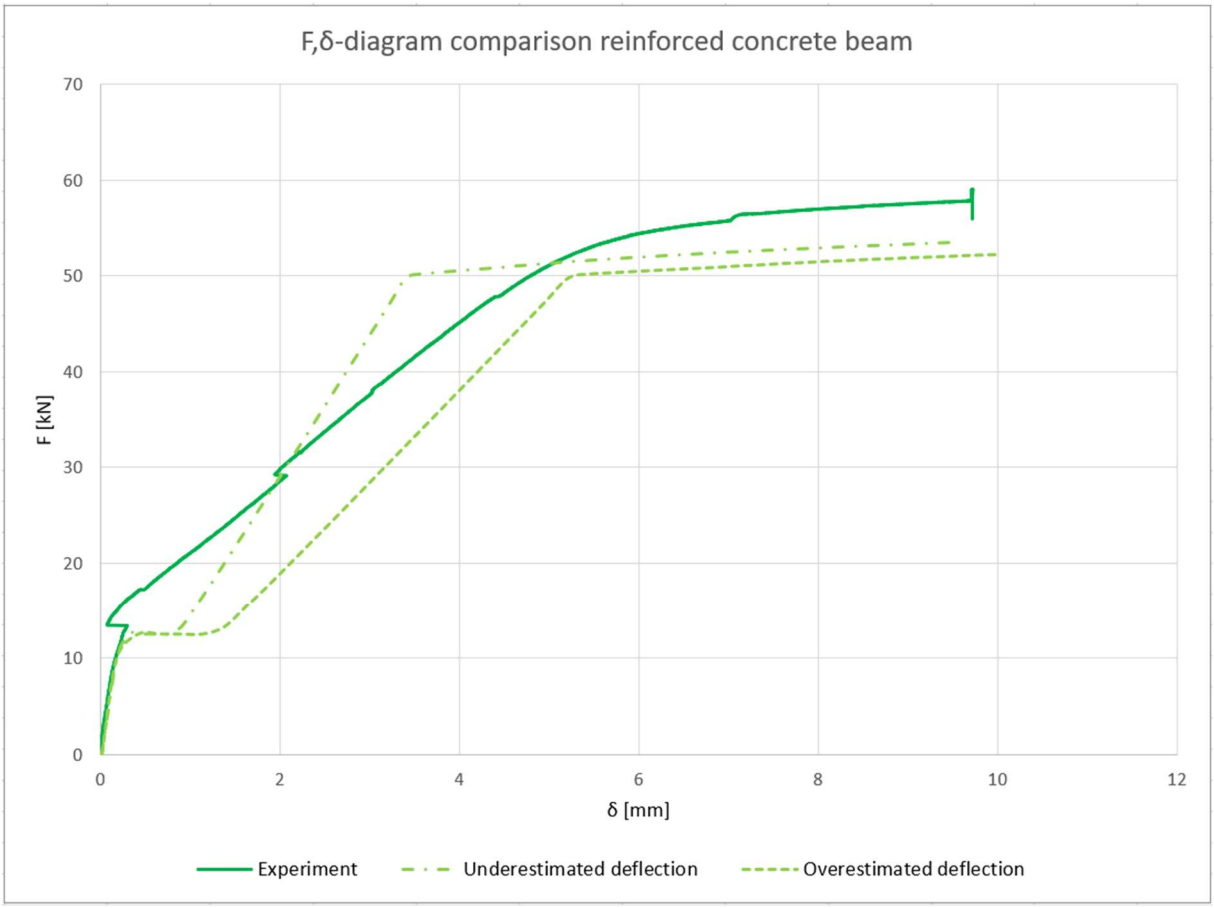

Figure 4-20: comparison of experimental deflection with under- and overestimated deflections

Now, the situation becomes different. The experimental results are not in line of what theoretically should be the case. The first noticeable part is the end resistance, which is higher than the two boundaries. This can have two explanations. The first explanation is that the input material parameters are assumed by (Huang, 2017); they are not based on experimental results. Those parameters have a massive influence on the results. The second possible explanation is that the steel reinforcement bars were not placed accurately during preparation of the beam; it could be the case that the reinforcement was placed a little bit lower, which increases the lever arm between the concrete compression zone and the steel reinforcement and therefore increases the resistance. A misplacement of 1 mm could already have a (noticeable) effect. Both causes can also explain the reason that the ATENA-model also does not correctly predict the end resistance.

Going back to the comparison shown in Figure 4-18, it can be noted that the beginning stage is exactly the same for the MLM, ATENA and experimental results; the initial stiffness is equal. After that, the MLM underestimates the resistance of the beam. Or in other words, the deflection for the same force is overestimated. This can be due to the earlier explained causes. However, the trend that both curves follow matches a lot. If a slope would be calculated for both curves, they would be quite similar; especially for the end phase (deflection $>$ 5 mm). The ATENA-results show much more compatibility with the experimental results in this stage.

Next, the crack widths that are obtained by (Huang, 2017) during the experiment are modelled in the MLM in order to also verify this part of the proposed MLM.

Using the same input as is shown in Figure 4-15, a comparison is made between the crack width-to-force diagram that follows from the proposed MLM and the experimental result that follows from the research of (Huang, 2017). This is shown in Figure 4-21.

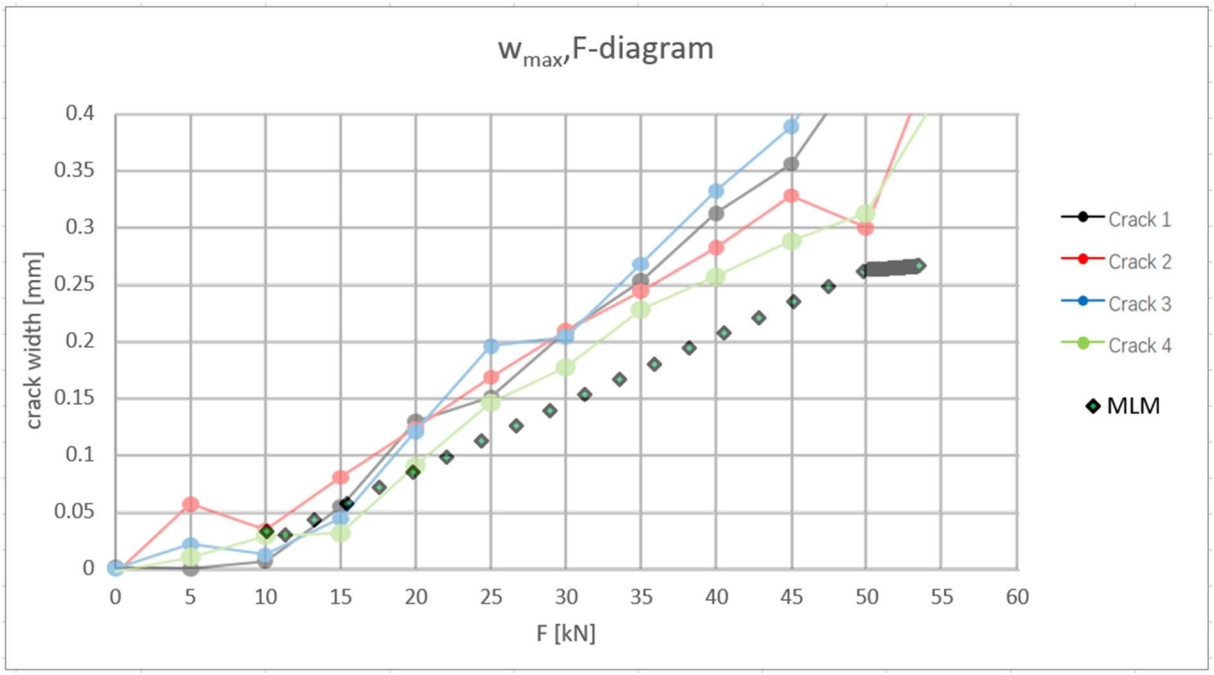

Figure 4-21: reinforced concrete crack width verification by comparing with (Huang, 2017)

In Figure 4-21, it can be seen that four cracks were measured during the experiment. The reason that this is done, is that those four cracks all occurred in the constant bending moment region. And as this region is large (500 mm), multiple cracks can occur.

One important conclusions can be drawn from the comparison; the MLM underestimates the crack width in the beam. For the same force, a larger crack width occurs in the experiment. A modification that can result in more aligned results, is the choice of the 'τ_{bm}' parameter. For lower values than '$\tau_{bm}=2f_{ctm}$', the crack width increases. However, this is only a possible cause.

The input parameters have already been shown in Figure 4-15. A screenshot of all the input and output of the developed MLM for this verification is shown in Appendix C.

4.3. Phase 3: reinforced hybrid section

The third phase is again related to the experiments performed by (Huang, 2017) and the modelled results of (Jayananda, 2017). The hybrid section that was tested is a beam with a bottom layer of SHCC, and a top layer of conventional concrete. It has the same dimensions as the non-hybrid beam: 1900x150x200 [mm]. Again, the span is equal to 1500 mm. The SHCC layer has a thickness of 70 mm, while the concrete layer has a thickness of 130 mm. The steel reinforcement is of the same configuration as the previous subchapter. The cross-section was shown in Figure 2-1. The

same 4-point bending test as was explained in the previous subchapter (4.2) was performed. As for the beam that was discussed in the previous subchapter, only the experimental results are available for comparison with the proposed MLM. What will be compared in this subchapter is the force-to-displacement curve.

In order to model this beam, the input parameters are chosen in accordance to what was assumed in the research of (Huang, 2017). The compressive input parameters that are assumed by (Huang, 2017) for concrete, and the tensional steel input parameters, were already discussed and are visualized in Figure 4-14.

The tensional input parameter for concrete was also discussed, but will be repeated. It is a single datapoint, which is the cracking stress and the cracking strain. The cracking stress is assumed to be 4.536 N/mm^2, while the strain that corresponds to it is assumed to be equal to 0.106 ‰.

The additional aspect that will be discussed in this subchapter, is the inclusion of SHCC as a material. Its tensional input parameters that are assumed by (Huang, 2017) are visualized in Figure 4-22.

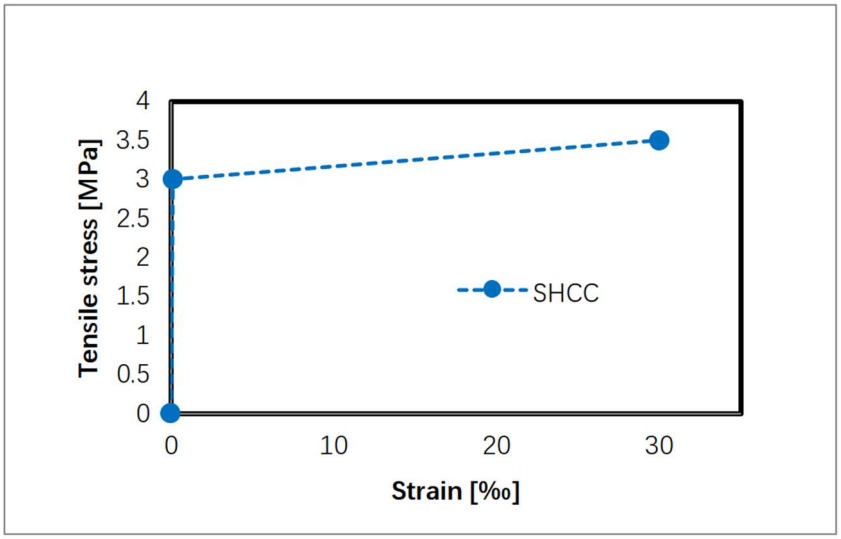

Figure 4-22: assumed tensional stress-to-strain relation for SHCC (Huang, 2017)

It is **assumed** that for compression, the same input as for concrete in compression can be used. This assumption was necessary because no other input was known. And as SHCC is only used as a bottom layer, it will only be loaded in tension. This input will therefore not affect the results at all. Using all the input in the MLM, it results in the input parameters shown in Figure 4-23.

BEAM INPUT		
Δh	0.05	mm
L	1500	mm
L_1	500	mm
L_2	500	mm
h	200	mm
n	200	[-]
t	1	mm
b	150	mm
$\Delta\kappa$	1E-6	mm^{-1}
n.a.	111.2	mm

MATERIALS				
	Concrete	SHCC	Steel	
E	34,000	18,000	200,000	N/mm^2
ρ	2300	2390.9	7850	Kg/m^3
Tension:				
f_1	4.536	3	550	N/mm^2
ε_1	1.33E-4	1.67E-4	2.75E-3	[-]
f_2	-	3.5	600	N/mm^2
ε_2	-	0.03	0.05	[-]
Compression:				
f_1	36	36	550	N/mm^2
ε_1	1.06E-3	2E-3	2.75E-3	[-]
f_2	36	36	600	N/mm^2
ε_2	3.5E-3	3.5E-3	0.05	[-]

REINFORCEMENT		
Top:		
φ	8	mm
c	31	mm
#	3	[-]
y	35	mm
Bottom:		
φ	8	mm
c	38	mm
#	2	[-]
y	158	mm

LAYER SPECS		
Top layer	✓	
Bottom layer	✓	
Web	×	
t_{TOP}	130	mm
t_{BOT}	70	mm

DEFLECTION		
Test type	4-point	
$\#_{seg}$	500	[-]
b_{seg}	< 1	mm

POINTS
60

Figure 4-23: input parameters used in the MLM to verify the results from (Huang, 2017)

This used input in the MLM results in the same stress-to-strain diagrams for concrete and steel that are previously shown in Figure 4-16 and Figure 4-17 are used again. Additionally, the stress-to-strain diagram in Figure 4-24 is found for SHCC.

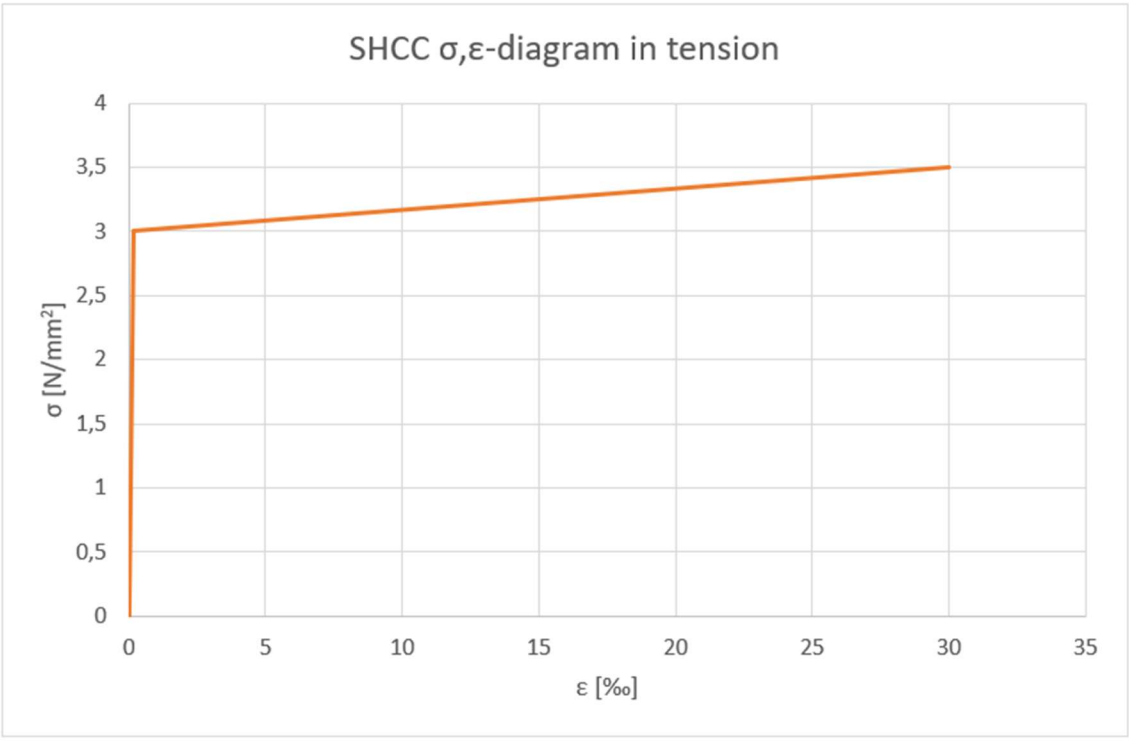

Figure 4-24: assumed SHCC stress-to-strain input in tension to use in the MLM

A comparison between the force-to-displacement diagram that follows from the proposed MLM, the modelled results with ATENA that follow from (Jayananda, 2017) and the experimental result that follows from the research of (Huang, 2017) is shown in Figure 4-25. Again, the recorded

deflections during the experiment were limited to around 10 mm, which is why the MLM results are also limited to 10 mm.

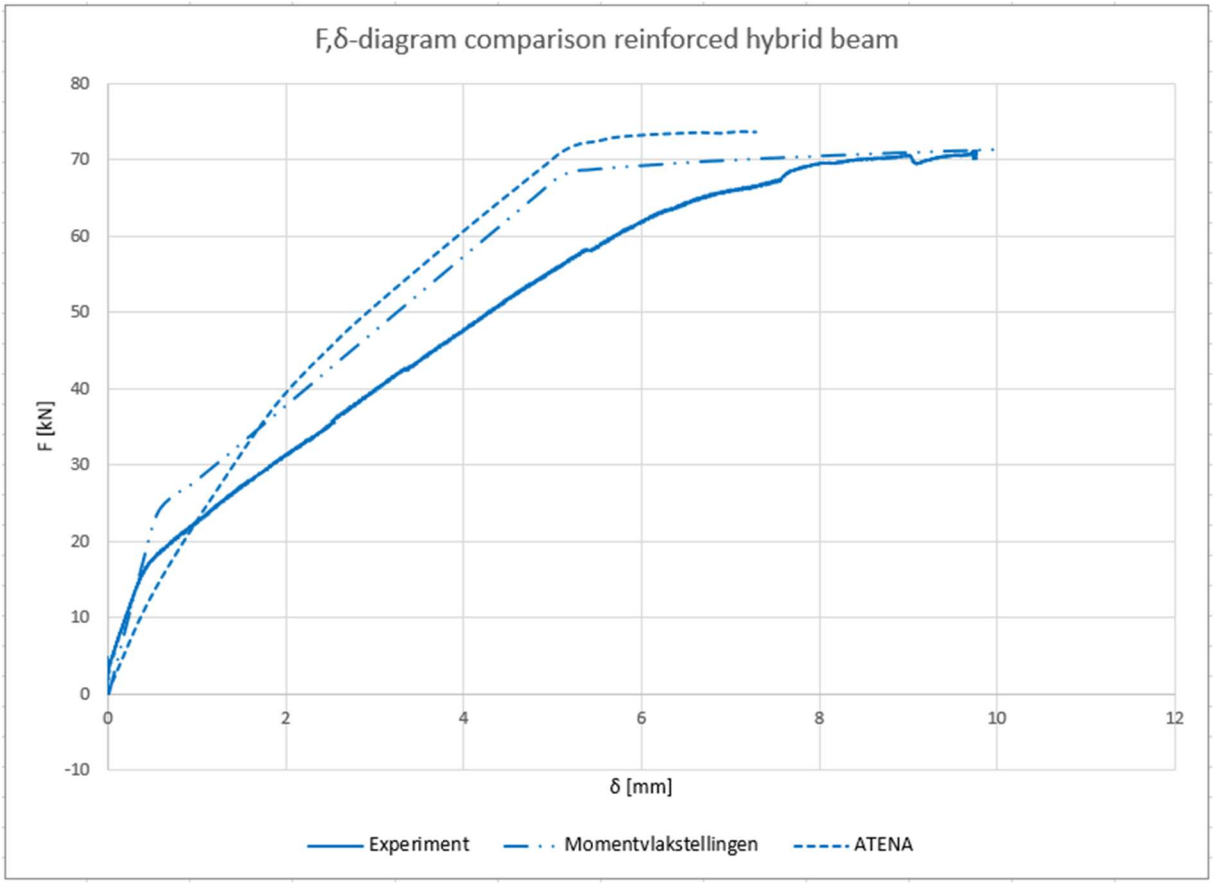

Figure 4-25: verification force-to-displacement of reinforced hybrid beam curve by comparing with (Huang, 2017) and (Jayananda, 2017)

As was done in the previous subchapter, a check is presented to verify if the curves shown in Figure 4-25 are logical. This was done by comparing with the under- and overestimated curves, in which the underestimated deflection was calculated using the 'constant curvature' method, and the overestimated deflection using the 'forget-me-nots'. The first check is performed for the deflection curve that is found using the momentvlakstellingen method. This is presented in Figure 4-26.

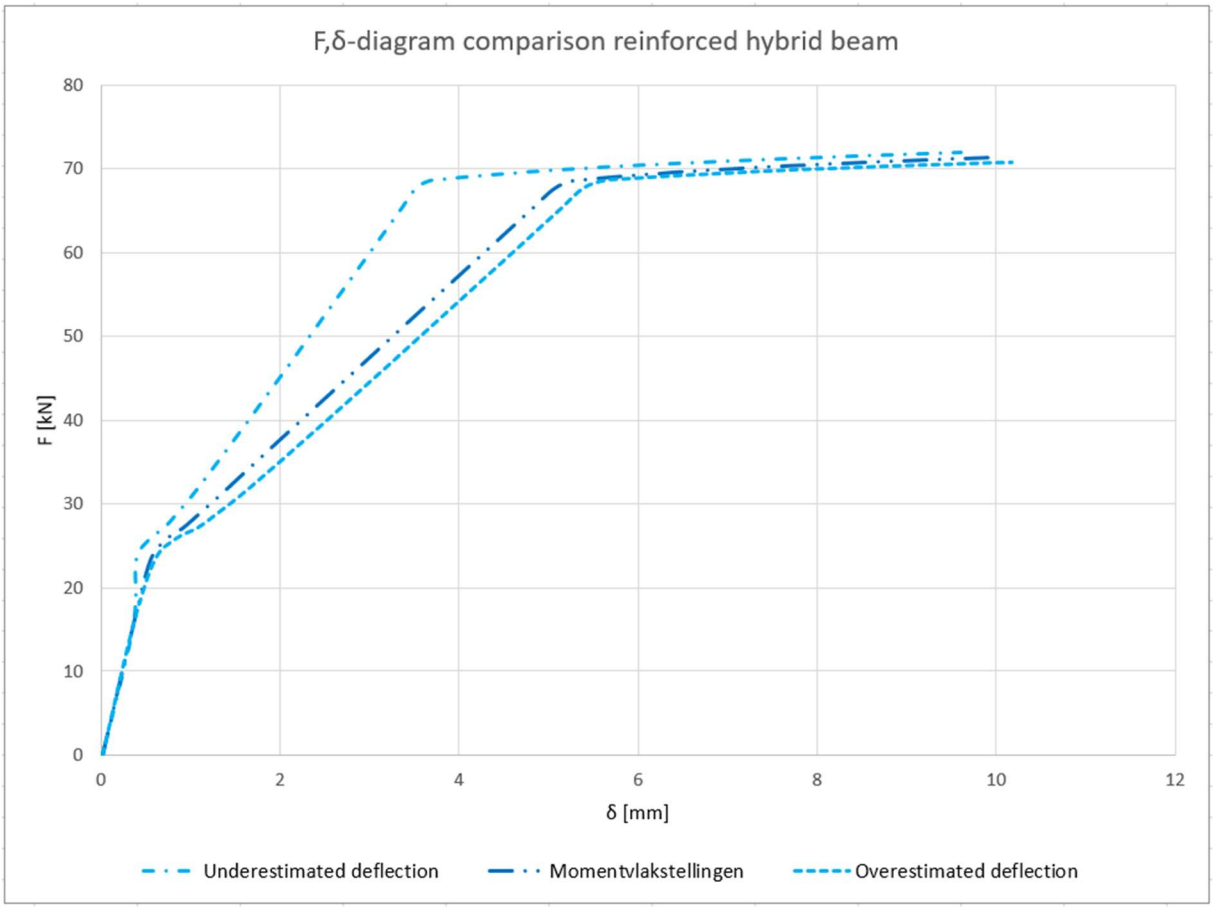

Figure 4-26: comparison of calculated MLM deflection with under- and overestimated deflections

As can be seen in Figure 4-26, the deflection curve that follows from the momentvlakstellingen method is always in between the under- and overestimated deflection. This indicates that the deflection that is found is logical. If the same comparison is made with the experimental result, it results in the curves that are shown in Figure 4-27.

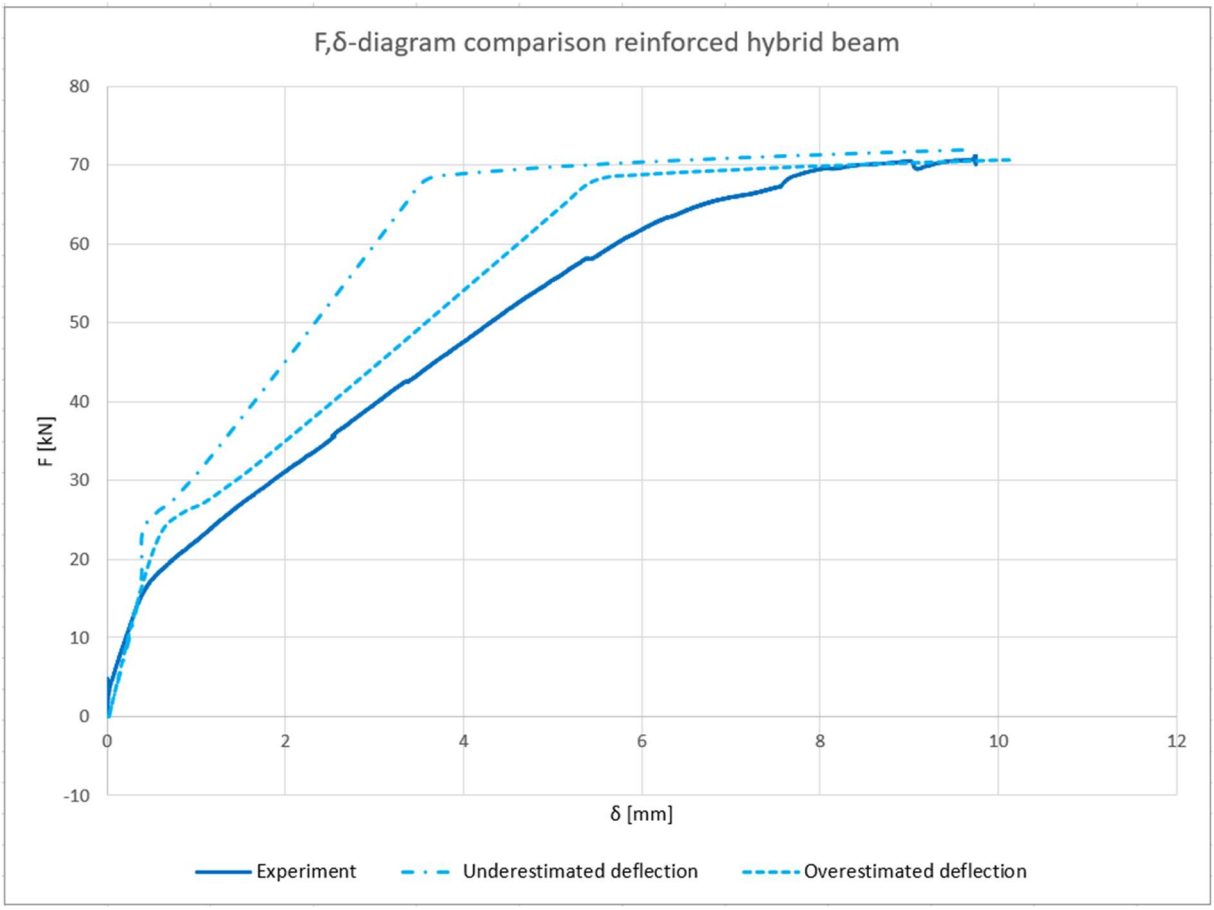

Figure 4-27: comparison of experimental deflection with under- and overestimated deflections

For the experimental results, the situation is completely different. The experimental results are not in line of what theoretically should be the case. This is the case for almost the entire curve. The deflection is higher than the theoretical overestimated deflection. The most plausible explanation for this behaviour is that the interface bond plays a huge role; in the MLM, it is assumed that the interface is perfect. In reality, this could have not been the case. If so, there will surely be a higher deflection than if the bond was perfect.

Going back to the comparison shown in Figure 4-25, it can be noted that the beginning stage is nearly the same for the MLM and the experiment; the initial stiffness is therefore also nearly the same. However, the initial stiffness is not predicted well by the ATENA-model. After that, the MLM overestimates the resistance of the beam. Or in other words, the deflection for the same force is underestimated. This is also the case for the ATENA-model. It is expected that this is due to the earlier mentioned interface effect. However, the trend that the MLM-curve follows matches a lot with the curve that follows from the experimental results. The most positive result that can be taken from this verification, is that the end resistance is predicted well; it is exactly the same for the MLM and the experiment. In this case, it is even reached at the same deflection for both curves. As was the case in phase 1 of the verification, the resistance of the beam itself is predicted very accurately. As for the ATENA-model, this end resistance is not predicted well. In this verification it is shown that the MLM performs better than the ATENA-

model for reinforced hybrid beams; for the reinforced non-hybrid beams, the ATENA-model performed better.

The input parameters have already been shown in Figure 4-23. A screenshot of all the input and output of the developed MLM for this verification is shown in Appendix C.

4.4. Phase 4: reinforced hybrid section with a U-shaped mould

In the last phase, a configuration will be proposed of which the experimental results can be obtained in future research. The reason that the experimental results can only be obtained in future research, is that no experiments have been performed before with such a configuration. In this subchapter, the bending resistance of this experimental setup will be modelled using the MLM. These results can then later be compared and verified by experimental results. The cross-section of the proposed configuration is a small alteration on the cross-section that has been shown before in Figure 2-1; the only difference is the addition of the 15 mm thick side webs of the U-shape. This is shown in Figure 4-28.

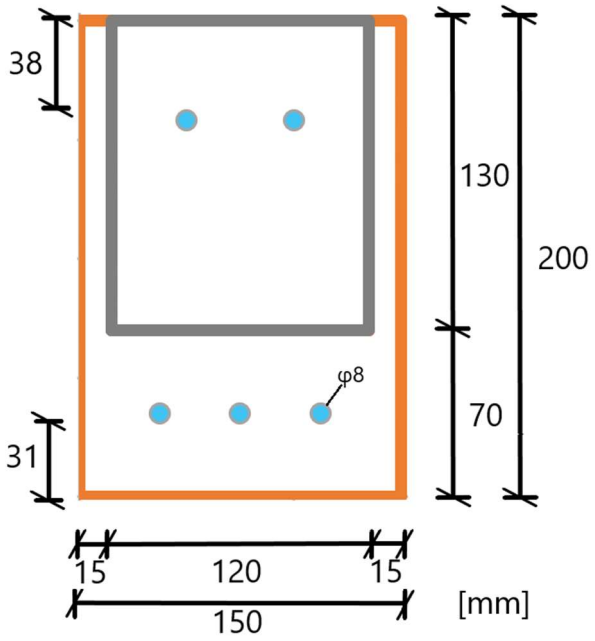

Figure 4-28: cross-section of reinforced hybrid concrete beam with a U-shaped SHCC mould

Not only the cross-section is very similar to the experiment that has been verified in the previous subchapter (4.3); in fact, the rest of the parameters are exactly the same. A 4-point bending test is proposed with a total span of 1500 mm (with three equal sub-spans of 500 mm), as was shown in Figure 2-2. The parameters are shown in Figure 4-29.

BEAM INPUT		
Δh	0.05	mm
L	1500	mm
L_1	500	mm
L_2	500	mm
h	200	mm
n	200	[-]
t	1	mm
b	150	mm
$\Delta\kappa$	1E-6	mm^{-1}
n.a.	109.5	mm

MATERIALS				
	Concrete	SHCC	Steel	
E	34,000	18,000	200,000	N/mm^2
ρ	2300	2390.9	7850	Kg/m^3
Tension:				
f_1	4.536	3	550	N/mm^2
ε_1	1.33E-4	1.67E-4	2.75E-3	[-]
f_2	-	3.5	600	N/mm^2
ε_2	-	0.03	0.05	[-]
Compression:				
f_1	36	36	550	N/mm^2
ε_1	1.06E-3	2E-3	2.75E-3	[-]
f_2	36	36	600	N/mm^2
ε_2	3.5E-3	3.5E-3	0.05	[-]

REINFORCEMENT		
Top:		
φ	8	mm
c	31	mm
#	3	[-]
y	35	mm
Bottom:		
φ	8	mm
c	38	mm
#	2	[-]
y	158	mm

LAYER SPECS		
Top layer	✓	
Bottom layer	✓	
Web	✓	
t_{TOP}	130	mm
t_{BOT}	70	mm
t_{WEB}	15	mm

DEFLECTION		
Test type	4-point	
$\#_{seg}$	500	[-]
b_{seg}	< 1	mm

POINTS
105

Figure 4-29: input parameters used in the MLM to model the bending resistance of the reinforced hybrid concrete beam with a U-shaped SHCC mould

This leads to the earlier shown stress-to-strain diagrams as material input. The diagrams were shown in Figure 4-16, Figure 4-17 and Figure 4-24. Using this input, the moment-to-curvature diagram that follows from the MLM is shown in Figure 4-30. Note however that a perfect bond between the SHCC and the concrete (also along the U-shaped mould) is a prerequisite for achieving the resistance that is shown in Figure 4-30.

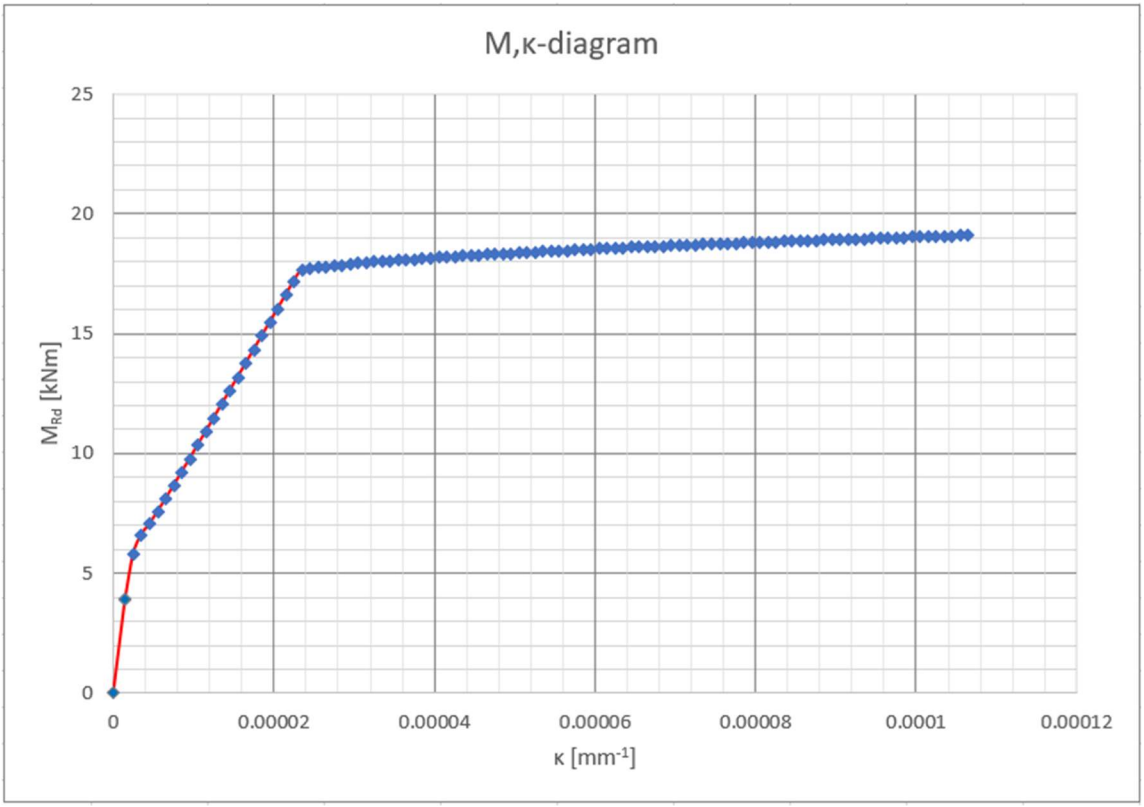

Figure 4-30: moment-to-curvature curve reinforced hybrid concrete beam with a U-shaped SHCC mould

Next to that, the force-to-displacement diagram that is found by modelling using the MLM is shown in Figure 4-31. Note that the deflection on the diagram is not limited as in the previous verifications; the diagram until failure is shown.

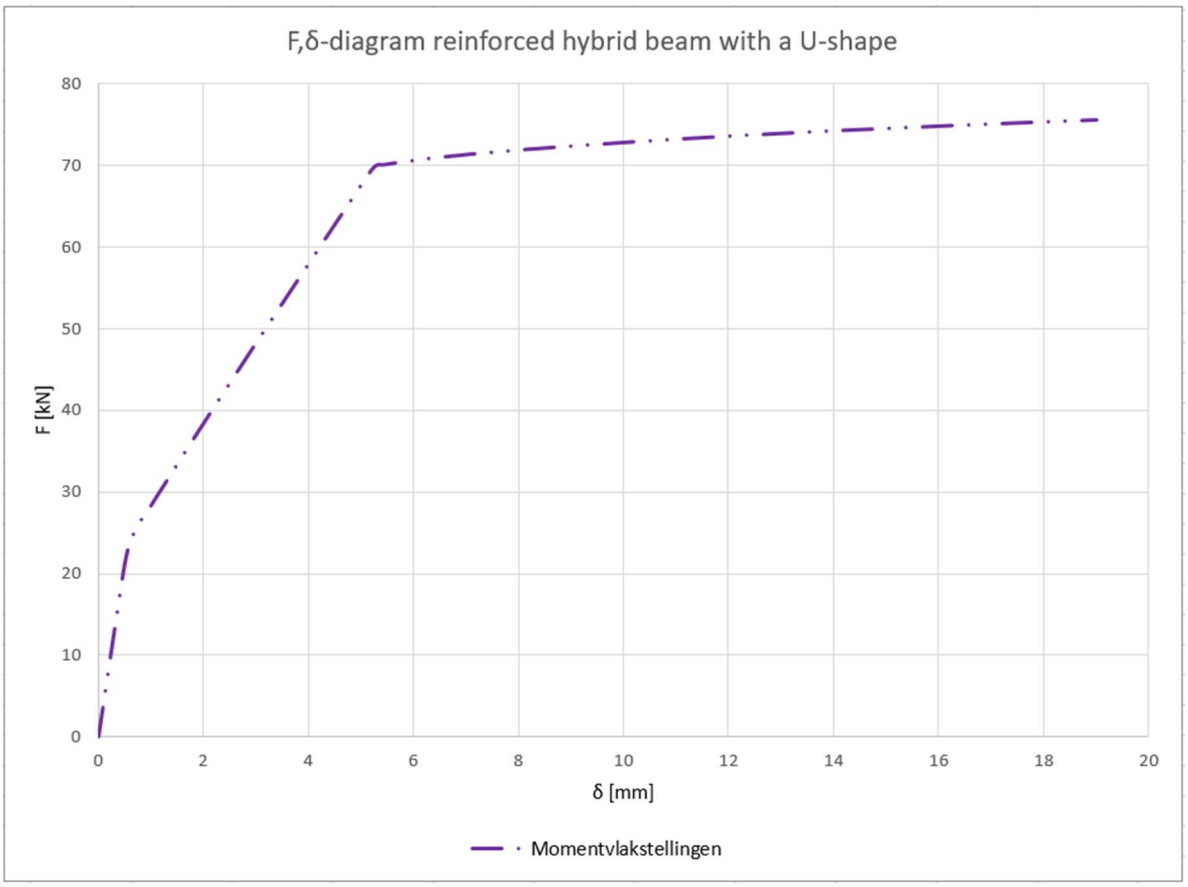

Figure 4-31: force-to-displacement curve reinforced hybrid concrete beam with a U-shaped SHCC mould

As was done in the previous subchapters, a check is presented to verify if the curve shown in Figure 4-25 is logical. This was done by comparing with the under- and overestimated curves, in which the underestimated deflection was calculated using the 'constant curvature' method, and the overestimated deflection using the 'forget-me-nots'. The results of this check are presented in Figure 4-32.

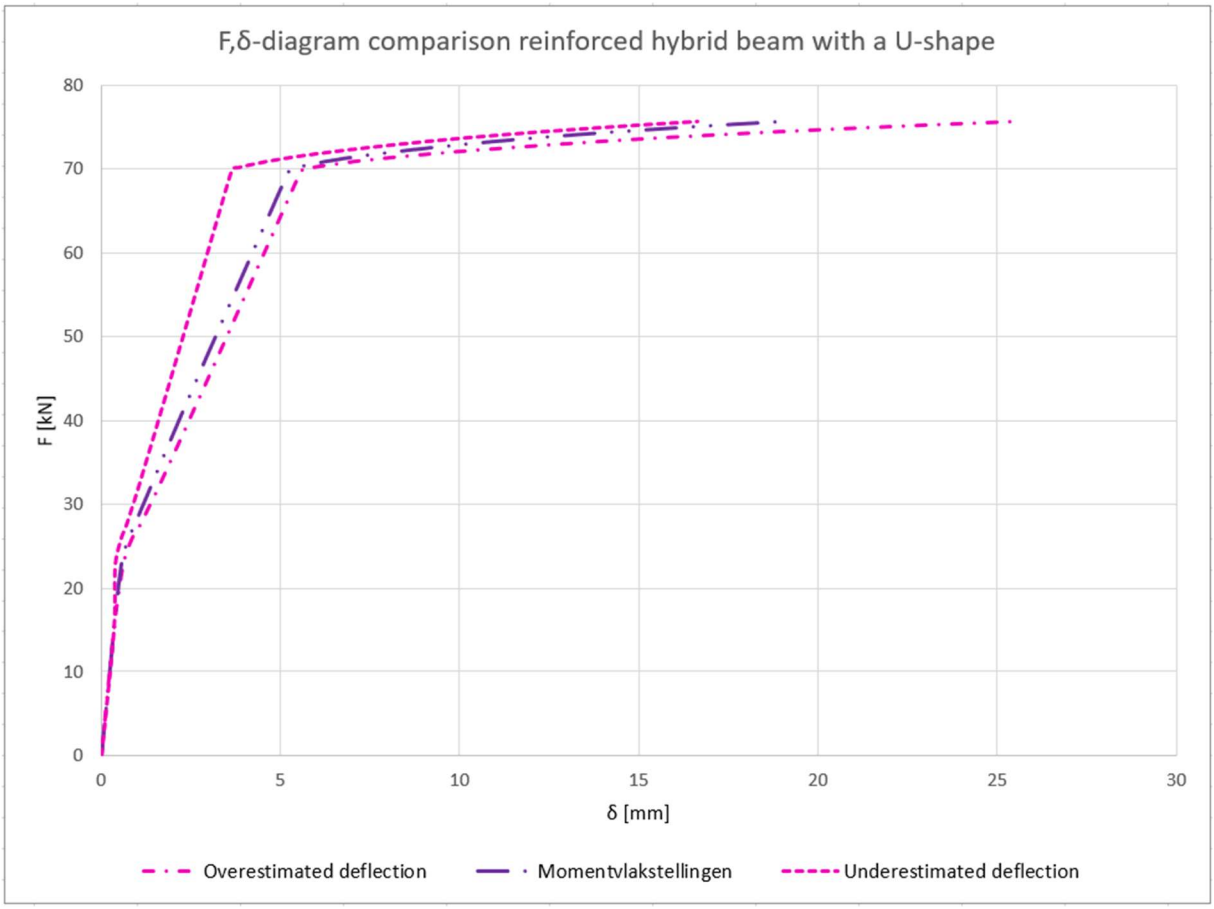

Figure 4-32: comparison of calculated MLM deflection with under- and overestimated deflections

As can be seen in Figure 4-32, the deflection curve that follows from the momentvlakstellingen method is always in between the under- and overestimated deflection. This indicates that the deflection that is found is logical.

4.5. Drying shrinkage

In subchapter 3.4.5, it was presented how the eigen-strains due to drying shrinkage can be calculated using the relative humidity profile. These strains could then be used to calculate the eigenstresses (in the linear elastic stage) that occur due to drying shrinkage. In the MLM, the eigen-strains are added as initial strains that effect the resistance of the specimen. In this subchapter, two verifications are shown. First of all, the calculation method of the eigen-strains using the relative humidity profile is verified. This is done by ultimately calculating the eigenstresses, and compare them with a finite-element program. This verification was made before by (Awasthy, 2019). The second verification that is shown is that of the results that follow if the eigen-strains are used as input in the MLM. For a specimen, the effect of the drying time on the flexural strength is verified.

4.5.1. Calculation of eigen-strains

For verification of the calculation method to obtain the eigen-strains, (Awasthy, 2019) used a finite-element program called FEMMASSE. First, it was checked whether the relative humidity

that was obtained with FEMMASSE was comparable with the results of (Hanson, 1968). That was the case. Note that the humidity data that was used in the analytical model of (Awasthy, 2019) was the same data that was obtained by FEMMASSE. Next, the stresses were calculated and compared to the stresses that follow from the earlier described analytical model. The result in Figure 4-33 was obtained.

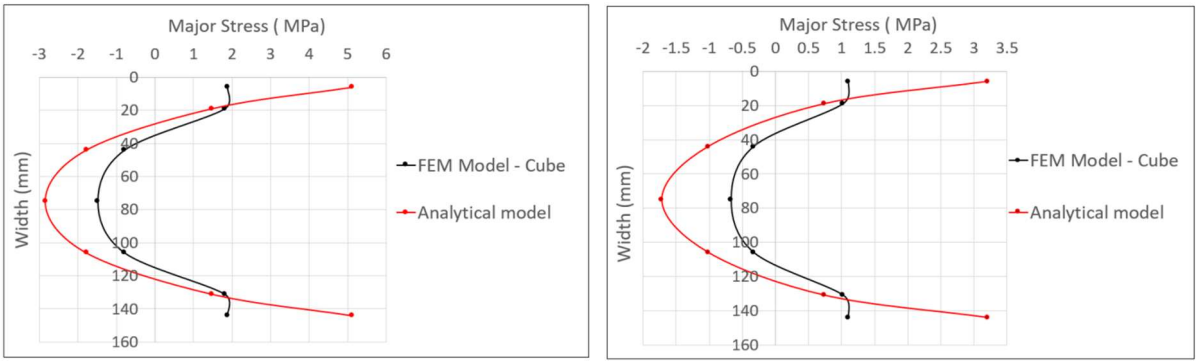

(a) 28 days of drying *(b) 1 year of drying*

Figure 4-33: comparison of eigenstresses between FEM and an analytical model (Awasthy, 2019)

The author (Awasthy, 2019) noted that the difference between the results was mainly due to the assumption of linear elastic behaviour in the analytical model. The stresses were calculated by multiplying the obtained strains by the linear Young's modulus (Awasthy, 2019). Even then, both lines in Figure 4-33 follow the same trend.

4.5.2. Effect of drying time on flexural strength

In the proposed MLM, the eigen-strains are calculated using the relative humidity profile. However, if those strains are known beforehand, they can directly be used as input. In this subchapter, the effect of the eigen-strains of different drying periods on the flexural strength will be verified. Again, a comparison will be made with results that follow from FEMMASSE. Two different specimens will be used in the verification: NSC (**N**ormal **S**trength **C**oncrete) and HSC (**H**igh **S**trength **C**oncrete). The specimen size is 400x100x100 [mm].

The material properties that are used in the calculation, are based on experimental results that are obtained by (Awasthy, 2019). Three material properties are available: the Young's modulus (shown in Figure 4-34), the compressive strength (shown in Figure 4-35) and the splitting tensile strength (shown in Figure 4-36). In the MLM, the direct tensile strength is needed to be able to model the specimen. As is assumed by (Awasthy, 2019), the direct tensile is assumed to be equal to 85% of the splitting tensile strength. As for the compressive strength, it is assumed that a bi-linear stress-to-strain diagram occurs, with failure at 3.5‰ (similar to conventional concrete). This holds for both NSC and HSC.

Compressive Strength (in MPa)										
Days	**Curing Regime**	**NSC**			**HSC**			**UHSC**		
		Value	*Mean*	*SD*	*Value*	*Mean*	*SD*	*Value*	*Mean*	*SD*
28	28DM	24.7	27.8	2.9	70.5	64.4	5.4	145.5	131.6	29.75
		29.6			62.7			151.8		
		29.3			60.1			97.4		
56	28DM	34.4	34.1	0.4	62.8	70.6	6.7	139.9	151.2	9.85
		33.9			73.9			157.8		
		33.8			75.1			155.8		
91	28DM	35.3	35.6	1.5	72.4	70.0	2.9	141.9	154.4	11.7
		37.2			66.5			156.2		
		34.2			72.4			165.2		
91	CM	38.1	41.6	3.1	66.3	70.1	4.3	155.9	160.3	4.3
		42.6			69.3			164.5		
		43.9			74.8			160.5		
155	28DM	36	32.8	2.9	61.2	66.1	5.7	152.0	163.0	9.6
		32			64.8			168.9		
		30.4			72.3			168.2		

Figure 4-34: experimental results of compressive strength of NSC and HSC

Splitting Tensile Strength (in MPa)										
Days	**Curing Regime**	**NSC**			**HSC**			**UHSC**		
		Value	*Mean*	*SD*	*Value*	*Mean*	*SD*	*Value*	*Mean*	*SD*
28	28DM	3.07	2.98	0.09	5.63	5.23	0.39	20.13	21.66	1.65
		2.96			4.84			21.43		
		2.89			5.22			23.41		
56	28DM	3.66	3.59	0.06	5.05	5.26	0.29	22.02	23.12	1.12
		3.55			5.13			23.07		
		3.57			5.60			24.26		
91	28DM	3.51	3.64	0.15	5.44	5.47	0.11	22.04	21.35	0.62
		3.61			5.59			21.19		
		3.80			5.39			20.83		
91	CM	3.76	3.79	0.02	5.35	5.39	0.08	21.59	19.40	1.91
		3.79			5.34			18.56		
		3.80			5.47			18.06		
155	28DM	3.68	3.71	0.03	5.26	5.22	0.03	19.9	19.6	0.31
		3.71			5.20			19.3		
		3.75			5.21			19.6		

Figure 4-35: experimental results of splitting tensile strength strength of NSC and HSC

		Elastic Modulus [in GPa]								
Days	**Curing Regime**	**NSC**			**HSC**			**UHSC**		
		Value	*Mean*	*SD*	*Value*	*Mean*	*SD*	*Value*	*Mean*	*SD*
28	28DM	29.0	31.0	1.9	36.7	37.3	0.7	44.6	45.4	1.0
		32.6			37.3			45.1		
		31.3			38.0			46.5		
56	28DM	32.2	34.0	1.7	38.1	38.9	0.7	46.6	46.7	0.4
		35.5			39.6			46.4		
		34.3			39.0			47.2		
								-		
91	28DM	32.6	34.4	2.6	38.7	39.6	0.8	47.4	47.5	0.4
		36.3			40.2			47.1		
		-			40			47.9		
91	CM	36.3	35.0	1.2	39.0	40.2	1.1	48.0	46.5	1.3
		34.7			40.9			46.0		
		34.1			40.8			45.5		
155	28DM	36.6	34.7	2.7	38.8	39.7	0.8	48.0	48.1	0.5
		32.8			40.4			47.7		
		-			39.9			48.6		

Figure 4-36: experimental results of Young's modulus of NSC and HSC

Two more assumptions are made. First of all, it is assumed that linear interpolation is possible between property quantities of known drying periods to calculate the quantities of untested drying periods. For example, if the Young's modulus at an age of 42 days is needed, the average value of the (mean) Young's modulus at 28 days and 56 days is taken. The second assumption is related to the material properties after an age of 155 days of the concrete. As there is no data available after this age, it is assumed that the material properties stay equal after this age.

In order to be able to compare with the results that follow from FEMMASSE, the same input has to be used. Therefore, the same tensile softening curve is used that is defined in FEMMASSE, which is shown in Figure 4-37.

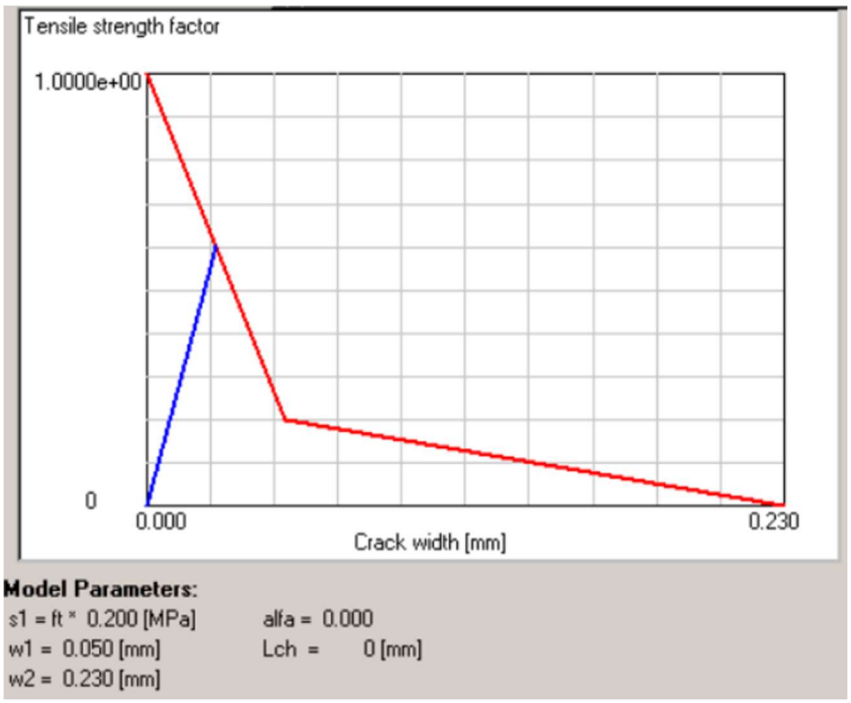

Figure 4-37: tensile softening curve as is defined in FEMMASSE (Awasthy, 2019)

The results that were available from (Awasthy, 2019) are the eigenstresses along the height, which were calculated using the linear elastic Young's modulus. To find the eigen-strains, the Young's modulus for each drying period was determined, after which the eigenstress was divided by the acquired Young's modulus to find the eigen-strain. The conversion from stresses to strains for NSC and HSC is shown in Appendix C.

4.5.2.1 Normal Strength Concrete

For this specimen, the used drying periods are listed in Table 4-2. These drying periods occur after the curing period of 28 days. So for 0 days of drying, the concrete age is 28 days.

Drying period [days]
0
3
10
14
21
28
63
337
702
1797
7272
18222

Table 4-2: drying periods after 28 days of curing of NSC specimen

In Figure 4-38, the input parameters that are used for NSC in the MLM are shown for 10 days of drying. Twelve different drying periods are defined in Table 4-2, but only the input for 10 days of drying is shown.

BEAM INPUT		
Δh	0.05	mm
L	400	mm
L_1	200	mm
h	100	mm
n	100	[-]
t	1	mm
b	100	mm
$\Delta\kappa$	1E-6	mm^{-1}
n.a.	50	mm

DRYING SHRINKAGE
10 days

POINTS
20

MATERIALS		
E	32,071	N/mm^2
ρ	2300	Kg/m^3
Tension:		
f_1	2.724	N/mm^2
ε_1	8.49E-5	[-]
Compression:		
f_1	30.05	N/mm^2
ε_1	9.37E-4	[-]
f_2	30.05	N/mm^2
ε_2	3.5E-3	[-]

DEFLECTION		
Test type	3-point	
$\#_{seg}$	200	[-]
b_{seg}	< 1	mm

LAYER SPECS		
Top layer	✓	
Bottom layer	×	
Web	×	
t	100	mm

CRACK INPUT		
L_{inf}	50	mm
$w_{c,2}$	0.05	mm
f_2	0.545	N/mm^2
ε_2	1.09E-3	[-]
$w_{c,3(END)}$	0.23	mm
$f_{3(END)}$	0	N/mm^2
$\varepsilon_{3(END)}$	4.69E-3	[-]

Figure 4-38: input parameters used in the MLM for 10 days of drying of NSC to verify the results from (Awasthy, 2019)

In the study of (Awasthy, 2019), the eigenstresses were known for this specimen (for all drying periods). These eigenstresses were translated to eigen-strains by dividing by the Young's modulus. This is correct as the material was still in the linear elastic stage. As an example, the eigenstresses for 10 days of drying (concrete age: 38 days) are shown in Figure 4-39. The eigenstresses for other drying periods are shown in Appendix C.

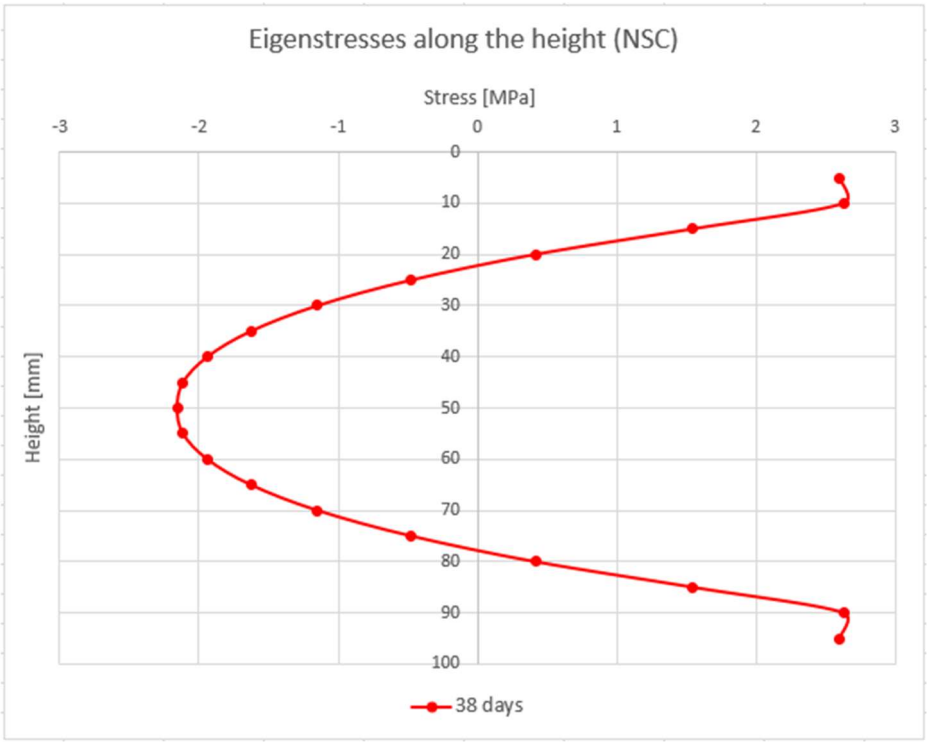

Figure 4-39: eigenstresses along the height for Normal Strength Concrete (Awasthy, 2019)

Comparing the results that follow from the developed MLM with the results from FEMMASSE (Awasthy, 2019) leads to the comparison in Figure 4-40.

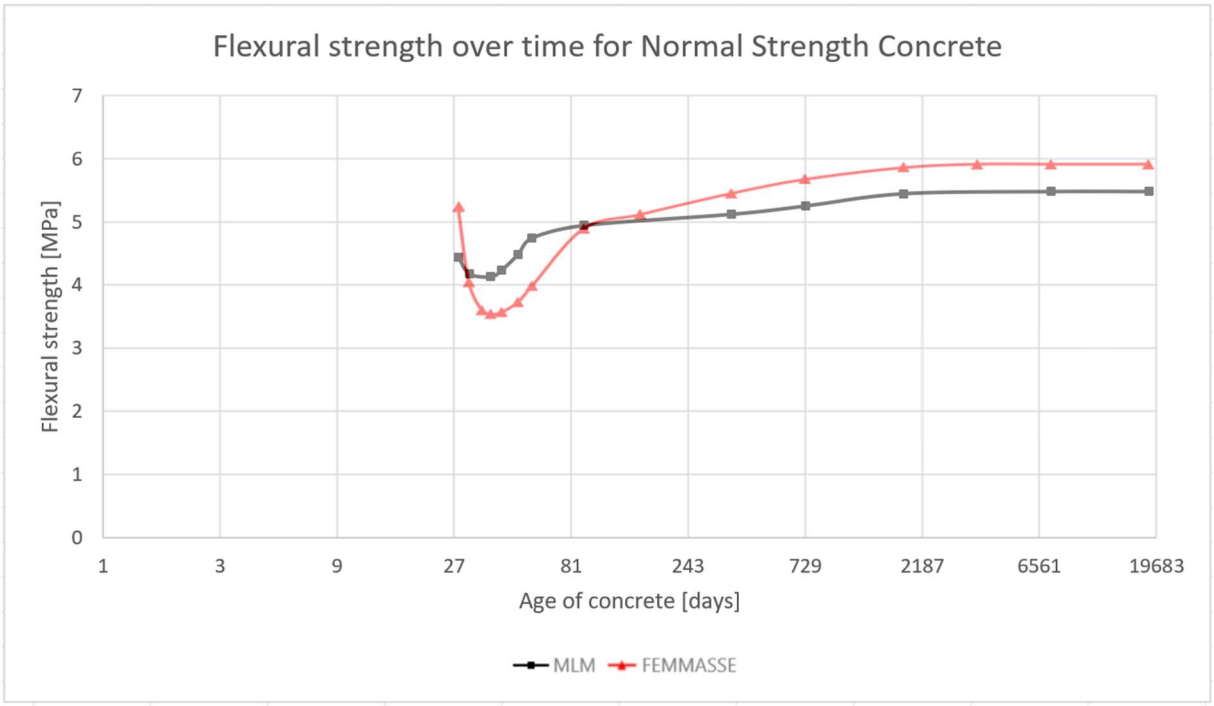

Figure 4-40: comparison of effect of drying periods on flexural strength of NSC between MLM and FEMMASSE (Awasthy, 2019)

Before comparing the results, it has to be noted that the eigen-strains in the top and bottom 5 mm were unknown (the distribution between 5 and 95 mm height was known). This could have an effect on the modelled results.

As can be seen in Figure 4-40, the trend that both lines follow is very similar. For both calculations, the flexural strength initially goes down, but starts increasing again after approximately 20 days of drying. The flexural strength keeps increasing with time to an extent that the initial flexural strength is exceeded. This is true for both sets of results. A difference between the two calculations is however the starting flexural strength (age of concrete of 28 days). Although the two lines in Figure 4-40 do not overlap, it can clearly be seen that the effect of drying on the flexural strength is similar.

The input parameters have already been shown in Figure 4-38. A screenshot of all the input and output of the developed MLM for this verification is shown in Appendix C.

4.5.2.2 High Strength Concrete

The same approach that is shown in the previous subchapter (4.5.2.1) is followed in this subchapter. First of all, the used drying periods are listed in Table 4-2.

Drying period [days]
0
3
10
63
152
337
702
1797
7272
18222

Table 4-3: drying periods after 28 days of curing of HSC specimen

In Figure 4-38, the input parameters that are used for HSC in the MLM are shown for 10 days of drying. Again, only the parameters for this period of drying are shown.

BEAM INPUT		
Δh	0.05	mm
L	400	mm
L_l	200	mm
h	100	mm
n	100	[-]
t	1	mm
b	100	mm
$\Delta\kappa$	1E-6	mm^{-1}
n.a.	50	mm

DRYING SHRINKAGE
10 days

POINTS
20

MATERIALS		
E	37,871	N/mm^2
ρ	2300	Kg/m^3
Tension:		
f_1	4.455	N/mm^2
ε_1	1.18E-4	[-]
Compression:		
f_1	66.614	N/mm^2
ε_1	1.76E-3	[-]
f_2	66.614	N/mm^2
ε_2	3.5E-3	[-]

DEFLECTION		
Test type	3-point	
$\#_{seg}$	200	[-]
b_{seg}	< 1	mm

LAYER SPECS		
Top layer	✓	
Bottom layer	×	
Web	×	
t	100	mm

CRACK INPUT		
L_{inf}	50	mm
$w_{c,2}$	0.05	mm
f_2	0.891	N/mm^2
ε_2	1.12E-3	[-]
$w_{c,3(END)}$	0.23	mm
$f_{3(END)}$	0	N/mm^2
$\varepsilon_{3(END)}$	4.72E-3	[-]

Figure 4-41: input parameters used in the MLM for 10 days of drying of HSC to verify the results from (Awasthy, 2019)

In the study of (Awasthy, 2019), the eigenstresses were also known for this specimen. These eigenstresses were translated to eigen-strains by dividing by the Young's modulus. As an example, the eigenstresses for 10 days of drying (concrete age: 38 days) are shown in Figure 4-42. The eigenstresses for other drying periods are shown in Appendix C.

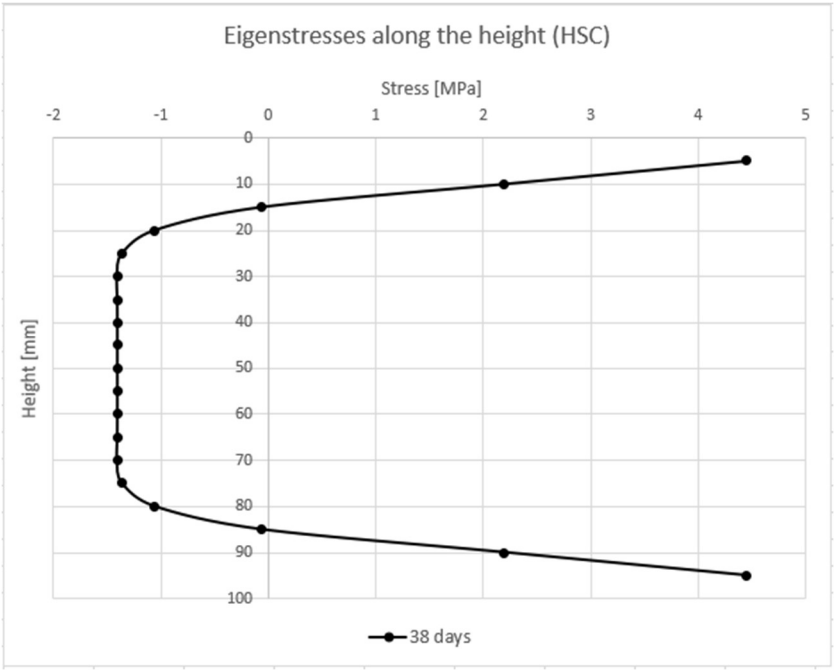

Figure 4-42: eigenstresses along the height for High Strength Concrete (Awasthy, 2019)

Comparing the results that follow from the developed MLM with the results from FEMMASSE (Awasthy, 2019) leads to the comparison in Figure 4-43.

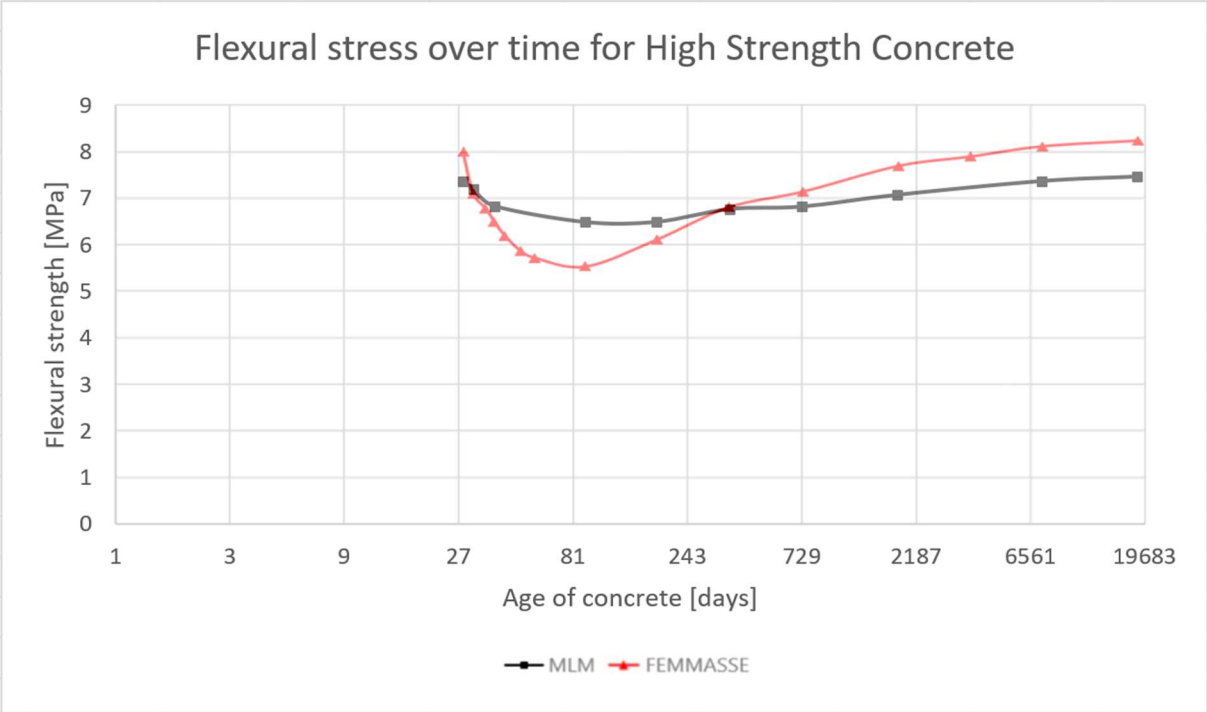

Figure 4-43: comparison of effect of drying periods on flexural strength of HSC between MLM and FEMMASSE (Awasthy, 2019)

Similarly to the NSC comparison, the eigen-strains in the top and bottom 5 mm were unknown (the distribution between 5 and 95 mm height was known). This could have an effect on the modelled results.

As can be seen in Figure 4-43, the trend that both lines follow is again similar. For both calculations, the flexural strength initially goes down, but starts increasing again. Different from the comparison in the previous subchapter, the flexural strength starts going up again after approximately 60 days of drying. Again, the flexural strength keeps increasing with time to an extent that the initial flexural strength is exceeded. This is true for both sets of results. The difference between the two calculations is similar to the previous subchapter: the initial flexural strength is not equal. What also is noticeable, is that for both the FEMMASSE and MLM results, the decrease and increase in flexural strength is described by a shallow curve. This was not the case for NSC; the decrease and increase at the start was described by a steep curve. What can be concluded from the results is, that the MLM predicts the trend that is followed well. For NSC, a steep curve was predicted, while for HSC, a shallow curve was predicted. That was in line with the predicted results in FEMASSE.

The input parameters have already been shown in Figure 4-41. A screenshot of all the input and output of the developed MLM for this verification is shown in Appendix C.

5. Discussion

5.1. Comparison between MLM's

In subchapter 4.1.1, the extended MLM, proposed in this research, was verified by comparing the results to previous research. In that research, also the results from an older version of the MLM were presented. The force-to-crack opening displacement curves of both MLM's overlapped, which indicates that the same input and calculation method is used. This also suggests that the force-to-displacement curve should be similar, but that was not the case. In order to be able to explain the difference, a similar check as was presented in subchapter 4.2 is used to verify if the previously found deflection curves are logical. This check will be done for the two MLM's, by comparing with the under- and overestimated deflection curves. First, the check is made for the calculated deflection using the extended MLM. This is shown in Figure 5-1.

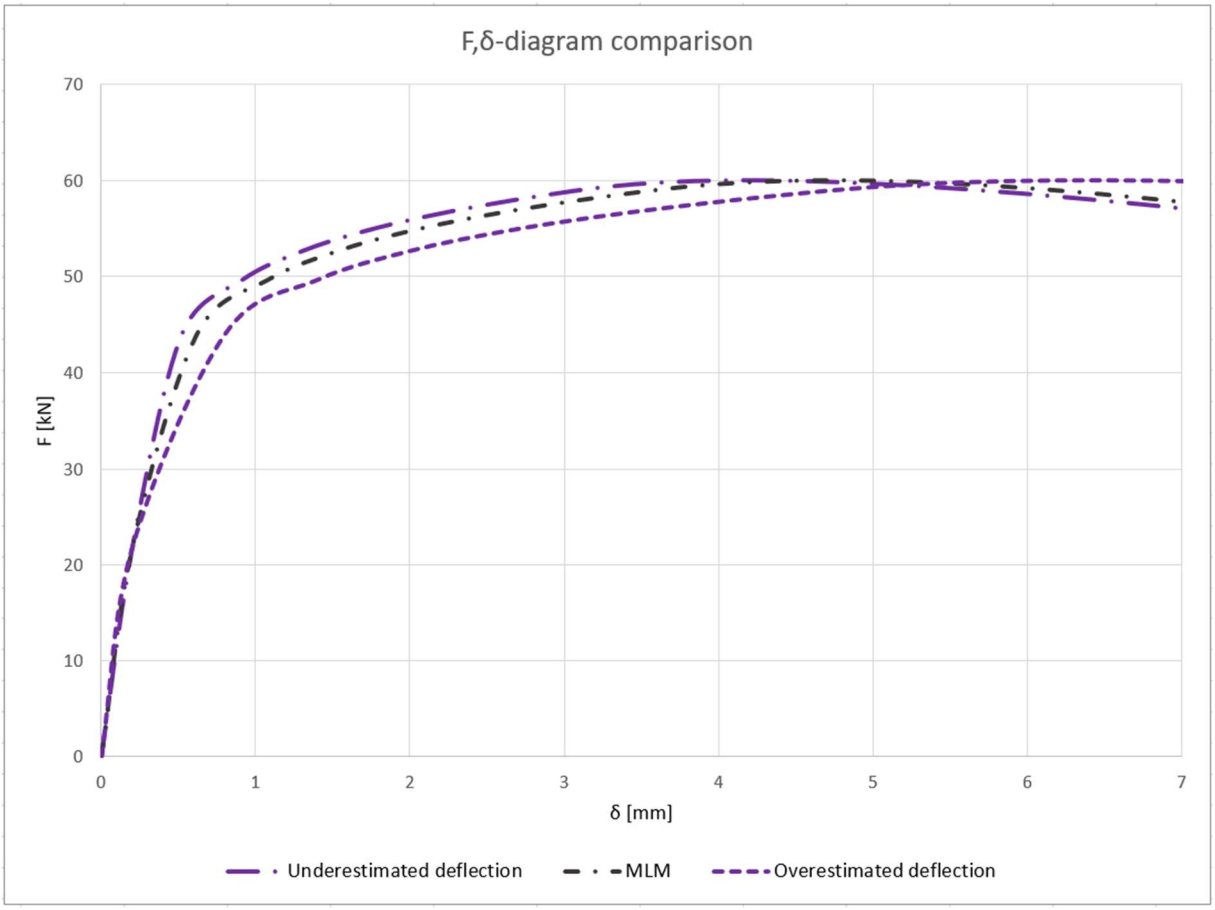

Figure 5-1: comparison of calculated MLM deflection with under- and overestimated deflections

When looking at the results in Figure 5-1, it seems like the under- and overestimated deflection curves cross each other in a way that the overestimated deflection becomes smaller than the underestimated deflection (from a deflection of approximately 5.3 mm and onwards), which

cannot be the case. To explain this, a larger part of the under- and overestimated deflection curves are shown in Figure 5-2.

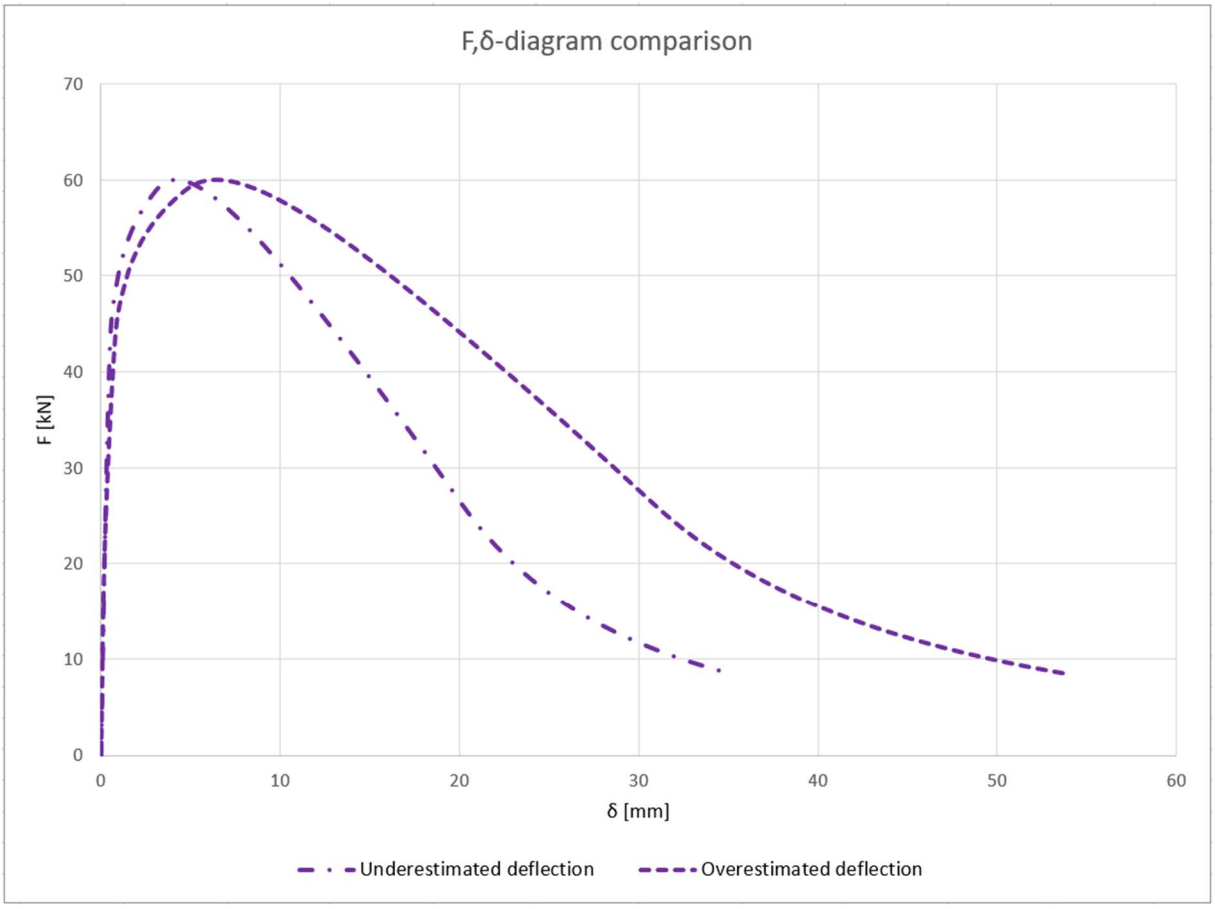

Figure 5-2: comparison between the under- and overestimated deflection curves

Now it becomes clear that both curves are correct. For the same force, the overestimated deflection curve is always on the right of the underestimated deflection curve, which means that the overestimated deflection is always larger than the underestimated deflection.

To go back at the deflection curve that is calculated using the MLM of this research; the curve always lies in between the under- and overestimated curve, so the acquired deflection is logical. Doing the same check for the deflection curve that is found by the MLM that was used by (Lappa, 2007), results in the comparison that is shown in Figure 5-3.

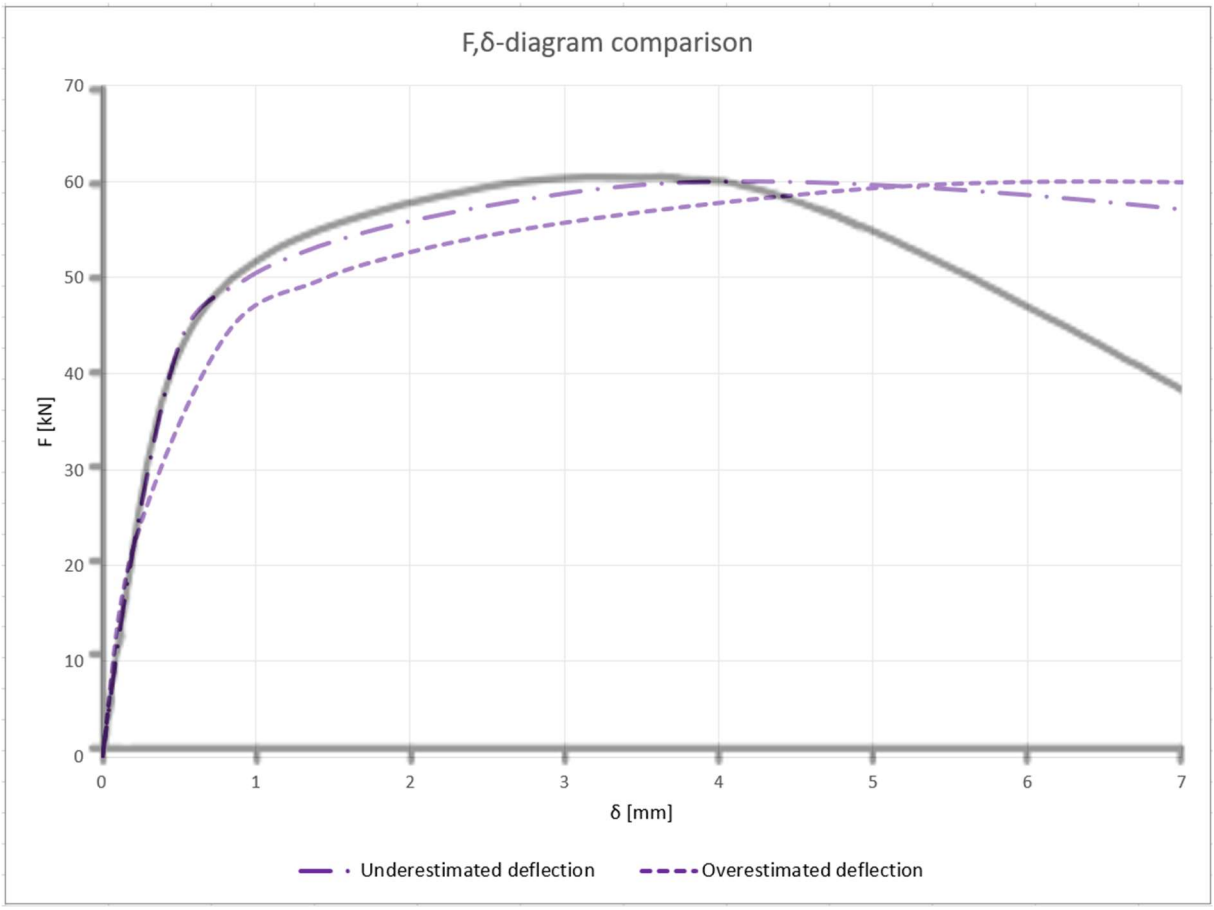

Figure 5-3: : comparison of under- and overestimated deflections with (Lappa, 2007)

As can be seen in Figure 5-3, the deflections as found by (Lappa, 2007) only lie in between the two curves for the beginning stage. After that, this is not the case anymore. As the verification in Figure 4-6 showed that the exact same curves were obtained for the force-to-crack opening displacement curves, it can be concluded that the same input was used in both MLM's. And using this input, the under- and overestimated deflections as in Figure 5-2 are found, which means that the 'real' deflection should lie in between those two curves. That is not the case for the results that are found by (Lappa, 2007).

The deflection is calculated differently in (Lappa, 2007). It is based on rigid body kinematics. Using Figure 3-35, the relationship in Eq. (5.1) is found (Lappa, 2007):

$$\frac{\delta}{w} = \frac{L}{4} \cdot \frac{1}{H} \qquad \textit{Eq. (5.1)}$$

The rotation depth 'H' is a variable that is determined by testing. For an unnotched bending test, it was found that this rotation depth can be assumed to be a constant value in the deflection hardening phase. The author notes that the deflection calculation is mainly suitable for

notched specimens, which could explain the difference that is found when calculating the deflection for the unnotched specimen. Next to that, it is noted that the deflection calculation is a curve fitting approach, which is not the case for the proposed MLM.

5.2. Structural contribution of webs in U-shape

The experimental setups presented in subchapters 4.3 and 4.4, of which the bending resistance was modelled using the MLM, were very similar. The presence of the U-shaped webs is the only difference. Because of that, the results can be compared to investigate the structural contribution of the webs of the U-shape. In both phases, the force-to-displacement diagram was modelled. These diagrams can be used for comparison. The only change is that the diagram that was found for the hybrid beam without a U-shape is not limited anymore by the 10 mm deflection (in the comparison with the experimental results). The comparison is shown in Figure 5-4.

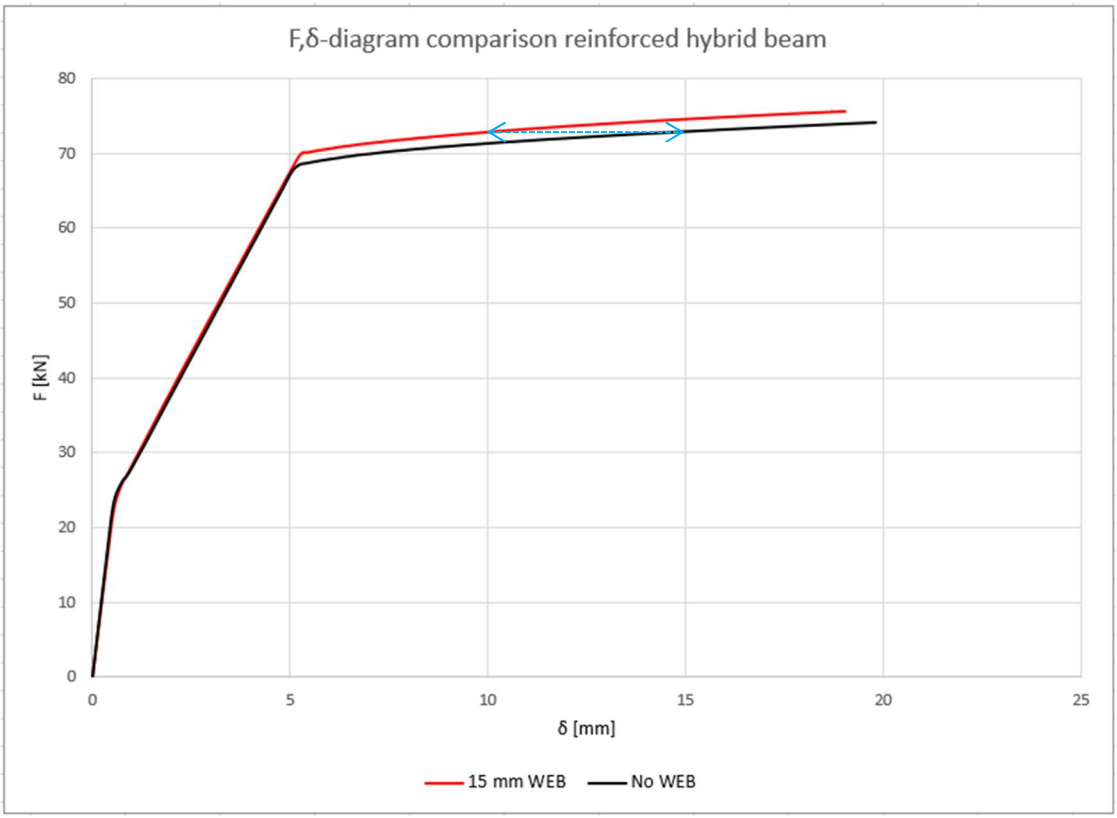

Figure 5-4: comparison between (MLM) modelled phase 3 & phase 4 force-to-displacement diagram

As can be seen in Figure 5-4, the effect on the ultimate force is not large; adding two webs of 15 mm thickness in a beam with a total width of 150 mm does not increase the resistance of the beam by much. The increase comes from the tensile properties of the SHCC (the material that was used in the webs). In the non-linear stage, the neutral axis moves upwards. At some point, the neutral axis reaches a position in which the webs are loaded in tension, and the cracking strain of concrete is exceeded. Then, only the SHCC contributes to the bending resistance. That happens at a deflection of approximately 5 mm in Figure 5-4.

The compressive material input parameters were assumed to be exactly the same for the concrete and the SHCC, so there is no contribution of the SHCC there. That is also why no effect is noticeable in the starting stages of the force-to-displacement curve, as the webs are mostly loaded in compression due to the location of the neutral axis.

However, there is a noticeable effect after a deflection of 5 mm. Because of the shallow slope after this deflection, the small difference in resistance causes a noticeable difference in deflection. As can be seen in Figure 5-4, the difference in deflection can be up to 5 mm when a force of approximately 73 kN is applied (marked in blue).

In short, before failure, the webs in the U-shape contribute by limiting the deflection. The ultimate force that the beam can carry is affected; the webs cause an increased resistance. However, this is not by much.

5.3. Stress-displacement verification

As was shown in subchapter 4.1.2, the verification of the stress-to-displacement diagram was not successful. In order to explain this, a comparison was made with results from an ongoing MSc thesis of Arif. A part of his research is about modelling the bending behaviour of beams in DIANA. One of the specimens that was modelled, was the same specimen that was verified in subchapter 4.1.2. In the MSc thesis, different tensile input is assumed to model this beam. This is shown in Figure 5-5.

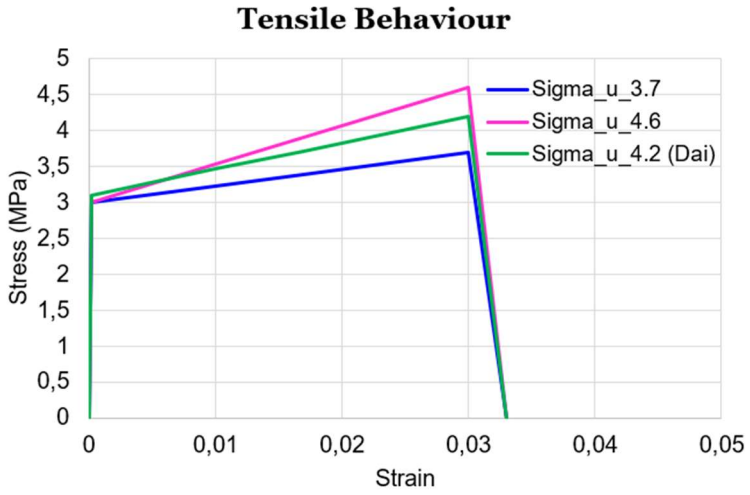

Figure 5-5: assumed tensile input for modelling using DIANA

In this subchapter, the blue line from Figure 5-5 is taken as input for the MLM, to compare with the results that follow from DIANA for this same input. The compressive input is also different from what is assumed in the MLM. This is shown in Figure 5-6.

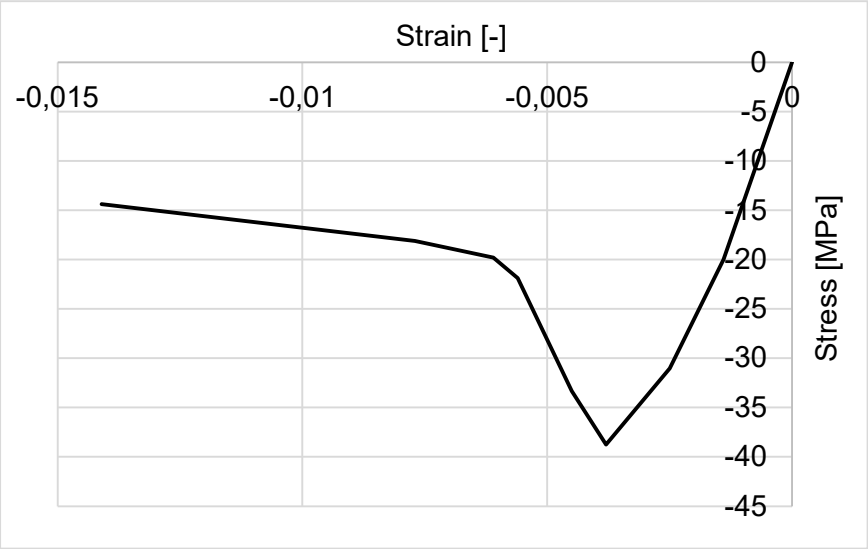

Figure 5-6: assumed compressive input for modelling using DIANA

This results in the input for the MLM that is shown in Figure 5-7.

BEAM INPUT		
Δh	0.05	mm
L	110	mm
L_1	40	mm
L_2	30	mm
h	10	mm
n	100	[-]
t	0.1	mm
b	30	mm
$\Delta\kappa$	1E-4	mm^{-1}
n.a.	5	mm

MATERIALS		
E	18,000	N/mm^2
ρ	2018	Kg/m^3
Tension:		
f_1	3	N/mm^2
ε_1	1.7E-4	[-]
f_2	3.7	N/mm^2
ε_2	0.03	[-]
f_3	0	N/mm^2
ε_3	0.033	[-]
Compression:		
f_1	38	N/mm^2
ε_1	0.004	[-]
f_2	20	N/mm^2
ε_2	0.006	[-]
f_3	15	N/mm^2
ε_3	0.014	[-]

LAYER SPECS		
Top layer	×	
Bottom layer	✓	
Web	×	
t	10	mm

POINTS
130

DEFLECTION		
Test type	4-point	
$\#_{seg}$	500	[-]
b_{seg}	< 0.5	mm

Figure 5-7: input parameters used in the MLM to compare with the results using DIANA

This used input in the MLM results in the stress-to-strain diagram that is shown in Figure 5-8.

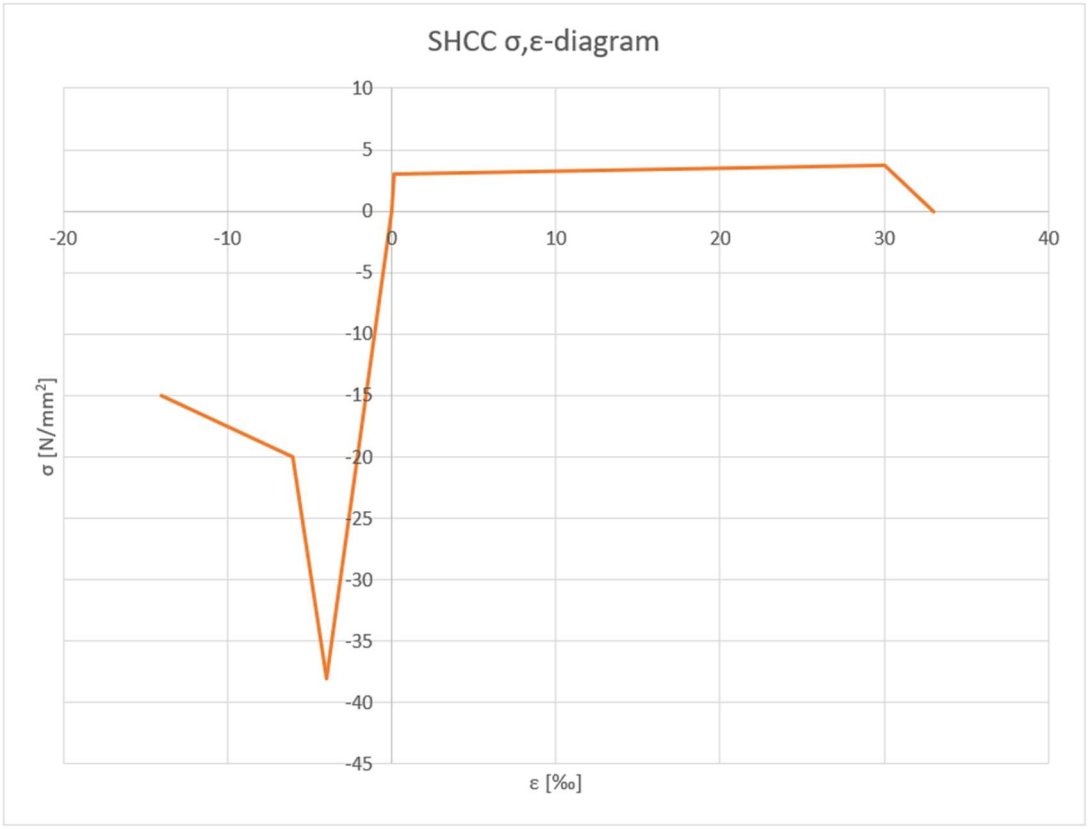

Figure 5-8: assumed SHCC stress-to-strain input to use in the MLM

A comparison with the results that follow from DIANA is shown in Figure 5-9.

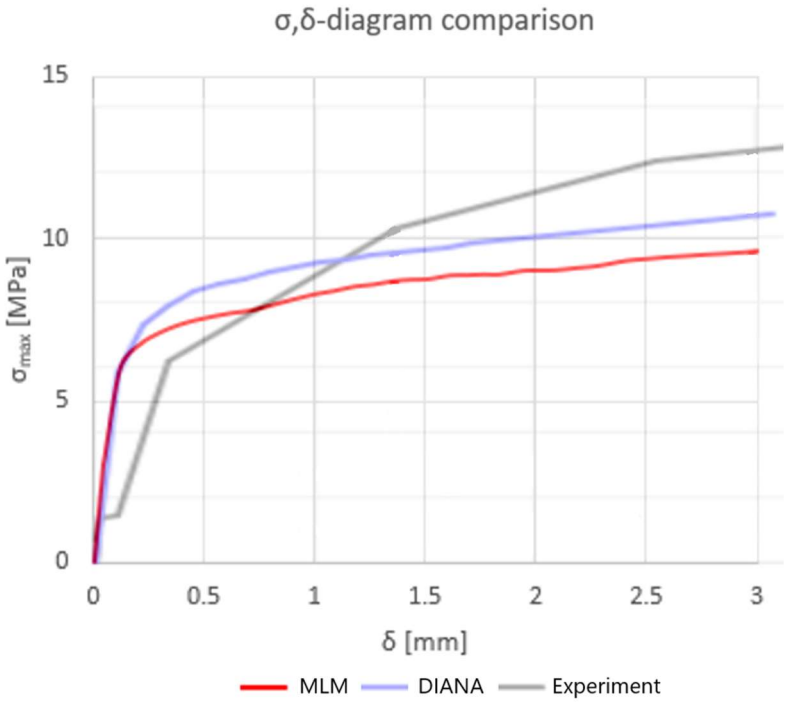

Figure 5-9: comparison between MLM and DIANA results with results from (Zhou, et al., 2010)

As is shown in Figure 5-9, the results from the MLM are very comparable with the results that follow from DIANA. Apart from the flexural strength, the behaviour is exactly the same. It could be the case that the DIANA model accounted for the resistance in the other direction, which explains the difference in strength. However, the result supports the statement that something might have been wrong in the experiment. Performing comparisons with the other input from Figure 5-5 leads to the same conclusion.

The input parameters have already been shown in Figure 5-7. A screenshot of all the input and output of the developed MLM for this comparison is shown in Appendix C.

5.4. MLM limitations

5.4.1. Crack width

The main added value of hybrid beams is the limitation of the crack width. As was explained before, the proposed MLM is able to calculate crack widths, but only for traditionally reinforced concrete beams, as the expressions that are needed for that calculation are known. For other materials, this is unknown, which means that the MLM cannot be used to determine this effect of limiting the crack width. If that would have been possible, the MLM could be used to find the optimal configurations of a hybrid beam in terms of crack width control. This is a limitation of the model, that could be solved if the expressions for calculating the crack width of other materials become known. The MLM will then be more powerful, as it will not only be able to model the bending resistance of each configuration, but also show what the effects are on crack width control. If these expressions become known, they can directly be implemented in the MLM, as the calculation process is already implemented in the MLM; only the expressions have to be changed.

5.4.2. Perfect bond

In the proposed MLM, a perfect bond between two materials in a hybrid beam is assumed. In reality, this will not always be the case. Next to that, a beam could start the experiment with a perfect bond, but after that lose this property. In a way, that is a limitation of the proposed model. Not only because of the dependency of a perfect bond in the experiment, but also because of calculations that are not suitable in the MLM because of the perfect bond. For example, the drying shrinkage calculation is not suitable for hybrid beams due to the assumed perfect bond.

5.4.3. Applicability

The proposed MLM is, as it stands now, suitable for experimental purposes. The calculation method that is applied to calculate the deflections is only useable for 3-point and 4-point bending tests, which typically are only used in experiments. However, the cross-sectional bending moment resistance is independent of the type of loading, so that could be used in practical applications, such as in the construction world.

The implementation of compressive reinforcement in the MLM is something that is very usable as it is also used at the construction site. However, it is assumed that only one row of reinforcement is used as (tensional or compressive) reinforcement. In reality, that is not always the case. Next to that, prestressed reinforcement is not taken into consideration in the MLM, which is used often in practice.

6. Conclusions

The main goal of this report was to be able to develop the 'reinforced hybrid concrete beams with a U-shaped SHCC mould' system and to be able to model the bending behaviour of it using the multi-layer model, including imposed deformations due to drying shrinkage. In order to do that, the basic multi-layer model for non-hybrid beams was rebuilt and expanded to be useable for hybrid beams. Next to that, several calculations were added. The following can be concluded after this research:

- → The added value of an SHCC U-shaped mould with concrete poured in it in comparison to a hybrid section is that formwork at the sides is not needed anymore. This leads to savings of costs.
- → The procedure of making such a U-shaped mould was developed. It consists of two moulds; the smaller mould is placed inside the larger mould, which results in an inverted U-shape after casting.
- → As long as the material input parameters in tension and compression are available, **any** material can be used as input in the multi-layer model. The proposed multi-layer model can handle four datapoints in tension, and three datapoints in compression. Each datapoint is a 'couple' of a stress and a strain to obtain a stress-to-strain input curve. However, the material input parameters are assumed to be unaffected by size effects.
- → The deflection that occurs is calculated using a theory called 'momentvlakstellingen'. The same model is also able to calculate the underestimated deflection based on curvature and the overestimated deflection based on 'forget-me-nots'. For the same input, the deflection curve that follows from the momentvlakstellingen is **always** between the under- and overestimated curve. This means that the obtained deflection is 'logical'.
- → Verification of the model showed that the end resistance of the beams (maximum force in the bending test) is predicted very accurately; also for hybrid beams. The initial stiffness of the beams is equal if the results of the model are compared with the results from the previous research. The differences are mainly in the stages in between. Generally, the same trend is found by the proposed multi-layer model. Or in other words, the slope of the curve that follows from the multi-layer model is very comparable to the slope that follows from the experimental results from previous research. However, the curves do not overlap. So the MLM can be used to accurately predict the end resistance of any (hybrid) beam, as long as the assumptions are the same as for the model. Until the MLM is verified for the hybrid beam containing a U-shaped mould, the results of for these configurations are not reliable.
- → Comparing the modelled results of the proposed experimental setup with a U-shaped mould to a very similar setup in which the only difference was the presence of the U-

shaped webs, showed that the structural contribution of the U-shaped webs is modest in terms of ultimate resistance. The main effect can be seen in the deflection at the end stage; for the same force, the beam containing a U-shape deflects up to 5 mm less than the beam that does not contain a U-shape.

→ Eigenstresses due to drying shrinkage were successfully implemented in the MLM. The results were verified with results obtained by a FEM-model called FEMMASSE. The implementation of the eigen-strains (that result in the eigenstresses) is only suitable for monolithic beams, of which the relative humidity profile is known (external input). The eigen-strains are calculated using the relative humidity profile, or they can directly be used as input. Hybrid beams are not suitable for the drying shrinkage calculation, as the main effect of drying shrinkage would be on the interface between the two materials, which is assumed to be a perfect interface in the proposed MLM.

→ The eigenstresses due to drying shrinkage have a negligible effect on the end resistance of a monolithic beam. The biggest effect is on the beginning stages; for the same force, there is a larger deflection of up to 39% for the same force when a specimen without drying is compared with a specimen that was exposed to 28 days of drying (the specimen that dried for 28 days deflects more).

→ The longitudinal shear calculation is not suitable for hybrid beams containing a U-shape, as the interface between the SHCC (for example) and the concrete is much larger and much different compared to a 'standard' hybrid beam. The shear stress is not only calculated for a certain position over the width, but also along the height. This can be improved in the future.

→ The crack width calculation in the proposed multi-layer model is only applicable for traditionally reinforced concrete beams. This was implemented by using the Eurocode expressions. It is recommended to expand the applicability of the calculation to the interface between the two layers in a hybrid section and to the interface between the bottom layer and the reinforcement (SHCC-steel for example) to be able to calculate the occurring crack width.

→ Implementing the crack width calculations for SHCC for example could lead to a powerful addition to the MLM. It can then also be used to find the most optimal configurations in terms of crack width control. In that way, the most optimal design that (Huang, 2017) found for the SHCC layer thickness could be found by the MLM without performing any experiments. That saves a lot of time. For now, this can already be done for traditionally reinforced beams to determine the most optimal reinforcement amount for reaching a certain bending moment resistance while at the same time meet the crack width requirements.

7. Further research

In this chapter, multiple subjects are proposed for future research.

7.1. Verification U-shaped mould

In chapter 2, an experimental setup was proposed containing a reinforced U-shaped SHCC mould. In subchapter 4.5, the bending resistance of the proposed experimental setup was calculated using the proposed MLM. However, as this type of experiment has never been performed before, the results could not be verified.

It is recommended to use the MLM results to compare with the results that follow from experimenting with this setup. The model can then also be improved and extended. The inclusion of webs in the MLM is already implemented, but again by assuming perfect bond between the SHCC and the concrete.

7.2. Longitudinal shear resistance

As was shown before in subchapter 3.4.7, a calculation of the maximum longitudinal shear stress between the two interfaces (SHCC and concrete for example) was implemented into the MLM. However, the resistance of this bond is not exactly known. If a perfect bond between the two layers is the goal, it should be further investigated what the maximum allowable shear stress is in different configurations. By comparing with the results of the MLM, it can then be stated whether there is a perfect bond or not. The maximum allowable shear stress is then the stress that causes any slip between the two layers. This is illustrated in Figure 7-1.

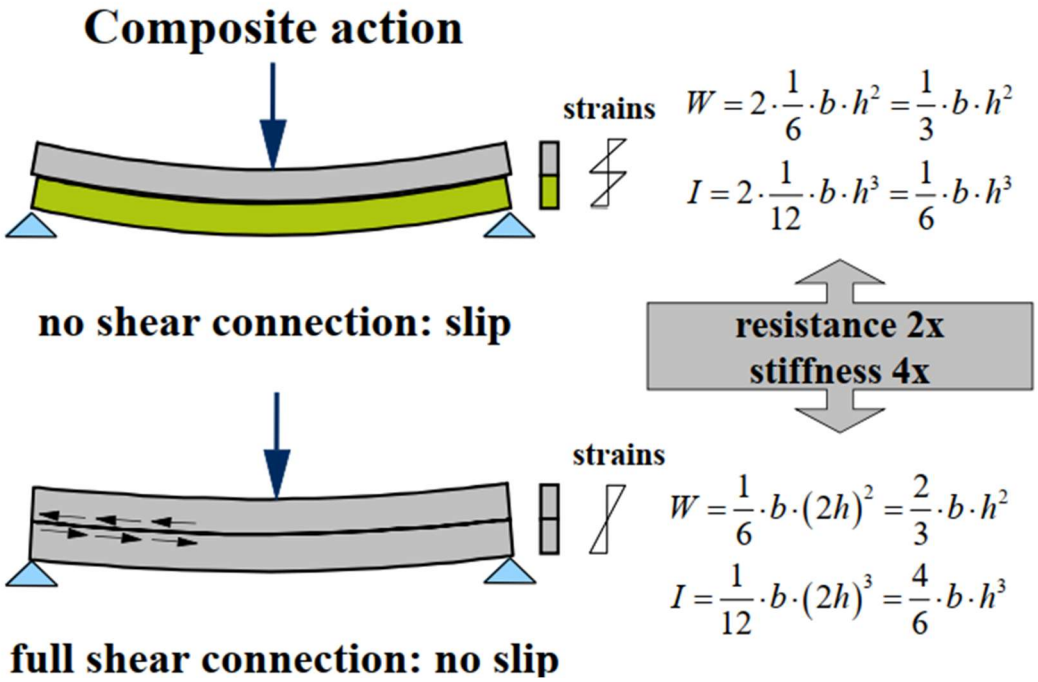

Figure 7-1: property differences between a hybrid beam with no bond and a perfect bond (Abspoel, 2019)

As can be seen in Figure 7-1, there are two extremes. One is a full shear connection, and the other is when there is no connection at all. It is clear that the resistance of the two extremes differs. That also means that the resistance for all situations **between** the two extremes are different. Therefore, if slip occurs, the resistance will go down. Because of this, the maximum allowable shear stress should be the stress at which slip occurs.

If the previously mentioned U-shaped mould is to be investigated, considering the longitudinal shear could add a challenging feature as there will be a much larger interface area between the two materials (SHCC and concrete for example). Next to that, the shear stress is not only calculated for a certain position over the width, but also along the height. It is recommended to implement this in the proposed MLM.

7.3. Crack width

In subchapter 7.2, it was explained that a perfect bond between the two layers is desired, as the current version of the MLM is only suitable for that situation. In future research, it could however be implemented in the MLM how the resistance decreases with increased slip. This also means that the effect of the bond on the crack width can be implemented in the MLM. In this research, it was shown how the bond between the steel reinforcement and the concrete was translated into the crack width in the tension zone. An example of those cracks is shown in Figure 7-2 as a DIC-image. In this image, all colors except blue show the strains that lead to cracks. The green colour indicates small strains, while the red colour indicates large strains. So the larger the strains, the more visible the cracks are.

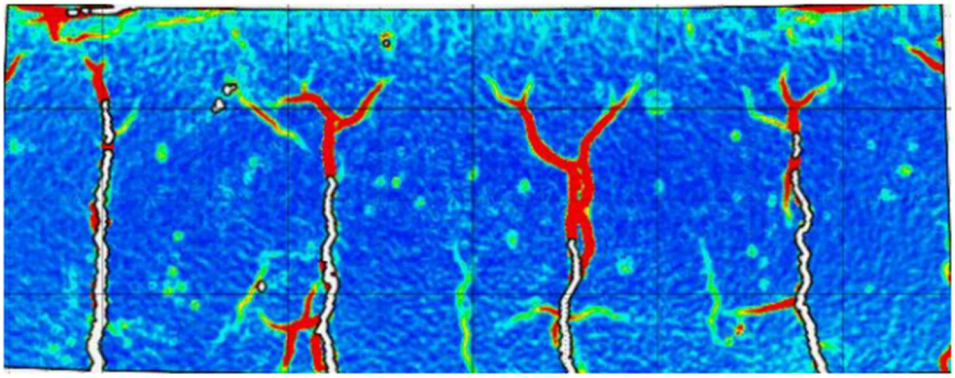

Figure 7-2: regular concrete cracks in a DIC-image (Singh, 2019)

If the bond between the two layers is translated into a crack width, it means that the crack width at the interface between the two layers can be found. Such cracks are illustrated in Figure 7-3. Again, a DIC-image is shown.

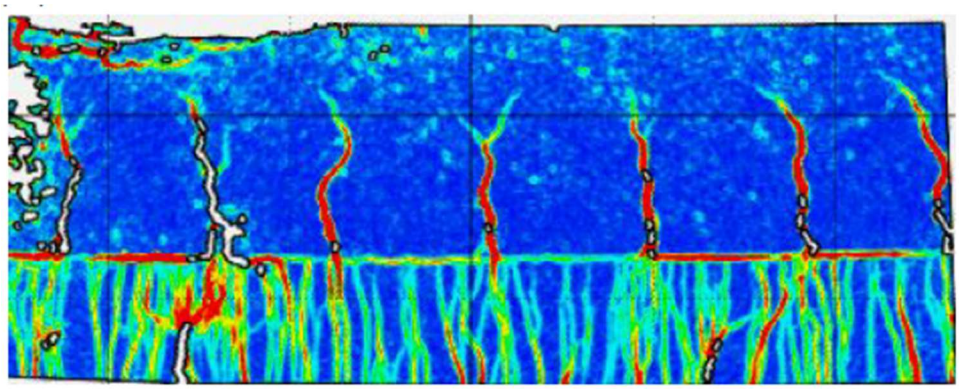

Figure 7-3: interface cracks in a DIC-image (Singh, 2019)

In this thesis, the bond between the steel reinforcement and the concrete was implemented by using an existing expression from the Eurocode. However, those expressions do not exist for the bond between SHCC and concrete, or between SHCC and steel reinforcement. Therefore, future research could be to find such expressions and propose them.

7.4. Drying shrinkage

In this research, the imposed deformations due to drying shrinkage were implemented in the MLM. This was done according to the findings of (Awasthy, 2019). The concept of the U-shaped mould can also be tested in combination with drying shrinkage. For example, what will be the effect of drying shrinkage on the resistance of the beam that is ultimately casted? Those are possible future research questions. This could then also be implemented in the MLM if the recommendation in the previous subchapter is implemented (cases in which there is no perfect bond, as that is a requirement to investigate the effect of drying shrinkage in hybrid beams).

Literature

Abspoel, R. (2019). Steel Structures 3 Introduction of the course [PowerPoint slides]. Retrieved from Delft University of Technology CIE4121 Steel Structures 3.

Awasthy, N. (2019). *Development of Mechanical Properties of Concrete with Time - Experimental and Numerical Study.* Delft.

Blagojević, A. (2016). *The Influence of Cracks on the Durability abd Service Life of Reinforced Concrete Structures in relation to Chloride-Induced Corrosion - A Look from a Different Perspective.* Delft: Ridderprint.

Grünewald, S. (2004). *Performance-based design of self-compacting fibre reinforced concrete.* Delft.

Hajializadeh, D., Eugene, O., Enright, B., & Schiels, E. (2012). *Nonlinear response of structures to characteristic loading scenarios.*

Hanson, J. (1968). Effects of curing and drying environments on splitting tensile strength of concrete. *Journal Proceedings volume 65*, 535-543.

Hartsuijker, C. (2001). *Toegepaste mechanica Deel 2 Spanning, vervormingen, verplaatsingen.* Academic Service, Schoonhoven.

Hartsuijker, C., & Welleman, H. (2013). *Mechanica Statisch onbepaalde constructies en bezwijkanalyse.* BIM Media, Den Haag.

Hendriks, M. A. (2018). Thick plates loaded perpendicular to their plane [PowerPoint slides]. Retrieved from Delft University of Technology CIE4180 Plates and Slabs.

Hordijk, D. A. (1991). *Local approach to fatigue of concrete.* Delft: W.D. Meinema b.v.

Huang, Z. (2017). *Flexural behaviour of reinforced concrete beams with a layer of SHCC in the tension zone - experimental study.* Delft.

Huijben, F., van Herweijnen, F., & Nijsse, R. (2010). VACUUMATICS; Systematic Flexural Rigidity Analysis. *Spatial Structures - Permanent and Temporary*, 8-12.

Jayananda, N. (2017). *Flexural Behaviour of Reinforced Concrete Beams with a Layer of SHCC in the Tension Zone - Numerical Study by ATENA Model.*

Kapteijn, T. (2020). *Feasibility study into the application of wrapped FRP joints on large diameter monopile dolphins - A study into the bending moment capacity of the wrapped pile splice.* Delft.

Kooiman, A. G. (2000). *Modelling Steel Fibre Reinforced Concrete for Structural Design.* Delft: Optima Grafische Communicatie, Rotterdam.

Lappa, E. S. (2007). *High Strength Fibre Reinforced Concrete - Static and fatigue behaviour in bending.* Delft: Gildeprint, Enschede.

Learneasy. (2020, July 16). Retrieved from Learneasy: http://www.learneasy.info/MDME/MEMmods/MEM09155A-CAE/050-Shear-in-Bending/shear-in-bending.html

Li, M., & Li, V. (2011). Behavior of ECC/Concrete Layered Repair System under Drying Shrinkage Conditions. *Journal of Restoration of Buildings and Monuments.*

Luković, M. (2016). *Influence of interface and strain hardening cementitious composite (SHCC) properties on the performance of concrete repairs.* Delft.

Luković, M., & van der Ham, H. (2020). Concrete structures 2 L03 Crack width [PowerPoint slides]. Retrieved from Delft University of Technology CIE3150 Concrete structures 2.

Luković, M., & van der Ham, H. (2020). Concrete structures 2 L04 Crack width [PowerPoint slides]. Retrieved from Delft University of Technology CIE3150 Concrete structures 2.

Luković, M., & van der Ham, H. (2020). Concrete structures 2 L05 Slabs [PowerPoint slides]. Retrieved from Delft University of Technology CIE3150 Concrete structures 2.

Luković, M., Hordijk, D., Huang, Z., & Schlangen, E. (2019). Strain Hardening Cementitious Composite (SHCC) for crack width control in reinforced concrete beams. *HERON Vol. 64*, 181-198.

Moris, P., & Dux, P. (2003). Cracking of plastic concrete. *Australian Journal of Civil Engineering*, 17-21.

NEN. (2011). *NEN-EN 1992-1-1+C2 (nl) Eurocode 2: Design of concrete structures - Part 1-1: General rules and rules for buildings.*

NEN. (2016). *NEN-EN 1992-1-1+C2/NB (nl) National Annex to NEN-EN 1992-1-1+C2 Eurocode 2: Design of concrete structures - Part 1-1: General rules and rules for buildings.*

Paul, S. C., & Babafemi, A. J. (2017). Performance of strain hardening cement-based composite (SHCC) under various exposure conditions. *Cogent Engineering*, 4:1.

Prinsse, S. (2017). *ALKALI -ACTIVATED CONCRETE: Development of material properties (strength and stiffness) and flexural behaviour of reinforced beams over time.* Delft.

Schumacher, P. (2006). *Rotation Capacity of Self-Compacting Steel Fiber Reinforced Concrete.* Delft.

Singh, S. (2019). *Influence of Interface and Type of Strain Hardening Cementitious Composite on Crack Control in SHCC-Concrete Hybrid Beams.* Delft.

Symbolab. (2020, July 15). Retrieved from Symbolab: https://www.symbolab.com/solver/definite-integral-calculator/%5Cfrac%7B12%7D%7Bh%5E%7B2%7D%7D%5Cint_%7B-%5Cfrac%7Bh%7D%7B2%7D%7D%5E%7B%5Cfrac%7Bh%7D%7B2%7D%7D%5Cleft(-4.1483E-9y%5E%7B4%7D%2B6.2342E-19y%5E%7B3%7D-2.6081E-5y%5E%7B2%7D%2B2.0074E-14y%2B1.1011

van Breugel, E. K. (2011). *Concrete Structures under Imposed Thermal and Shrinkage Deformations Theory and Practice.* Delft.

Welleman, H. (2018). Slender Structures Load carrying principles [PowerPoint slides]. Retrieved from Delft University of Technology CIE4190 Analysis of Slender Structures. Delft.

Zhou, J., Qian, S., Beltran, M. G., Ye, G., Breguel, v., Klaas, & Li, V. C. (2010). Development of engineered cementitious composites with limestone powder and blast furnace slag. *Materials and structures 43*, 803-814.

Appendix A: MLM script

First, the programming code is shown of the proposed MLM. After that, the calculations that are made separately by Excel are shown. The programming code is shown in the original font that is used in VBA Excel:

```
Private Sub Layers()

'IMPORTANT NOTE: webs are of the same material as the bottom layer

'#PARAMETERS
Border1 = 42
Points = Range("H23")
L = Range("D3")
NofLayers = Range("D7")
b = Range("D9")
L1 = Range("D4")
L2 = Range("D5")
Segments = Range("M31")
h = Range("D6")

'INITIAL NEUTRAL AXIS POSITION (neutral axis will go up in non-linear stage)
NA = Range("D11")

Density = Range("K15")
DensitySHCC = Range("K17")
DensityS = Range("K19")
E = Range("D15")
ESHCC = Range("D17")
ES = Range("D19")

tTOP = Range("D24")
tBOT = Range("D25")
tWEB = Range("D26")
Pi = Application.WorksheetFunction.Pi()

PhiBOT = Range("D29")
PhiTOP = Range("F29")

'The 'SH' below is the 500 data points limit. To change the limit, expand this + expand the
data in the 'Input' worksheet

'#CLEAR everything before filling the cells again. Note that the numbers below are the parame-
ters + 1

'Don't use "Range(Range("E17"), Range("E24").End(xlToRight)).Clear" instead of line below!
Gaps will then not be taken into consideration
Range("C34:SH41").Clear
Range("C34:SH41").HorizontalAlignment = xlCenter

'When everything is finished, substitute 'SH46' below by 'C46'
Range(Range("B46"), Range("SH46").End(xlDown)).ClearContents

Range(Range("E44"), Range("E44").End(xlToRight)).ClearContents
Range(Range("E42"), Range("E42").End(xlToRight)).ClearContents
Range(Range("E42"), Range("E42").End(xlToRight)).Borders.LineStyle = xlNone

Cells(26, 9).Value = 0

Dim i As Integer

'#LAYERS DEFINITION
```

```
SHCCLayers = Int(tBOT / Range("D8"))

'Choose between the simple and the advanced method
If tBOT / Range("D8") = Int(tBOT / Range("D8")) Then
    For i = 1 To NofLayers
        Cells(Border1 + 3 + i, 2).Value = i
        Cells(Border1 + 3 + i, 3).Value = i * Range("D8") - Range("D8") / 2
    Next i
Else
    For i = 1 To SHCCLayers
        Cells(Border1 + 3 + i, 2).Value = i
        Cells(Border1 + 3 + i, 3).Value = i * Range("D8") - Range("D8") / 2
    Next i

    Cells(Border1 + 3 + (SHCCLayers + 1), 2).Value = SHCCLayers + 1 & "A"
    Cells(Border1 + 3 + (SHCCLayers + 1), 3).Value = tBOT - (tBOT - SHCCLayers * Range("D8"))
/ 2

    Cells(Border1 + 3 + (SHCCLayers + 2), 2).Value = SHCCLayers + 1 & "B"
    Cells(Border1 + 3 + (SHCCLayers + 2), 3).Value = tBOT - (tBOT - SHCCLayers * Range("D8"))
/ 2 + Range("D8") / 2

    For i = SHCCLayers + 2 To NofLayers + 1
        Cells(Border1 + 4 + i, 2).Value = i
        Cells(Border1 + 4 + i, 3).Value = i * Range("D8") - Range("D8") / 2
    Next i
End If

'#START
For i = 1 To 5
    Cells(Border1 - i, 3).Value = 0
Next i

'Manually insert the n.a. value
Cells(Border1 - 6, 3).Value = NA

'#SELF-WEIGHT
q = Density * (tTOP / 1000) * ((b - tWEB) / 1000) * 9.81 / 1000 'N/mm
qSHCC = DensitySHCC * ((tTOP / 1000) * (tWEB / 1000) + (tBOT / 1000) * (b / 1000)) * 9.81 /
1000 'N/mm
qS = DensityS * (Pi / 4 * PhiBOT ^ 2 / 1000000) * 9.81 / 1000 + DensityS * (Pi / 4 * PhiTOP ^
2 / 1000000) * 9.81 / 1000 'N/mm

qtot = q + qSHCC + qS

'Additional moment at all times due to self-weight
MG = 1 / 8 * qtot * L ^ 2

'Iy is considered the moment of inertia around the STRONG axis
Iy = 1 / 12 * (b - 2 * tWEB) * tTOP ^ 3 + ((tBOT + 1 / 2 * tTOP) - NA) ^ 2 * (tTOP * (b - 2 *
tWEB))
IySHCC = 1 / 12 * b * tBOT ^ 3 + (1 / 2 * tBOT - NA) ^ 2 * (tBOT * b)
IyWEB = 2 * (1 / 12 * tWEB * tTOP ^ 3 + ((tBOT + 1 / 2 * tTOP) - NA) ^ 2 * (tTOP * tWEB))
IySBOT = Range("D31") * ((Pi / 4 * (PhiBOT / 2) ^ 4) + (Range("D32") - NA) ^ 2 * (Pi / 4 *
PhiBOT ^ 2))
IySTOP = Range("F31") * ((Pi / 4 * (PhiTOP / 2) ^ 4) + (Range("F32") - NA) ^ 2 * (Pi / 4 *
PhiTOP ^ 2))

EIlinear = (E * Iy + ESHCC * (IySHCC + IyWEB) + ES * (IySBOT + IySTOP))

'Initial displacement due to self-weight
wG = 5 / 384 * qtot * L ^ 4 / EIlinear

Cells(Border1 + 2, 3).Value = MG
Cells(Border1 + 2, 4).Value = MG

Cells(Border1 - 7, 3).Value = wG
```

```
'Show progess in %
Cells(26, 9).Value = 1 / (Points + 2)
'-------------------------------------------------------------------------------------------------
'#INITIAL STRAIN DUE TO DRYING SHRINKAGE

'Determine the slopes between the regions for interpolation:
region1slope = (Range("O12") - Range("O13")) / (Range("N12") - Range("N13"))
region2slope = (Range("O11") - Range("O12")) / (Range("N11") - Range("N12"))
region3slope = (Range("O10") - Range("O11")) / (Range("N10") - Range("N11"))
region4slope = (Range("O9") - Range("O10")) / (Range("N9") - Range("N10"))
region5slope = (Range("O8") - Range("O9")) / (Range("N8") - Range("N9"))
region6slope = (Range("O7") - Range("O8")) / (Range("N7") - Range("N8"))
region7slope = (Range("O6") - Range("O7")) / (Range("N6") - Range("N7"))
region8slope = (Range("O5") - Range("O6")) / (Range("N5") - Range("N6"))

'Determine for each layer what the strain is:

'Choose between the simple and the advanced method
If tBOT / Range("D8") = Int(tBOT / Range("D8")) Then
    For i = 1 To NofLayers
        center = Cells(Border1 + 3 + i, 3)
        If center >= 0 And center < Range("N12") Then
            Cells(Border1 + 3 + i, 4).Value = Range("O13") + center * region1slope
        ElseIf center >= Range("N12") And center < Range("N11") Then
            Cells(Border1 + 3 + i, 4).Value = Range("O12") + (center - Range("N12")) * re-
gion2slope
        ElseIf center >= Range("N11") And center < Range("N10") Then
            Cells(Border1 + 3 + i, 4).Value = Range("O11") + (center - Range("N11")) * re-
gion3slope
        ElseIf center >= Range("N10") And center < Range("N9") Then
            Cells(Border1 + 3 + i, 4).Value = Range("O10") + (center - Range("N10")) * re-
gion4slope
        ElseIf center >= Range("N9") And center < Range("N8") Then
            Cells(Border1 + 3 + i, 4).Value = Range("O9") + (center - Range("N9")) * re-
gion5slope
        ElseIf center >= Range("N8") And center < Range("N7") Then
            Cells(Border1 + 3 + i, 4).Value = Range("O8") + (center - Range("N8")) * re-
gion6slope
        ElseIf center >= Range("N7") And center < Range("N6") Then
            Cells(Border1 + 3 + i, 4).Value = Range("O7") + (center - Range("N7")) * re-
gion7slope
        ElseIf center >= Range("N6") And center <= Range("N5") Then
            Cells(Border1 + 3 + i, 4).Value = Range("O6") + (center - Range("N6")) * re-
gion8slope
        End If
    Next i
Else
    For i = 1 To NofLayers + 1
        center = Cells(Border1 + 3 + i, 3)
        If center >= 0 And center < Range("N12") Then
            Cells(Border1 + 3 + i, 4).Value = Range("O13") + center * region1slope
        ElseIf center >= Range("N12") And center < Range("N11") Then
            Cells(Border1 + 3 + i, 4).Value = Range("O12") + (center - Range("N12")) * re-
gion2slope
        ElseIf center >= Range("N11") And center < Range("N10") Then
            Cells(Border1 + 3 + i, 4).Value = Range("O11") + (center - Range("N11")) * re-
gion3slope
        ElseIf center >= Range("N10") And center < Range("N9") Then
            Cells(Border1 + 3 + i, 4).Value = Range("O10") + (center - Range("N10")) * re-
gion4slope
        ElseIf center >= Range("N9") And center < Range("N8") Then
            Cells(Border1 + 3 + i, 4).Value = Range("O9") + (center - Range("N9")) * re-
gion5slope
        ElseIf center >= Range("N8") And center < Range("N7") Then
            Cells(Border1 + 3 + i, 4).Value = Range("O8") + (center - Range("N8")) * re-
gion6slope
```

```
        ElseIf center >= Range("N7") And center < Range("N6") Then
            Cells(Border1 + 3 + i, 4).Value = Range("O7") + (center - Range("N7")) * re-
gion7slope
        ElseIf center >= Range("N6") And center <= Range("N5") Then
            Cells(Border1 + 3 + i, 4).Value = Range("O6") + (center - Range("N6")) * re-
gion8slope
        End If
    Next i
End If

'Determine what the strain is for the reinforcement:

'bottom reinforcement:
If Range("D32") >= 0 And Range("D32") < Range("N12") Then
    epsSDRYBOT = Range("O13") + Range("D32") * region1slope
ElseIf Range("D32") >= Range("N12") And Range("D32") < Range("N11") Then
    epsSDRYBOT = Range("O12") + (Range("D32") - Range("N12")) * region2slope
ElseIf Range("D32") >= Range("N11") And Range("D32") < Range("N10") Then
    epsSDRYBOT = Range("O11") + (Range("D32") - Range("N11")) * region3slope
ElseIf Range("D32") >= Range("N10") And Range("D32") < Range("N9") Then
    epsSDRYBOT = Range("O10") + (Range("D32") - Range("N10")) * region4slope
ElseIf Range("D32") >= Range("N9") And Range("D32") < Range("N8") Then
    epsSDRYBOT = Range("O9") + (Range("D32") - Range("N9")) * region5slope
ElseIf Range("D32") >= Range("N8") And Range("D32") < Range("N7") Then
    epsSDRYBOT = Range("O8") + (Range("D32") - Range("N8")) * region6slope
ElseIf Range("D32") >= Range("N7") And Range("D32") < Range("N6") Then
    epsSDRYBOT = Range("O7") + (Range("D32") - Range("N7")) * region7slope
ElseIf Range("D32") >= Range("N6") And Range("D32") <= Range("N5") Then
    epsSDRYBOT = Range("O6") + (Range("D32") - Range("N6")) * region8slope
End If

'top reinforcement:
If Range("F32") >= 0 And Range("F32") < Range("N12") Then
    epsSDRYTOP = Range("O13") + Range("F32") * region1slope
ElseIf Range("F32") >= Range("N12") And Range("F32") < Range("N11") Then
    epsSDRYTOP = Range("O12") + (Range("F32") - Range("N12")) * region2slope
ElseIf Range("F32") >= Range("N11") And Range("F32") < Range("N10") Then
    epsSDRYTOP = Range("O11") + (Range("F32") - Range("N11")) * region3slope
ElseIf Range("F32") >= Range("N10") And Range("F32") < Range("N9") Then
    epsSDRYTOP = Range("O10") + (Range("F32") - Range("N10")) * region4slope
ElseIf Range("F32") >= Range("N9") And Range("F32") < Range("N8") Then
    epsSDRYTOP = Range("O9") + (Range("F32") - Range("N9")) * region5slope
ElseIf Range("F32") >= Range("N8") And Range("F32") < Range("N7") Then
    epsSDRYTOP = Range("O8") + (Range("F32") - Range("N8")) * region6slope
ElseIf Range("F32") >= Range("N7") And Range("F32") < Range("N6") Then
    epsSDRYTOP = Range("O7") + (Range("F32") - Range("N7")) * region7slope
ElseIf Range("F32") >= Range("N6") And Range("F32") <= Range("N5") Then
    epsSDRYTOP = Range("O6") + (Range("F32") - Range("N6")) * region8slope
End If
'-----------------------------------------------------------------------------------------
'#LINEAR ELASTIC STAGE

'If the web thickness is equal to half the width, it means that there is no concrete (theoret-
ical situation):
If tWEB = b / 2 Then
    tTOP = 0
End If

'SHCC + CONCRETE:
epsLIM1 = Range("F15")
epsLIM1SHCC = Range("F17")

'Find the curvature that marks the end of the linear elastic stage:
If Range("N22") <> "NONE" Then

    'Choose between the simple and the advanced method
    If tBOT / Range("D8") = Int(tBOT / Range("D8")) Then
```

```
        kappa0 = 9999
        For i = 1 To NofLayers
            epsDRY = Cells(Border1 + 3 + i, 4)

            'Implement bottom layer
            If Cells(Border1 + 3 + i, 3) < tBOT Then
                epsMAX = epsLIM1SHCC
            Else
                epsMAX = epsLIM1
            End If

            epsPOSSIBLE = epsMAX - epsDRY
            kappaMAX = epsPOSSIBLE / (NA - Cells(Border1 + 3 + i, 3))

            If kappaMAX > 0 Then
                If kappaMAX < kappa0 Then
                    kappa0 = kappaMAX
                End If
            End If
        Next i

    Else
        kappaPOSSIBLESHCC = 9999
        For i = 1 To SHCCLayers
            epsDRY = Cells(Border1 + 3 + i, 4)
            epsMAX = epsLIM1SHCC
            epsPOSSIBLE = epsMAX - epsDRY

            kappaMAX = epsPOSSIBLE / (NA - Cells(Border1 + 3 + i, 3))

            If kappaMAX > 0 Then
                If kappaMAX < kappaPOSSIBLESHCC Then
                    kappaPOSSIBLESHCC = kappaMAX
                End If
            End If
        Next i

        kappaPOSSIBLECON = 9999
        For i = SHCCLayers + 2 To NofLayers + 1
            epsDRY = Cells(Border1 + 4 + i, 4)
            epsMAX = epsLIM1
            epsPOSSIBLE = epsMAX - epsDRY

            kappaMAX = epsPOSSIBLE / (NA - Cells(Border1 + 4 + i, 3))

            If kappaMAX > 0 Then
                If kappaMAX < kappaPOSSIBLECON Then
                    kappaPOSSIBLECON = kappaMAX
                End If
            End If
        Next i

        kappa0 = WorksheetFunction.Min(kappaPOSSIBLECON, kappaPOSSIBLESHCC)
    End If
Else

    If tTOP <> 0 Then

        If tBOT >= NA Then
            kappaPOSSIBLESHCC = epsLIM1SHCC / NA

            kappa0 = kappaPOSSIBLESHCC
        Else
            kappaPOSSIBLECON = epsLIM1 / (NA - tBOT)
            kappaPOSSIBLESHCC = epsLIM1SHCC / NA

            kappa0 = WorksheetFunction.Min(kappaPOSSIBLECON, kappaPOSSIBLESHCC)
```

```
        End If

    ElseIf tTOP = 0 Then
        kappa0 = epsLIM1SHCC / NA
    ElseIf tBOT = 0 Then
        kappa0 = epsLIM1 / NA
    End If

End If

Cells(Border1 - 1, 4).Value = kappa0

'Manually insert the n.a. value
Cells(Border1 - 6, 4).Value = NA

'Slopes of stress-strain diagrams (both are also for compression in the first part, so rc1 =
rc1min!)
rc1 = Range("E15") / epsLIM1
rc1SHCC = Range("E17") / epsLIM1SHCC

'+3 below is to include steel reinforcement (one for bottom layer; one for top layer) +
'if advanced method is used (if the simple method is used, there will be one empty cell)
Dim arrN() As Long
ReDim arrN(0 To NofLayers + 3)
Dim arrM() As Long
ReDim arrM(0 To NofLayers + 3)

'Choose between the simple and the advanced method
If tBOT / Range("D8") = Int(tBOT / Range("D8")) Then
    For i = 1 To NofLayers
        eps = (NA - Cells(Border1 + 3 + i, 3)) * kappa0

        'Implement bottom layer
        If Cells(Border1 + 3 + i, 3) < tBOT Then
            Sigma = rc1SHCC * eps
        Else
            'SigmaSHCC below also includes compressive resistance:
            SigmaSHCC = rc1SHCC * eps
            SigmaCON = rc1 * eps
            Sigma = (2 * tWEB) / b * SigmaSHCC + (1 - (2 * tWEB) / b) * SigmaCON
        End If

        arrN(i) = Sigma * Range("D8") * b
        arrM(i) = arrN(i) * (NA - Cells(Border1 + 3 + i, 3))
    Next i
Else
    'SHCC:
    For i = 1 To SHCCLayers
        eps = (NA - Cells(Border1 + 3 + i, 3)) * kappa0
        Sigma = rc1SHCC * eps

        arrN(i) = Sigma * Range("D8") * b
        arrM(i) = arrN(i) * (NA - Cells(Border1 + 3 + i, 3))
    Next i

    'Partial SHCC:
    eps = (NA - Cells(Border1 + 3 + (SHCCLayers + 1), 3)) * kappa0
    Sigma = rc1SHCC * eps

    arrN(SHCCLayers + 1) = Sigma * (tBOT / Range("D8") - SHCCLayers) * Range("D8") * b
    arrM(SHCCLayers + 1) = arrN(SHCCLayers + 1) * (NA - Cells(Border1 + 3 + (SHCCLayers + 1),
3))

    'Partial CONCRETE (+WEBS):
    eps = (NA - Cells(Border1 + 3 + (SHCCLayers + 2), 3)) * kappa0
    SigmaSHCC = rc1SHCC * eps
    SigmaCON = rc1 * eps
```

```
    Sigma = (2 * tWEB) / b * SigmaSHCC + (1 - (2 * tWEB) / b) * SigmaCON

    arrN(SHCCLayers + 2) = Sigma * (1 - (tBOT / Range("D8") - SHCCLayers)) * Range("D8") * b
    arrM(SHCCLayers + 2) = arrN(SHCCLayers + 2) * (NA - Cells(Border1 + 3 + (SHCCLayers + 2),
3))

    'CONCRETE (+WEBS):
    For i = SHCCLayers + 2 To NofLayers + 1
        eps = (NA - Cells(Border1 + 4 + i, 3)) * kappa0
        SigmaSHCC = rc1SHCC * eps
        SigmaCON = rc1 * eps
        Sigma = (2 * tWEB) / b * SigmaSHCC + (1 - (2 * tWEB) / b) * SigmaCON

        arrN(i + 1) = Sigma * Range("D8") * b
        arrM(i + 1) = arrN(i + 1) * (NA - Cells(Border1 + 4 + i, 3))
    Next i
End If

'STEEL REINFORCEMENT:
epsLIM1S = Range("F19")
rc1S = Range("E19") / epsLIM1S

'Bottom reinforcement:
AreaSBOT = Pi / 4 * PhiBOT ^ 2 * Range("D31")
epsSBOT = (NA - Range("D32")) * kappa0
SigmaSBOT = rc1S * epsSBOT
arrN(NofLayers + 2) = SigmaSBOT * AreaSBOT
arrM(NofLayers + 2) = arrN(NofLayers + 2) * (NA - Range("D32"))

Cells(Border1 - 8, 4).Value = SigmaSBOT * AreaSBOT

'Top reinforcement:
AreaSTOP = Pi / 4 * PhiTOP ^ 2 * Range("F31")
epsSTOP = (NA - Range("F32")) * kappa0
SigmaSTOP = rc1S * epsSTOP
arrN(NofLayers + 3) = SigmaSTOP * AreaSTOP
arrM(NofLayers + 3) = arrN(NofLayers + 3) * (NA - Range("F32"))

'-----------------------------------
''Show Delta - N'S FOR FIRST STEP
'For n = 1 To NofLayers + 3
'    Cells(50 + n, 5).Value = arrN(n)
'Next n

''Show Delta - M'S FOR FIRST STEP
'For n = 1 To NofLayers + 3
'    Cells(50 + n, 6).Value = arrM(n)
'Next n
'-----------------------------------

'#SUM OF N
Cells(Border1 - 3, 4).Value = WorksheetFunction.Sum(arrN)

'#CALCULATE MOMENT
Mlinear = WorksheetFunction.Sum(arrM)
Cells(Border1 - 5, 4).Value = Mlinear

'#CALCULATE APPLIED FORCE; note that moment due to selfweight is reduced from occuring moment
If Range("M30") = "4-point" Then
    'M=FL/6
    Flinear = 6 * (Cells(Border1 - 5, 4) - MG) / L
Else
    'M=FL/4
    Flinear = 4 * (Cells(Border1 - 5, 4) - MG) / L
End If

Cells(Border1 - 4, 4).Value = Flinear
```

```
'#CALCULATE DISPLACEMENT (using Momentvlakstellingen):
If Range("M30") = "4-point" Then
    'Reduced moment diagram consists of ONLY 3 constant parts: Area1 and Area7 are triangles;
Area4 is a rectangle
    Theta1 = 1 / 2 * (Mlinear - MG) / EIlinear * L1
    Theta4 = (Mlinear - MG) / EIlinear * L2
    Theta7 = Theta1

    Distance1 = L - 2 / 3 * L1
    Distance4 = L / 2
    Distance7 = 2 / 3 * L1

    'All thetas times their distances are equal to PhiA times L (so that the displacement at
the second support = 0
    PhiA = (Theta1 * Distance1 + Theta4 * Distance4 + Theta7 * Distance7) / L

    'Split Theta4 in two to get the deflection at midspan
    Theta4B = Theta4 / 2

    w = PhiA * L / 2 - Theta1 * (Distance1 - L / 2) - Theta4B * L2 / 4
Else
    'Reduced moment diagram consists of ONLY 2 constant parts: Area1 and Area7 are triangles
    Theta1 = 1 / 2 * (Mlinear - MG) / EIlinear * L1
    Theta7 = Theta1

    Distance1 = L - 2 / 3 * L1
    Distance7 = 2 / 3 * L1

    'All thetas times their distances are equal to PhiA times L (so that the displacement at
the second support = 0
    PhiA = (Theta1 * Distance1 + Theta7 * Distance7) / L

    w = PhiA * L / 2 - Theta1 * (Distance1 - L / 2)
End If

Cells(Border1 - 7, 4).Value = w + wG

''#CALCULATE STRAIN AT TOP
'Cells(Border1 - 8, 4).Value = -kappa0 * (h - NA)

'Show progess in %
Cells(26, 9).Value = 2 / (Points + 2)

'Implement the case that the initial drying shrinkage strain is exceeding the linear elastic
stage:
epsDRYmax = Range("O13")

If tTOP = 0 And epsDRYmax >= epsLIM1SHCC Then
    Cells(Border1 - 7, 4).Value = wG

    For i = 1 To 5
        Cells(Border1 - i, 4).Value = 0
    Next i

    kappa0 = 0
ElseIf tBOT = 0 And epsDRYmax >= epsLIM1 Then
    Cells(Border1 - 7, 4).Value = wG

    For i = 1 To 5
        Cells(Border1 - i, 4).Value = 0
    Next i

    kappa0 = 0
ElseIf tBOT <> 0 Then
    If epsDRYmax >= epsLIM1SHCC Then
        Cells(Border1 - 7, 4).Value = wG
```

```
        For i = 1 To 5
            Cells(Border1 - i, 4).Value = 0
        Next i

        kappa0 = 0
    Else
        'Note that tBOT is used as that marks the bottom of the top layer
        If tBOT >= 0 And tBOT < Range("N12") Then
            epsDRYmax = Range("O13") + tBOT * region1slope
        ElseIf tBOT >= Range("N12") And tBOT < Range("N11") Then
            epsDRYmax = Range("O12") + (tBOT - Range("N12")) * region2slope
        ElseIf tBOT >= Range("N11") And tBOT < Range("N10") Then
            epsDRYmax = Range("O11") + (tBOT - Range("N11")) * region3slope
        ElseIf tBOT >= Range("N10") And tBOT < Range("N9") Then
            epsDRYmax = Range("O10") + (tBOT - Range("N10")) * region4slope
        ElseIf tBOT >= Range("N9") And tBOT < Range("N8") Then
            epsDRYmax = Range("O9") + (tBOT - Range("N9")) * region5slope
        ElseIf tBOT >= Range("N8") And tBOT < Range("N7") Then
            epsDRYmax = Range("O8") + (tBOT - Range("N8")) * region6slope
        ElseIf tBOT >= Range("N7") And tBOT < Range("N6") Then
            epsDRYmax = Range("O7") + (tBOT - Range("N7")) * region7slope
        ElseIf tBOT >= Range("N6") And tBOT <= Range("N5") Then
            epsDRYmax = Range("O6") + (tBOT - Range("N6")) * region8slope
        End If

        If epsDRYmax >= epsLIM1 Then
            Cells(Border1 - 7, 4).Value = wG

            For i = 1 To 5
                Cells(Border1 - i, 4).Value = 0
            Next i

            kappa0 = 0
        End If
    End If
End If

'-----------------------------------------------------------------------------------------------
'NON-LINEAR STAGE

'+3 below is to include steel reinforcement (one for bottom layer; one for top layer) +
'if advanced method is used (if the simple method is used, there will be one empty cell)
Dim arrN1() As Long
ReDim arrN1(0 To NofLayers + 3)
Dim arrN2() As Long
ReDim arrN2(0 To NofLayers + 3)

If tTOP <> 0 Then
    'Choose between crack inclusion or exclusion for concrete:
    If Range("L26") = "NO" And Range("G15") <> "" Then
        epsLIM2 = Range("H15")

        'Slope of stress-strain diagram (rcmin1 = rc1 -> see L.E. stage)
        rc2 = (Range("G15") - Range("E15")) / (epsLIM2 - epsLIM1)

        'Add possible third point in tension
        If Range("I15") <> "" Then
            epsLIM3 = Range("J15")
            rc3 = (Range("I15") - Range("G15")) / (epsLIM3 - epsLIM2)
        End If
    ElseIf Range("L26") = "YES" And Range("G15") <> "" And Range("N26") = "" Then
        epsLIM2 = Range("H15")

        'Slope of stress-strain diagram (rcmin1 = rc1 -> see L.E. stage)
        rc2 = (Range("G15") - Range("E15")) / (epsLIM2 - epsLIM1)
```

```
        epsLIM3 = Range("S26")
        rc3 = (Range("R26") - Range("G15")) / (epsLIM3 - epsLIM2)
    ElseIf Range("L26") = "YES" And Range("G15") = "" And Range("N26") <> "" Then
        epsLIM2 = Range("P26")

        'Slope of stress-strain diagram (rcmin1 = rc1 -> see L.E. stage)
        rc2 = (Range("O26") - Range("E15")) / (epsLIM2 - epsLIM1)

        epsLIM3 = Range("S26")
        rc3 = (Range("R26") - Range("O26")) / (epsLIM3 - epsLIM2)
    ElseIf Range("L26") = "YES" And Range("G15") <> "" And Range("N26") <> "" Then
        epsLIM2 = Range("H15")

        'Slope of stress-strain diagram (rcmin1 = rc1 -> see L.E. stage)
        rc2 = (Range("G15") - Range("E15")) / (epsLIM2 - epsLIM1)

        epsLIM3 = Range("P26")
        rc3 = (Range("O26") - Range("G15")) / (epsLIM3 - epsLIM2)

        epsLIM4 = Range("S26")
        rc4 = (Range("R26") - Range("O26")) / (epsLIM4 - epsLIM3)
    ElseIf Range("L26") = "YES" And Range("G15") = "" And Range("N26") = "" Then
        epsLIM2 = Range("S26")

        'Slope of stress-strain diagram (rcmin1 = rc1 -> see L.E. stage)
        rc2 = (Range("R26") - Range("E15")) / (epsLIM2 - epsLIM1)
    End If
End If

If tBOT <> 0 Or tWEB <> 0 Then
    'Choose between crack inclusion or exclusion for SHCC:
    If Range("L27") = "NO" And Range("G17") <> "" Then
        epsLIM2SHCC = Range("H17")

        'Slope of stress-strain diagram
        rc2SHCC = (Range("G17") - Range("E17")) / (epsLIM2SHCC - epsLIM1SHCC)

        'Add possible third point in tension
        If Range("I17") <> "" Then
            epsLIM3SHCC = Range("J17")
            rc3SHCC = (Range("I17") - Range("G17")) / (epsLIM3SHCC - epsLIM2SHCC)
        End If
    ElseIf Range("L27") = "YES" And Range("G17") <> "" And Range("N27") = "" Then
        epsLIM2SHCC = Range("H17")

        'Slope of stress-strain diagram
        rc2SHCC = (Range("G17") - Range("E17")) / (epsLIM2SHCC - epsLIM1SHCC)

        epsLIM3SHCC = Range("S27")
        rc3SHCC = (Range("R27") - Range("G17")) / (epsLIM3SHCC - epsLIM2SHCC)
    ElseIf Range("L27") = "YES" And Range("N27") <> "" Then
        epsLIM2SHCC = Range("P27")

        'Slope of stress-strain diagram
        rc2SHCC = (Range("O27") - Range("E17")) / (epsLIM2SHCC - epsLIM1SHCC)

        epsLIM3SHCC = Range("S27")
        rc3SHCC = (Range("R27") - Range("O27")) / (epsLIM3SHCC - epsLIM2SHCC)
    ElseIf Range("L27") = "YES" And Range("G17") <> "" And Range("N27") <> "" Then
        epsLIM2SHCC = Range("H17")

        'Slope of stress-strain diagram
        rc2SHCC = (Range("G17") - Range("E17")) / (epsLIM2SHCC - epsLIM1SHCC)

        epsLIM3SHCC = Range("P27")
        rc3SHCC = (Range("O27") - Range("G17")) / (epsLIM3SHCC - epsLIM2SHCC)
```

```
        epsLIM4SHCC = Range("S27")
        rc4SHCC = (Range("R27") - Range("O27")) / (epsLIM4SHCC - epsLIM3SHCC)
    ElseIf Range("L27") = "YES" And Range("G17") = "" And Range("N27") = "" Then
        epsLIM2SHCC = Range("S27")

        'Slope of stress-strain diagram (rcmin1 = rc1 -> see L.E. stage)
        rc2 = (Range("R27") - Range("E17")) / (epsLIM2 - epsLIM1)
    End If
End If

epsLIMmin1 = -Range("F16")

epsLIMmin1SHCC = -Range("F18")

epsLIMmin1S = -Range("F20")
epsLIMmin2S = -Range("H20")
epsLIM2S = Range("H19")

'Slopes of stress-strain diagrams
rcmin2S = (-Range("E20") - -Range("G20")) / (epsLIMmin1S - epsLIMmin2S)
rc2S = (Range("G19") - Range("E19")) / (epsLIM2S - epsLIM1S)

'Use conditions for second and/or third compression point (in case it is not necessary so the
code does not crash):

'CONCRETE:
If Range("G16") <> "" And Range("I16") = "" Then
    epsLIMmin2 = -Range("H16")
    rcmin2 = (-Range("E16") - -Range("G16")) / (epsLIMmin1 - epsLIMmin2)
ElseIf Range("G16") <> "" And Range("I16") <> "" Then
    epsLIMmin2 = -Range("H16")
    rcmin2 = (-Range("E16") - -Range("G16")) / (epsLIMmin1 - epsLIMmin2)

    epsLIMmin3 = -Range("J16")
    rcmin3 = (-Range("G16") - -Range("I16")) / (epsLIMmin2 - epsLIMmin3)
End If

'SHCC:
If Range("G18") <> "" And Range("I18") = "" Then
    epsLIMmin2SHCC = -Range("H18")
    rcmin2SHCC = (-Range("E18") - -Range("G18")) / (epsLIMmin1SHCC - epsLIMmin2SHCC)
ElseIf Range("G18") <> "" And Range("I18") <> "" Then
    epsLIMmin2SHCC = -Range("H18")
    rcmin2SHCC = (-Range("E18") - -Range("G18")) / (epsLIMmin1SHCC - epsLIMmin2SHCC)

    epsLIMmin3SHCC = -Range("J18")
    rcmin3SHCC = (-Range("G18") - -Range("I18")) / (epsLIMmin2SHCC - epsLIMmin3SHCC)
End If

'MAXIMUM NUMBER OF STEPS
deltah = Range("D2")
Steps = (h - NA) / deltah
deltakappa = Range("D10")

'n.a. before the first iteration (end of LE-stage)
naSTEP = NA

For n = 1 To Points
    Cells(Border1, 4 + n).Value = n
    Cells(Border1 + 2, 4 + n).Value = MG

    kappa = kappa0 + n * deltakappa
    For j = 1 To Steps
        NA1 = naSTEP + (j - 1) * deltah
        NA2 = naSTEP + j * deltah

        'Choose between the simple and the advanced method
```

```
        If tBOT / Range("D8") = Int(tBOT / Range("D8")) Then
            For i = 1 To NofLayers

            'SHCC + CONCRETE:
                'First of two parts that will be compared
                epsDRY = Cells(Border1 + 3 + i, 4)
                epsLOAD = (NA1 - Cells(Border1 + 3 + i, 3)) * kappa

                eps = epsDRY + epsLOAD

                If Cells(Border1 + 3 + i, 3) < tBOT Then
                    'SHCC bottom layer:
                    If eps >= epsLIMmin3SHCC And eps < epsLIMmin2SHCC Then
                        Sigma = -Range("G18") + rcmin3SHCC * (eps - epsLIMmin2SHCC)
                    ElseIf eps >= epsLIMmin2SHCC And eps < epsLIMmin1SHCC Then
                        Sigma = -Range("E18") + rcmin2SHCC * (eps - epsLIMmin1SHCC)
                    ElseIf eps >= epsLIMmin1SHCC And eps <= epsLIM1SHCC Then
                        Sigma = rc1SHCC * eps
                    ElseIf eps > epsLIM1SHCC And eps <= epsLIM2SHCC Then
                        Sigma = Range("E17") + rc2SHCC * (eps - epsLIM1SHCC)
                    'ElseIf below only fulfilled if there is a third point in tension (other-
wise the statement is never fulfilled)
                    ElseIf eps > epsLIM2SHCC And eps <= epsLIM3SHCC Then
                        Sigma = Range("G17") + rc3SHCC * (eps - epsLIM2SHCC)
                    'ElseIf below only fulfilled if there is a fourth point in tension (other-
wise the statement is never fulfilled)
                    ElseIf eps > epsLIM3SHCC And eps <= epsLIM4SHCC Then
                        Sigma = Range("O27") + rc4SHCC * (eps - epsLIM3SHCC)
                    Else
                        Sigma = 0
                    End If
                Else
                    'SHCC web (if present):
                    If eps >= epsLIMmin3SHCC And eps < epsLIMmin2SHCC Then
                        SigmaSHCC = -Range("G18") + rcmin3SHCC * (eps - epsLIMmin2SHCC)
                    ElseIf eps >= epsLIMmin2SHCC And eps < epsLIMmin1SHCC Then
                        SigmaSHCC = -Range("E18") + rcmin2SHCC * (eps - epsLIMmin1SHCC)
                    ElseIf eps >= epsLIMmin1SHCC And eps <= epsLIM1SHCC Then
                        SigmaSHCC = rc1SHCC * eps
                    ElseIf eps > epsLIM1SHCC And eps <= epsLIM2SHCC Then
                        SigmaSHCC = Range("E17") + rc2SHCC * (eps - epsLIM1SHCC)
                    'ElseIf below only fulfilled if there is a third point in tension (other-
wise the statement is never fulfilled)
                    ElseIf eps > epsLIM2SHCC And eps <= epsLIM3SHCC Then
                        SigmaSHCC = Range("G17") + rc3SHCC * (eps - epsLIM2SHCC)
                    'ElseIf below only fulfilled if there is a fourth point in tension (other-
wise the statement is never fulfilled)
                    ElseIf eps > epsLIM3SHCC And eps <= epsLIM4SHCC Then
                        SigmaSHCC = Range("O27") + rc4SHCC * (eps - epsLIM3SHCC)
                    Else
                        SigmaSHCC = 0
                    End If

                    'CONCRETE:
                    If eps >= epsLIMmin3 And eps < epsLIMmin2 Then
                        SigmaCON = -Range("G16") + rcmin3 * (eps - epsLIMmin2)
                    ElseIf eps >= epsLIMmin2 And eps < epsLIMmin1 Then
                        SigmaCON = -Range("E16") + rcmin2 * (eps - epsLIMmin1)
                    ElseIf eps >= epsLIMmin1 And eps <= epsLIM1 Then
                        SigmaCON = rc1 * eps
                    ElseIf eps > epsLIM1 And eps <= epsLIM2 Then
                        SigmaCON = Range("E15") + rc2 * (eps - epsLIM1)
                    'ElseIf below only fulfilled if there is a third point in tension (other-
wise the statement is never fulfilled)
                    ElseIf eps > epsLIM2 And eps <= epsLIM3 Then
                        SigmaCON = Range("G15") + rc3 * (eps - epsLIM2)
```

```
                    'ElseIf below only fulfilled if there is a fourth point in tension (other-
wise the statement is never fulfilled)
                    ElseIf eps > epsLIM3 And eps <= epsLIM4 Then
                        SigmaCON = Range("O26") + rc4 * (eps - epsLIM3)
                    Else
                        SigmaCON = 0
                    End If

                    Sigma = (2 * tWEB) / b * SigmaSHCC + (1 - (2 * tWEB) / b) * SigmaCON

                End If

                arrN1(i) = Sigma * Range("D8") * b

                'Second of two parts that will be compared
                epsDRY = Cells(Border1 + 3 + i, 4)
                epsLOAD = (NA2 - Cells(Border1 + 3 + i, 3)) * kappa

                eps = epsDRY + epsLOAD

                If Cells(Border1 + 3 + i, 3) < tBOT Then
                    'SHCC bottom layer:
                    If eps >= epsLIMmin3SHCC And eps < epsLIMmin2SHCC Then
                        Sigma = -Range("G18") + rcmin3SHCC * (eps - epsLIMmin2SHCC)
                    ElseIf eps >= epsLIMmin2SHCC And eps < epsLIMmin1SHCC Then
                        Sigma = -Range("E18") + rcmin2SHCC * (eps - epsLIMmin1SHCC)
                    ElseIf eps >= epsLIMmin1SHCC And eps <= epsLIM1SHCC Then
                        Sigma = rc1SHCC * eps
                    ElseIf eps > epsLIM1SHCC And eps <= epsLIM2SHCC Then
                        Sigma = Range("E17") + rc2SHCC * (eps - epsLIM1SHCC)
                    'ElseIf below only fulfilled if there is a third point in tension (other-
wise the statement is never fulfilled)
                    ElseIf eps > epsLIM2SHCC And eps <= epsLIM3SHCC Then
                        Sigma = Range("G17") + rc3SHCC * (eps - epsLIM2SHCC)
                    'ElseIf below only fulfilled if there is a fourth point in tension (other-
wise the statement is never fulfilled)
                    ElseIf eps > epsLIM3SHCC And eps <= epsLIM4SHCC Then
                        Sigma = Range("O27") + rc4SHCC * (eps - epsLIM3SHCC)
                    Else
                        Sigma = 0
                    End If
                Else
                    'SHCC web (if present):
                    If eps >= epsLIMmin3SHCC And eps < epsLIMmin2SHCC Then
                        SigmaSHCC = -Range("G18") + rcmin3SHCC * (eps - epsLIMmin2SHCC)
                    ElseIf eps >= epsLIMmin2SHCC And eps < epsLIMmin1SHCC Then
                        SigmaSHCC = -Range("E18") + rcmin2SHCC * (eps - epsLIMmin1SHCC)
                    ElseIf eps >= epsLIMmin1SHCC And eps <= epsLIM1SHCC Then
                        SigmaSHCC = rc1SHCC * eps
                    ElseIf eps > epsLIM1SHCC And eps <= epsLIM2SHCC Then
                        SigmaSHCC = Range("E17") + rc2SHCC * (eps - epsLIM1SHCC)
                    'ElseIf below only fulfilled if there is a third point in tension (other-
wise the statement is never fulfilled)
                    ElseIf eps > epsLIM2SHCC And eps <= epsLIM3SHCC Then
                        SigmaSHCC = Range("G17") + rc3SHCC * (eps - epsLIM2SHCC)
                    'ElseIf below only fulfilled if there is a fourth point in tension (other-
wise the statement is never fulfilled)
                    ElseIf eps > epsLIM3SHCC And eps <= epsLIM4SHCC Then
                        SigmaSHCC = Range("O27") + rc4SHCC * (eps - epsLIM3SHCC)
                    Else
                        SigmaSHCC = 0
                    End If

                    'CONCRETE:
                    If eps >= epsLIMmin3 And eps < epsLIMmin2 Then
                        SigmaCON = -Range("G16") + rcmin3 * (eps - epsLIMmin2)
                    ElseIf eps >= epsLIMmin2 And eps < epsLIMmin1 Then
```

```
                    SigmaCON = -Range("E16") + rcmin2 * (eps - epsLIMmin1)
                ElseIf eps >= epsLIMmin1 And eps <= epsLIM1 Then
                    SigmaCON = rc1 * eps
                ElseIf eps > epsLIM1 And eps <= epsLIM2 Then
                    SigmaCON = Range("E15") + rc2 * (eps - epsLIM1)
                'ElseIf below only fulfilled if there is a third point in tension (other-
wise the statement is never fulfilled)
                ElseIf eps > epsLIM2 And eps <= epsLIM3 Then
                    SigmaCON = Range("G15") + rc3 * (eps - epsLIM2)
                'ElseIf below only fulfilled if there is a fourth point in tension (other-
wise the statement is never fulfilled)
                ElseIf eps > epsLIM3 And eps <= epsLIM4 Then
                    SigmaCON = Range("O26") + rc4 * (eps - epsLIM3)
                Else
                    SigmaCON = 0
                End If

                Sigma = (2 * tWEB) / b * SigmaSHCC + (1 - (2 * tWEB) / b) * SigmaCON
            End If

            arrN2(i) = Sigma * Range("D8") * b

        Next i
    Else
        'First of two parts that will be compared

        'SHCC:
        For i = 1 To SHCCLayers
            epsDRY = Cells(Border1 + 3 + i, 4)
            epsLOAD = (NA1 - Cells(Border1 + 3 + i, 3)) * kappa

            eps = epsDRY + epsLOAD

            If eps >= epsLIMmin3SHCC And eps < epsLIMmin2SHCC Then
                Sigma = -Range("G18") + rcmin3SHCC * (eps - epsLIMmin2SHCC)
            ElseIf eps >= epsLIMmin2SHCC And eps < epsLIMmin1SHCC Then
                Sigma = -Range("E18") + rcmin2SHCC * (eps - epsLIMmin1SHCC)
            ElseIf eps >= epsLIMmin1SHCC And eps <= epsLIM1SHCC Then
                Sigma = rc1SHCC * eps
            ElseIf eps > epsLIM1SHCC And eps <= epsLIM2SHCC Then
                Sigma = Range("E17") + rc2SHCC * (eps - epsLIM1SHCC)
            'ElseIf below only fulfilled if there is a third point in tension (otherwise
the statement is never fulfilled)
            ElseIf eps > epsLIM2SHCC And eps <= epsLIM3SHCC Then
                Sigma = Range("G17") + rc3SHCC * (eps - epsLIM2SHCC)
            'ElseIf below only fulfilled if there is a fourth point in tension (otherwise
the statement is never fulfilled)
            ElseIf eps > epsLIM3SHCC And eps <= epsLIM4SHCC Then
                Sigma = Range("O27") + rc4SHCC * (eps - epsLIM3SHCC)
            Else
                Sigma = 0
            End If

            arrN1(i) = Sigma * Range("D8") * b
        Next i

        'Partial SHCC:
        epsDRY = Cells(Border1 + 3 + (SHCCLayers + 1), 4)
        epsLOAD = (NA1 - Cells(Border1 + 3 + (SHCCLayers + 1), 3)) * kappa

        eps = epsDRY + epsLOAD

        If eps >= epsLIMmin3SHCC And eps < epsLIMmin2SHCC Then
            Sigma = -Range("G18") + rcmin3SHCC * (eps - epsLIMmin2SHCC)
        ElseIf eps >= epsLIMmin2SHCC And eps < epsLIMmin1SHCC Then
            Sigma = -Range("E18") + rcmin2SHCC * (eps - epsLIMmin1SHCC)
        ElseIf eps >= epsLIMmin1SHCC And eps <= epsLIM1SHCC Then
```

```
            Sigma = rc1SHCC * eps
        ElseIf eps > epsLIM1SHCC And eps <= epsLIM2SHCC Then
            Sigma = Range("E17") + rc2SHCC * (eps - epsLIM1SHCC)
        'ElseIf below only fulfilled if there is a third point in tension (otherwise the
statement is never fulfilled)
        ElseIf eps > epsLIM2SHCC And eps <= epsLIM3SHCC Then
            Sigma = Range("G17") + rc3SHCC * (eps - epsLIM2SHCC)
        'ElseIf below only fulfilled if there is a fourth point in tension (otherwise the
statement is never fulfilled)
        ElseIf eps > epsLIM3SHCC And eps <= epsLIM4SHCC Then
            Sigma = Range("O27") + rc4SHCC * (eps - epsLIM3SHCC)
        Else
            Sigma = 0
        End If

        arrN1(SHCCLayers + 1) = Sigma * (tBOT / Range("D8") - SHCCLayers) * Range("D8") *
b

        'Partial CONCRETE (+WEBS):
        epsDRY = Cells(Border1 + 3 + (SHCCLayers + 2), 4)
        epsLOAD = (NA1 - Cells(Border1 + 3 + (SHCCLayers + 2), 3)) * kappa

        eps = epsDRY + epsLOAD

        'SHCC web (if present):
        If eps >= epsLIMmin3SHCC And eps < epsLIMmin2SHCC Then
            SigmaSHCC = -Range("G18") + rcmin3SHCC * (eps - epsLIMmin2SHCC)
        ElseIf eps >= epsLIMmin2SHCC And eps < epsLIMmin1SHCC Then
            SigmaSHCC = -Range("E18") + rcmin2SHCC * (eps - epsLIMmin1SHCC)
        ElseIf eps >= epsLIMmin1SHCC And eps <= epsLIM1SHCC Then
            SigmaSHCC = rc1SHCC * eps
        ElseIf eps > epsLIM1SHCC And eps <= epsLIM2SHCC Then
            SigmaSHCC = Range("E17") + rc2SHCC * (eps - epsLIM1SHCC)
        'ElseIf below only fulfilled if there is a third point in tension (otherwise the
statement is never fulfilled)
        ElseIf eps > epsLIM2SHCC And eps <= epsLIM3SHCC Then
            SigmaSHCC = Range("G17") + rc3SHCC * (eps - epsLIM2SHCC)
        'ElseIf below only fulfilled if there is a fourth point in tension (otherwise the
statement is never fulfilled)
        ElseIf eps > epsLIM3SHCC And eps <= epsLIM4SHCC Then
            SigmaSHCC = Range("O27") + rc4SHCC * (eps - epsLIM3SHCC)
        Else
            SigmaSHCC = 0
        End If

        'CONCRETE:
        If eps >= epsLIMmin3 And eps < epsLIMmin2 Then
            SigmaCON = -Range("G16") + rcmin3 * (eps - epsLIMmin2)
        ElseIf eps >= epsLIMmin2 And eps < epsLIMmin1 Then
            SigmaCON = -Range("E16") + rcmin2 * (eps - epsLIMmin1)
        ElseIf eps >= epsLIMmin1 And eps <= epsLIM1 Then
            SigmaCON = rc1 * eps
        ElseIf eps > epsLIM1 And eps <= epsLIM2 Then
            SigmaCON = Range("E15") + rc2 * (eps - epsLIM1)
        'ElseIf below only fulfilled if there is a third point in tension (otherwise the
statement is never fulfilled)
        ElseIf eps > epsLIM2 And eps <= epsLIM3 Then
            SigmaCON = Range("G15") + rc3 * (eps - epsLIM2)
        'ElseIf below only fulfilled if there is a fourth point in tension (otherwise the
statement is never fulfilled)
        ElseIf eps > epsLIM3 And eps <= epsLIM4 Then
            SigmaCON = Range("O26") + rc4 * (eps - epsLIM3)
        Else
            SigmaCON = 0
        End If

        Sigma = (2 * tWEB) / b * SigmaSHCC + (1 - (2 * tWEB) / b) * SigmaCON
```

```
            arrN1(SHCCLayers + 2) = Sigma * (1 - (tBOT / Range("D8") - SHCCLayers)) *
Range("D8") * b

            'CONCRETE (+WEBS)
            For i = SHCCLayers + 2 To NofLayers + 1
                epsDRY = Cells(Border1 + 4 + i, 4)
                epsLOAD = (NA1 - Cells(Border1 + 4 + i, 3)) * kappa

                eps = epsDRY + epsLOAD

                'SHCC web (if present):
                If eps >= epsLIMmin3SHCC And eps < epsLIMmin2SHCC Then
                    SigmaSHCC = -Range("G18") + rcmin3SHCC * (eps - epsLIMmin2SHCC)
                ElseIf eps >= epsLIMmin2SHCC And eps < epsLIMmin1SHCC Then
                    SigmaSHCC = -Range("E18") + rcmin2SHCC * (eps - epsLIMmin1SHCC)
                ElseIf eps >= epsLIMmin1SHCC And eps <= epsLIM1SHCC Then
                    SigmaSHCC = rc1SHCC * eps
                ElseIf eps > epsLIM1SHCC And eps <= epsLIM2SHCC Then
                    SigmaSHCC = Range("E17") + rc2SHCC * (eps - epsLIM1SHCC)
                'ElseIf below only fulfilled if there is a third point in tension (otherwise
the statement is never fulfilled)
                ElseIf eps > epsLIM2SHCC And eps <= epsLIM3SHCC Then
                    SigmaSHCC = Range("G17") + rc3SHCC * (eps - epsLIM2SHCC)
                'ElseIf below only fulfilled if there is a fourth point in tension (otherwise
the statement is never fulfilled)
                ElseIf eps > epsLIM3SHCC And eps <= epsLIM4SHCC Then
                    SigmaSHCC = Range("O27") + rc4SHCC * (eps - epsLIM3SHCC)
                Else
                    SigmaSHCC = 0
                End If

                'CONCRETE:
                If eps >= epsLIMmin3 And eps < epsLIMmin2 Then
                    SigmaCON = -Range("G16") + rcmin3 * (eps - epsLIMmin2)
                ElseIf eps >= epsLIMmin2 And eps < epsLIMmin1 Then
                    SigmaCON = -Range("E16") + rcmin2 * (eps - epsLIMmin1)
                ElseIf eps >= epsLIMmin1 And eps <= epsLIM1 Then
                    SigmaCON = rc1 * eps
                ElseIf eps > epsLIM1 And eps <= epsLIM2 Then
                    SigmaCON = Range("E15") + rc2 * (eps - epsLIM1)
                'ElseIf below only fulfilled if there is a third point in tension (otherwise
the statement is never fulfilled)
                ElseIf eps > epsLIM2 And eps <= epsLIM3 Then
                    SigmaCON = Range("G15") + rc3 * (eps - epsLIM2)
                'ElseIf below only fulfilled if there is a fourth point in tension (otherwise
the statement is never fulfilled)
                ElseIf eps > epsLIM3 And eps <= epsLIM4 Then
                    SigmaCON = Range("O26") + rc4 * (eps - epsLIM3)
                Else
                    SigmaCON = 0
                End If

                Sigma = (2 * tWEB) / b * SigmaSHCC + (1 - (2 * tWEB) / b) * SigmaCON

                arrN1(i + 1) = Sigma * Range("D8") * b
            Next i

            'Second of two parts that will be compared

            'SHCC:
            For i = 1 To SHCCLayers
                epsDRY = Cells(Border1 + 3 + i, 4)
                epsLOAD = (NA2 - Cells(Border1 + 3 + i, 3)) * kappa

                eps = epsDRY + epsLOAD
```

```
                If eps >= epsLIMmin3SHCC And eps < epsLIMmin2SHCC Then
                    Sigma = -Range("G18") + rcmin3SHCC * (eps - epsLIMmin2SHCC)
                ElseIf eps >= epsLIMmin2SHCC And eps < epsLIMmin1SHCC Then
                    Sigma = -Range("E18") + rcmin2SHCC * (eps - epsLIMmin1SHCC)
                ElseIf eps >= epsLIMmin1SHCC And eps <= epsLIM1SHCC Then
                    Sigma = rc1SHCC * eps
                ElseIf eps > epsLIM1SHCC And eps <= epsLIM2SHCC Then
                    Sigma = Range("E17") + rc2SHCC * (eps - epsLIM1SHCC)
                'ElseIf below only fulfilled if there is a third point in tension (otherwise
the statement is never fulfilled)
                ElseIf eps > epsLIM2SHCC And eps <= epsLIM3SHCC Then
                    Sigma = Range("G17") + rc3SHCC * (eps - epsLIM2SHCC)
                'ElseIf below only fulfilled if there is a fourth point in tension (otherwise
the statement is never fulfilled)
                ElseIf eps > epsLIM3SHCC And eps <= epsLIM4SHCC Then
                    Sigma = Range("O27") + rc4SHCC * (eps - epsLIM3SHCC)
                Else
                    Sigma = 0
                End If

                arrN2(i) = Sigma * Range("D8") * b
            Next i

            'Partial SHCC:
            epsDRY = Cells(Border1 + 3 + (SHCCLayers + 1), 4)
            epsLOAD = (NA2 - Cells(Border1 + 3 + (SHCCLayers + 1), 3)) * kappa

            eps = epsDRY + epsLOAD

            If eps >= epsLIMmin3SHCC And eps < epsLIMmin2SHCC Then
                Sigma = -Range("G18") + rcmin3SHCC * (eps - epsLIMmin2SHCC)
            ElseIf eps >= epsLIMmin2SHCC And eps < epsLIMmin1SHCC Then
                Sigma = -Range("E18") + rcmin2SHCC * (eps - epsLIMmin1SHCC)
            ElseIf eps >= epsLIMmin1SHCC And eps <= epsLIM1SHCC Then
                Sigma = rc1SHCC * eps
            ElseIf eps > epsLIM1SHCC And eps <= epsLIM2SHCC Then
                Sigma = Range("E17") + rc2SHCC * (eps - epsLIM1SHCC)
            'ElseIf below only fulfilled if there is a third point in tension (otherwise the
statement is never fulfilled)
            ElseIf eps > epsLIM2SHCC And eps <= epsLIM3SHCC Then
                Sigma = Range("G17") + rc3SHCC * (eps - epsLIM2SHCC)
            'ElseIf below only fulfilled if there is a fourth point in tension (otherwise the
statement is never fulfilled)
            ElseIf eps > epsLIM3SHCC And eps <= epsLIM4SHCC Then
                Sigma = Range("O27") + rc4SHCC * (eps - epsLIM3SHCC)
            Else
                Sigma = 0
            End If

            arrN2(SHCCLayers + 1) = Sigma * (tBOT / Range("D8") - SHCCLayers) * Range("D8") *
b

            'Partial CONCRETE (+WEBS):
            epsDRY = Cells(Border1 + 3 + (SHCCLayers + 2), 4)
            epsLOAD = (NA2 - Cells(Border1 + 3 + (SHCCLayers + 2), 3)) * kappa

            eps = epsDRY + epsLOAD

            'SHCC web (if present):
            If eps >= epsLIMmin3SHCC And eps < epsLIMmin2SHCC Then
                SigmaSHCC = -Range("G18") + rcmin3SHCC * (eps - epsLIMmin2SHCC)
            ElseIf eps >= epsLIMmin2SHCC And eps < epsLIMmin1SHCC Then
                SigmaSHCC = -Range("E18") + rcmin2SHCC * (eps - epsLIMmin1SHCC)

            ElseIf eps >= epsLIMmin1SHCC And eps <= epsLIM1SHCC Then
                SigmaSHCC = rc1SHCC * eps
            ElseIf eps > epsLIM1SHCC And eps <= epsLIM2SHCC Then
```

```
                SigmaSHCC = Range("E17") + rc2SHCC * (eps - epsLIM1SHCC)
            'ElseIf below only fulfilled if there is a third point in tension (otherwise the
statement is never fulfilled)
            ElseIf eps > epsLIM2SHCC And eps <= epsLIM3SHCC Then
                SigmaSHCC = Range("G17") + rc3SHCC * (eps - epsLIM2SHCC)
            'ElseIf below only fulfilled if there is a fourth point in tension (otherwise the
statement is never fulfilled)
            ElseIf eps > epsLIM3SHCC And eps <= epsLIM4SHCC Then
                SigmaSHCC = Range("O27") + rc4SHCC * (eps - epsLIM3SHCC)
            Else
                SigmaSHCC = 0
            End If

            'CONCRETE:
            If eps >= epsLIMmin3 And eps < epsLIMmin2 Then
                SigmaCON = -Range("G16") + rcmin3 * (eps - epsLIMmin2)
            ElseIf eps >= epsLIMmin2 And eps < epsLIMmin1 Then
                SigmaCON = -Range("E16") + rcmin2 * (eps - epsLIMmin1)
            ElseIf eps >= epsLIMmin1 And eps <= epsLIM1 Then
                SigmaCON = rc1 * eps
            ElseIf eps > epsLIM1 And eps <= epsLIM2 Then
                SigmaCON = Range("E15") + rc2 * (eps - epsLIM1)
            'ElseIf below only fulfilled if there is a third point in tension (otherwise the
statement is never fulfilled)
            ElseIf eps > epsLIM2 And eps <= epsLIM3 Then
                SigmaCON = Range("G15") + rc3 * (eps - epsLIM2)
            'ElseIf below only fulfilled if there is a fourth point in tension (otherwise the
statement is never fulfilled)
            ElseIf eps > epsLIM3 And eps <= epsLIM4 Then
                SigmaCON = Range("O26") + rc4 * (eps - epsLIM3)
            Else
                SigmaCON = 0
            End If

            Sigma = (2 * tWEB) / b * SigmaSHCC + (1 - (2 * tWEB) / b) * SigmaCON

            arrN2(SHCCLayers + 2) = Sigma * (1 - (tBOT / Range("D8") - SHCCLayers)) *
Range("D8") * b

            'CONCRETE (+WEBS)
            For i = SHCCLayers + 2 To NofLayers + 1
                epsDRY = Cells(Border1 + 4 + i, 4)
                epsLOAD = (NA2 - Cells(Border1 + 4 + i, 3)) * kappa

                eps = epsDRY + epsLOAD

                'SHCC web (if present):
                If eps >= epsLIMmin3SHCC And eps < epsLIMmin2SHCC Then
                    SigmaSHCC = -Range("G18") + rcmin3SHCC * (eps - epsLIMmin2SHCC)
                ElseIf eps >= epsLIMmin2SHCC And eps < epsLIMmin1SHCC Then
                    SigmaSHCC = -Range("E18") + rcmin2SHCC * (eps - epsLIMmin1SHCC)
                ElseIf eps >= epsLIMmin1SHCC And eps <= epsLIM1SHCC Then
                    SigmaSHCC = rc1SHCC * eps
                ElseIf eps > epsLIM1SHCC And eps <= epsLIM2SHCC Then
                    SigmaSHCC = Range("E17") + rc2SHCC * (eps - epsLIM1SHCC)
                'ElseIf below only fulfilled if there is a third point in tension (otherwise
the statement is never fulfilled)
                ElseIf eps > epsLIM2SHCC And eps <= epsLIM3SHCC Then
                    SigmaSHCC = Range("G17") + rc3SHCC * (eps - epsLIM2SHCC)
                'ElseIf below only fulfilled if there is a fourth point in tension (otherwise
the statement is never fulfilled)
                ElseIf eps > epsLIM3SHCC And eps <= epsLIM4SHCC Then
                    SigmaSHCC = Range("O27") + rc4SHCC * (eps - epsLIM3SHCC)
                Else
                    SigmaSHCC = 0
                End If
```

```
                'CONCRETE:
                If eps >= epsLIMmin3 And eps < epsLIMmin2 Then
                    SigmaCON = -Range("G16") + rcmin3 * (eps - epsLIMmin2)
                ElseIf eps >= epsLIMmin2 And eps < epsLIMmin1 Then
                    SigmaCON = -Range("E16") + rcmin2 * (eps - epsLIMmin1)
                ElseIf eps >= epsLIMmin1 And eps <= epsLIM1 Then
                    SigmaCON = rc1 * eps
                ElseIf eps > epsLIM1 And eps <= epsLIM2 Then
                    SigmaCON = Range("E15") + rc2 * (eps - epsLIM1)
                'ElseIf below only fulfilled if there is a third point in tension (otherwise
the statement is never fulfilled)
                ElseIf eps > epsLIM2 And eps <= epsLIM3 Then
                    SigmaCON = Range("G15") + rc3 * (eps - epsLIM2)
                'ElseIf below only fulfilled if there is a fourth point in tension (otherwise
the statement is never fulfilled)
                ElseIf eps > epsLIM3 And eps <= epsLIM4 Then
                    SigmaCON = Range("O26") + rc4 * (eps - epsLIM3)
                Else
                    SigmaCON = 0
                End If

                Sigma = (2 * tWEB) / b * SigmaSHCC + (1 - (2 * tWEB) / b) * SigmaCON

                arrN2(i + 1) = Sigma * Range("D8") * b
            Next i
        End If

        'STEEL REINFORCEMENT:
        'Continuation of first of two parts

        'Bottom reinforcement:

        epsSBOT = (NA1 - Range("D32")) * kappa

        If epsSBOT >= epsLIMmin2S And epsSBOT < epsLIMmin1S Then
            SigmaSBOT = -Range("E20") + rcmin2S * (epsSBOT - epsLIMmin1S)
        ElseIf epsSBOT >= epsLIMmin1S And epsSBOT <= epsLIM1S Then
            SigmaSBOT = rc1S * epsSBOT
        ElseIf epsSBOT > epsLIM1S And epsSBOT <= epsLIM2S Then
            SigmaSBOT = Range("E19") + rc2S * (epsSBOT - epsLIM1S)
        Else
            SigmaSBOT = 0
        End If

        arrN1(NofLayers + 2) = SigmaSBOT * AreaSBOT

        'Top reinforcement:
        epsSTOP = (NA1 - Range("F32")) * kappa

        If epsSTOP >= epsLIMmin2S And epsSTOP < epsLIMmin1S Then
            SigmaSTOP = -Range("E20") + rcmin2S * (epsSTOP - epsLIMmin1S)
        ElseIf epsSTOP >= epsLIMmin1S And epsSTOP <= epsLIM1S Then
            SigmaSTOP = rc1S * epsSTOP
        ElseIf epsSTOP > epsLIM1S And epsSTOP <= epsLIM2S Then
            SigmaSTOP = Range("E19") + rc2S * (epsSTOP - epsLIM1S)
        Else
            SigmaSTOP = 0
        End If

        arrN1(NofLayers + 3) = SigmaSTOP * AreaSTOP

        'Sum up the whole array, so CONCRETE + SHCC + STEEL (sum of horizontal forces first
step)
        SumN1 = WorksheetFunction.Sum(arrN1)

        'Continuation of second of two parts
```

```
        'Bottom reinforcement:
        epsSLOADBOT = (NA2 - Range("D32")) * kappa
        epsSBOT = epsSLOADBOT + epsSDRYBOT

        If epsSBOT >= epsLIMmin2S And epsSBOT < epsLIMmin1S Then
            SigmaSBOT = -Range("E20") + rcmin2S * (epsSBOT - epsLIMmin1S)
        ElseIf epsSBOT >= epsLIMmin1S And epsSBOT <= epsLIM1S Then
            SigmaSBOT = rc1S * epsSBOT
        ElseIf epsSBOT > epsLIM1S And epsSBOT <= epsLIM2S Then
            SigmaSBOT = Range("E19") + rc2S * (epsSBOT - epsLIM1S)
        Else
            SigmaSBOT = 0
        End If

        arrN2(NofLayers + 2) = SigmaSBOT * AreaSBOT

        'Top reinforcement:
        epsSLOADTOP = (NA2 - Range("F32")) * kappa
        epsSTOP = epsSLOADTOP + epsSDRYTOP

        If epsSTOP >= epsLIMmin2S And epsSTOP < epsLIMmin1S Then
            SigmaSTOP = -Range("E20") + rcmin2S * (epsSTOP - epsLIMmin1S)
        ElseIf epsSTOP >= epsLIMmin1S And epsSTOP <= epsLIM1S Then
            SigmaSTOP = rc1S * epsSTOP
        ElseIf epsSTOP > epsLIM1S And epsSTOP <= epsLIM2S Then
            SigmaSTOP = Range("E19") + rc2S * (epsSTOP - epsLIM1S)
        Else
            SigmaSTOP = 0
        End If

        arrN2(NofLayers + 3) = SigmaSTOP * AreaSTOP

        'Sum up the whole array, so CONCRETE + SHCC + STEEL (sum of horizontal forces first
step)
        SumN2 = WorksheetFunction.Sum(arrN2)

        'When one of the two steps is positive and the other negative, it means, that sum of
forces = 0 is in between (so equilibrium)
        If SumN1 > 0 And SumN2 < 0 Or SumN1 < 0 And SumN2 > 0 Then
            Cells(Border1 - 1, 4 + n).Value = kappa

            '#MEAN/INTERPOLATION METHOD: in this method, the step that is closest to zero con-
tributes relatively more to the result
            TotalSum = Abs(SumN1) + Abs(SumN2)

            'The interpolated n.a. position that will also be used in the next iteration
            naSTEP = (1 - Abs(SumN1) / TotalSum) * NA1 + (1 - Abs(SumN2) / TotalSum) * NA2

            Cells(Border1 - 6, 4 + n).Value = naSTEP

            SumSTEPmax = WorksheetFunction.Max(Abs(SumN1), Abs(SumN2))

            If SumSTEPmax = Abs(SumN1) Then
                Cells(Border1 - 2, 4 + n).Value = SumN1
                Cells(Border1 - 3, 4 + n).Value = SumN2
            Else
                Cells(Border1 - 2, 4 + n).Value = SumN2
                Cells(Border1 - 3, 4 + n).Value = SumN1
            End If

            '#CALCULATE MOMENT

            'SHCC + CONCRETE:

            'Choose between the simple and the advanced method
            If tBOT / Range("D8") = Int(tBOT / Range("D8")) Then
                For i = 1 To NofLayers
```

```
                    'Take the seperate contributions into account. Therefore, NA1 and NA2 are
used and not naSTEP!
                    MofN1 = (1 - Abs(SumN1) / TotalSum) * arrN1(i) * (NA1 - Cells(Border1 + 3
+ i, 3))
                    MofN2 = (1 - Abs(SumN2) / TotalSum) * arrN2(i) * (NA2 - Cells(Border1 + 3
+ i, 3))

                    arrM(i) = MofN1 + MofN2
                Next i
            Else
                'SHCC:
                For i = 1 To SHCCLayers
                    'Take the seperate contributions into account. Therefore, NA1 and NA2 are
used and not naSTEP!
                    MofN1 = (1 - Abs(SumN1) / TotalSum) * arrN1(i) * (NA1 - Cells(Border1 + 3
+ i, 3))
                    MofN2 = (1 - Abs(SumN2) / TotalSum) * arrN2(i) * (NA2 - Cells(Border1 + 3
+ i, 3))

                    arrM(i) = MofN1 + MofN2
                Next i

                'Partial SHCC:
                MofN1 = (1 - Abs(SumN1) / TotalSum) * arrN1(SHCCLayers + 1) * (NA1 -
Cells(Border1 + 3 + (SHCCLayers + 1), 3))
                MofN2 = (1 - Abs(SumN2) / TotalSum) * arrN2(SHCCLayers + 1) * (NA2 -
Cells(Border1 + 3 + (SHCCLayers + 1), 3))

                arrM(SHCCLayers + 1) = MofN1 + MofN2

                'Partial CONCRETE (+WEBS):
                MofN1 = (1 - Abs(SumN1) / TotalSum) * arrN1(SHCCLayers + 2) * (NA1 -
Cells(Border1 + 3 + (SHCCLayers + 2), 3))
                MofN2 = (1 - Abs(SumN2) / TotalSum) * arrN2(SHCCLayers + 2) * (NA2 -
Cells(Border1 + 3 + (SHCCLayers + 2), 3))

                arrM(SHCCLayers + 2) = MofN1 + MofN2

                'CONCRETE (+WEBS):
                For i = SHCCLayers + 2 To NofLayers + 1
                    'Take the seperate contributions into account. Therefore, NA1 and NA2 are
used and not naSTEP!
                    MofN1 = (1 - Abs(SumN1) / TotalSum) * arrN1(i + 1) * (NA1 - Cells(Border1
+ 4 + i, 3))
                    MofN2 = (1 - Abs(SumN2) / TotalSum) * arrN2(i + 1) * (NA2 - Cells(Border1
+ 4 + i, 3))

                    arrM(i + 1) = MofN1 + MofN2
                Next i
            End If

            'STEEL REINFORCEMENT:
            'Take the seperate contributions into account. Therefore, NA1 and NA2 are used and
not naSTEP!

            'Bottom reinforcement:
            MofN1 = (1 - Abs(SumN1) / TotalSum) * arrN1(NofLayers + 2) * (NA1 - Range("D32"))
            MofN2 = (1 - Abs(SumN2) / TotalSum) * arrN2(NofLayers + 2) * (NA2 - Range("D32"))

            arrM(NofLayers + 2) = MofN1 + MofN2
            NinSteel = (1 - Abs(SumN1) / TotalSum) * arrN1(NofLayers + 2) + (1 - Abs(SumN2) /
TotalSum) * arrN2(NofLayers + 2)

            'Top reinforcement:
            MofN1 = (1 - Abs(SumN1) / TotalSum) * arrN1(NofLayers + 3) * (NA1 - Range("F32"))
            MofN2 = (1 - Abs(SumN2) / TotalSum) * arrN2(NofLayers + 3) * (NA2 - Range("F32"))
```

```
            arrM(NofLayers + 3) = MofN1 + MofN2

            Mtotal = WorksheetFunction.Sum(arrM)
            Cells(Border1 - 5, 4 + n).Value = Mtotal

            '#CALCULATE APPLIED FORCE; note that moment due to selfweight is reduced from oc-
curing moment

            'M=(F/2)*L1
            F = 2 * (Mtotal - MG) / L1
            If F < 0 Then
            'When the force is displayed as zero, it means that failure has occured (MG > M);
            'the beam cannot carry its own weight anymore
                Cells(Border1 - 4, 4 + n).Value = 0
            Else
                Cells(Border1 - 4, 4 + n).Value = F
            End If

            '#CALCULATE STRAIN AT TOP
'            Cells(Border1 - 8, 4 + n).Value = -kappa * (h - naSTEP)
            Cells(Border1 - 8, 4 + n).Value = NinSteel

            '#CALCULATE DISPLACEMENT:
            If Range("M30") = "4-point" Then
                If Mtotal > Mlinear Then

                    'MOMENTVLAKSTELLINGEN:
                    'Reduced moment diagram consists of 3 constant parts and a non-linear
part; Area1 and Area7 are triangles;
                    'Area4 is a rectangle
                    Llinear = (Mlinear / Mtotal) * L1

                    Theta1 = 1 / 2 * kappa0 * Llinear
                    Theta4 = kappa * L2
                    Theta7 = Theta1

                    Distance1 = L - 2 / 3 * Llinear
                    Distance4 = L / 2
                    Distance7 = 2 / 3 * Llinear

                    'Define segments between constant parts (non-linear)
                    SegLength = (L1 - Llinear) / Segments

                    PhiSeg0B = 0
                    PhiSeg0A = 0
                    DispSeg0 = 0

                    For a = 1 To Segments
                        Mslope = (Mtotal - Mlinear) / (L1 - Llinear)
                        'Moment at centerline of segment:
                        MSeg = Mlinear + Mslope * (a - 1 / 2) * SegLength

                        For s = 1 To n
                            Mcell = Cells(Border1 - 5, 4 + (s - 1))

                            If Mcell <> "" And Mcell <= MSeg Then
                                C = s
                            End If
                        Next s

                        kappaSeg = Cells(Border1 - 1, 4 + (C - 1))

                        Theta = kappaSeg * SegLength

                        'For finding phiA (A is the left support; B is the right support):
                        DisToB = L1 + L2 + (Segments + 1 / 2 - a) * SegLength
```

```
                    'Ditance to A = Distance to B for the other non-linear part of the di-
agram
                    DisToA = L - DisToB

                    PhiSegB = PhiSeg0B + Theta * DisToB
                    PhiSeg0B = PhiSegB

                    PhiSegA = PhiSeg0A + Theta * DisToA
                    PhiSeg0A = PhiSegA

                    'For finding deflection at midspan
                    DisToMid = L2 / 2 + (Segments + 1 / 2 - a) * SegLength

                    DispSeg = DispSeg0 + Theta * DisToMid
                    DispSeg0 = DispSeg

                Next a

                'All thetas times their distances are equal to PhiA times L (so that the
displacement at the second support = 0
                PhiA = (Theta1 * Distance1 + Theta4 * Distance4 + Theta7 * Distance7 +
PhiSegB + PhiSegA) / L

                'Split Theta4 in two to get the deflection at midspan
                Theta4B = Theta4 / 2

                w = PhiA * L / 2 - Theta1 * (Distance1 - L / 2) - Theta4B * L2 / 4 -
DispSeg

            Else
                'Reduced moment diagram consists of ONLY 3 constant parts: Area1 and Area7
are triangles; Area4 is a rectangle
                Theta1 = 1 / 2 * (Mtotal / EIlinear) * L1
                Theta4 = kappa * L2
                Theta7 = Theta1

                Distance1 = L - 2 / 3 * L1
                Distance4 = L / 2
                Distance7 = 2 / 3 * L1

                'All thetas times their distances are equal to PhiA times L (so that the
displacement at the second support = 0
                PhiA = (Theta1 * Distance1 + Theta4 * Distance4 + Theta7 * Distance7) / L

                'Split Theta4 in two to get the deflection at midspan
                Theta4B = Theta4 / 2

                w = PhiA * L / 2 - Theta1 * (Distance1 - L / 2) - Theta4B * L2 / 4

            End If

'               'UNDERESTIMATED DEFLECTION:
'               R = 1 / kappa
'               w = L2 ^ 2 / (8 * R) + L1 * L2 / (2 * R)

'               'OVERESTIMATED DEFLECTION
'               R = 1 / kappa
'               w = L ^ 2 / (8 * R) - L1 ^ 2 / (6 * R)

        Else    '3-point bending'
            If Mtotal > Mlinear Then
                'MOMENTVLAKSTELLINGEN:
                'Reduced moment diagram consists of 2 constant parts and a non-linear
part; Area1 and Area7 are triangles
                Llinear = (Mlinear / Mtotal) * L1

                Theta1 = 1 / 2 * kappa0 * Llinear
```

```
                    Theta7 = Theta1

                    Distance1 = L - 2 / 3 * Llinear
                    Distance7 = 2 / 3 * Llinear

                    'Define segments between constant parts (non-linear)
                    SegLength = (L1 - Llinear) / Segments

                    PhiSeg0 = 0
                    DispSeg0 = 0

                    For a = 1 To Segments
                        Mslope = (Mtotal - Mlinear) / (L1 - Llinear)
                        'Moment at centerline of segment:
                        MSeg = Mlinear + Mslope * (a - 1 / 2) * SegLength

                        For s = 1 To n
                            Mcell = Cells(Border1 - 5, 4 + (s - 1))

                            If Mcell <> "" And Mcell <= MSeg Then
                                C = s
                            End If
                        Next s

                        kappaSeg = Cells(Border1 - 1, 4 + (C - 1))

                        Theta = kappaSeg * SegLength

                        'For finding phiA:
                        DisToB = L1 + (Segments + 1 / 2 - a) * SegLength
                        PhiSeg = PhiSeg0 + Theta * DisToB
                        PhiSeg0 = PhiSeg

                        'For finding deflection at midspan
                        DisToMid = (Segments + 1 / 2 - a) * SegLength
                        DispSeg = DispSeg0 + Theta * DisToMid
                        DispSeg0 = DispSeg

                    Next a

                    'All thetas times their distances are equal to PhiA times L (so that the
displacement at the second support = 0
                    PhiA = (Theta1 * Distance1 + Theta7 * Distance7 + PhiSeg) / L

                    w = PhiA * L / 2 - Theta1 * (Distance1 - L / 2) - DispSeg

                Else
                    'Reduced moment diagram consists of 3 constant parts: Area1 and Area7 are
triangles;
                    'Area4 is a rectangle (the damaged region)
                    'Assume that the damaged region has a length of  5 mm
                    Damage = 5 'mm

                    Mslope = Mtotal / L1

                    'Maximum moment just before damaged region:
                    Mundamaged = Mslope * (L1 - Damage / 2)

                    Theta1 = 1 / 2 * (Mundamaged / EIlinear) * (L1 - Damage / 2)
                    Theta4 = kappa * Damage
                    Theta7 = Theta1

                    Distance1 = L - 2 / 3 * (L1 - Damage / 2)
                    Distance4 = L / 2
                    Distance7 = 2 / 3 * (L1 - Damage / 2)
```

```
                    'All thetas times their distances are equal to PhiA times L (so that the
displacement at the second support = 0
                    PhiA = (Theta1 * Distance1 + Theta4 * Distance4 + Theta7 * Distance7) / L

                    'Split Theta4 in two to get the deflection at midspan
                    Theta4B = Theta4 / 2

                    w = PhiA * L / 2 - Theta1 * (Distance1 - L / 2) - Theta4B * (Damage / 2)

                End If
            End If

            Cells(Border1 - 7, 4 + n).Value = w

            Exit For
        'In the case all material properties are symmetrical (so no difference between tension
and compression):
        ElseIf Abs(SumN1) = 0 Then

            '#CALCULATE MOMENT

            'SHCC + CONCRETE:
            'Choose between the simple and the advanced method
            If tBOT / Range("D8") = Int(tBOT / Range("D8")) Then
                For i = 1 To NofLayers
                    arrM(i) = arrN1(i) * (naSTEP - Cells(Border1 + 3 + i, 3))
                Next i
            Else
                'SHCC:
                For i = 1 To SHCCLayers
                    arrM(i) = arrN1(i) * (naSTEP - Cells(Border1 + 3 + i, 3))
                Next i

                'Partial SHCC:
                arrM(SHCCLayers + 1) = arrN1(SHCCLayers + 1) * (naSTEP - Cells(Border1 + 3 +
(SHCCLayers + 1), 3))

                'Partial CONCRETE (+WEBS):
                arrM(SHCCLayers + 2) = arrN1(SHCCLayers + 2) * (naSTEP - Cells(Border1 + 3 +
(SHCCLayers + 2), 3))

                'CONCRETE (+WEBS):
                For i = SHCCLayers + 2 To NofLayers + 1
                    arrM(i + 1) = arrN1(i + 1) * (naSTEP - Cells(Border1 + 4 + i, 3))
                Next i
            End If

            'STEEL REINFORCEMENT:
            arrM(NofLayers + 2) = arrN1(NofLayers + 2) * (naSTEP - Range("D32"))
            arrM(NofLayers + 3) = arrN1(NofLayers + 3) * (naSTEP - Range("F32"))

            Mtotal = WorksheetFunction.Sum(arrM)
            Cells(Border1 - 5, 4 + n).Value = Mtotal

            '#CALCULATE APPLIED FORCE; note that moment due to selfweight is reduced from oc-
curing moment
            'M=(F/2)*L1
            F = 2 * (Mtotal - MG) / L1
            If F < 0 Then
            'When the force is displayed as zero, it means that failure has occured (MG > M);
            'the beam cannot carry its own weight anymore
                Cells(Border1 - 4, 4 + n).Value = 0
            Else
                Cells(Border1 - 4, 4 + n).Value = F
            End If

            '#CALCULATE DISPLACEMENT:
```

```
            If Range("M30") = "4-point" Then
                If Mtotal > Mlinear Then

                    'MOMENTVLAKSTELLINGEN:
                    'Reduced moment diagram consists of 3 constant parts and a non-linear
part; Area1 and Area7 are triangles;
                    'Area4 is a rectangle
                    Llinear = (Mlinear / Mtotal) * L1

                    Theta1 = 1 / 2 * kappa0 * Llinear
                    Theta4 = kappa * L2
                    Theta7 = Theta1

                    Distance1 = L - 2 / 3 * Llinear
                    Distance4 = L / 2
                    Distance7 = 2 / 3 * Llinear

                    'Define segments between constant parts (non-linear)
                    SegLength = (L1 - Llinear) / Segments

                    PhiSeg0B = 0
                    PhiSeg0A = 0
                    DispSeg0 = 0

                    For a = 1 To Segments
                        Mslope = (Mtotal - Mlinear) / (L1 - Llinear)
                        'Moment at centerline of segment:
                        MSeg = Mlinear + Mslope * (a - 1 / 2) * SegLength

                        For s = 1 To n
                            Mcell = Cells(Border1 - 5, 4 + (s - 1))

                            If Mcell <> "" And Mcell <= MSeg Then
                                C = s
                            End If
                        Next s

                        kappaSeg = Cells(Border1 - 1, 4 + (C - 1))

                        Theta = kappaSeg * SegLength

                        'For finding phiA (A is the left support; B is the right support):
                        DisToB = L1 + L2 + (Segments + 1 / 2 - a) * SegLength

                        'Ditance to A = Distance to B for the other non-linear part of the di-
agram
                        DisToA = L - DisToB

                        PhiSegB = PhiSeg0B + Theta * DisToB
                        PhiSeg0B = PhiSegB

                        PhiSegA = PhiSeg0A + Theta * DisToA
                        PhiSeg0A = PhiSegA

                        'For finding deflection at midspan
                        DisToMid = L2 / 2 + (Segments + 1 / 2 - a) * SegLength

                        DispSeg = DispSeg0 + Theta * DisToMid
                        DispSeg0 = DispSeg

                    Next a

                    'All thetas times their distances are equal to PhiA times L (so that the
displacement at the second support = 0
                    PhiA = (Theta1 * Distance1 + Theta4 * Distance4 + Theta7 * Distance7 +
PhiSegB + PhiSegA) / L
```

```
                    'Split Theta4 in two to get the deflection at midspan
                    Theta4B = Theta4 / 2

                    w = PhiA * L / 2 - Theta1 * (Distance1 - L / 2) - Theta4B * L2 / 4 -
DispSeg

                Else
                    'Reduced moment diagram consists of ONLY 3 constant parts: Area1 and Area7
are triangles; Area4 is a rectangle
                    Theta1 = 1 / 2 * (Mtotal / EIlinear) * L1
                    Theta4 = kappa * L2
                    Theta7 = Theta1

                    Distance1 = L - 2 / 3 * L1
                    Distance4 = L / 2
                    Distance7 = 2 / 3 * L1

                    'All thetas times their distances are equal to PhiA times L (so that the
displacement at the second support = 0
                    PhiA = (Theta1 * Distance1 + Theta4 * Distance4 + Theta7 * Distance7) / L

                    'Split Theta4 in two to get the deflection at midspan
                    Theta4B = Theta4 / 2

                    w = PhiA * L / 2 - Theta1 * (Distance1 - L / 2) - Theta4B * L2 / 4

                End If

'                'UNDERESTIMATED DEFLECTION:
'                R = 1 / kappa
'                w = L2 ^ 2 / (8 * R) + L1 * L2 / (2 * R)

'                'OVERESTIMATED DEFLECTION
'                R = 1 / kappa
'                w = L ^ 2 / (8 * R) - L1 ^ 2 / (6 * R)

            Else    '3-point bending'
                If Mtotal > Mlinear Then
                    'MOMENTVLAKSTELLINGEN:
                    'Reduced moment diagram consists of 2 constant parts and a non-linear
part; Area1 and Area7 are triangles
                    Llinear = (Mlinear / Mtotal) * L1

                    Theta1 = 1 / 2 * kappa0 * Llinear
                    Theta7 = Theta1

                    Distance1 = L - 2 / 3 * Llinear
                    Distance7 = 2 / 3 * Llinear

                    'Define segments between constant parts (non-linear)
                    SegLength = (L1 - Llinear) / Segments

                    PhiSeg0 = 0
                    DispSeg0 = 0

                    For a = 1 To Segments
                        Mslope = (Mtotal - Mlinear) / (L1 - Llinear)
                        'Moment at centerline of segment:
                        MSeg = Mlinear + Mslope * (a - 1 / 2) * SegLength

                        For s = 1 To n
                            Mcell = Cells(Border1 - 5, 4 + (s - 1))

                            If Mcell <> "" And Mcell <= MSeg Then
                                C = s
                            End If
                        Next s
```

```
                        kappaSeg = Cells(Border1 - 1, 4 + (C - 1))

                        Theta = kappaSeg * SegLength

                        'For finding phiA:
                        DisToB = L1 + (Segments + 1 / 2 - a) * SegLength
                        PhiSeg = PhiSeg0 + Theta * DisToB
                        PhiSeg0 = PhiSeg

                        'For finding deflection at midspan
                        DisToMid = (Segments + 1 / 2 - a) * SegLength
                        DispSeg = DispSeg0 + Theta * DisToMid
                        DispSeg0 = DispSeg

                    Next a

                    'All thetas times their distances are equal to PhiA times L (so that the
displacement at the second support = 0
                    PhiA = (Theta1 * Distance1 + Theta7 * Distance7 + PhiSeg) / L

                    w = PhiA * L / 2 - Theta1 * (Distance1 - L / 2) - DispSeg

                Else
                    'Reduced moment diagram consists of 3 constant parts: Area1 and Area7 are
triangles;
                    'Area4 is a rectangle (the damaged region)
                    'Assume that the damaged region has a length of  5 mm
                    Damage = 5 'mm

                    Mslope = Mtotal / L1

                    'Maximum moment just before damaged region:
                    Mundamaged = Mslope * (L1 - Damage / 2)

                    Theta1 = 1 / 2 * (Mundamaged / EIlinear) * (L1 - Damage / 2)
                    Theta4 = kappa * Damage
                    Theta7 = Theta1

                    Distance1 = L - 2 / 3 * (L1 - Damage / 2)
                    Distance4 = L / 2
                    Distance7 = 2 / 3 * (L1 - Damage / 2)

                    'All thetas times their distances are equal to PhiA times L (so that the
displacement at the second support = 0
                    PhiA = (Theta1 * Distance1 + Theta4 * Distance4 + Theta7 * Distance7) / L

                    'Split Theta4 in two to get the deflection at midspan
                    Theta4B = Theta4 / 2

                    w = PhiA * L / 2 - Theta1 * (Distance1 - L / 2) - Theta4B * (Damage / 2)

                End If
            End If

'            Cells(Border1 - 8, 4 + n).Value = -kappa * (h - naSTEP)
            Cells(Border1 - 8, 4 + n).Value = arrN1(NofLayers + 2)
            Cells(Border1 - 7, 4 + n).Value = w
            Cells(Border1 - 6, 4 + n).Value = naSTEP
            Cells(Border1 - 3, 4 + n).Value = SumN1
            Cells(Border1 - 1, 4 + n).Value = kappa

            Exit For
        End If
    Next j
'Show progress in %
Cells(26, 9).Value = (n + 2) / (Points + 2)
```

```
Next n

'-----------------------------------
''SHOW DELTA-N'S FOR LAST STEP (not necessarily a correct step!)
'For n = 1 To NofLayers + 3
'    Cells(50 + n, 7).Value = arrN1(n)
'    Cells(50 + n, 8).Value = arrN2(n)
'Next n
'
''SHOW DELTA-M'S FOR LAST STEP (not necessarily a correct step!)
'For n = 1 To NofLayers + 3
'    Cells(50 + n, 10).Value = arrM(n)
'Next n
'-----------------------------------

'#DRAW BORDERS
Range(Cells(Border1 - 5, 2), Cells(Border1 - 5, 2 + Points + 2)).BorderAround (xlDouble)
Range(Cells(Border1 - 1, 2), Cells(Border1 - 1, 2 + Points + 2)).BorderAround (xlDouble)

With Range(Range("C42"), Range("C42").End(xlToRight)).Borders(xlEdgeBottom)
.LineStyle = xlContinuous
.Weight = xlMedium
End With

End Sub

Private Sub CommandButton1_Click()

Call Layers

End Sub
```

Excel calculations

Crack width calculation for w,F-diagram → **only valid if a reinforced concrete beam is considered without drying shrinkage!**

Find σ_{sr}

d	α_e	A_s	ρ_l	x	z	σ_{sr}
[mm]	[-]	[mm²]	[-]	[mm]	[mm]	[N/mm²]
165	5.882353	150.7964	0.006093	38.65607	152.1146	118.4013

w_{max} parameters

τ_{bm}	α	h_{eff}	ρ_{eff}
[N/mm²]	[-]	[mm]	[-]
9.072	0.5	53.78131	0.018693

N_{steel}	[N]	0	1464.347	4463.338	8795.512	12970.85	16982.54	20942.18	24876.24	28804.35	32646.43	36507.28	40384.67	44207.98	48039.79
w_{max}	[mm]	-0.03167	-0.02648	-0.01584	-0.00047	0.014345	0.028577	0.042625	0.056581	0.070517	0.084147	0.097844	0.1116	0.125164	0.138758
$w_{max,adjusted}$	[mm]		0.031671				0.028577	0.042625	0.056581	0.070517	0.084147	0.097844	0.1116	0.125164	0.138758
$F_{adjusted}$	[N]		10.09351				11.29278	13.27069	15.37945	17.54999	19.81642	22.07952	24.3441	26.64392	28.94321
$w_{max,adjusted}$	[mm]	0.031671	0.028577	0.042625	0.056581	0.070517	0.084147	0.097844	0.1116	0.125164	0.138758	0.152373	0.166009	0.17966	0.193073
$F_{adjusted}$	[N]	10.09351	11.29278	13.27069	15.37945	17.54999	19.81642	22.07952	24.3441	26.64392	28.94321	31.24179	33.54119	35.8416	38.16536

Interface shear calculation → **only valid if a hybrid beam is considered (no webs)**

I	b	S
[mm⁴]	[mm]	[mm³]
1.00E+08	150	0

$F_{adjusted}$	[kN]		0												
$F_{adjusted}$	[kN]	0													
V_{max}	[kN]	0													
$\tau_{long,max}$	[N/mm²]	0													
$V_{long,max/m}$	[N/m]	0													

Stress calculation for σ,δ-diagram → **only valid if a non-hybrid beam is considered (no webs)**

I	z
[mm⁴]	[mm]
1.00E+08	99.26

M	[Nmm]	0	2715930	3323229	2462835	2598191	3015748	3510226	4037415	4580050	5146658	5712432	6278578	6853532	7428355
$\sigma_{bot,fiber}$	[N/mm²]	0	2.695776	3.298569	2.444559	2.578911	2.99337	3.484178	4.007455	4.546064	5.108467	5.670043	6.231988	6.802675	7.373233
δ	[mm]	0.012555	0.180737	0.347736	0.487658	0.647046	0.882836	1.158137	1.426834	1.688719	1.947415	2.200333	2.450381	2.698856	2.945573

Appendix figure 1: Excel calculations in the MLM

Appendix B: MLM parameters

In this Appendix, all available parameters in the proposed MLM are explained. This is done by going through all the presented sections of Figure 3-18. In this Appendix, the parameters will be shown as they are shown in the proposed MLM itself. All possible input is shown in Appendix figure 2. In this figure, also the cross-section that follows from the input is shown. Although there is some explanation in some sections, it is not always enough to fully understand the purpose of the corresponding parameter.

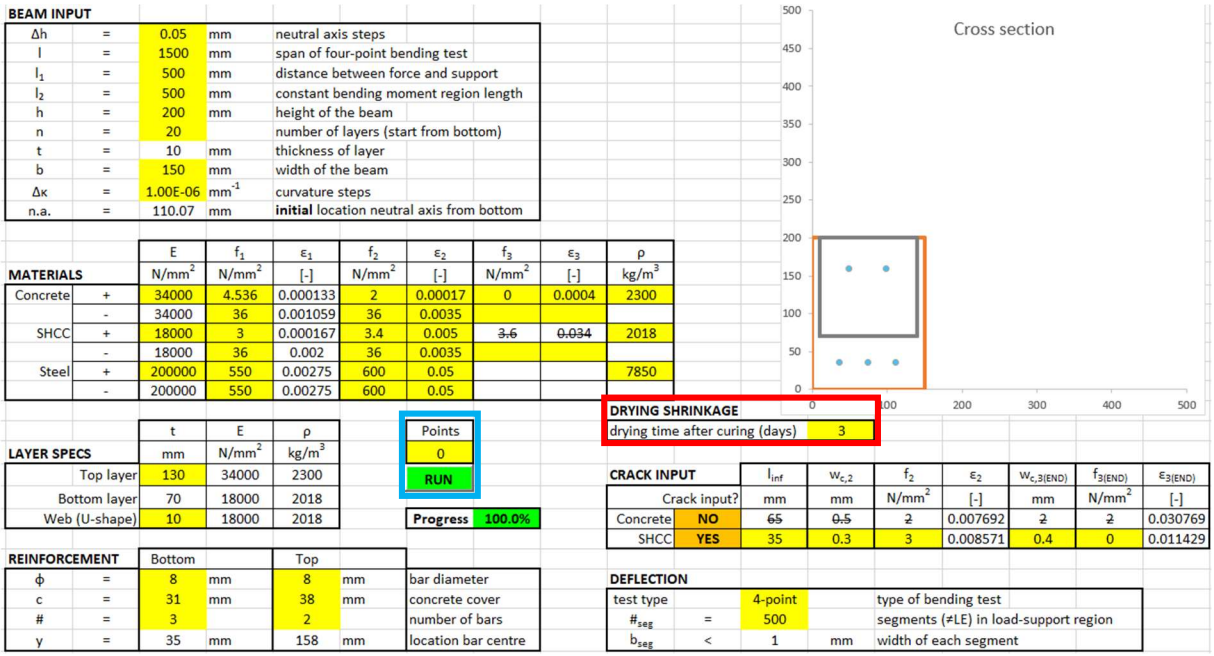

Appendix figure 2: MLM parameters as in the MLM itself

Every cell in Appendix figure 2 that is marked in yellow corresponds to an input parameter that the user needs to define. Some parameters are not marked; they are determined based on the other parameters.

Section 1: points

The first section that is explained, is the 'points' section, which is the section that needs the shortest explanation. It is marked in blue in Appendix figure 2. The input that is used here is the desired number of datapoints in the output diagrams. The number of datapoints is by default limited to 500 datapoints, but it can be extended. The reason that it is limited, is that there are processes that are performed in the background and are dependent on the maximum number of datapoints. The more points there are, the more time those processes will take, and therefore increase the computation time.

Section 2: beam input

The second section that is explained, is the 'beam input' section. The required parameters are shown in Appendix figure 3.

BEAM INPUT
Δh
L
L_1
L_2
h
n
t
b
Δκ
n.a.

Appendix figure 3: beam input section parameters in the developed MLM

The 'Δh' represents the magnitude of the 'neutral axis steps'. In the non-linear stage, the neutral axis will move upwards in order to assure that there is horizontal equilibrium in the cross-section. In the iterative process, the neutral axis is moved up (by this 'neutral axis steps') in each iteration until horizontal equilibrium is found. That was explained more in detail in subchapter 3.1.1.2. With this parameter, it can be determined how big or small these steps are. The larger the step, the less the probability is that equilibrium is found. This is because it might be the case that the position that would have led to equilibrium is missed because of the larger steps.

The 'L', 'L_1' and 'L_2' parameters are related to the span of the beam that is considered. If a 4-point bending test is considered, both 'L_1' and 'L_2' are present. This was shown before in Figure 3-21. In a 3-point bending test, the 'L_2' is not present. When this type of bending test is chosen in the MLM, the 'L_2' automatically disappears.

The cross-sectional dimensions are also input in this section, and are given by 'h' and 'b'. Those are already drawn in Appendix figure 2.

Next, the 'Δκ' parameter is explained. This parameter determines how much the difference is between the curvature of two datapoints in the moment-to-curvature diagram. The larger this difference is, the less fluent/accurate the diagram becomes. This was explained more in detail in subchapter 3.1.1.2.

Moreover, the 'n.a' parameter is present in this section. This gives the initial neutral axis position of the cross-section, which is calculated automatically. Although this means that this is not really 'input', it is used as input for the calculation process of the MLM. Here, it will be explained how the initial neutral axis position is calculated. This location is determined with respect to the bottom axis, and its magnitude is determined as follows:

$$y = \frac{E * S}{E * A} \qquad \textit{Appendix eq. (1)}$$

In this expression, 'E' is the Young's modulus [N/mm^2], 'S' is the first moment of area [mm^3] and 'A' the area [mm^2]. In this expression, it seems that the 'E' parameter can be left out because it is present in both the nominator and the denominator. That is true for homogeneous sections. However, when dealing with inhomogeneous sections, the situation becomes different. Different materials have different contributions. That is described in the different Young's moduli.

Last but not least, the parameters that form the core of the MLM are explained: the 'n' and the 't', which are related to the layers. 'n' gives the number of layers. This is illustrated in Appendix figure 4; in this figure, 20 layers in a beam of 200 mm height are shown. The thickness 't' of the layer therefore becomes 200/20 = 10 mm.

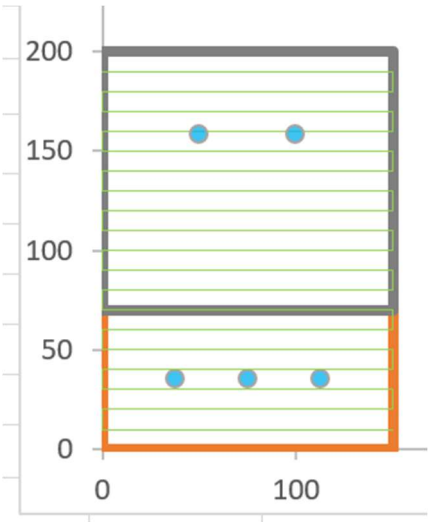

Appendix figure 4: visualization of the layers (green lines) in the MLM; dimensions in [mm]

As the number of layers is in fact the core of the multi-**layer** model, its effects are also explained here.

Effect of number of layers

The number of layers that is used in a multi-layer model has to be chosen wisely. Choosing a small number of layers gives inaccurate results, while a large number will require more computing time. The concept of inaccurate results is illustrated in Appendix figure 5. To show the extent of the possible error, only two layers are used. The internal lever arm is in reality equal to $\frac{2}{3}$ times the height. When there are only two layers, this internal lever arm becomes equal to half the height. For increasing number of layers, this effect is reduced.

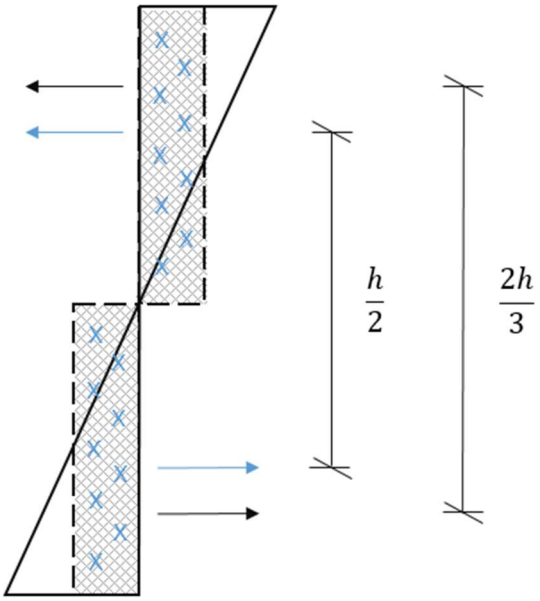

Appendix figure 5: comparing two layers to an infinite amount of layers in the MLM

For different numbers of layers, the results of the cracking force were recorded. This was done for a hypothetical case of which the input is shown in Appendix figure 6. In this hypothetical case a cross section consisting of only concrete is considered. As only the cracking force is recorded, only the linear elastic behaviour is of importance.

BEAM INPUT

Δh	=	0.05	mm	neutral axis steps
l	=	1500	mm	span of four-point bending test
l_1	=	500	mm	distance between force and support
l_2	=	500	mm	constant bending moment region length
h	=	200	mm	height of the beam
n	=	20		number of layers (start from bottom)
t	=	10	mm	thickness of layer
b	=	150	mm	width of the beam
Δκ	=	1.00E-06	mm^{-1}	curvature steps
n.a.	=	100.00	mm	**initial** location neutral axis from bottom

MATERIALS		E N/mm^2	f_1 N/mm^2	ε_1 [-]	f_2 N/mm^2	ε_2 [-]	f_3 N/mm^2	ε_3 [-]	ρ kg/m^3
Concrete	+	34000	4.536	0.000133					2300
	-	34000	36	0.001059	36	0.0035			
SHCC	+	18000	3	0.000167	3.4	0.015	3.6	0.034	2018
	-	18000	36	0.002	36	0.0035			
Steel	+	200000	550	0.00275	600	0.05			7850
	-	200000	550	0.00275	600	0.05			

LAYER SPECS	t mm	E N/mm^2	ρ kg/m^3
Top layer	200	34000	2300
Bottom layer	0	18000	2018
Web (U-shape)	0	18000	2018

Points: 0
RUN
Progress: 100.0%

REINFORCEMENT		Bottom		Top		
ϕ	=	8	mm	8	mm	bar diameter
c	=	31	mm	38	mm	concrete cover
#	=	0		0		number of bars
y	=	35	mm	158	mm	location bar centre

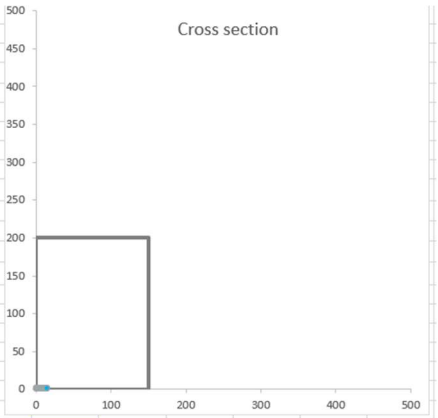

DRYING SHRINKAGE

drying time after curing (days)	NONE

CRACK INPUT		l_{inf}	$w_{c,2}$	f_2	ε_2	$w_{c,3(END)}$	$f_{3(END)}$	$\varepsilon_{3(END)}$
Crack input?		mm	mm	N/mm^2	[-]	mm	N/mm^2	[-]
Concrete	NO	~~100~~	~~0.5~~	~~2~~	~~0.005~~	~~2~~	~~2~~	~~0.02~~
SHCC	NO	~~5~~	~~0.165~~	~~3.4~~	~~0.033~~	~~0.185~~	~~2.8~~	~~0.037~~

DEFLECTION

test type		4-point		type of bending test
$\#_{seg}$	=	500		segments (≠LE) in load-support region
b_{seg}	<	1	mm	width of each segment

Appendix figure 6: material properties in an MLM calculation to determine the effect of the number of layers

In Appendix figure 7, the assumed concrete properties of concrete in tension are shown. The softening behaviour could also be defined, but in this case, only the cracking force is searched for, so only the linear elastic input is needed.

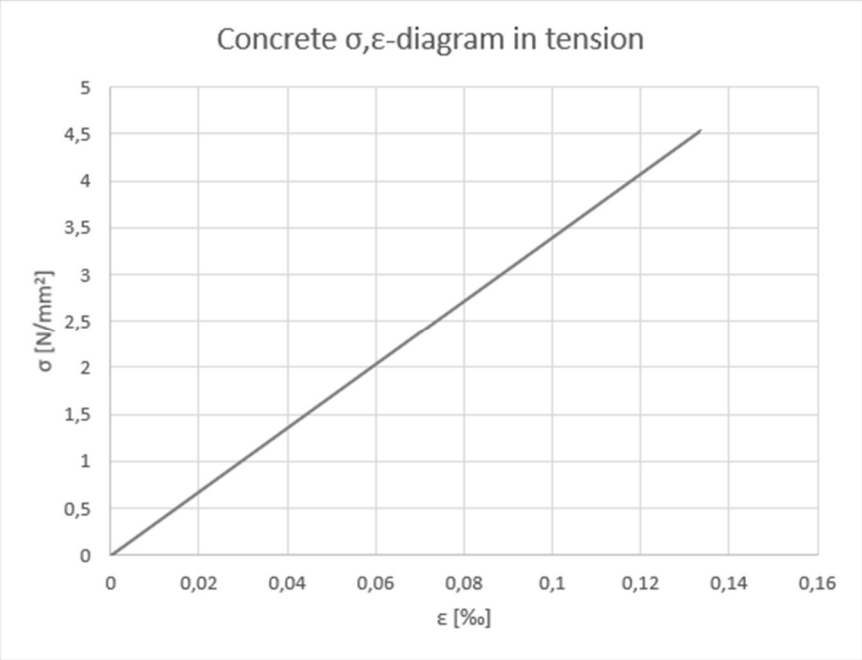

Appendix figure 7: assumed (linear) concrete properties in tension

As can be seen, the cracking stress is at around 4.5 N/mm^2. The 'true' cracking force is calculated and compared with different numbers of layers. Using Eq. (3.1), the true cracking force is calculated:

$$\sigma = \frac{M}{W} \rightarrow \sigma = f_1 \rightarrow M_{Rd} = f_1 * W = 4.536 * \frac{1}{6} * 150 * 200^2 = 4.54\ kNm$$

This bending moment follows from the static scheme in Appendix figure 8. For the sake of simplicity, it is assumed in this case that there are three equal spans. From that, the cracking force can be calculated back. It is equal to:

$$M = \frac{1}{6} * F * L \rightarrow F_{cr} = \frac{6 * M}{L} = \frac{6 * 4.54}{1.5} = \mathbf{18.14\ kN}$$

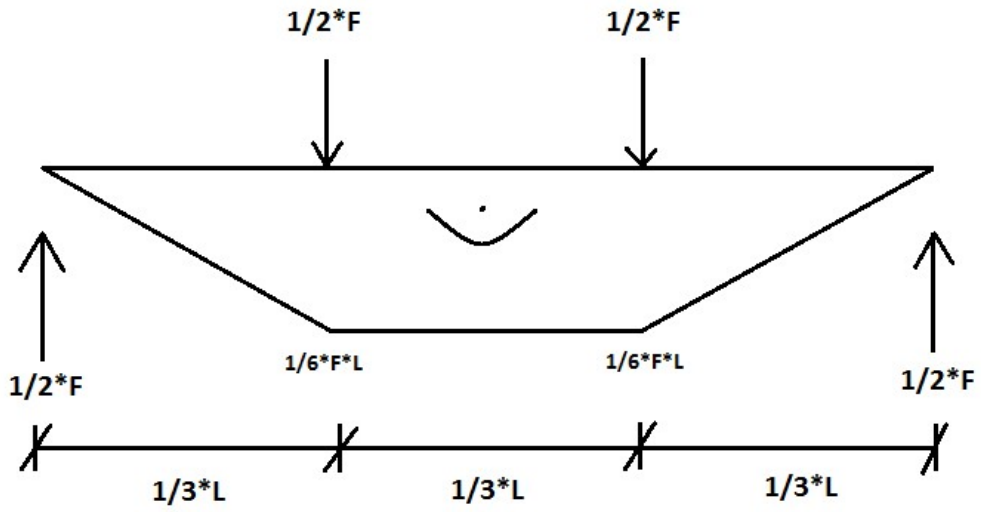

Appendix figure 8: bending moment distribution of a 4-point bending test

In Appendix figure 9, a comparison is made between this result and the result that follows from the proposed MLM for different numbers of layers.

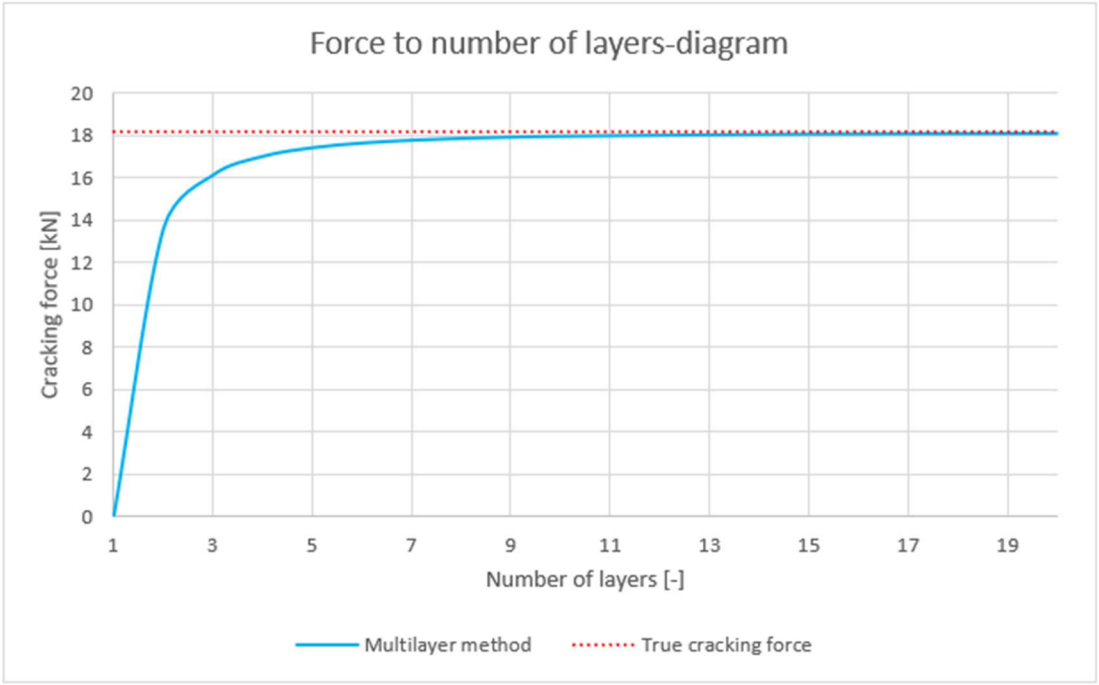

Appendix figure 9: comparison between the real cracking force and what follows from the MLM

As can be seen in Appendix figure 9, the results are very inaccurate for small numbers of layers. But after that, the results quickly converge. When using 10 layers, the difference with the 'true' value is only 1%. From this, it can be concluded that a relatively small number of layers can give accurate results. Although this difference of 1% is found for this particular example, the main message that can be drawn from this result is that using much more layers will not improve the accuracy much. It will only cost extra computation time for a slight improvement in results. At the other hand, using two or three layers in total would result in very inaccurate results. To

conclude, a balance needs to be found when modelling with the MLM, depending on the desired accuracy.

Section 3: materials

The third section that is explained, is the 'materials' section. The required parameters are shown in Appendix figure 10.

MATERIALS
E
f_1
ε_1
f_2
ε_2
f_3
ε_3
ρ

Appendix figure 10: materials section parameters in the developed MLM

In the proposed MLM, the material input parameters can be defined tension and compression. That can be seen in the screenshot of the model that is shown in Appendix figure 11. The '+' sign in that figure stands for 'tension', and the '-' sign stands for 'compression'. In Appendix figure 11, concrete, SHCC and steel are used as materials. The steel indicates the material of the reinforcement; the other two are what the cross-section is composed of. It is not necessary to use SHCC and concrete; any material of which the material input is known can in theory be modelled in the MLM.

		E	f_1	ε_1	f_2	ε_2	f_3	ε_3	ρ
MATERIALS		N/mm^2	N/mm^2	[-]	N/mm^2	[-]	N/mm^2	[-]	kg/m^3
Concrete	+	34000	4.536	0.000133	2	0.00017	0	0.0004	2300
	-	34000	36	0.001059	36	0.0035			
SHCC	+	18000	3	0.000167	3.4	0.015	3.6	0.034	2018
	-	18000	36	0.002	36	0.0035			
Steel	+	200000	550	0.00275	600	0.05			7850
	-	200000	550	0.00275	600	0.05			

Appendix figure 11: materials section in the developed MLM

First, the parameters that require no explanation are mentioned, namely the Young's modulus 'E' and the density 'ρ'. The density is used to calculate the self-weight of the beam, which ultimately is translated into a deflection that is presented in the MLM before any other calculation is made. The most noticeable effect of the density is when the moment of failure of the specimen needs to be specified. The self-weight causes a certain bending moment. If at some

point the resistance of the beam is smaller than this moment, it means that no force is needed to reach this bending moment; the beam has then failed.

After that, the 'f' and the 'ε' parameters are explained, which in fact form a couple as they are the input of the stress-to-strain diagrams that show the material input. The best way to illustrate this is by showing the diagrams that correspond to the input in Appendix figure 11. This is done for concrete, and it is shown in Appendix figure 12 and Appendix figure 13. Note that this is only an example to illustrate the input parameters.

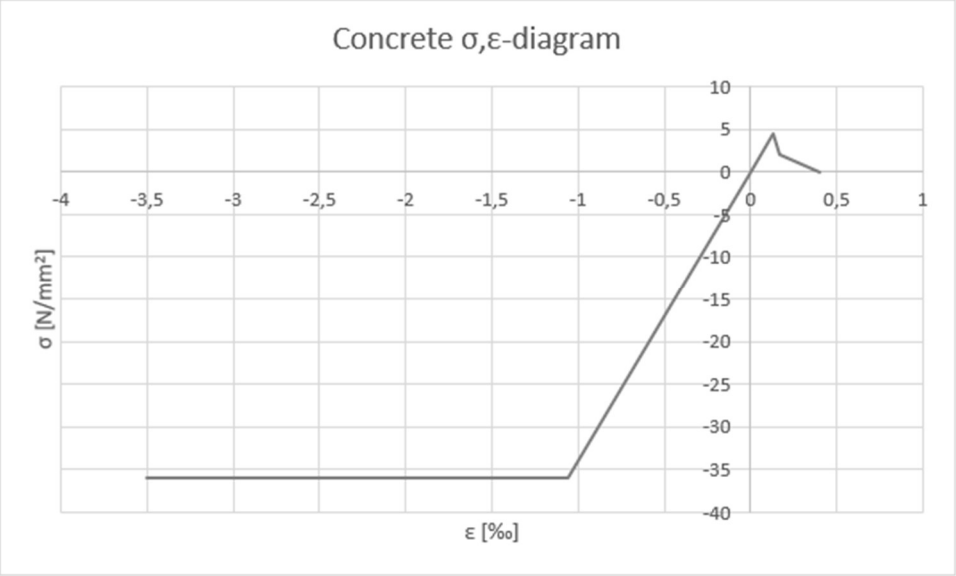

Appendix figure 12: assumed stress-to-strain input diagram of concrete

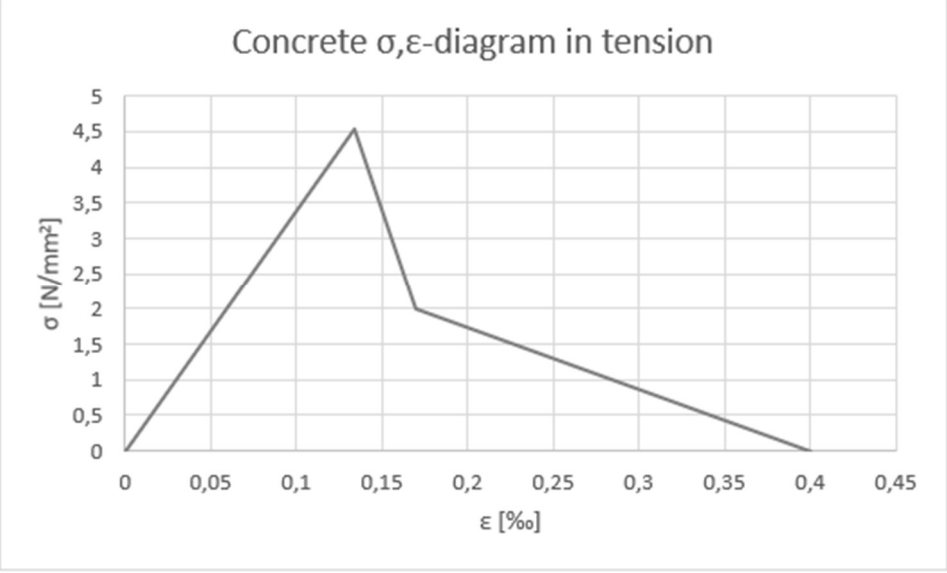

Appendix figure 13: assumed stress-to-strain input diagram of concrete in tension

For the first 'couple', which are 'f_1' and 'ε_1' it can be seen in Appendix figure 11 that the strain is not marked yellow, which means that it is calculated automatically. This is true because for

the linear elastic stage, Eq. (3.3) holds, which means that the strain can be calculated from the stress and the Young's modulus. For the second and third couple, this is not the case anymore because the non-linear stage is entered. Therefore, both components of the couple are marked yellow.

The purpose of those input diagrams is to relate the strains that occur in each layer of the cross-section to its corresponding stress, and then use it to find the force that occurs in each layer. Therefore, this is crucial input which greatly affects the output.

As can be seen in Appendix figure 11, there are up to three possible stress-to-strain couples possible for use in the stress-to-strain diagrams (not for the reinforcement as the third couple is not marked yellow; only two couples are possible). If there is also crack input available (see explanation in 'crack input' section), this number can be increased up to four. If an experimental stress-strain curve is to be used as input, this experimental stress-strain curve can be approximated best if many 'couples' are used. However, this number is limited up to four in the proposed MLM.

Section 4: layer specifications

The fourth section that will be explained is the 'layer specifications' section. The required parameters are shown in Appendix figure 14.

LAYER SPECS
Top layer
Bottom layer
Web
t
E
ρ

Appendix figure 14: layer specifications section parameters in the developed MLM

There are two important notes that have to be made here. First of all, the top layer **always** corresponds to the input of the concrete in the materials section. The bottom layer **always** corresponds to the SHCC input from the materials section. This also holds for the web in case a U-shape is modelled.

Two of the three parameters that are shown in Appendix figure 14 were mentioned earlier, namely the Young's modulus 'E' and the density 'ρ'. The parameter 't' shows the thickness of the material layer that is considered. For the top and bottom layer, it is the thickness of the layers themselves. If the two thicknesses are summed up, they should result in the total height of the beam that was entered in the 'beam input' section. The thickness of the web however, is the width of one web of a U-shape. So if a thickness of 10 mm is used, each web of the U-shape has a thickness of 10 mm.

Section 5: reinforcement

The fifth section that is explained, is the 'reinforcement' section. Note that this section is purely related to the steel. In other words, the reinforcement that is meant here is composed of the steel of which the input comes from the materials section. Theoretically, other materials can be used as reinforcement. However, the reinforcement should then consist of circular bars, as the calculation is based on that type of reinforcement. The material should then be specified in the materials section. The required parameters for the reinforcement section are shown in Appendix figure 15.

REINFORCEMENT
ϕ
c
#
y

Appendix figure 15: reinforcement section parameters in the developed MLM

Note that two different reinforcement types are present, which can be seen in Appendix figure 16: tension reinforcement at the bottom of the beam (denoted as 'bottom'), and compression reinforcement at the top of the beam (denoted as 'top').

REINFORCEMENT		Bottom		Top		
ϕ	=	8	mm	8	mm	bar diameter
c	=	31	mm	38	mm	concrete cover
#	=	3		2		number of bars
y	=	35	mm	158	mm	location bar centre

Appendix figure 16: reinforcement section in the developed MLM

First of all, the reinforcement bar diameter can be specified. However, only the practically used bar diameters can be chosen. Those are shown in Appendix figure 17.

Bar ϕ [mm]
6
8
10
12
14
16
20
25
32
40

Appendix figure 17: practical bar diameters

The other two parameters are the concrete cover 'c', and the number of bars that are used in the beam. This parameters is defined as '#'. The final parameter that is present is the 'y', which is the location of the bar center. This parameter is calculated automatically from the other input, and is of importance because it is a necessary part of the bending moment resistance calculation (it determines the lever arm to the neutral axis).

A limitation in the proposed MLM is that only one row of reinforcement is allowed. So if there are too many bars that are inserted, it is not an option to have two layers of reinforcement instead. This can be extended in the future. The maximum quantity of reinforcement bars is determined according to the Eurocode (NEN, 2011). This code prescribes that the minimum distance between reinforcement bars should be equal to:

$$d_{\emptyset,min} = max\{k_1\emptyset; d_g + k_2; 20\} \text{ in mm} \qquad \textit{Appendix eq. (2)}$$

The 'k_1' and 'k_2' parameters are dependent on the region. For the Netherlands, 'k_1' is equal to 1, and 'k_2' is equal to 5 (NEN, 2016). That gives the following expression:

$$d_{\emptyset,min} = max\{\emptyset; d_g + 5; 20\} \text{ in mm} \qquad \textit{Appendix eq. (3)}$$

The 'd_g' parameter is the maximum aggregate size of the mixture. No coarse aggregates are present if SHCC is made, so in that case, this parameter can be neglected. However, for traditionally reinforced beams, this is not true. However, this is dependent on the beam. For now, it is assumed that the aggregate size is not governing, and the expression that is used in this MLM is:

$$d_{\emptyset,min} = max\{\emptyset; 20\} \text{ in mm} \qquad \textit{Appendix eq. (4)}$$

Now that the minimum required distance is known, it can be compared with the actual distance. An important **assumption** here is that the horizontal concrete cover is assumed to be equal to the vertical concrete cover. So the concrete cover that is inserted is normally the cover from the bottom of the beam; it is now assumed that it is also equal to the cover from the side. This is made clear in Appendix figure 18.

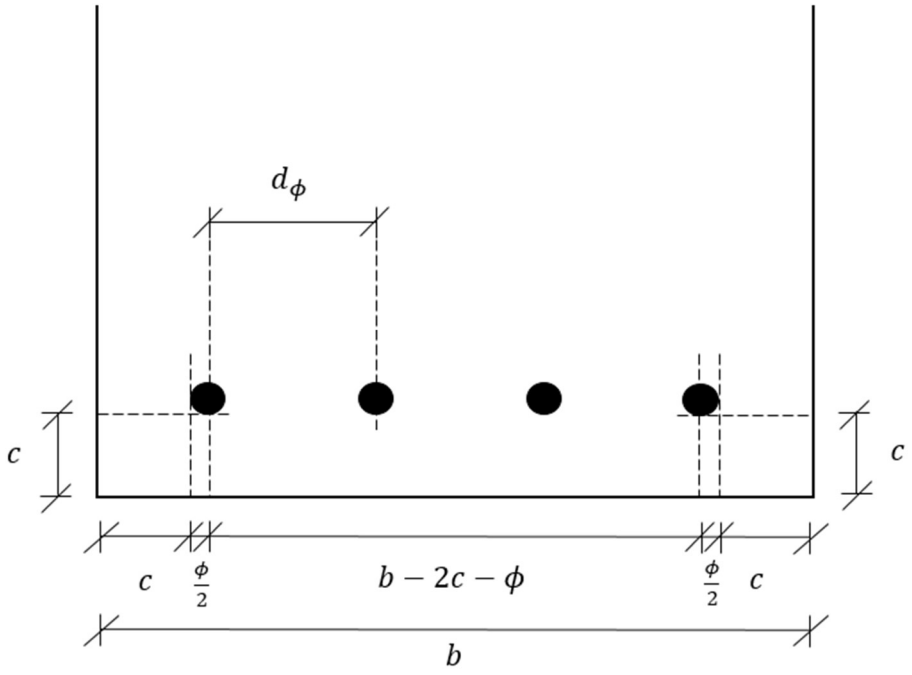

Appendix figure 18: needed scheme for calculating the distance between the reinforcement bars

With this, the distance between the center of the two outer reinforcement bars becomes 'b - 2c - ϕ'. To find the distance between the center of two bars next to each other, it should be divided by 'the number of bars minus one'. The last step is to find the distance between the bars. This is the last found distance minus two times half the diameter of the bar. That leads to:

$$d_\emptyset = \frac{b-2c-\phi}{\#-1} - \phi \text{ in mm} \qquad \textit{Appendix eq. (5)}$$

In the MLM, this distance is compared to the maximum allowable distance. If it exceeds it, a warning is prompted in the model.

Section 6: drying shrinkage

The sixth section that is explained, is the 'drying shrinkage' section. This section is marked in red in Appendix figure 2. The parameter in this section gives how long the specimen has been drying since curing. Here, the curing period is set to be 28 days. If 'NONE' is chosen, it means that the bending test is performed on the same day that the specimen is taken out of the curing room. However, the options are limited. The choices in Appendix table 1 can be made. However, those are only for a specimen height of 150 mm. If a different specimen size is to be tested, the relative humidity profile (or the eigen-strains) for different drying periods has to be provided in the MLM.

Days of drying
NONE
3
7
14
28
90
180
365
730
1095

Appendix table 1: time of drying options in the proposed MLM

If drying has occurred before testing, internal strains/stresses develop that affect the bending test results. Those are taken into consideration in the MLM. An example of this is shown in Appendix figure 19 (for 3 days of drying).

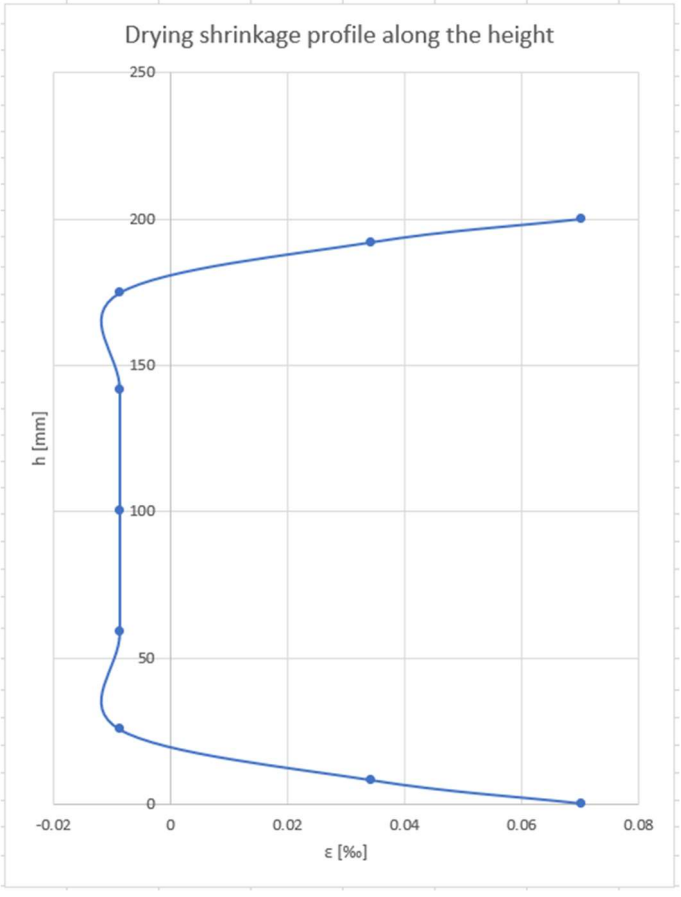

Appendix figure 19: drying shrinkage profile including eigen-strains for 3 days of drying of concrete

This drying shrinkage profile is determined by (Awasthy, 2019) for the drying periods that are shown in Appendix table 1. The other drying shrinkage profiles were shown in Figure 3-39. How

those drying profiles are found, how they affect the results, and how the drying shrinkage is implemented in the MLM, was explained in subchapter 3.4.5.

Section 7: crack input

The next section that is explained, is the 'crack input' section. The input in this section ultimately leads to the same stress-to-strain diagrams that are explained in the 'materials section'. The required parameters are shown in Appendix figure 20.

CRACK INPUT
L_{inf}
$w_{c,2}$
f_2
ε_2
$w_{c,3(END)}$
$f_{3(END)}$
$\varepsilon_{3(END)}$

Appendix figure 20: crack input section in the developed MLM

Two parameters have been explained before, namely the stress 'f' and the strain 'ε'. Also the crack opening displacement and the influence length were explained before, although it was in different subchapters. The crack opening displacement was explained in subchapter 3.4.4, while the influence length was explained in subchapter 3.3.

If the critical crack opening displacement is known, it can be inserted in Eq. (3.8) and translated to the strain by dividing by the influence length; this leads to the strain that is used in the calculations. Normally, the critical crack opening displacement is found in the stress-to-crack opening relation (in tension). An example is shown in Appendix figure 21. The starting point of the horizontal axis is a crack opening of zero, which marks the start of the non-linear stage. So, there is also linear input that comes before this. That is covered in the materials section that was explained before in this Appendix.

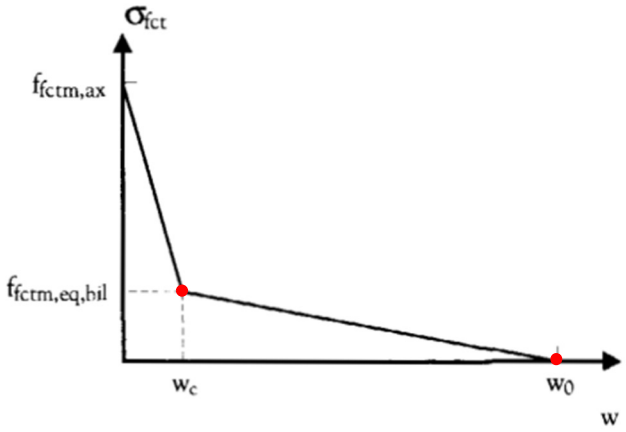

Appendix figure 21: example of a stress-to-crack opening relation (Kooiman, 2000); edited

As is shown in Appendix figure 21, two stress-crack opening couples can be formed (marked in red) if a bi-linear softening curve is assumed. That can also be used as input in the proposed MLM. As was explained in subchapter 3.3, these couples can be translated to stress-strain couples. An important note that needs to be made here, is that the strains that are found by translating the crack opening are **only** the non-linear strains. In the stress-to-strain diagrams, the **total** strains are used. To find the total strain, the non-linear strain has to be added up to the maximum corresponding (tensile) strain from the materials section. This is illustrated in Appendix figure 22. On the left, the stress-to-strain input is shown. On the right, the stress-to-crack opening input is shown. So first, the stress-to-crack opening input is translated to stress-to-strain input, then it is **added up** to the stress-to-strain input on the left.

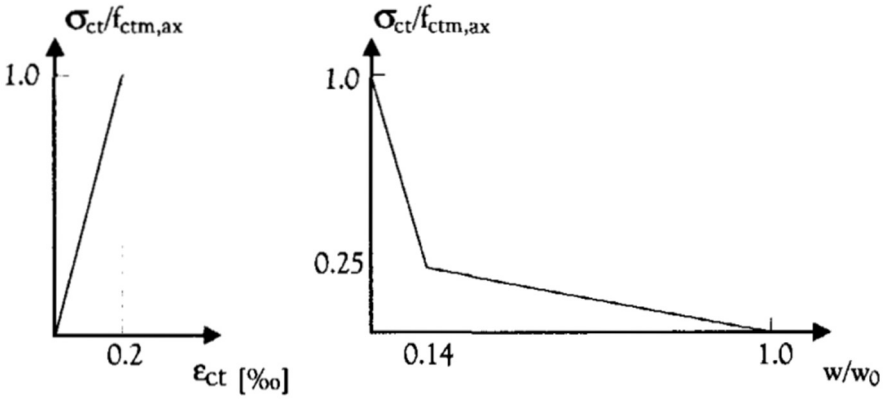

Appendix figure 22: stress-to-strain added with the stress-to-crack opening diagram (Kooiman, 2000)

The stress-to-strain input on the left in Appendix figure 22 can also be bilinear in the proposed MLM. That means that there can be two manually inserted couples (for example as is shown in Appendix figure 23 for SHCC; marked in blue). This leads to a maximum of four couples in the stress-to-strain diagram that forms the input.

MATERIALS		E N/mm²	f_1 N/mm²	ε_1 [-]	f_2 N/mm²	ε_2 [-]	f_3 N/mm²	ε_3 [-]	ρ kg/m³
Concrete	+	34000	4.536	0.000133	2	0.00017	0	0.0004	2300
	-	34000	36	0.001059	36	0.0035			
SHCC	+	18000	3	0.000167	3.4	0.005	~~3.6~~	~~0.034~~	2018
	-	18000	36	0.002	36	0.0035			
Steel	+	200000	550	0.00275	600	0.05			7850
	-	200000	550	0.00275	600	0.05			

Appendix figure 23: two manual stress-to-strain couples for SHCC marked in blue

An example of a case in which there are four couples in tension is shown in Appendix figure 23. Currently, this is the maximum amount of datapoints in tensional properties that the proposed MLM can handle. If more datapoints are desired, the proposed MLM should be expanded.

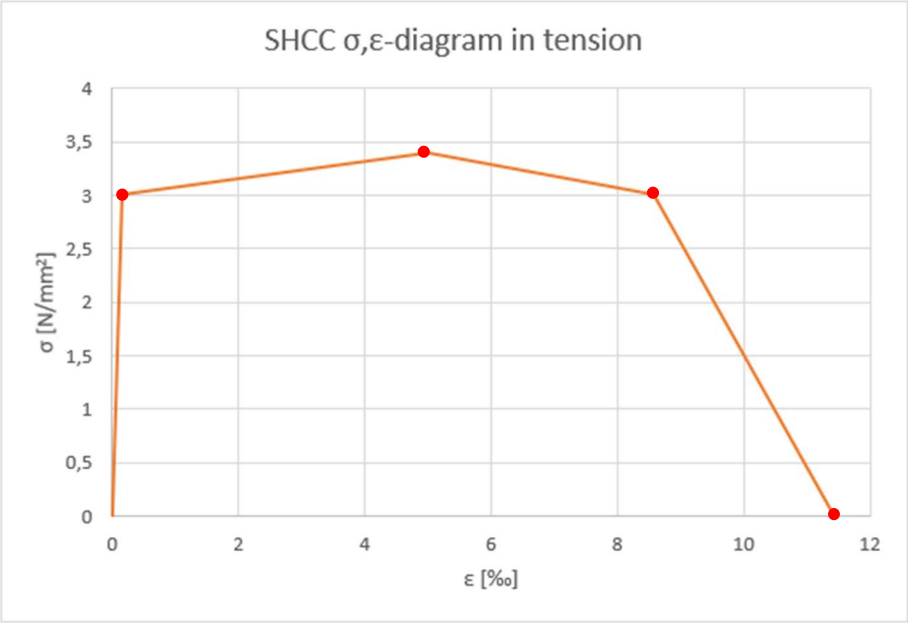

Appendix figure 24: maximum amount of four stress-to-strain couples in tension

As was explained before, only three datapoints can be used as input if there is no crack input available. If there is crack input available, this increases to four datapoints. This can be explained as follows: the crack input section is added to the materials section if there is crack input. This means that two datapoints can be added. That would suggest that five datapoints are possible in total, as the materials section already contains three datapoints. However, the proposed MLM is programmed such that if there is crack input, the materials section can only produce two datapoints. That results in four possible datapoints in total.

Section 8: deflection

Finally, the parameters of the 'deflection' section are explained. The required parameters are shown in Appendix figure 25.

DEFLECTION
Test type
$\#_{seg}$
b_{seg}

Appendix figure 25: deflection section in the developed MLM

First of all, it can be chosen which type of bending test is performed. The two options are a 3-point and a 4-point bending test. The reason that the type of bending test is input in this section, is that mainly the deflection is affected by different types of bending tests.

The next parameter is the number of segments '$\#_{seg}$'. Because this parameter cannot be explained on its own, only the visualization of it is shown. That is shown in Figure 3-28. In short, it prescribes the number of segments between the maximum bending moment and the maximum linear elastic moment. This is needed for determining the deflection. This was explained more in detail in subchapter 3.4.2.2.2.

The final parameter is the width of those segments (given by 'b_{seg}'). Note that a 'smaller than' sign is used in Appendix figure 25, and not an 'equal to' sign. This is done because the length of the non-linear region (region 2 in Figure 3-28) is different for each iteration. Therefore, the maximum possible value is chosen, namely:

$$b_{seg} = \frac{L_1}{\#_{seg}} \qquad \textit{Appendix eq. (6)}$$

The L_1 is the total left span as was described earlier. In this way, the 'smaller than' sign is always true as the length of the region always has to be smaller than the total left/right span. This parameter is only included in the model to give an indication of how wide each segment is to have an idea of the accuracy that can be expected from the results.

Appendix C: MLM verification

Phase 1: HSFRC

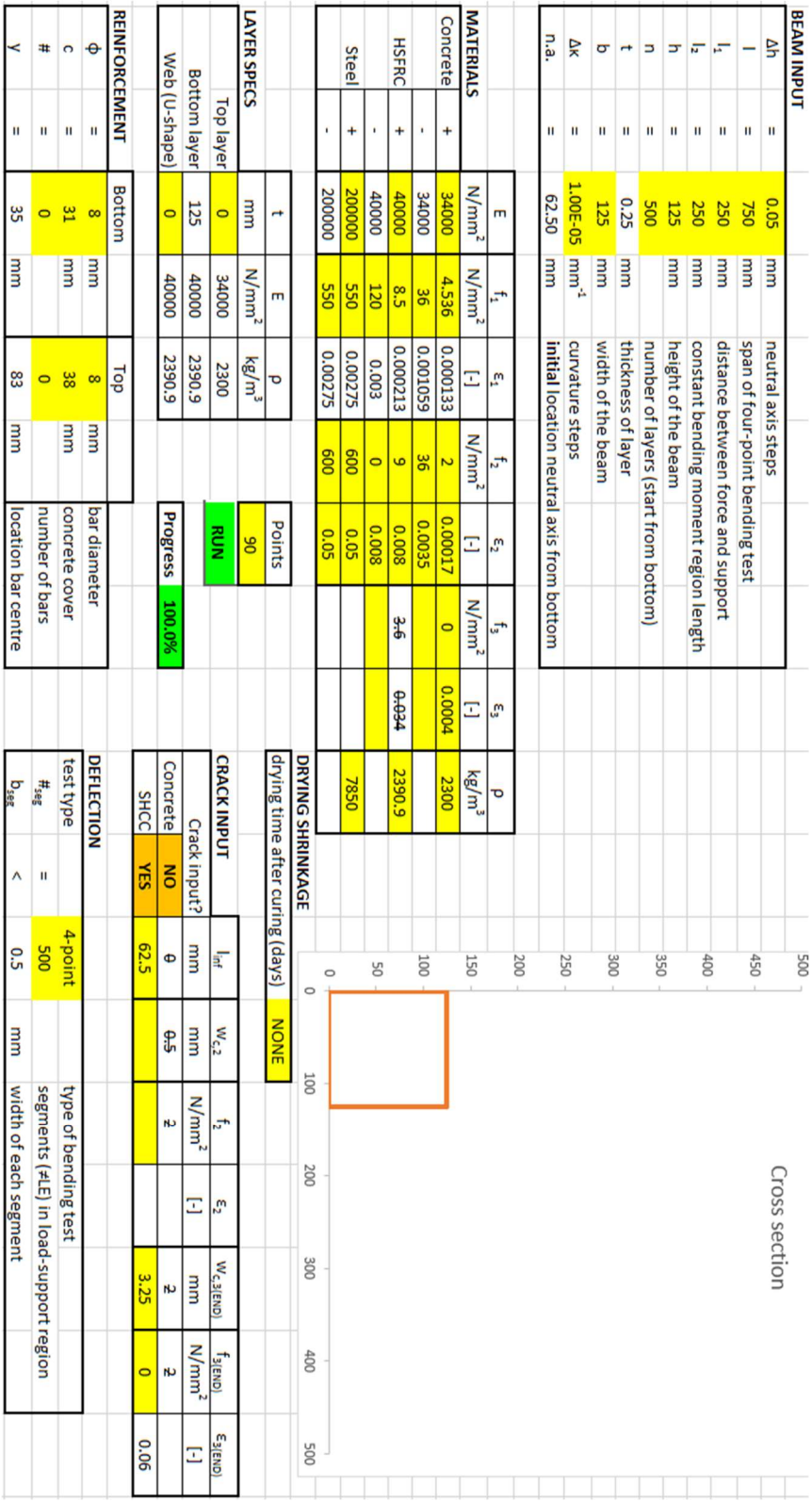

Appendix figure 26: input parameters verification phase 1; HSFRC

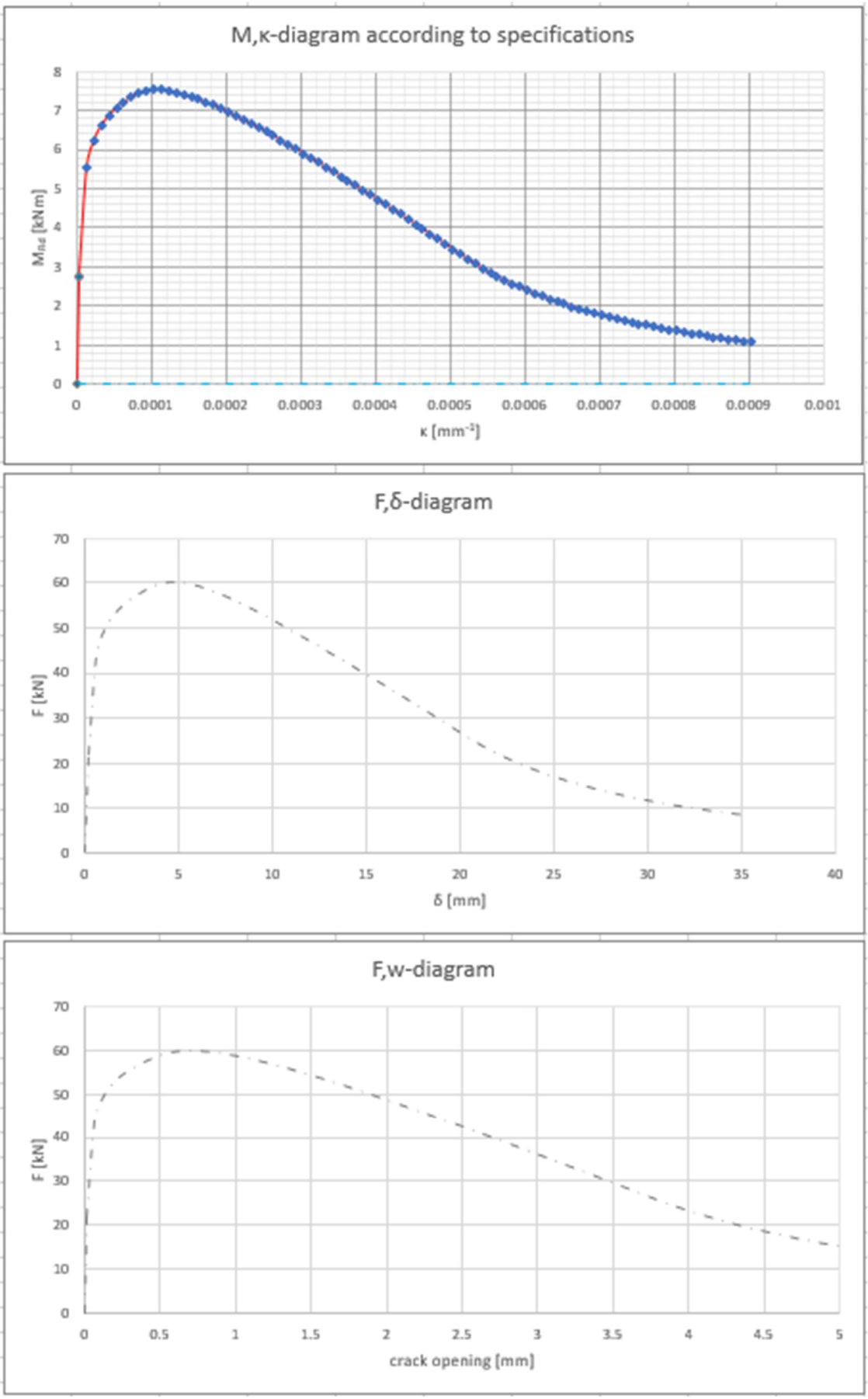

Appendix figure 27: output verification phase 1; HSFRC

Phase 1: SHCC

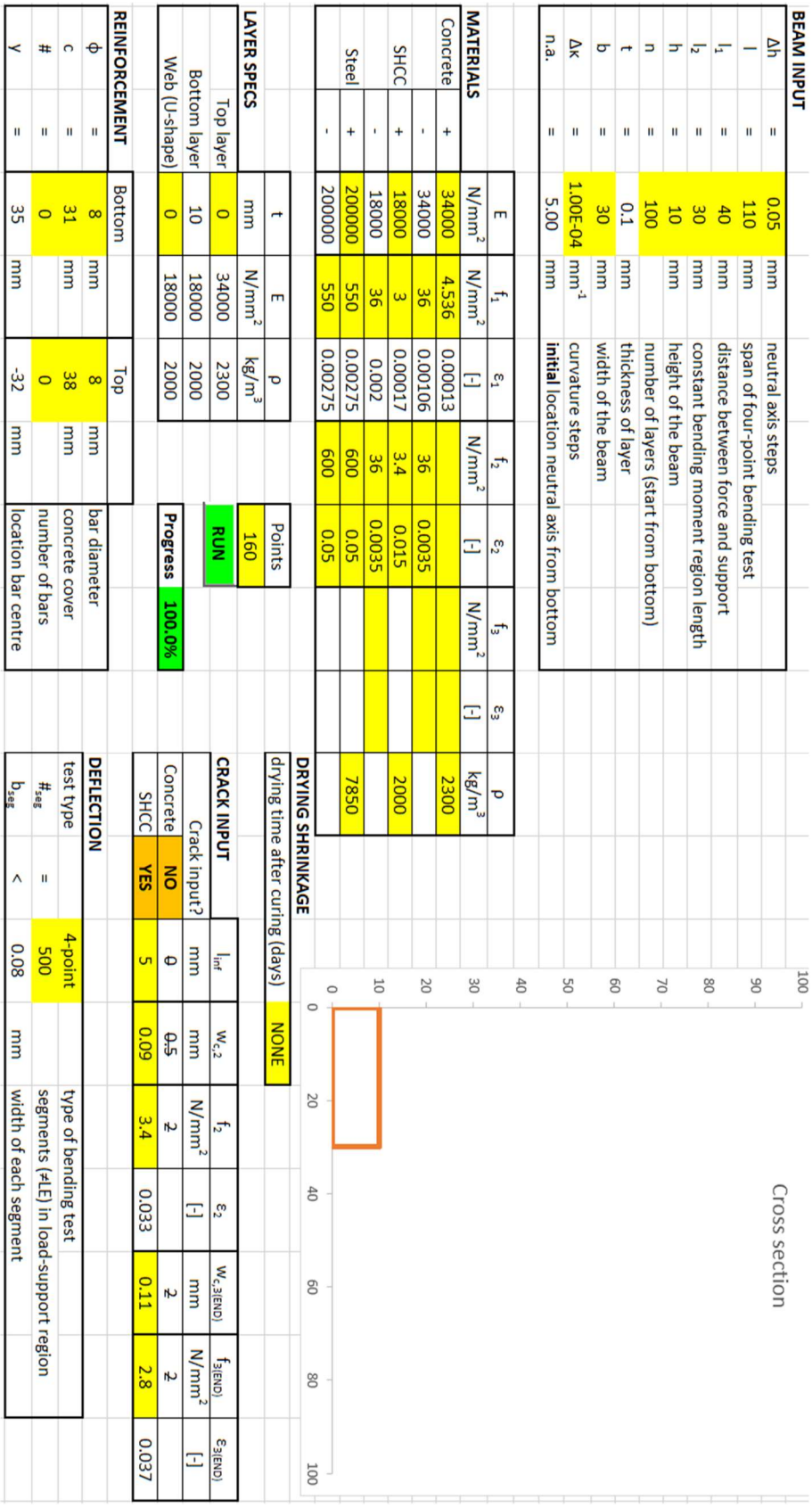

Appendix figure 28: input parameters verification phase 1; HSFRC

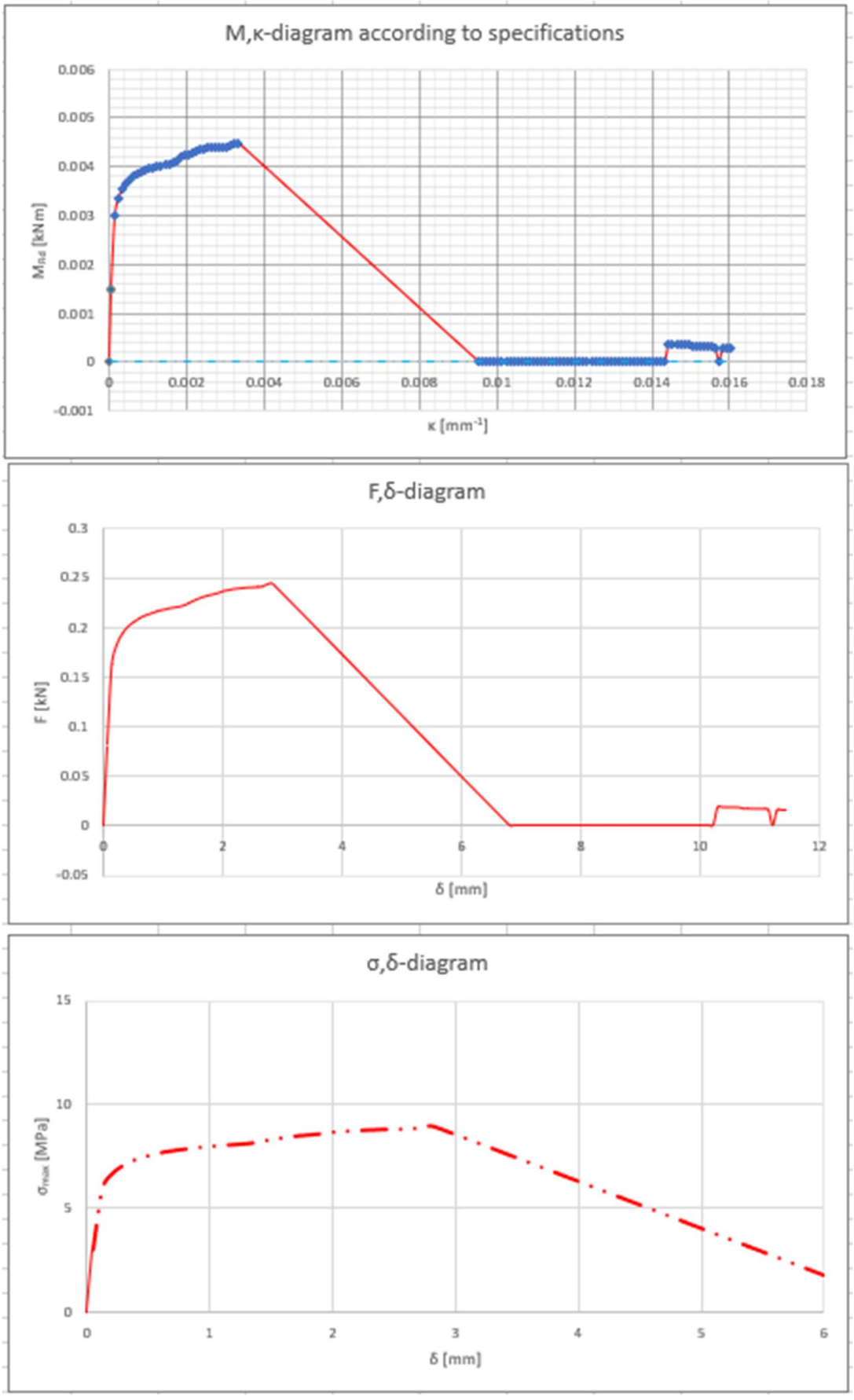

Appendix figure 29: output verification phase 1; HSFRC

Phase 2

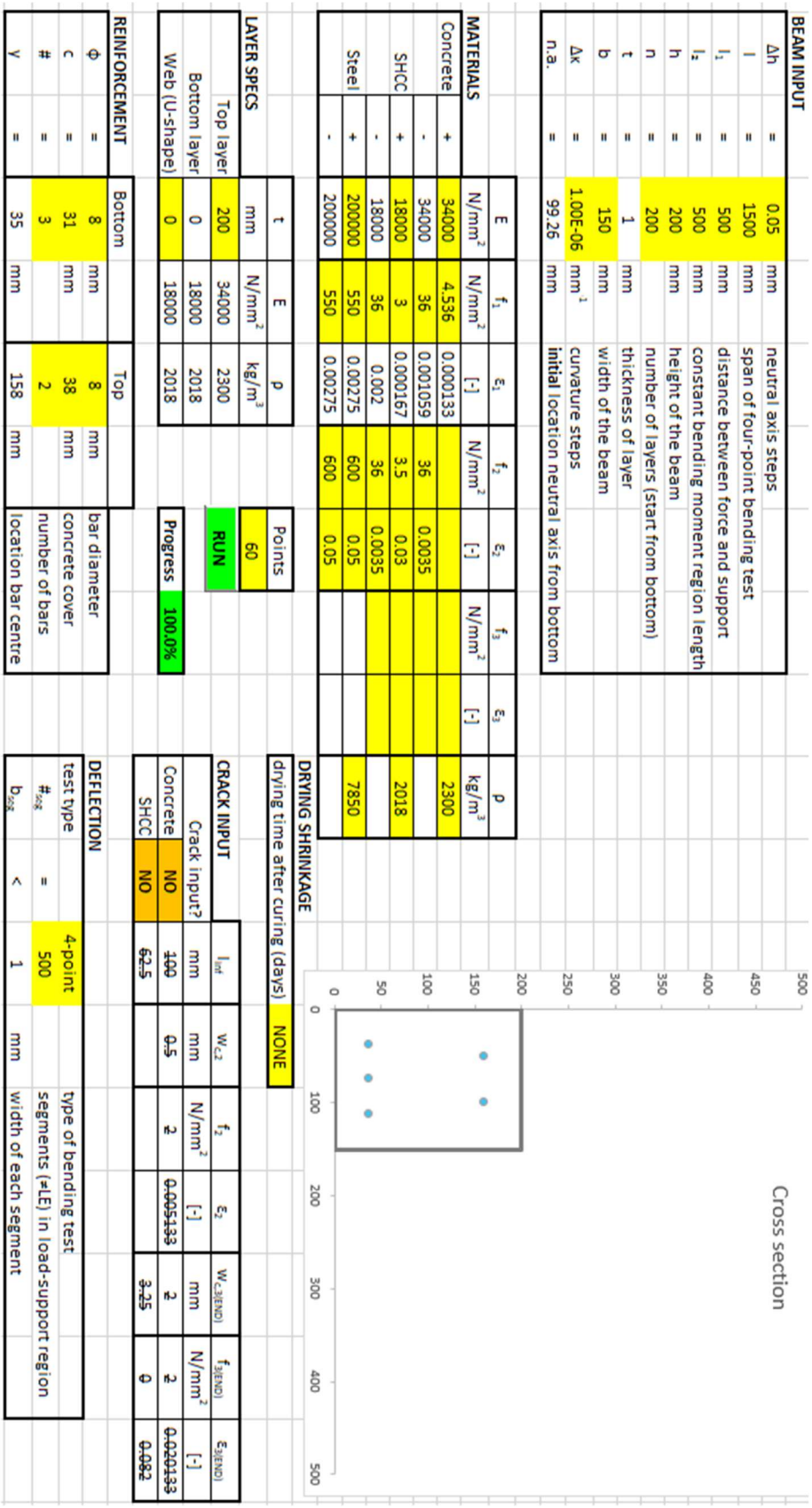

Appendix figure 30: input parameters verification phase 2

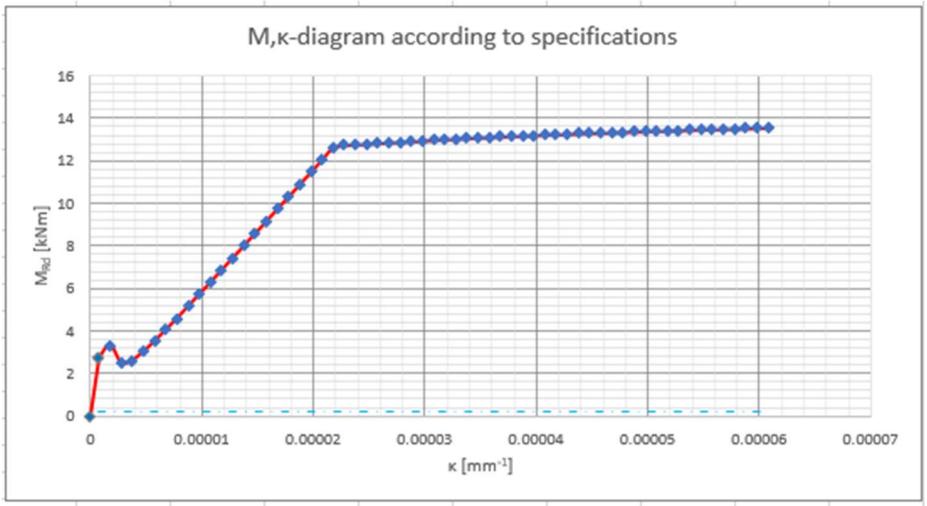

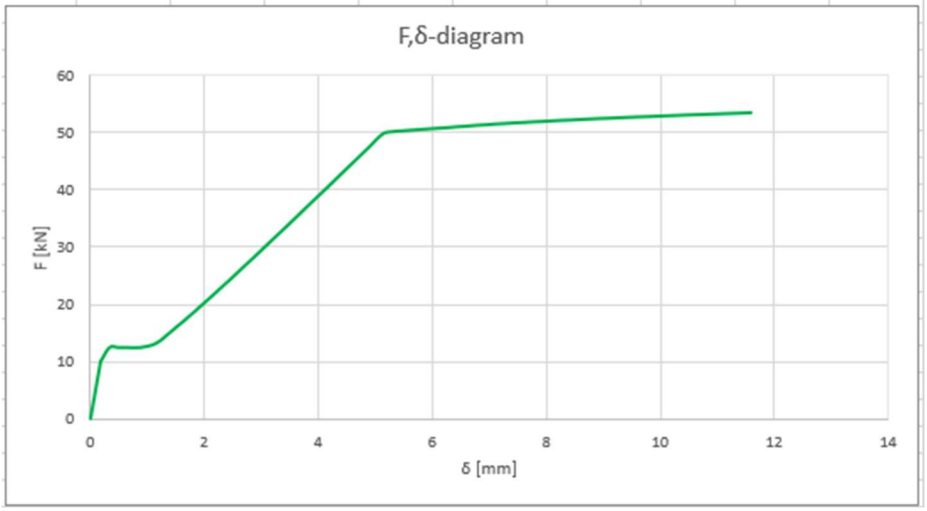

Appendix figure 31: output verification phase 2

Find σ_{sr}

d	α_e	A_s	ρ_l	x	z	σ_{sr}
[mm]	[-]	[mm^2]	[-]	[mm]	[mm]	[N/mm^2]
165	5.882353	150.7964	0.006093	38.65607	152.1146	118.4013

w_{max} parameters

τ_{bm}	α	h_{eff}	ρ_{eff}
[N/mm^2]	[-]	[mm]	[-]
9.072	0.5	53.78131	0.018693

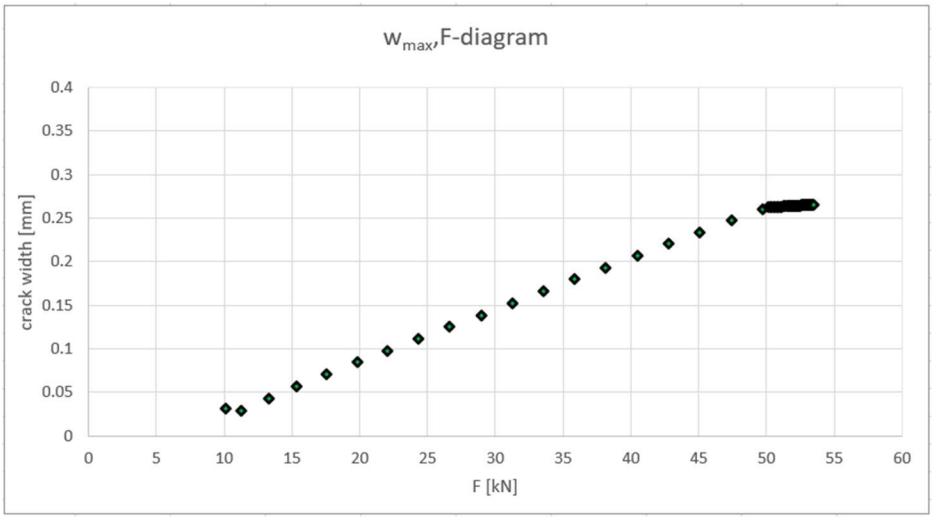

Appendix figure 32: crack width calculation output phase 2

Phase 3

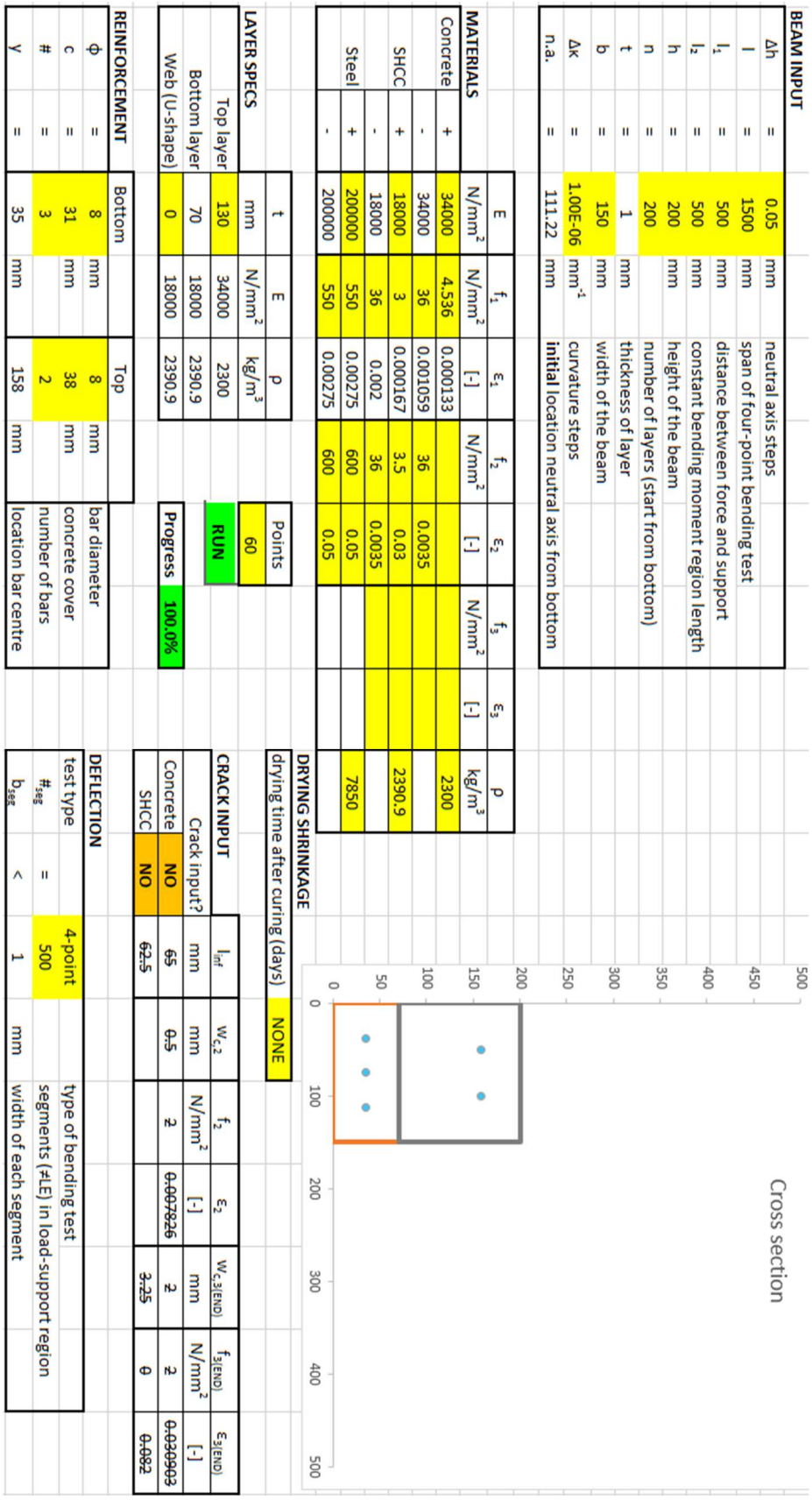

Appendix figure 33: input parameters verification phase 3

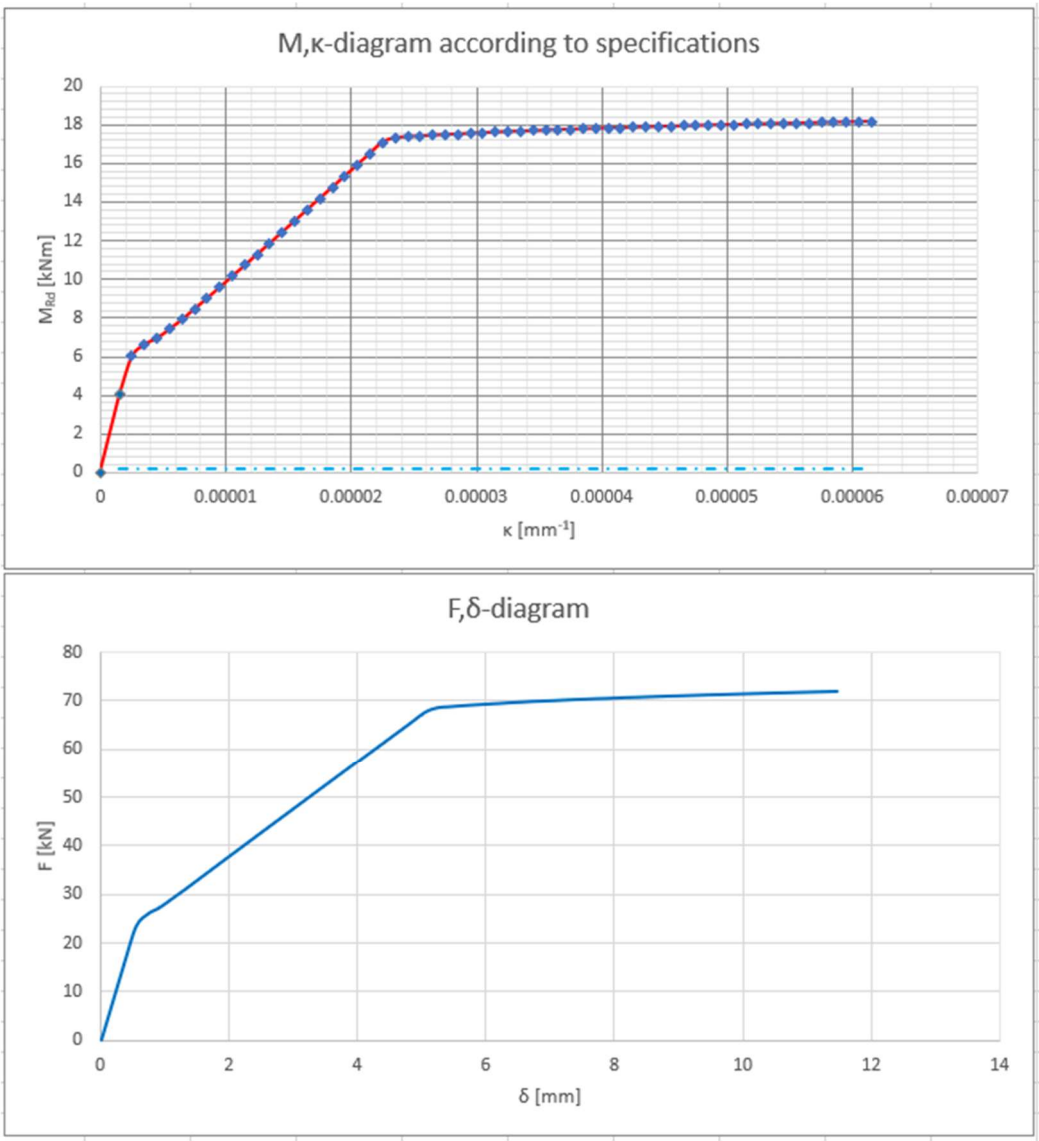

Appendix figure 34: output verification phase 3

Phase 4

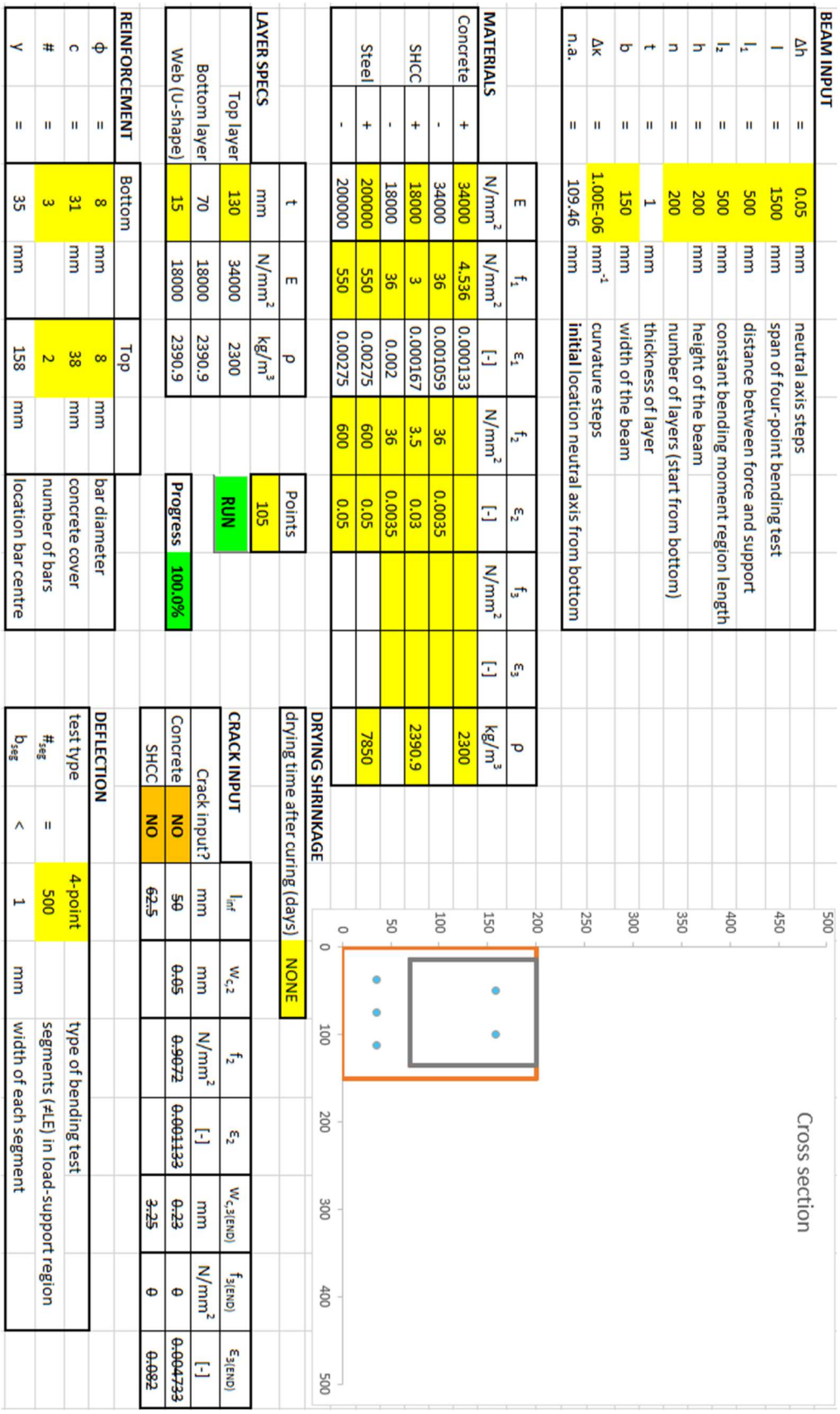

Appendix figure 35: input parameters verification phase 4

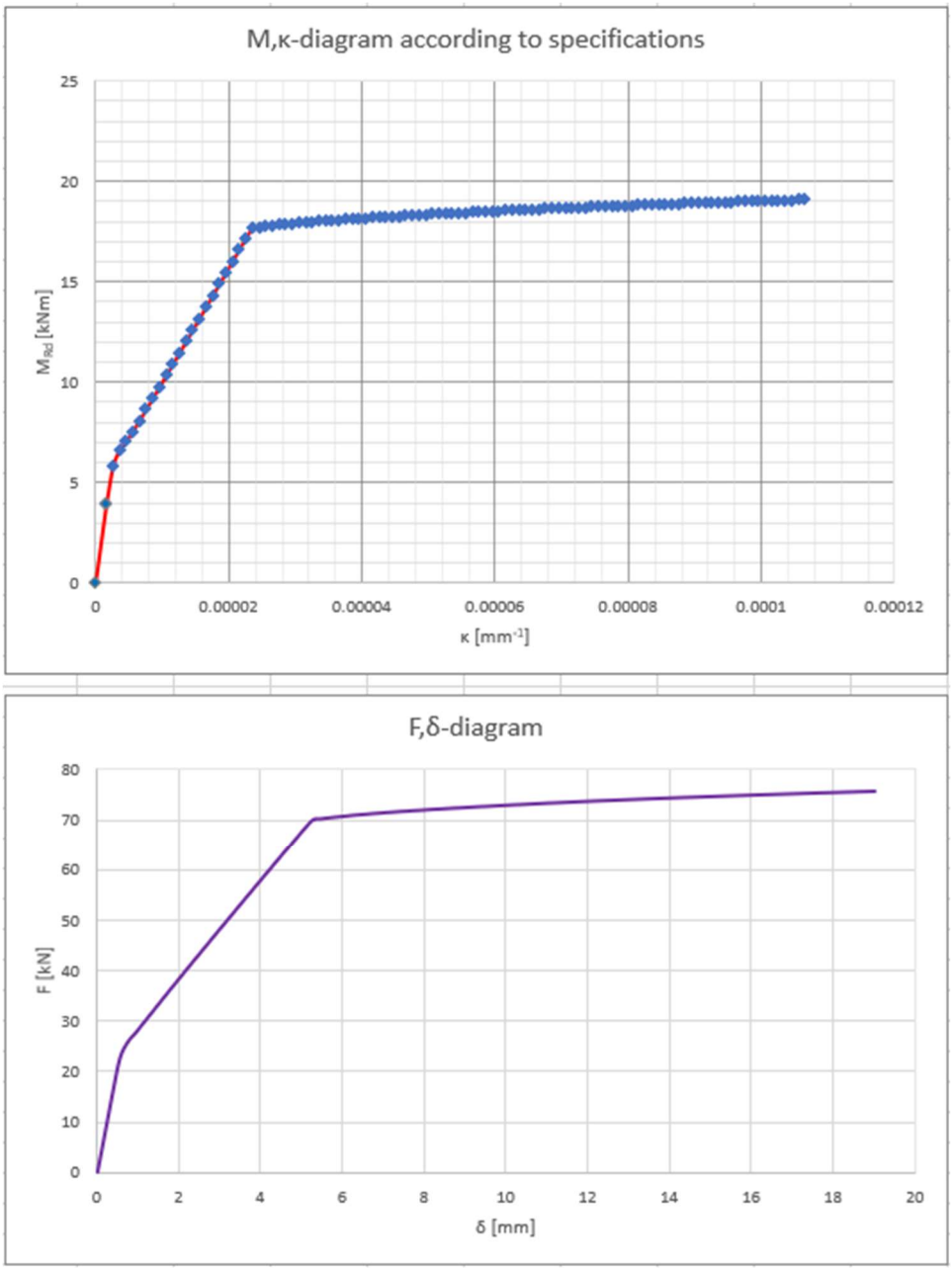

Appendix figure 36: output verification phase 4

Drying shrinkage: NSC

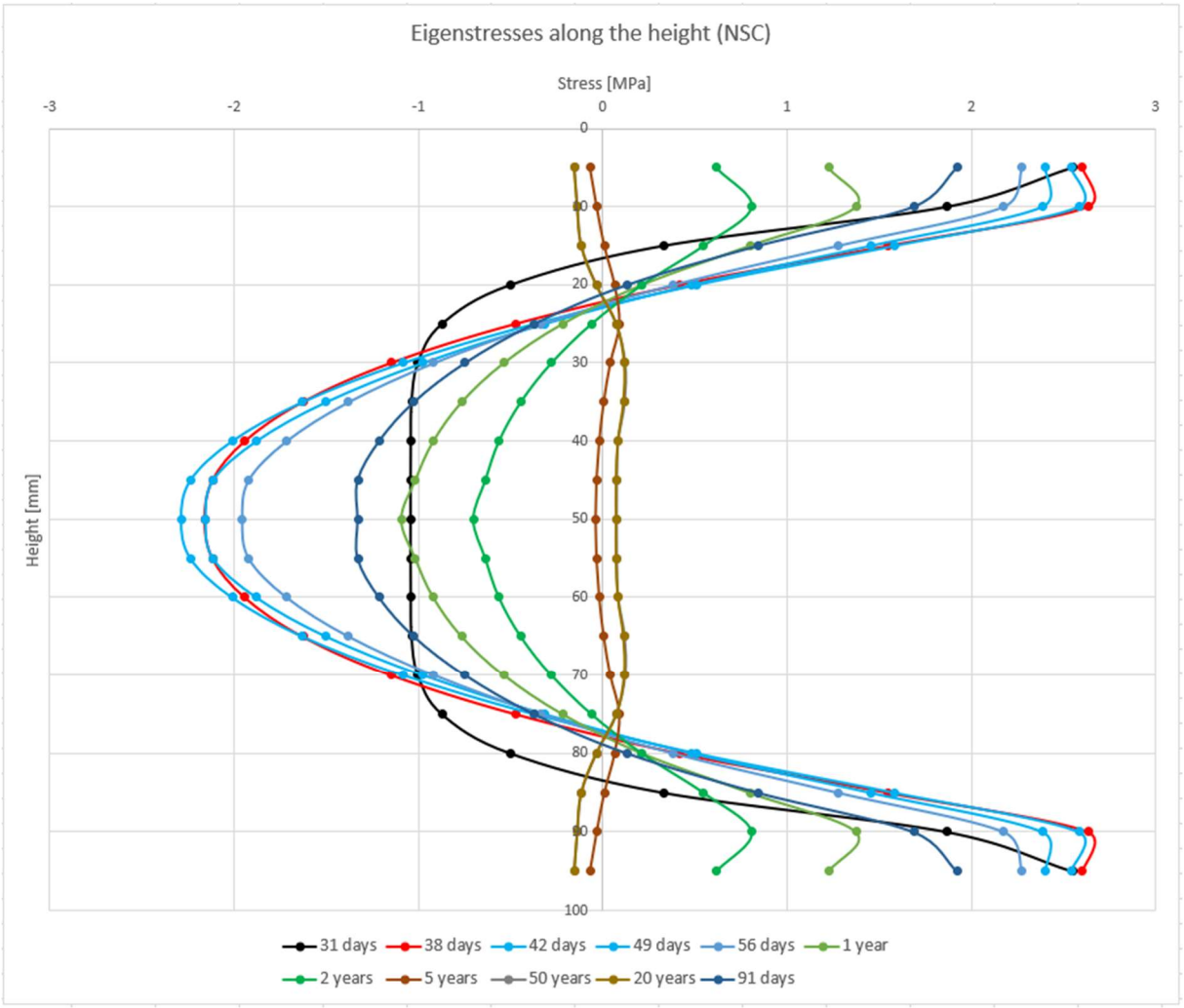

Appendix figure 37: eigenstresses along the height for Normal Strength Concrete (Awasthy, 2019)

NSC

Days	[-]	31	38	42	49	56	91	365	730	1825	7300	18250
E-modulus	N/mm^2	31321	32071	32500	33250	34000	34400	34700	34700	34700	34700	34700

Depth		Stress	Stress	Stress	Stress	Stress	Stress	Stress	Stress	Stress	Stress	Stress
[mm]		$[N/mm^2]$	$[N/mm^2]$	$[N/mm^2]$	$[N/mm^2]$	$[N/mm^2]$	$[N/mm^2]$	$[N/mm^2]$	$[N/mm^2]$	$[N/mm^2]$	$[N/mm^2]$	$[N/mm^2]$
5		2.548	2.603	2.542	2.404	2.273	1.923	1.227	0.616	-0.069	-0.151	-0.151
10		1.87	2.633	2.586	2.389	2.174	1.688	1.375	0.808	-0.032	-0.135	-0.134
15		0.33	1.549	1.586	1.456	1.276	0.844	0.799	0.547	0.01	-0.113	-0.113
20		-0.499	0.416	0.511	0.484	0.383	0.135	0.215	0.214	0.067	-0.032	-0.033
25		-0.871	-0.473	-0.371	-0.316	-0.333	-0.371	-0.217	-0.06	0.093	0.079	0.074
30		-1.001	-1.147	-1.083	-0.976	-0.916	-0.745	-0.535	-0.277	0.043	0.12	0.122
35		-1.035	-1.626	-1.628	-1.501	-1.379	-1.022	-0.763	-0.443	0.007	0.116	0.119
40		-1.039	-1.939	-2.01	-1.88	-1.715	-1.211	-0.917	-0.561	-0.018	0.086	0.084
45		-1.04	-2.114	-2.236	-2.115	-1.921	-1.327	-1.015	-0.635	-0.033	0.076	0.077
50		-1.04	-2.156	-2.287	-2.156	-1.956	-1.327	-1.091	-0.7	-0.038	0.076	0.076
55		-1.04	-2.114	-2.236	-2.115	-1.921	-1.327	-1.015	-0.635	-0.033	0.076	0.077
60		-1.039	-1.939	-2.01	-1.88	-1.715	-1.211	-0.917	-0.561	-0.018	0.086	0.084
65		-1.035	-1.626	-1.628	-1.501	-1.379	-1.022	-0.763	-0.443	0.007	0.116	0.119
70		-1.001	-1.147	-1.083	-0.976	-0.916	-0.745	-0.535	-0.277	0.043	0.12	0.122
75		-0.871	-0.473	-0.371	-0.316	-0.333	-0.371	-0.217	-0.06	0.093	0.079	0.074
80		-0.499	0.416	0.511	0.484	0.383	0.135	0.215	0.214	0.067	-0.032	-0.033
85		0.33	1.549	1.586	1.456	1.276	0.844	0.799	0.547	0.01	-0.113	-0.113
90		1.87	2.633	2.586	2.389	2.174	1.688	1.375	0.808	-0.032	-0.135	-0.134
95		2.548	2.603	2.542	2.404	2.273	1.923	1.227	0.616	-0.069	-0.151	-0.151

Depth		Strain	Strain	Strain	Strain	Strain	Strain	Strain	Strain	Strain	Strain	Strain
[mm]		[-]	[-]	[-]	[-]	[-]	[-]	[-]	[-]	[-]	[-]	[-]
5		8.1351E-05	8.1E-05	7.8E-05	7.2E-05	6.7E-05	5.6E-05	3.5E-05	1.8E-05	-2E-06	-4E-06	-4E-06
10		5.9704E-05	8.2E-05	8E-05	7.2E-05	6.4E-05	4.9E-05	4E-05	2.3E-05	-9E-07	-4E-06	-4E-06
15		1.0536E-05	4.8E-05	4.9E-05	4.4E-05	3.8E-05	2.5E-05	2.3E-05	1.6E-05	2.9E-07	-3E-06	-3E-06
20		-1.593E-05	1.3E-05	1.6E-05	1.5E-05	1.1E-05	3.9E-06	6.2E-06	6.2E-06	1.9E-06	-9E-07	-1E-06
25		-2.781E-05	-1E-05	-1E-05	-1E-05	-1E-05	-1E-05	-6E-06	-2E-06	2.7E-06	2.3E-06	2.1E-06
30		-3.196E-05	-4E-05	-3E-05	-3E-05	-3E-05	-2E-05	-2E-05	-8E-06	1.2E-06	3.5E-06	3.5E-06
35		-3.304E-05	-5E-05	-5E-05	-5E-05	-4E-05	-3E-05	-2E-05	-1E-05	2E-07	3.3E-06	3.4E-06
40		-3.317E-05	-6E-05	-6E-05	-6E-05	-5E-05	-4E-05	-3E-05	-2E-05	-5E-07	2.5E-06	2.4E-06
45		-3.32E-05	-7E-05	-7E-05	-6E-05	-6E-05	-4E-05	-3E-05	-2E-05	-1E-06	2.2E-06	2.2E-06
50		-3.32E-05	-7E-05	-7E-05	-6E-05	-6E-05	-4E-05	-3E-05	-2E-05	-1E-06	2.2E-06	2.2E-06
55		-3.32E-05	-7E-05	-7E-05	-6E-05	-6E-05	-4E-05	-3E-05	-2E-05	-1E-06	2.2E-06	2.2E-06
60		-3.317E-05	-6E-05	-6E-05	-6E-05	-5E-05	-4E-05	-3E-05	-2E-05	-5E-07	2.5E-06	2.4E-06
65		-3.304E-05	-5E-05	-5E-05	-5E-05	-4E-05	-3E-05	-2E-05	-1E-05	2E-07	3.3E-06	3.4E-06
70		-3.196E-05	-4E-05	-3E-05	-3E-05	-3E-05	-2E-05	-2E-05	-8E-06	1.2E-06	3.5E-06	3.5E-06
75		-2.781E-05	-1E-05	-1E-05	-1E-05	-1E-05	-1E-05	-6E-06	-2E-06	2.7E-06	2.3E-06	2.1E-06
80		-1.593E-05	1.3E-05	1.6E-05	1.5E-05	1.1E-05	3.9E-06	6.2E-06	6.2E-06	1.9E-06	-9E-07	-1E-06
85		1.0536E-05	4.8E-05	4.9E-05	4.4E-05	3.8E-05	2.5E-05	2.3E-05	1.6E-05	2.9E-07	-3E-06	-3E-06
90		5.9704E-05	8.2E-05	8E-05	7.2E-05	6.4E-05	4.9E-05	4E-05	2.3E-05	-9E-07	-4E-06	-4E-06
95		8.1351E-05	8.1E-05	7.8E-05	7.2E-05	6.7E-05	5.6E-05	3.5E-05	1.8E-05	-2E-06	-4E-06	-4E-06

Appendix figure 38: conversion from eigenstresses to eigen-strain for a NSC specimen of 100 mm

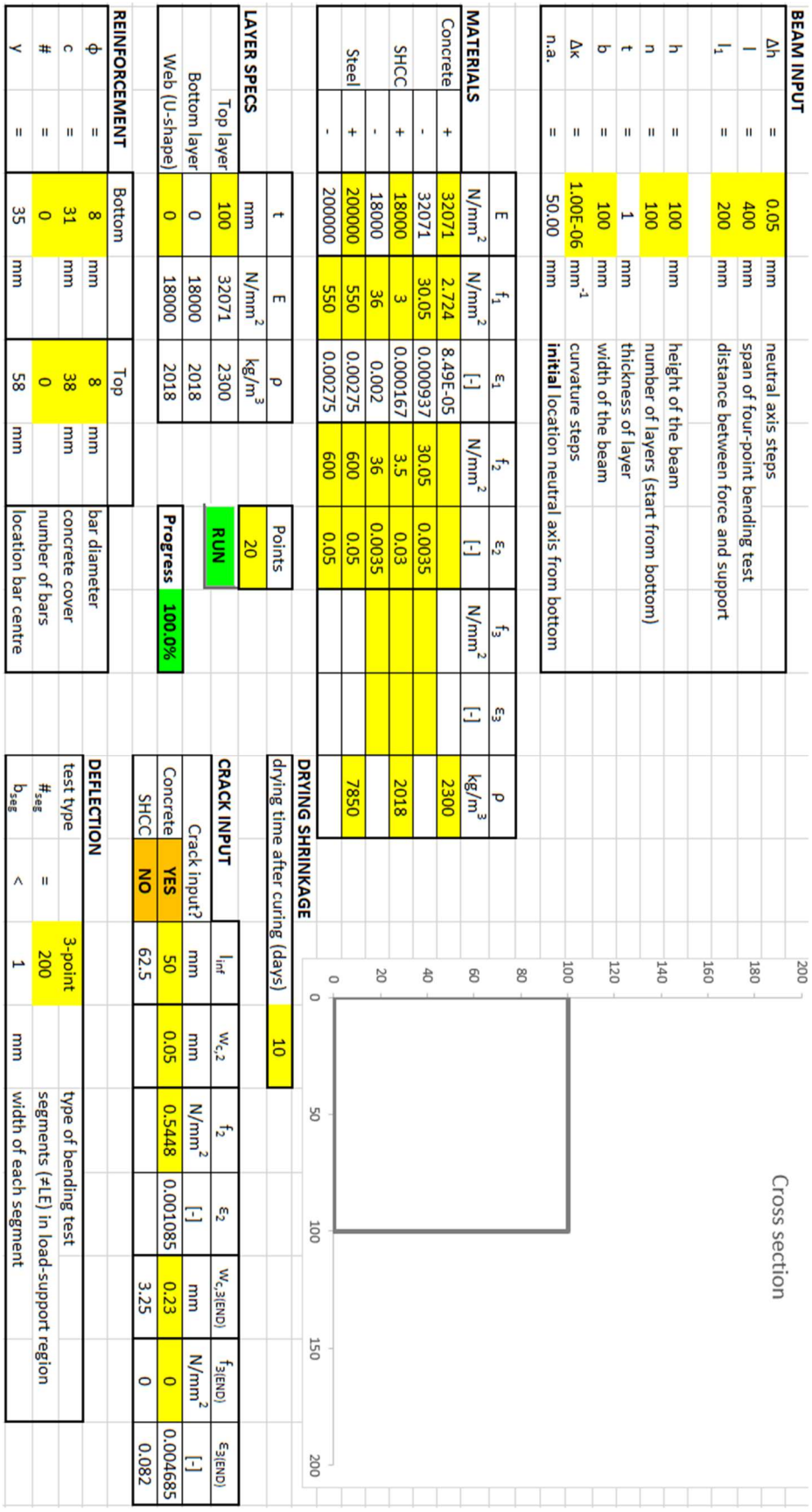

Appendix figure 39: input parameters NSC drying shrinkage verification

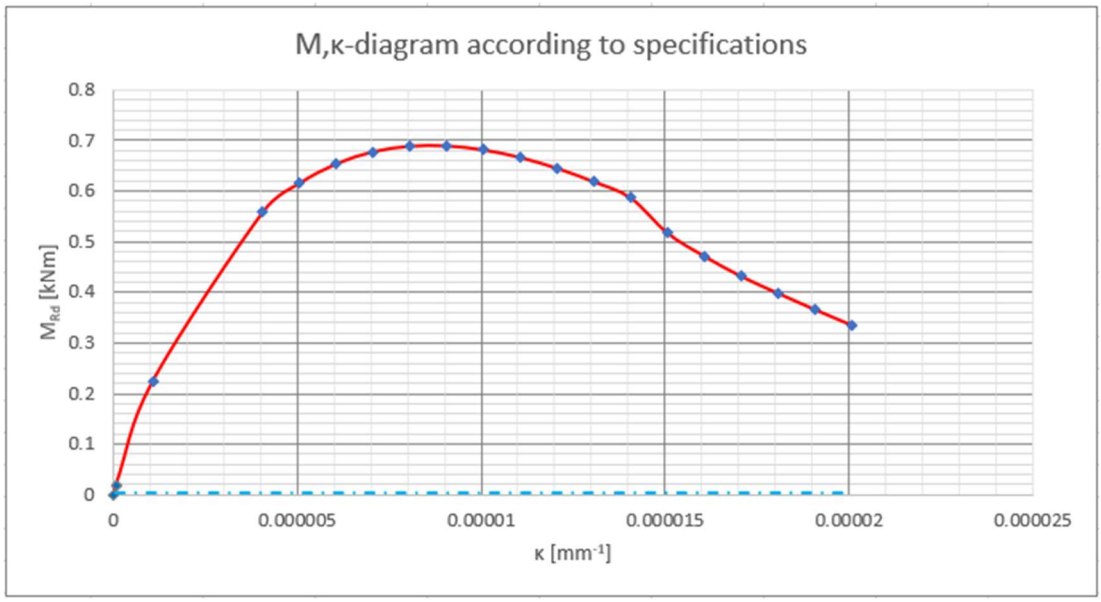

Stress calculation for σ,δ-diagram → **only valid if a non-hybrid beam is considered (no webs)**

I	z
[mm^4]	[mm]
8.33E+06	50.00

M	[Nmm]	0	19294	223894	558520	615357	653910	677772	688698	689331	681377	666445
$\sigma_{bot.fiber}$	[N/mm^2]	0	0.115764	1.343364	3.35112	3.692142	3.92346	4.066632	4.132188	4.135986	4.088262	3.99867
δ	[mm]	0.000291	0.001021	0.000725	0.009113	0.014655	0.018797	0.021642	0.023227	0.02332	0.022162	0.020324

σ_{max}	[N/mm^2]	4.135986

Appendix figure 40: output NSC drying shrinkage verification

Drying shrinkage: HSC

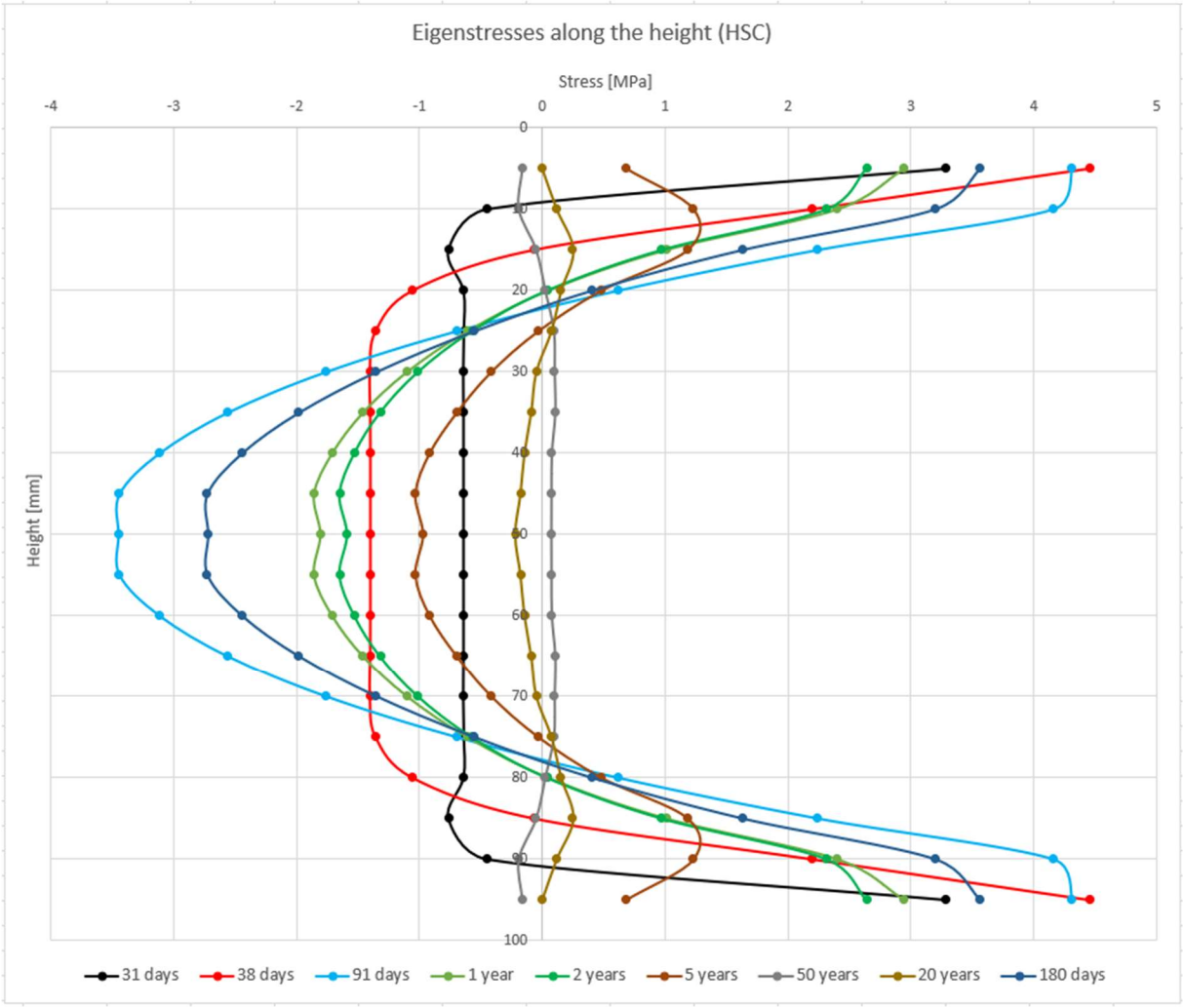

Appendix figure 41: eigenstresses along the height for High Strength Concrete (Awasthy, 2019)

HSC

Days	[-]	31	38	91	180	365	730	1825	7300	18250
E-modulus	N/mm^2	37471	37871	39600	39700	39700	39600	39600	39600	39600

Depth		Stress	Stress	Stress	Stress	Stress	Stress	Stress	Stress	Stress
[mm]		[N/mm^2]	[N/mm^2]	[N/mm^2]	[N/mm^2]	[N/mm^2]	[N/mm^2]	[N/mm^2]	[N/mm^2]	[N/mm^2]
5		3.285	4.451	4.311	3.56	2.944	2.638	0.68	0	-0.164
10		-0.445	2.193	4.157	3.194	2.399	2.314	1.227	0.116	-0.193
15		-0.76	-0.066	2.243	1.628	1.007	0.973	1.18	0.249	-0.052
20		-0.637	-1.055	0.618	0.404	0.046	0.041	0.48	0.152	0.021
25		-0.634	-1.356	-0.698	-0.555	-0.611	-0.571	-0.033	0.074	0.091
30		-0.639	-1.402	-1.758	-1.35	-1.101	-1.009	-0.414	-0.047	0.097
35		-0.637	-1.399	-2.558	-1.98	-1.459	-1.317	-0.694	-0.088	0.102
40		-0.637	-1.398	-3.114	-2.444	-1.71	-1.526	-0.915	-0.142	0.074
45		-0.637	-1.398	-3.44	-2.726	-1.858	-1.646	-1.031	-0.174	0.071
50		-0.637	-1.398	-3.449	-2.721	-1.807	-1.585	-0.969	-0.216	0.07
55		-0.637	-1.398	-3.44	-2.726	-1.858	-1.646	-1.031	-0.174	0.071
60		-0.637	-1.398	-3.114	-2.444	-1.71	-1.526	-0.915	-0.142	0.074
65		-0.637	-1.399	-2.558	-1.98	-1.459	-1.317	-0.694	-0.088	0.102
70		-0.639	-1.402	-1.758	-1.35	-1.101	-1.009	-0.414	-0.047	0.097
75		-0.634	-1.356	-0.698	-0.555	-0.611	-0.571	-0.033	0.074	0.091
80		-0.637	-1.055	0.618	0.404	0.046	0.041	0.48	0.152	0.021
85		-0.76	-0.066	2.243	1.628	1.007	0.973	1.18	0.249	-0.052
90		-0.445	2.193	4.157	3.194	2.399	2.314	1.227	0.116	-0.193
95		3.285	4.451	4.311	3.56	2.944	2.638	0.68	0	-0.164

Depth		Strain	Strain	Strain	Strain	Strain	Strain	Strain	Strain	Strain
[mm]		[-]	[-]	[-]	[-]	[-]	[-]	[-]	[-]	[-]
5		8.7668E-05	0.00012	0.00011	9E-05	7.4E-05	6.7E-05	1.7E-05	0	-4E-06
10		-1.188E-05	5.8E-05	0.0001	8E-05	6E-05	5.8E-05	3.1E-05	2.9E-06	-5E-06
15		-2.028E-05	-2E-06	5.7E-05	4.1E-05	2.5E-05	2.5E-05	3E-05	6.3E-06	-1E-06
20		-1.7E-05	-3E-05	1.6E-05	1E-05	1.2E-06	1E-06	1.2E-05	3.8E-06	5.3E-07
25		-1.692E-05	-4E-05	-2E-05	-1E-05	-2E-05	-1E-05	-8E-07	1.9E-06	2.3E-06
30		-1.705E-05	-4E-05	-4E-05	-3E-05	-3E-05	-3E-05	-1E-05	-1E-06	2.4E-06
35		-1.7E-05	-4E-05	-6E-05	-5E-05	-4E-05	-3E-05	-2E-05	-2E-06	2.6E-06
40		-1.7E-05	-4E-05	-8E-05	-6E-05	-4E-05	-4E-05	-2E-05	-4E-06	1.9E-06
45		-1.7E-05	-4E-05	-9E-05	-7E-05	-5E-05	-4E-05	-3E-05	-4E-06	1.8E-06
50		-1.7E-05	-4E-05	-9E-05	-7E-05	-5E-05	-4E-05	-2E-05	-5E-06	1.8E-06
55		-1.7E-05	-4E-05	-9E-05	-7E-05	-5E-05	-4E-05	-3E-05	-4E-06	1.8E-06
60		-1.7E-05	-4E-05	-8E-05	-6E-05	-4E-05	-4E-05	-2E-05	-4E-06	1.9E-06
65		-1.7E-05	-4E-05	-6E-05	-5E-05	-4E-05	-3E-05	-2E-05	-2E-06	2.6E-06
70		-1.705E-05	-4E-05	-4E-05	-3E-05	-3E-05	-3E-05	-1E-05	-1E-06	2.4E-06
75		-1.692E-05	-4E-05	-2E-05	-1E-05	-2E-05	-1E-05	-8E-07	1.9E-06	2.3E-06
80		-1.7E-05	-3E-05	1.6E-05	1E-05	1.2E-06	1E-06	1.2E-05	3.8E-06	5.3E-07
85		-2.028E-05	-2E-06	5.7E-05	4.1E-05	2.5E-05	2.5E-05	3E-05	6.3E-06	-1E-06
90		-1.188E-05	5.8E-05	0.0001	8E-05	6E-05	5.8E-05	3.1E-05	2.9E-06	-5E-06
95		8.7668E-05	0.00012	0.00011	9E-05	7.4E-05	6.7E-05	1.7E-05	0	-4E-06

Appendix figure 42: conversion from eigenstresses to eigen-strain for an HSC specimen of 100 mm

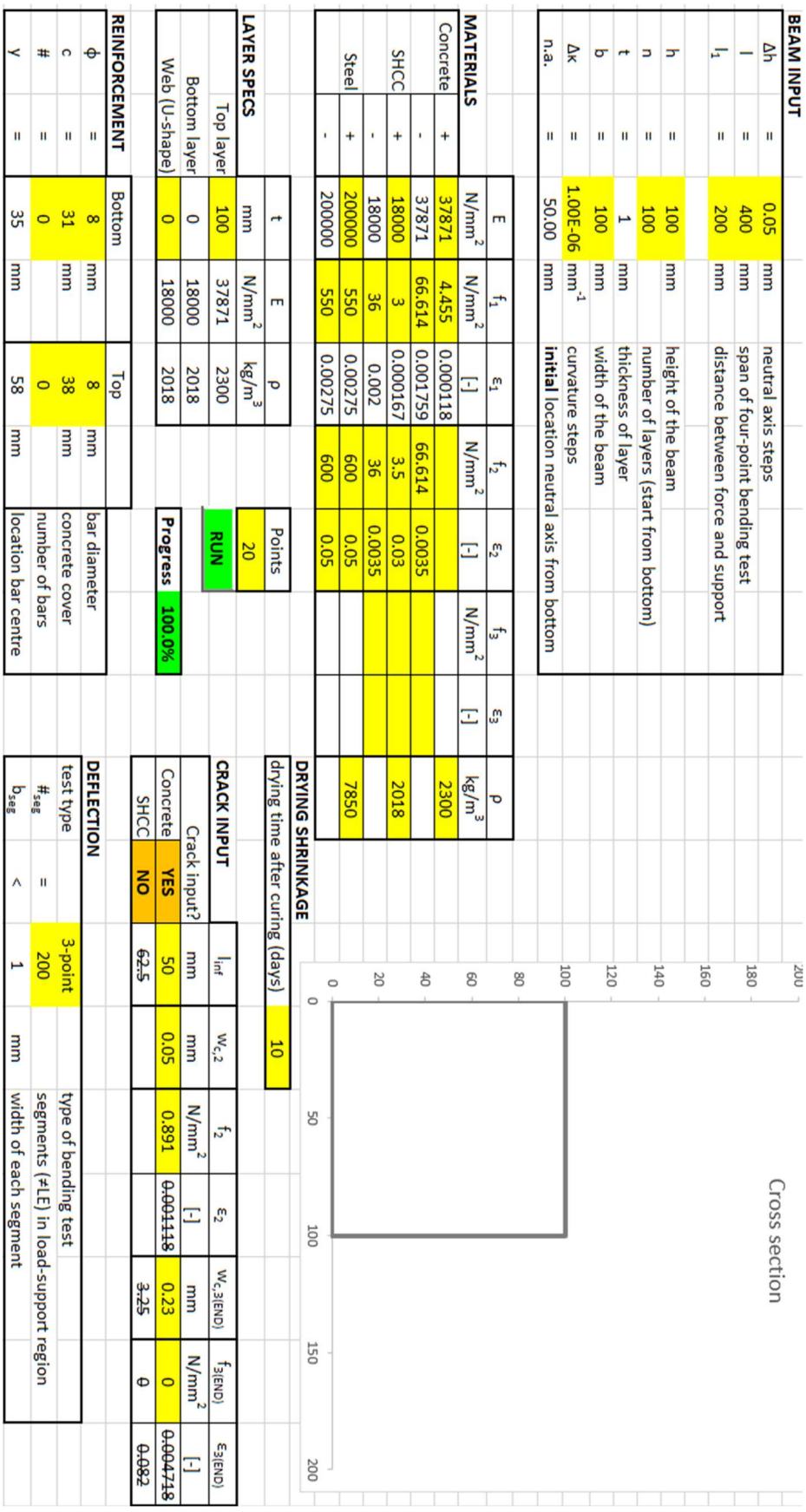

Appendix figure 43: input parameters HSC drying shrinkage verification

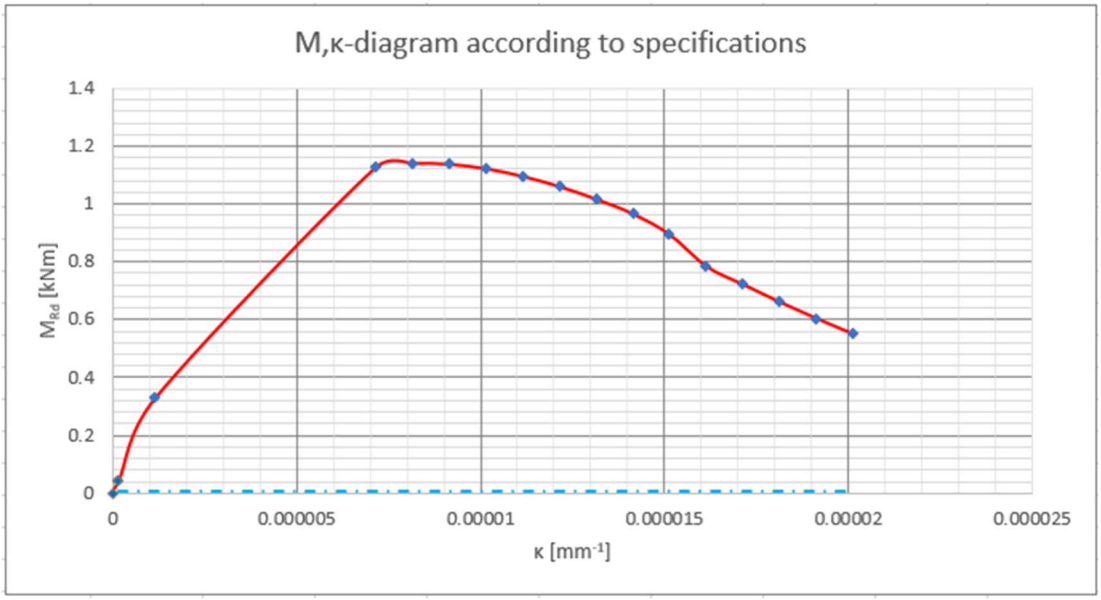

Stress calculation for σ,δ-diagram → **only valid if a non-hybrid beam is considered (no webs)**

I	z
[mm^4]	[mm]
8.33E+06	50.00

M	[Nmm]	0	42974	330323	1126864	1140177	1137414	1121792	1095471	1060137	1016622	965908
$\sigma_{bot.fiber}$	[N/mm^2]	0	0.257844	1.981938	6.761184	6.841062	6.824484	6.730752	6.572826	6.360822	6.099732	5.795448
δ	[mm]	0.000246	0.001865	0.001371	0.010506	0.011685	0.011656	0.010505	0.010444	0.010378	0.010309	0.010204

σ_{max}	[N/mm^2]	6.841062

Appendix figure 44: output HSC drying shrinkage verification

Comparison with DIANA

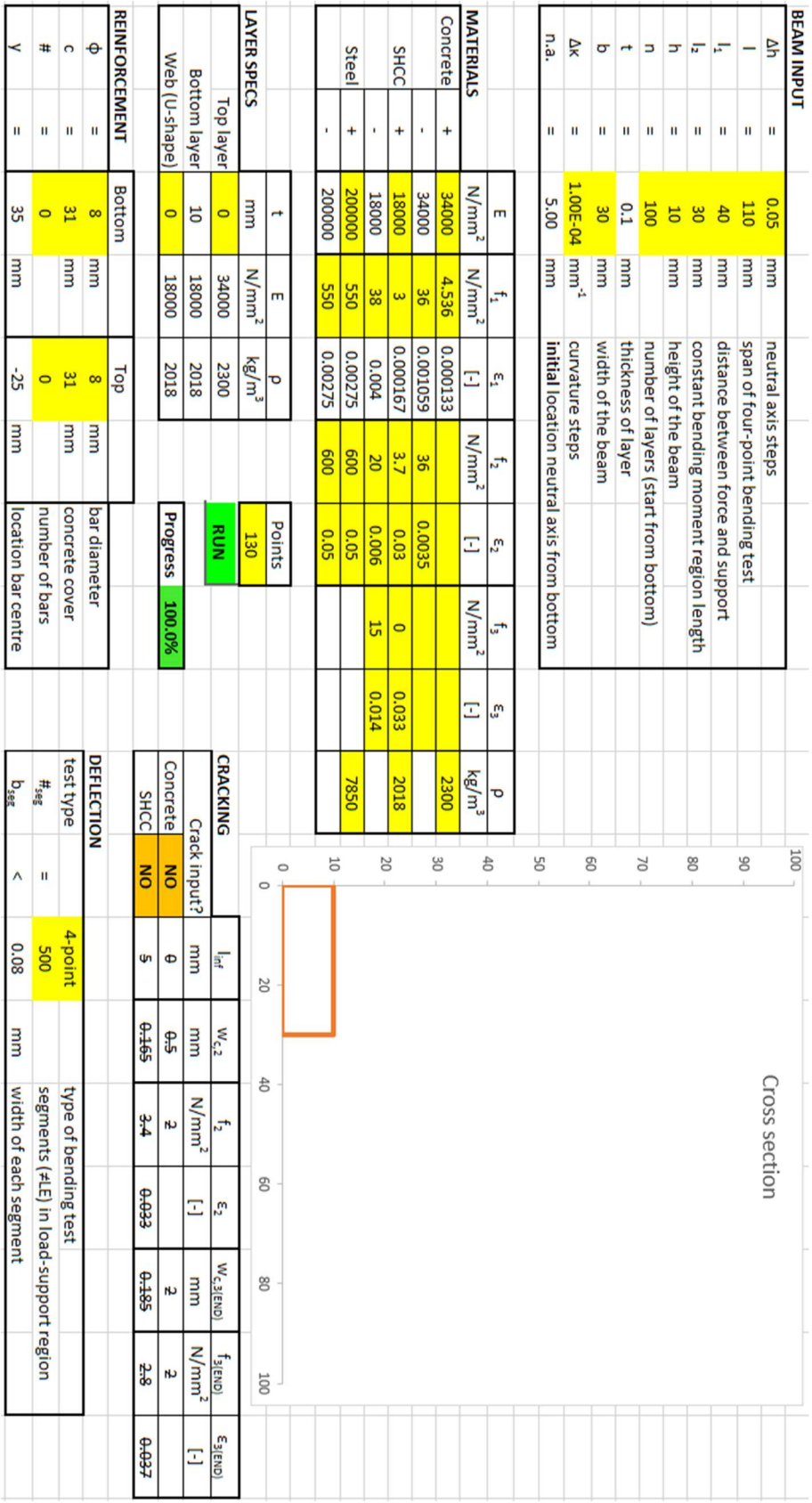

Appendix figure 45: input parameters comparison with DIANA

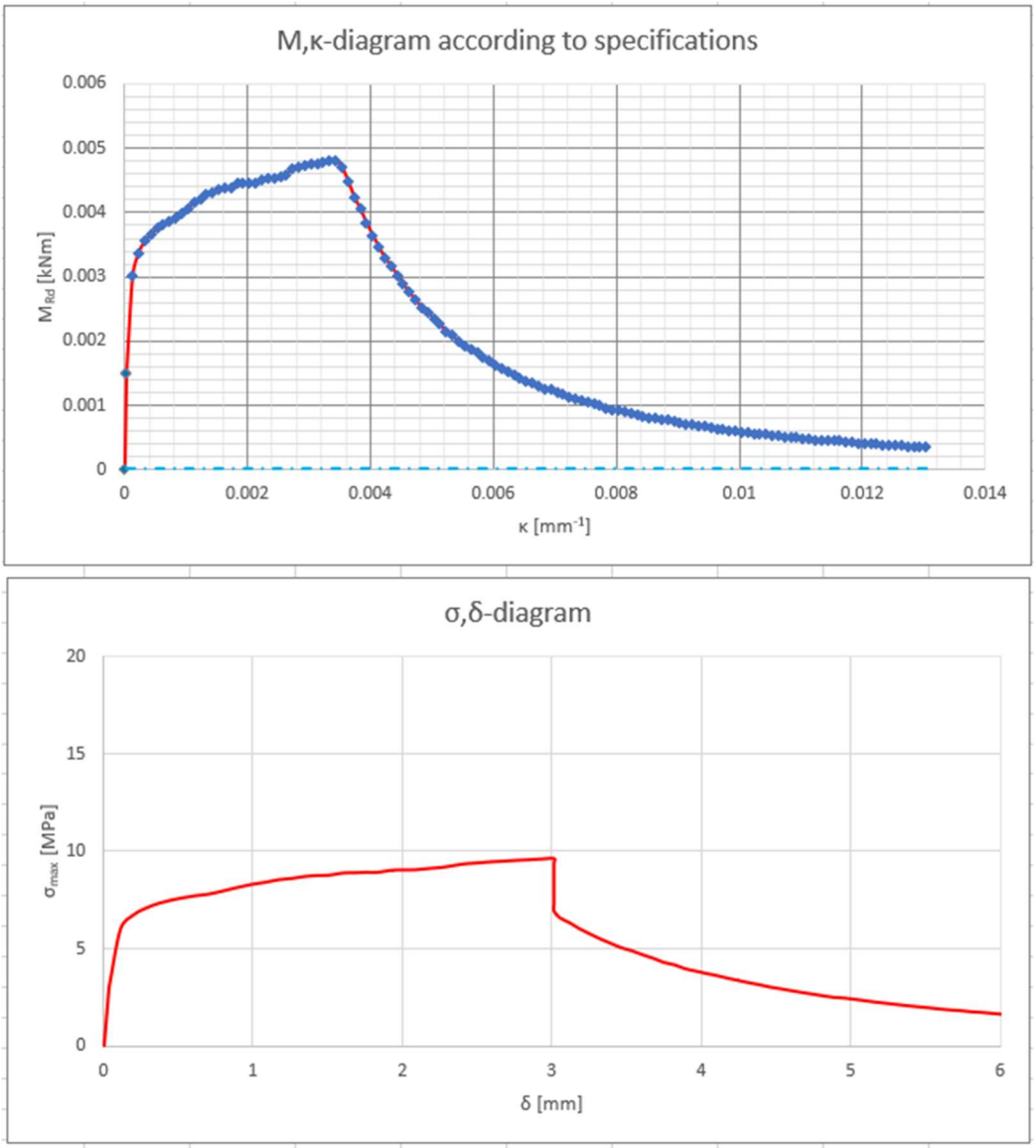

Appendix figure 46: output comparison with DIANA

Appendix D: deflection

Method 1: constant curvature

First, the derivation of the general expression is shown for the constant curvature method. In Figure 3-23, the geometrical properties were visualized. The 'f' was considered, which is equal to:

$$f = \frac{L^2}{8R} \qquad \textit{Appendix eq. (7)}$$

Using the terms that are used in this thesis, Appendix eq. (7) translates into:

$$f = \frac{L_2^2}{8R} \qquad \textit{Appendix eq. (8)}$$

Zooming in Figure 3-23 gives the situation as in Appendix figure 47:

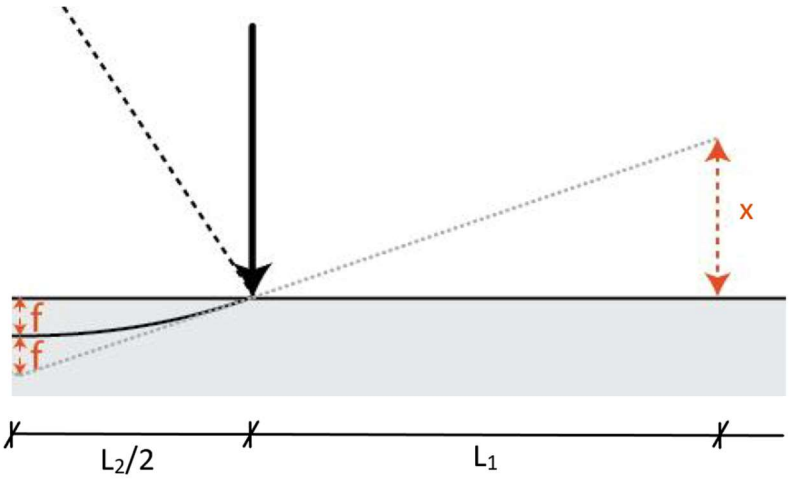

Appendix figure 47: edited version of Figure 3-23

By using geometry, the 'x' in Appendix figure 47 can be expressed as:

$$x = 2f\frac{L_1}{\frac{L_2}{2}} = 4f\frac{L_1}{L_2} \qquad \textit{Appendix eq. (9)}$$

That gives a total deflection of:

$$w_1 = f + x = \frac{L_2^2}{8R} + 4f\frac{L_1}{L_2} = \frac{L_2^2}{8R} + 4\frac{L_2^2}{8R}\frac{L_1}{L_2} = \frac{L_2^2}{8R} + \frac{L_1 L_2}{2R} = \frac{\boldsymbol{L_2}}{\boldsymbol{2R}}\left(\frac{\boldsymbol{L_2}}{\boldsymbol{4}} + \boldsymbol{L_1}\right) \qquad \textit{Appendix eq. (10)}$$

Method 2: momentvlakstellingen; theory

The 'momentvlakstellingen' method is based on the information from (Hartsuijker, 2001). It only holds for structures of which the bending moment distribution is known. For a 3-point or 4-point bending test, the bending moment distribution is known. This method is based on translating the known bending moment line into a 'reduced' bending moment line, by dividing the bending moment line by the stiffness. This is shown in Appendix figure 48.

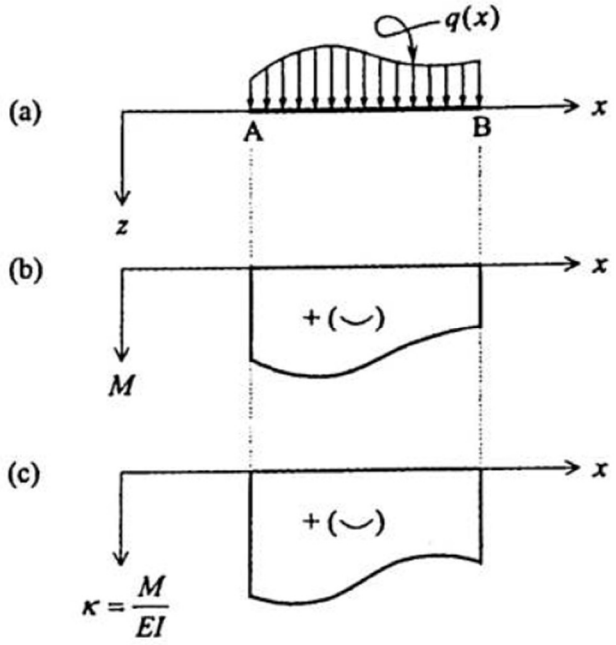

Appendix figure 48: definition of the reduced bending moment line (Hartsuijker, 2001)

Note that this reduced bending moment line is in fact a line that shows the curvature at each point. This theory is split into two parts: the first momentvlakstelling and the second momentvlakstelling. The first one is related to the rotation angle; the second one is related to the deflection. In this Appendix, the generic case is explained. The specific application was shown in subchapter 3.4.2.2.

First momentvlakstelling

From mechanics, it is known that:

$$\kappa = \frac{d\varphi}{dx} \qquad \textit{Appendix eq. (11)}$$

Substituting this in Appendix eq. (12) gives the result in Appendix eq. (13):

$$M = EI\kappa \rightarrow \kappa = \frac{M}{EI} \qquad \textit{Appendix eq. (12)}$$

$$\frac{d\varphi}{dx} = \frac{M}{EI} \rightarrow d\varphi = \frac{M}{EI}dx \qquad \textit{Appendix eq. (13)}$$

Integrating this over the length AB in Appendix figure 48 gives that the increase of the angle '$\Delta\varphi$' between A and B is equal to the area of the reduced bending moment line. This angle is required for finding the deflection (Hartsuijker, 2001).

Second momentvlakstelling

From mechanics, it is also know that:

$$\varphi = -\frac{dw}{dx} \rightarrow dw = -\varphi dx \qquad \textit{Appendix eq. (14)}$$

Integrating this over the length AB in Appendix figure 48 gives that the increase of the deflection Δw between A and B is equal to the previously found angle times the distance from the centerpoint of part AB to B. Next to that, if there is a known angle at A, the so called 'kwispeleffect' appears. That is equal to the angle at A times the distance to B. Those two together determine the deflection at B (Hartsuijker, 2001). This is shown in Appendix figure 49.

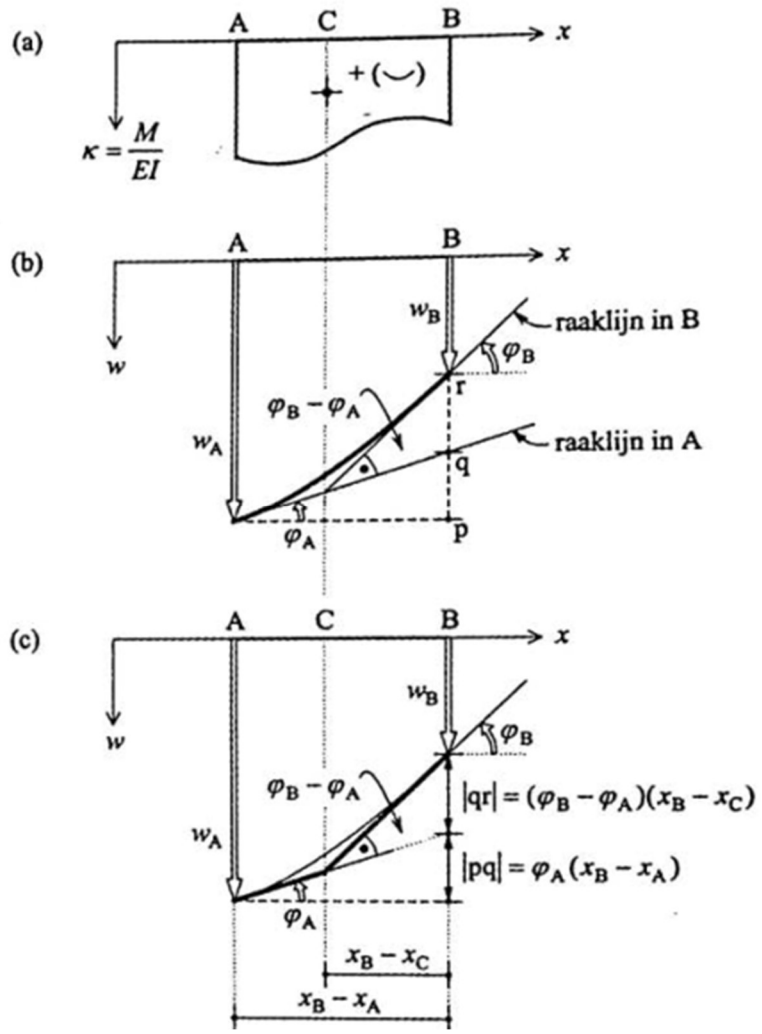

Appendix figure 49: calculation of the deflection according to the momentvlakstellingen (Hartsuijker, 2001)

Method 2: momentvlakstellingen; 3-point bending test

Here, the same procedure of subchapter 3.4.2.2 will be explained for a 3-point bending test.

Linear elastic stage

In Appendix figure 50, the bending moment diagram is shown for a 3-point bending test.

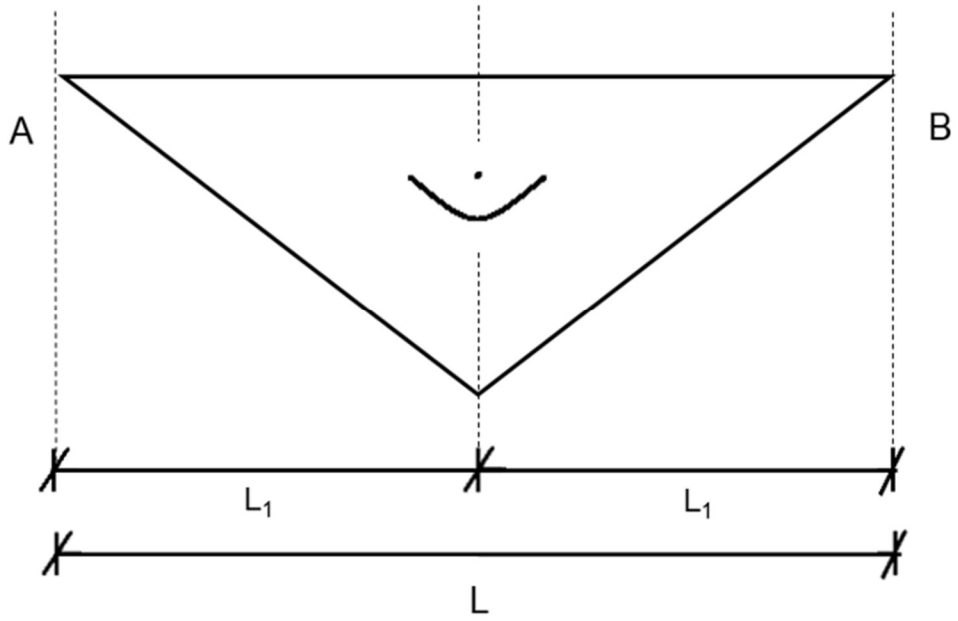

Appendix figure 50: bending moment diagram for a 3-point bending test

The reduced moment diagram has exactly the same shape as the original bending moment diagram. This is shown in Appendix figure 51.

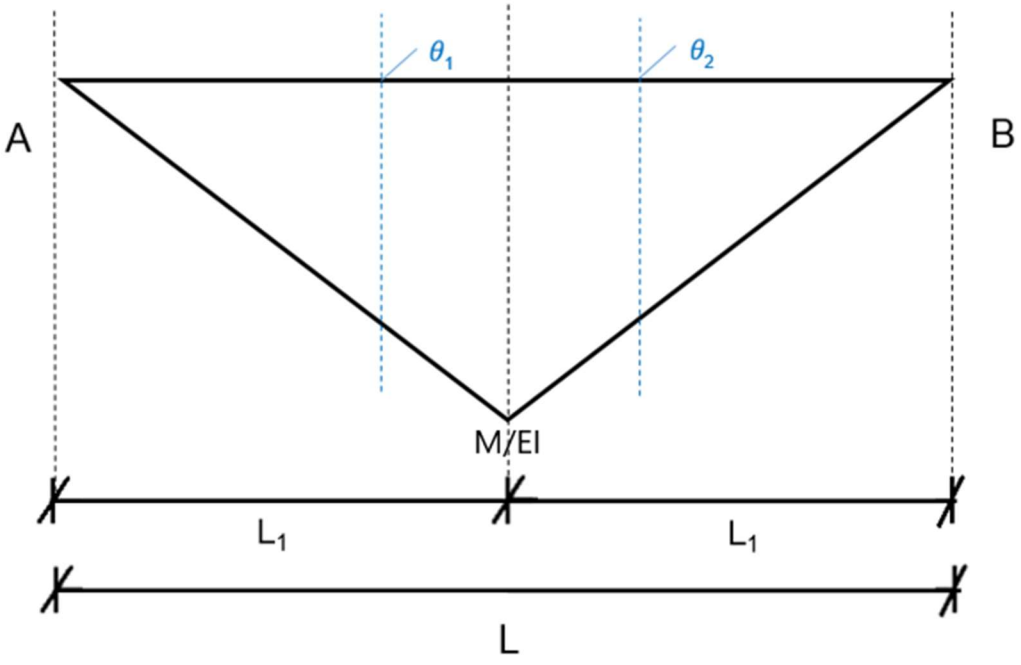

Appendix figure 51: reduced bending moment diagram for a 3-point bending test

The beam is split into straightforward geometrical parts. In this case, the diagram is split into two triangles. Those lead to the 'θ_1' and 'θ_2'. As the two triangles have exactly the same area, $\theta_1 = \theta_2$. The location of the angles is at one-third of the width of each triangle from the highest point.

Again, first the rotation at support A has to be found, in order to mitigate the deflection at support B that would occur if there was no rotation at A. This rotation is shown in Appendix figure 52.

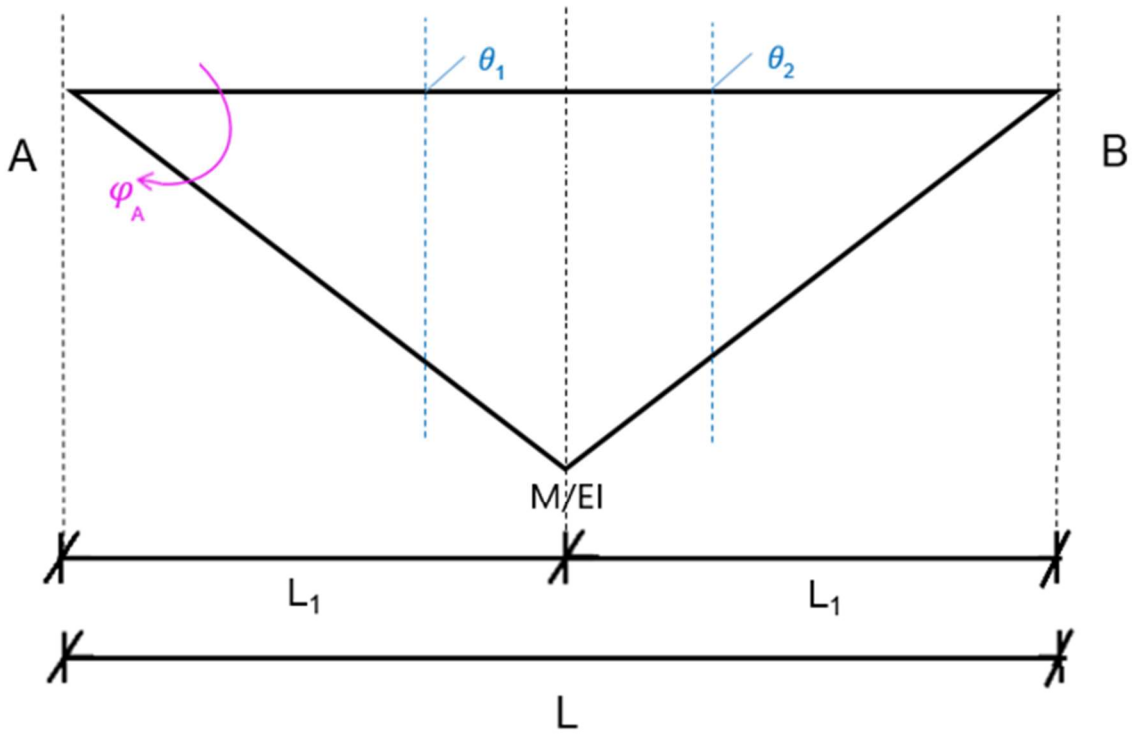

Appendix figure 52: rotation φ_A at point A to compensate for the imaginary displacement at support B

The equation in this case (with respect to point B) becomes:

$$\varphi_A L = \theta_1 \left(L - \frac{2}{3}L_1\right) + \theta_2 \frac{2}{3}L_1 \qquad \textit{Appendix eq. (15)}$$

After this is found, and after it is known that the deflection at midspan is desired, the reduced bending moment diagram could be split in half again. However, in this case, taking out 'θ_2' is sufficient as 'θ_1' already is equal to the area of half of the beam. Now the deflection at midspan becomes:

$$w_{midspan} = \varphi_A \frac{L}{2} - \theta_1 \frac{1}{3}L_1 \qquad \textit{Appendix eq. (16)}$$

Note the minus signs because of the different directions of the rotations.

Non-linear stage

Following the same approach as in subchapter 3.4.2.2.2, the bending moment diagram for the 3-point bending test is taken into account again. it can be split into two regions that are shown in Appendix figure 53.

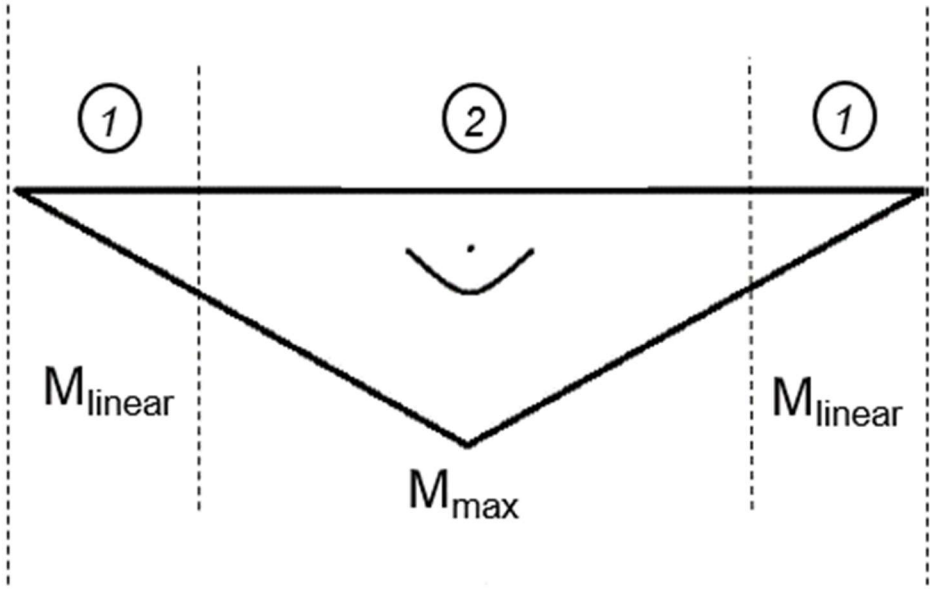

Appendix figure 53: two regions in the bending moment diagram in the non-linear stage for a 3-point bending test

Those two regions can be explained as follows:

→ *Region 1*: linear elastic region. In this region, the undamaged material is taken into consideration; the material is acting linearly. The geometrical figure that results in the reduced bending moment diagram is a triangle near the support.

→ *Region 2*: non-linear segments region. Between the location of the end of the undamaged material and the location of the applied force, the bending moment varies. Therefore, this region has to be split into multiple segments, that have the shape of a rectangle. The bending moment at the centerline of each segment is coupled with the corresponding curvature. For a large amount of segments, the approximation is accurate.

This is all summarized in Appendix figure 54. A sketch is shown of a possible configuration.

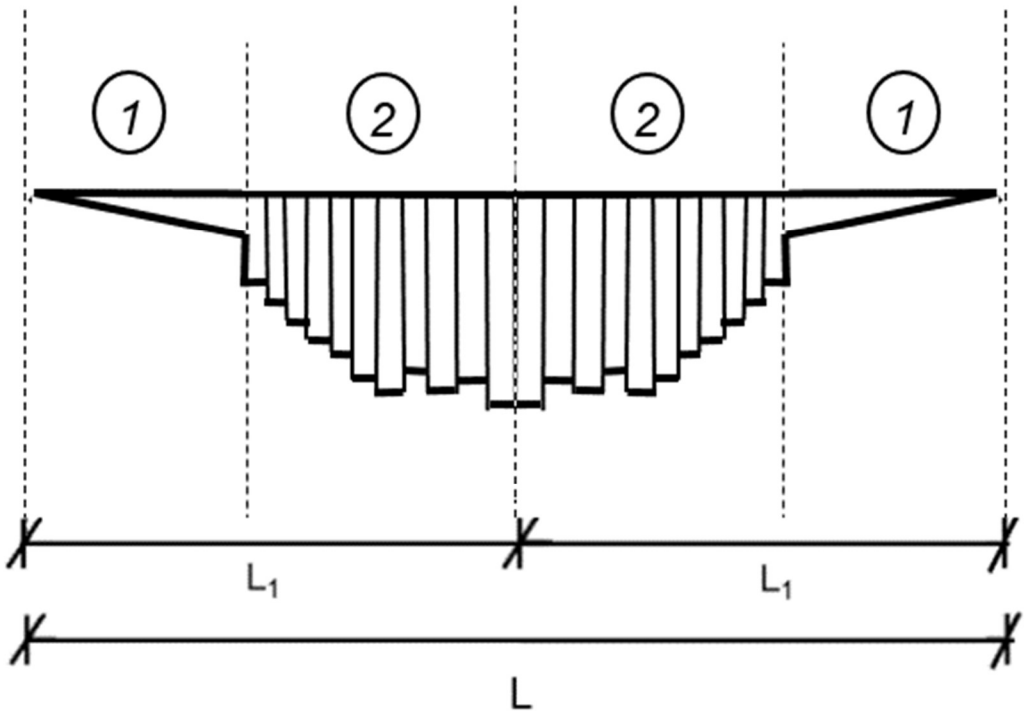

Appendix figure 54: reduced bending moment diagram regions in the non-linear stage for a 3-point bending test

As can be seen in Appendix figure 54, region two is not a straight line between region 1 and the location of the applied force. Next to that, region 1 has a very shallow slope. Both observations are explained in subchapter 3.4.2.2.2.

In order to find the deflection at midspan, all areas that are shown in Appendix figure 54 have to be found and multiplied with their distance to support B in order to find the rotation at support A. After that, the reduced bending moment diagram can be split into two, and all areas including the rotation at support A have to be multiplied with their distance to midspan.

Method 3: small scale geometry

In this method, the total beam is split into small segments. Because of symmetry around the midpoint, only half of the beam needs to be considered. Therefore, only half of the beam is divided into segments. Each segment is under a certain rotation, which can be approximated. The approximations are shown in Appendix figure 55.

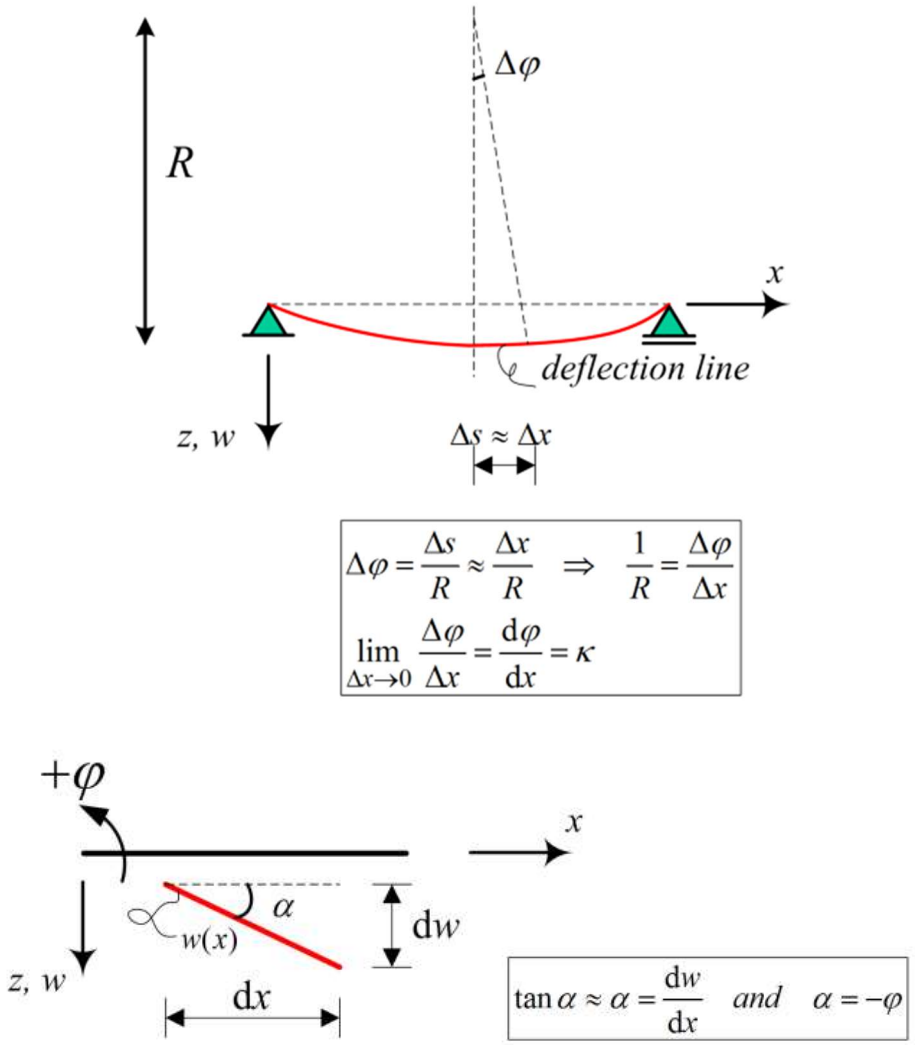

Appendix figure 55: small scale geometrical approximations (Welleman, 2018)

The angle 'ϕ', which is related to the curvature, can be approximated by:

$$d\phi = \kappa * dx \qquad \textit{Appendix eq. (17)}$$

The angle 'ϕ' is only equal to 'dϕ' for very small rotations. Translating this all to words, it means that the angle of a segment is equal to the curvature of the segment times the width of the segment. The width is translated from 'dx', which again, is only equal to the width of the segment for very small 'x'. This angle is, as can be seen in Appendix figure 55, equal to the angle

'α', which is related to the deflection. Multiplying this angle with the distance to a certain point gives the deflection at that point (Hartsuijker, 2001).

As was discussed before, only half of the span needs to be considered. The typical deflection of half a span is shown in Appendix figure 56.

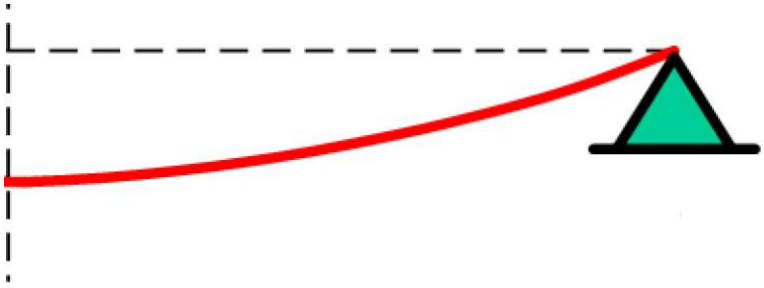

Appendix figure 56: deflection of half a span for a simply supported beam (Welleman, 2018)

In this method, the calculation is started from midspan, as the angle there is equal to zero. It is assumed that this is also the origin of a reference axis 'y', as is shown in Appendix figure 57. So the deflection is zero at this location. Now, the support is taken as a reference point to multiply the angles with (to find the deflection). However, the deflection that follows is located at the support, which never can be satisfied as the deflection at the support must be equal to zero. This is shown in Appendix figure 57. In this figure, the imaginary deflection line is shown in red (which follows from the calculation).

Appendix figure 57: imaginary deflection of half a span for a simply supported beam (Welleman, 2018)

As is explained, this deflection cannot happen. Therefore, the whole red line has to be move downwards by the same (deflection) amount that is found. Therefore, the deflection at midspan is exactly the deflection that was calculated at the support. In this way, the deflection at midspan is found.

For segments that are infinitesimal, this method provides the **exact and real** deflection. However, in reality, each segment will have a certain length. Therefore, the provided deflection is an **approximation** of the deflection.

Although the small scale geometry theory is applicable for a 4-point bending test, it provides less accurate results compared to the momentvlakstellingen method if the same parameters are used. This has to do with the number of segments and will be explained below.

As was explained before, the bending stiffness is different for each segment between the force and the support after the linear elastic stage. So the scaling of the bending moment diagram to the curvature is not by a constant factor (as is the case in the linear elastic stage). This step is exactly the same as in the momentvlakstellingen method. Therefore, for each segment, the occurring bending moment has to be matched with the corresponding curvature. The more datapoints (in the moment-to-curvature diagram) there are, the more accurate this process becomes. This also implies that having a limited amount of datapoints can give inaccurate deflections as incorrect curvatures are used (because they are approximated due to the lack of a match). This implies that this method is only accurate if very small curvature steps and very small segments are used.

As the 4-point bending test consists of a constant bending moment region, and therefore it is unnecessary to split that part into segments, it means that the second method (momentvlakstellingen) is more accurate. The 'momentvlakstellingen' method only splits the non-linear part between the force and the support into segments, while this method splits the whole half span into segments. So for the same number of segments, the momentvlakstellingen method performs better. Note that this holds for the 4-point bending test only. For the 3-point bending test, the two methods show similar behaviour. Therefore, the small scale geometry method can better only be used in case of 3-point bending tests. But as the two methods show similar behaviour, and the 'momentvlakstellingen' method is already used for the 4-point bending test in the proposed MLM, the latter method will also be used for the 3-point bending test.

Method 4: forget-me-nots; 4-point bending

Here, the derivation of Eq. (3.19) and Eq. (3.20) is shown for the forget-me-not method. As was shown before, the deflection for a 4-point bending test is calculated using Eq. (3.18). By rewriting Eq. (3.12), the curvature can be found:

$$\kappa = \frac{1}{R} \qquad \textit{Appendix eq. (18)}$$

By using Appendix eq. (18), Eq. (3.17) can be rewritten as:

$$EI = MR \qquad \textit{Appendix eq. (19)}$$

Using a = L/3 in Eq. (3.18), and entering the found expression for the bending stiffness into the same equation gives:

$$w_2 = \frac{L^2}{24R}\left(3 - 4\frac{\left(\frac{L}{3}\right)^2}{L^2}\right) = \frac{L^2}{24R}\left(3 - 4\frac{1}{9}\right) = \mathbf{\frac{23}{216}\frac{L^2}{R}} \qquad \textit{Appendix eq. (20)}$$

To find the general expression for the deflection, 'a' is substituted with 'L_1'. This gives:

$$w_2 = \frac{L^2}{24R}\left(3 - 4\frac{L_1^2}{L^2}\right) = \frac{L^2}{8R} - \frac{L_1^2}{6R} = \mathbf{\frac{1}{2R}\left(\frac{L^2}{4} - \frac{L_1^2}{3}\right)} \qquad \textit{Appendix eq. (21)}$$

Method 4: forget-me-nots; 3-point bending

The derivation of Eq. (3.21) is shown here. The deflection for a 3-point bending test is calculated by:

$$w_3 = \frac{1}{48}\frac{FL^3}{EI} \qquad \textit{Appendix eq. (22)}$$

Using the expression in Appendix eq. (19), and using the maximum moment that was given in Eq. (3.11), the stiffness can be rewritten to:

$$EI = \frac{F}{2}L_1 R \qquad \textit{Appendix eq. (23)}$$

Using the expression in Appendix eq. (23), the deflection in Appendix eq. (22) can be rewritten to:

$$w_3 = \frac{1}{48}\frac{FL^3}{\frac{1}{2}FL_1 R} = \boldsymbol{\frac{1}{24}\frac{L^3}{L_1 R}} \qquad \textit{Appendix eq. (24)}$$

Appendix E: drying shrinkage

In Appendix figure 58, the eigen-strains due to drying shrinkage profile for different drying periods are shown for a specimen of 150 mm.

	Days	Days	Days	Days	Days	Days	Days	Days	Days	Days	
	NONE	3	7	14	28	90	180	365	730	1095	
Depth	Strain	Strain	Strain	Strain	Strain	Strain	Strain	Strain	Strain	Strain	Height from bottom
[mm]	[-]	[-]	[-]	[-]	[-]	[-]	[-]	[-]	[-]	[-]	[-]
75	0	7.04E-05	0.00011	0.000144973	0.00019	0.0002	0.000168	0.000127	7.65E-05	4.59E-05	150
69	0	3.44E-05	7.52E-05	0.000110973	0.00015	0.000136	0.00012	9.6E-05	6.35E-05	3.99E-05	144
56	0	-8.6E-06	-9.8E-06	1.09733E-05	4.01E-05	2.33E-05	2.03E-05	2.6E-05	2.25E-05	1.99E-05	131
31	0	-8.6E-06	-2E-05	-3.90267E-05	-6E-05	-4.7E-05	-4E-05	-3.4E-05	-2.3E-05	-1.8E-05	106
0	0	-8.6E-06	-2E-05	-3.90267E-05	-7E-05	-6.7E-05	-6E-05	-5.4E-05	-4.1E-05	-2.5E-05	75
-31	0	-8.6E-06	-2E-05	-3.90267E-05	-6E-05	-4.7E-05	-4E-05	-3.4E-05	-2.3E-05	-1.8E-05	44
-56	0	-8.6E-06	-9.8E-06	1.09733E-05	4.01E-05	2.33E-05	2.03E-05	2.6E-05	2.25E-05	1.99E-05	19
-69	0	3.44E-05	7.52E-05	0.000110973	0.00015	0.000136	0.00012	9.6E-05	6.35E-05	3.99E-05	6
-75	0	7.04E-05	0.00011	0.000144973	0.00019	0.0002	0.000168	0.000127	7.65E-05	4.59E-05	0

Appendix figure 58: calculated eigen-strains along the height due to drying shrinkage for different drying periods

Proof of linear component equal to zero

The drying shrinkage profiles that are shown in Figure 3-39 are all symmetric around the midpoint. That leads to a 'linear component' that is equal to 0. The derivation of this is shown here. The linear component is calculated as follows:

$$\Delta T_b = \frac{h}{I} \int_{x_1}^{x_2} T(x) * b(x) * x \, dx \qquad \textit{Appendix eq. (25)}$$

The T(x) is the function of the relative humidity in this case, and the b(x) is the width that can be a function of the location (varying width). The limit values 'x_1' and 'x_2' are equal to 0 and 'h' respectively. The 'I' is the known '$\frac{1}{12}bh^3$' value. As a constant width is assumed in the proposed MLM, and as it is also possible to calculate per unit of width, it is assumed that b(x) = b = 1. That gives the following expression for the linear component:

$$\Delta T_b = \frac{h}{\frac{1}{12}h^3} \int_0^h T(x) * x \, dx = \frac{12}{h^2} \int_0^h T(x) * x \, dx \qquad \textit{Appendix eq. (26)}$$

It is assumed that the vertical axis is the y-axis, and not the x-axis as is shown in the expression. The integral should be over the height, and not over the width. Therefore, the expression becomes:

$$\Delta T_b = \frac{12}{h^2} \int_0^h T(y) * y \, dy \qquad \textit{Appendix eq. (27)}$$

Now, an expression needs to be found for the relative humidity distribution. In this proof, the profile for 28 days of drying is taken. The result in Appendix figure 59 is obtained.

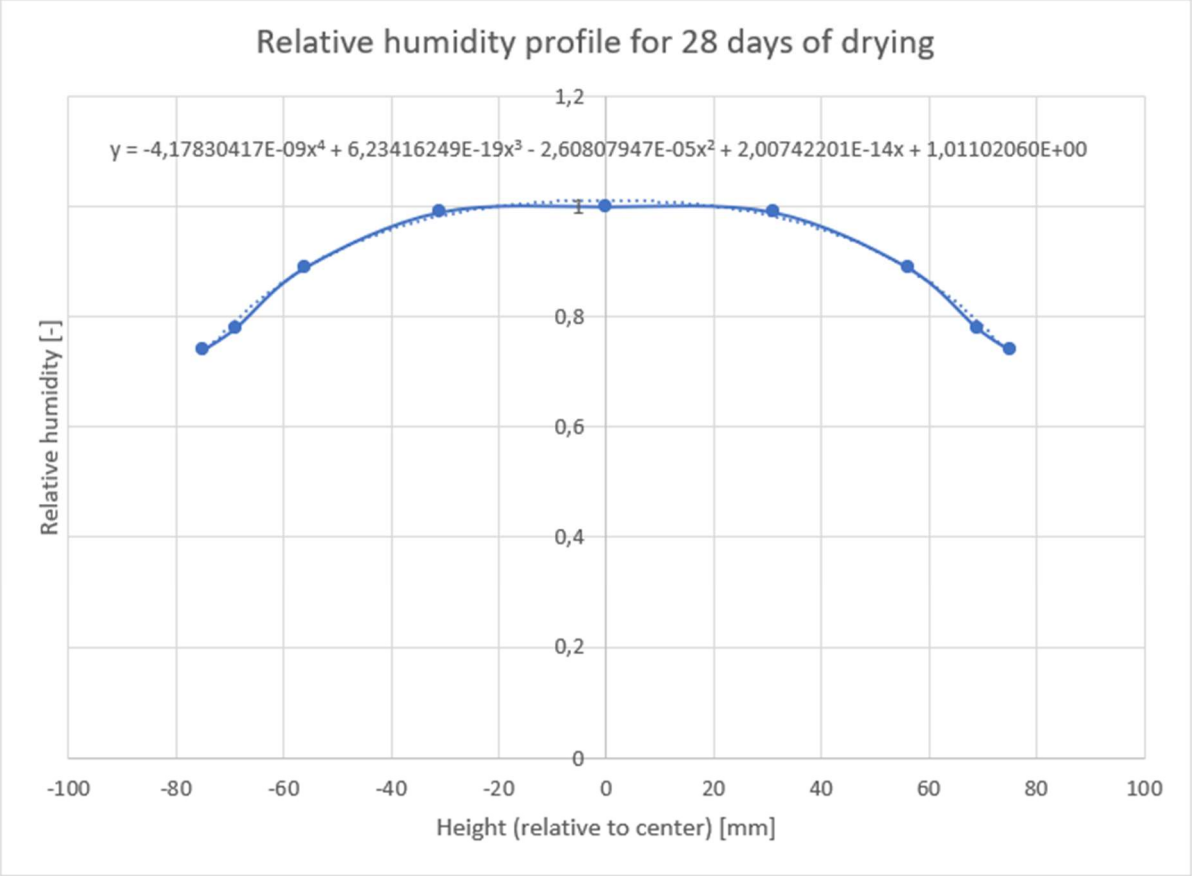

Appendix figure 59: fourth-order polynomial trendline of relative humidity profile for 28 days of drying

Based on the profile, a fourth-order polynomial fitting line was needed to approximate the humidity profile correctly. As is shown in Appendix figure 59, the axes are flipped compared to what was shown earlier. This was necessary to obtain the expression of the trendline. It is now as a function of 'x', but it can be flipped, which leads to the following expression:

$$\Delta T(y) = -4.1483 * 10^{-9} y^4 + 6.2342 * 10^{-19} y^3 - 2.6081 * 10^{-5} y^2 + 2.0074 * 10^{-14} y + 1.1011 \qquad \textit{Appendix eq. (28)}$$

As the height is now described relative to the center of the cross-section, the integral limits also have to change. The integral becomes:

$$\Delta T_b = \frac{12}{h^2} \int_{-\frac{h}{2}}^{\frac{h}{2}} T(y) * y \, dy \qquad \textit{Appendix eq. (29)}$$

The calculation of the integral is shown in Appendix figure 60.

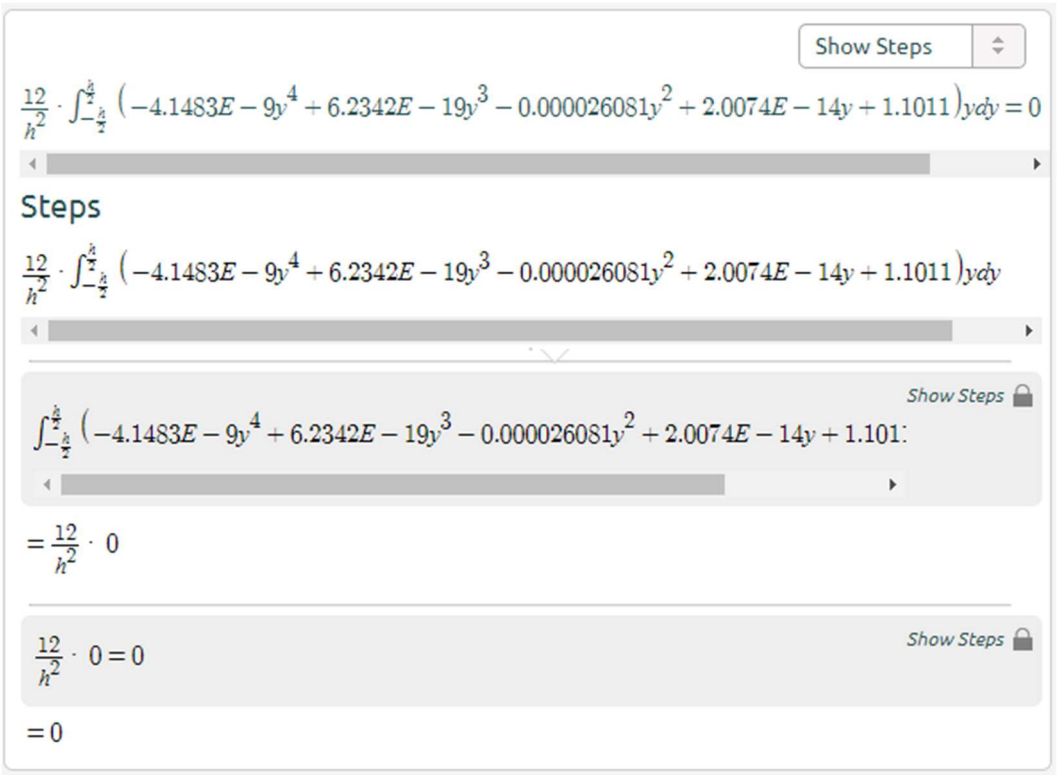

Appendix figure 60: calculation of the linear component integral for symmetric drying profiles (Symbolab, 2020)

As is shown in Appendix figure 60, the integral is equal to zero. Therefore, it is proven that the linear component does not contribute to the eigen-strains that are used in the MLM. This is true for all symmetric profiles. And as is shown in Figure 3-39, all profiles are symmetric. If different input is used, the drying shrinkage profile has to be symmetric in order to follow the calculation method that is used in the proposed MLM.

Average component calculation example

Again, the humidity profile of 28 days drying is used for the calculation. Now, it is shown how the mean component is calculated. The relative humidity data that is available is given in the form of datapoints for a specimen of 150 mm height. The data is shown in Appendix table 2.

Height [mm]	RH [-]
75	0.74
69	0.78
56	0.89
31	0.99
0	1
-31	0.99
-56	0.89
-69	0.78
-75	0.74

Appendix table 2: relative humidity input data for a specimen of 150 mm height and a drying period of 28 days

To know the average component, the specimen is divided into segments. The segments are the regions between the datapoints. That gives the regions as in Appendix table 3.

Region [mm]
75
75 to 69
69 to 56
56 to 31
31 to 0
0 to -31
-31 to -56
-56 to -69
-69 to -75

Appendix table 3: regions of humidity input data

For each region, the average relative humidity is calculated. For example, the average of the region between 75 to 69 mm is equal to (0.74+0.78) / 2= 0.76. Then, the average has to be multiplied with the height of the region. That needs to be done because the regions all have different heights. If all heights were the same, this was not necessary. Now, every region contributes differently to the total average. So for the region between 75 to 69 mm, the 0.76 value still needs to be multiplied with (75-69)= 6, which gives 0.76*6= 4.56. Doing this for all regions gives the results as is shown in Appendix table 4.

Region [mm]	MEAN
75	0
75 to 69	4.56
69 to 56	10.855
56 to 31	23.5
31 to 0	30.845
0 to -31	30.845
-31 to -56	23.5
-56 to -69	10.855
-69 to -75	4.56

Appendix table 4: average contribution of each region to the total average

The final step is to sum up all the individual contributions, which is in this case the sum of the 'MEAN' column. That is equal to 139.52. Dividing this number by the total height gives the total average, or in other words: the average component. In this case, it is equal to: 139.52/150= 0.93. So the average relative humidity of a beam exposed to 28 days of drying is equal to 0.93.

CRITICAL ASSUMPTION: 28 days of curing before drying

h	time of drying					
[mm]	3 days	7 days	14 days	28 days	90 days	180 days
150						
Depth [mm]	Relative humidity (input from FEMMASSE)					
75	0.921	0.87	0.816	0.74	0.593	0.542
69	0.957	0.905	0.85	0.78	0.657	0.59
56	1	0.99	0.95	0.89	0.77	0.69
31	1	1	1	0.99	0.84	0.75
0	1	1	1	1	0.86	0.77
-31	1	1	1	0.99	0.84	0.75
-56	1	0.99	0.95	0.89	0.77	0.69
-69	0.957	0.905	0.85	0.78	0.657	0.59
-75	0.921	0.87	0.816	0.74	0.593	0.542

3 days						7 days						14 days						28 days						90 days						180 days			
Region [mm]		MEAN	EIGEN		EIGEN		MEAN	EIGEN		EIGEN		MEAN	EIGEN		EIGEN		MEAN	EIGEN		EIGEN		MEAN	EIGEN		EIGEN		MEAN	EIGEN		EIGEN	
					ADJUSTED	Depth [mm]				ADJUSTED					ADJUSTED					ADJUSTED					ADJUSTED					ADJUSTED	
75	0		-7.03933E-05		7.04E-05	75				0.00011			-0.00014		0.000145			-0.00019		0.00019			-0.0002		0.0002			-0.00017		0.000168
75 to 69	5.634		-3.43933E-05		3.44E-05	69		5.325	-7.5E-05	7.52E-05		4.998	-0.00011	0.000111	1.1E-05		4.56	-0.00015	4.01E-05	0.00015		3.75	-0.00014	0.000136		3.396	-0.00012	0.00012		2.03E-05
69 to 56	12.7205		8.60667E-06		-8.6E-06	56		12.3175	9.77E-06	-9.8E-06		11.7	-1.1E-05	0.000111	1.1E-05		10.855	-4E-05	4.01E-05	-6E-05		9.2755	-2.3E-05	2.33E-05		8.32	-2E-05	2.03E-05		-4E-05
56 to 31	25		8.60667E-06		-8.6E-06	31		24.875	1.98E-05	-2E-05		24.375	3.9E-05	-3.9E-05	-3.9E-05		23.5	5.99E-05	-6E-05	-7E-05		20.125	4.67E-05	-4.7E-05		18	3.97E-05	-4E-05		-6E-05
31 to 0	31		8.60667E-06		-8.6E-06	0		31	1.98E-05	-2E-05		31	3.9E-05	-3.9E-05	-3.9E-05		30.845	6.99E-05	-6E-05	-7E-05		26.35	6.67E-05	-6.7E-05		23.56	5.97E-05	-6E-05		-6E-05
0 to -31	31		8.60667E-06		-8.6E-06	-31		31	1.98E-05	-2E-05		31	3.9E-05	-3.9E-05	-3.9E-05		30.845	5.99E-05	-6E-05	-6E-05		26.35	4.67E-05	-4.7E-05		23.56	3.97E-05	-4E-05		-4E-05
-31 to -56	25		8.60667E-06		-8.6E-06	-56		24.875	1.97E-06	-9.8E-06		24.375	-1.1E-05	1.1E-05	1.1E-05		23.5	-4E-05	4.01E-05	6E-05		20.125	-2.3E-05	2.33E-05		18	-2E-05	2.03E-05		4E-05
-56 to -69	12.7205		-3.43933E-05		3.44E-05	-69		12.3175	-7.5E-05	7.52E-05		11.7	-0.0001	0.000111	1.1E-05		10.855	-0.00015	0.00015	6E-05		9.2755	-0.00014	0.000136		8.32	-0.00012	0.00012		4E-05
-69 to -75	5.634		-7.03933E-05		7.04E-05	-75		5.325	-0.00011	0.00011		4.998	-0.00014	0.000145	1.1E-05		4.56	-0.00019	0.00019	7E-05		3.75	-0.0002	0.0002		3.396	-0.00017	0.000168		6E-05
	MEAN	0.991393					MEAN	0.980233				MEAN	0.960973				MEAN	0.930133				MEAN	0.79334				MEAN	0.710347			

Appendix figure 61: calculation of eigen-strains due to drying shrinkage in the MLM

Input of drying shrinkage calculation example

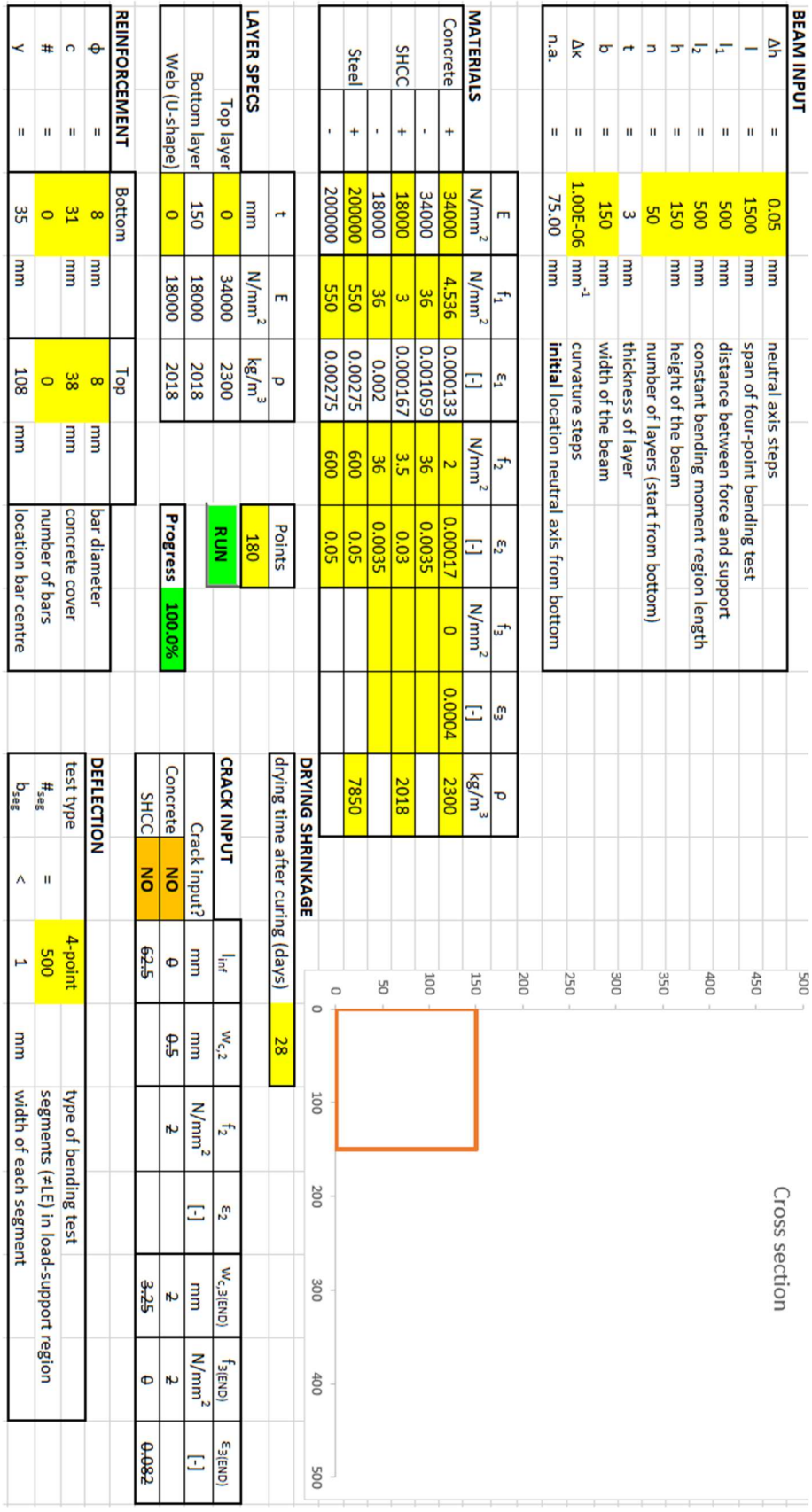

Appendix figure 62: input in MLM of drying shrinkage calculation example for 28 days of drying

Appendix F: U-shaped mould

The process of finding the easiest way of producing a U-shaped mould was done in two stages. In the first stage, an outside mould of 400x100x100 mm was used (called 'small scale experiment' in this Appendix). In the second stage, an outside mould of 600x150x150 mm was used (called 'medium scale experiment' in this Appendix). The design of the U-shaped mould is meant to be used in future experiments at the TU Delft. When that happens, beams of 1900x150x200 mm are recommended to be used in the experiments (called 'large scale experiment' in this Appendix). Those are also the dimensions that were used in (Huang, 2017). Furthermore, additional information on the large scale experiment is presented in this Appendix.

Small scale experiment

The goal of the small scale experiments was to find a way of making a U-shape.

Step 1

The inside and outside mould that were chosen were based on the availability of materials in the TU Delft concrete lab. The moulds are shown in Figure 2-4. The dimensions of the outside mould are 400x100x100 mm, and the dimensions of the inside mould are 400x75.5x47.2 mm. The outside mould was made out of steel, and the inside mould was made out of wood. Oil was applied to the surface of both moulds. However, the inside mould was not made to be used as an inside mould, as the outside surface (that was used as the inside mould) was not smooth. That gave some implications during demoulding, which resulted in some cracks. Those cracks were the result of excessive hammering during demoulding. Because of the wood surface that was not smooth (and even cross-laminated), the oil was absorbed by the wood, which made the SHCC stick to the wood. The results are shown in Appendix figure 63 and Appendix figure 64. Note that a different SHCC mixture was used compared to the experiments of (Huang, 2017) for this experiment; a mixture which consisted of blast-furnace slag and Portland cement CEM I was used while a mixture with Portland cement CEM III was desired (more practical for structural applications).

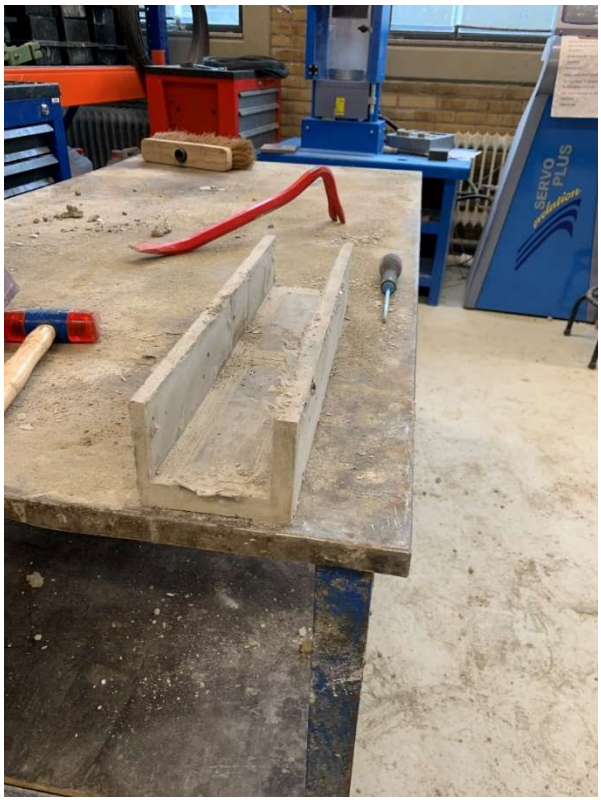

Appendix figure 63: U-shape made out of SHCC

Appendix figure 64: longitudinal cracks as a result of excessive hammering during demoulding

Step 2

In this step, the same mixture as (Huang, 2017) was used (as is shown in Table 2-1). Next to that, the goal was to prevent cracking as in the previous step from happening. The hypothesis was that the hammering caused the cracking, so when demoulding this time, the usage of the hammer was limited to a minimum. Those were the only differences compared to the previous step. The SHCC was however still stuck because of the wood that was not smooth, so that also needed to be solved in future experiments. The result is shown in Appendix figure 65 and Appendix figure 66. As can be seen, there are no cracks, so the hypothesis was correct.

Appendix figure 65: U-shape made out of the correct SHCC mixture

Appendix figure 66: top view of the SHCC U-shape

Step 3

The next step was to try a different material for the inside mould. Styrofoam was used, but it was of a low quality. Seven plates of Styrofoam were stacked up to reach a desirable height. The stacking resulted however in the problem that SHCC slipped in between the plates, which made demoulding much harder. Although this was not a very successful experiment, the hypothesis was that high quality Styrofoam would perform better. The results of this experiment are shown in Appendix figure 67 and Appendix figure 68. Everything except the inside mould was kept the same compared to the previous step.

Appendix figure 67: demoulding of an SHCC U-shape with Styrofoam as the inside mould

Appendix figure 68: the effect of Styrofoam plates on the demoulding process

Medium scale experiment

The next stage was about performing the medium scale experiments. The meaning of this step was to try everything that could be thought of before presenting a design for a large scale experiment. That included for example thinking of how to prevent leakage or how to prevent the usage of spacers to not make it mix up with the 'fresh' mixture. When these experiments were finished, it was known exactly how the large scale specimens should be casted. Therefore, a useful guide is left in this thesis, so that the experiments in the future can easily be performed.

Note that in the description of the large scale experiments in this thesis, it is assumed that exactly the same setup as the experiment of (Huang, 2017) will be used. The steel reinforcement can be tweaked a bit so that it fits better in the U-shaped mould, but everything that has effect on the resistance should stay the same. The concrete cover (31 mm) and the thickness of the SHCC layer (70 mm) are examples of parameters that should stay the same.

Step 1

As was explained before, high-quality Styrofoam could be a better option than the Styrofoam that was used before. Therefore, high-quality Styrofoam was ordered via the TU Delft. It consisted of plates of 60 mm thickness, which made it very suitable for the large scale testing, as two plates would make a thickness of 120 mm, which was exactly the required width of the inside mould. In this step, also steel reinforcement was added. The main challenge was with the stirrups. The dimension of the outside mould was now 600x150x150 mm. Although this seems much smaller than the large scale dimensions (1900x150x200 mm), the width and height were comparable. The most important dimension was however the width, and that was exactly the same (150 mm). The reason that this is the most important dimension, is that the webs and stirrups have to fit in this small space. If that would work, the rest would not be an issue. The inside mould was also cut in a way to get an SHCC layer of 70 mm, as that would be the case in the large scale beam. Also, the reinforcement cover was set to 31 mm (as the large scale beam). The reinforcement that was prepared, is shown in Appendix figure 69.

Appendix figure 69: prepared reinforcement for medium scale experiment

Although everything seemed correct, there were some problems after casting. As the Styrofoam was cut (from the top and the bottom) using a manual saw, it was not completely flat. That caused leakage which made the demoulding very difficult. Next to that, the Styrofoam contained a certain texture which made it stick to the SHCC. That needed to be solved in the next step. The problem of the texture is shown in Appendix figure 70. The result after the demoulding was completed was shown before in Figure 2-9.

Appendix figure 70: Styrofoam sticking to the SHCC

Step 2

The last step was to solve the problems that occurred in the previous step. The cutting was not done by hand anymore, but by the timber shop at the university. Machines were used which meant that the cutting was precise. To solve the problem of the texture of the Styrofoam, the Styrofoam was wrapped in tape (see Appendix figure 71). And to make sure that there was no leakage from below the inside mould, the inside mould was taped to the bottom of the outside mould. That gave the result that was shown before in Figure 2-6. As can be seen, the result was much better. It was even so promising that there is a possibility to reuse the Styrofoam that was used as an inside mould.

Appendix figure 71: inside Styrofoam mould wrapped in tape

Pressure check

When concrete is casted in the U-shaped mould, it is pressuring the webs of the mould. It is comparable with the load from water on a water lock. An overview of that is shown in Appendix figure 72.

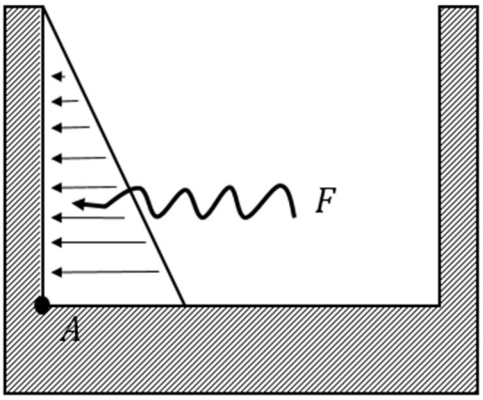

Appendix figure 72: front view U-shape mould pressured by casted concrete

The pressure is equal to:

$$p_A = \rho g h = 2018 * 9.81 * 0.13 = 2573\ N/m^2$$

In which 'h' is not the total height, but only the height over which there is pressure by the concrete. The pressure can be translated into a force, by calculating the area of the triangle in Appendix figure 72. Its resultant is on one third of the height of the triangle.

$$F = \frac{1}{2} * h * p_A = 0.5 * 0.13 * 2573 = 167.3\ N/m$$

Note that this force is per unit meter depth (into the paper if looking at Appendix figure 72). The force results in a bending moment that acts on point A in Appendix figure 72. It is equal to:

$$M_A = F * \frac{1}{3} h = 167.3 * \frac{1}{3} * 0.13 = 7.25\ Nm/m = 7250\ Nmm/m$$

As this load is acting per unit meter depth, the cross section that can be considered for calculation of the stresses has a height of 15 mm and a width of 1000 mm. That gives:

$$\sigma = \frac{M}{W} = \frac{7250}{\frac{1}{6} * 1000 * 15^2} = 0.19\ N/mm^2$$

As this is considerably lower than the cracking stress of SHCC (3 N/mm^2), the SHCC webs will not crack when concrete is casted into the U-shaped mould. In fact, this stress will only be reached if the web has a height of 3.25 m (and pressured by concrete along this height).

If the webs had a thickness of 10 mm, the stress would be equal to 0.43 N/mm^2, and it would only crack if a web height of 2.47 m was used.

Appendix G: crack width

In this Appendix, the parameters in Eq. (3.25) are explained. The first parameter is 'ϕ', which represents the bar diameter of the (ribbed) steel reinforcement bar. Secondly, the 'E_s' parameter is the Young's modulus of the steel that is used. The final parameter is the 'σ_s', which is the stress in the steel reinforcement bar. This stress is calculated using Appendix eq. (30):

$$\sigma_s = \frac{N_s}{A_s} \qquad \textit{Appendix eq. (30)}$$

Or in other words, the stress is equal to the force in the bar divided by the area of the bar. The two remaining parameters are 'ρ_{eff}' and 'σ_{sr}', which need more explanation.

Effective area

The 'ρ' parameter normally indicates the reinforcement ratio of a specimen. In this case, it is not different. However, now the subscript 'eff' comes in to play, which stands for 'effective'. In a beam, the reinforcement only controls the cracks in a certain area. For a beam loading in bending, where tensions occurs at the bottom of the beam, it is shown in Appendix figure 73 how this effective area looks like (marked in red).

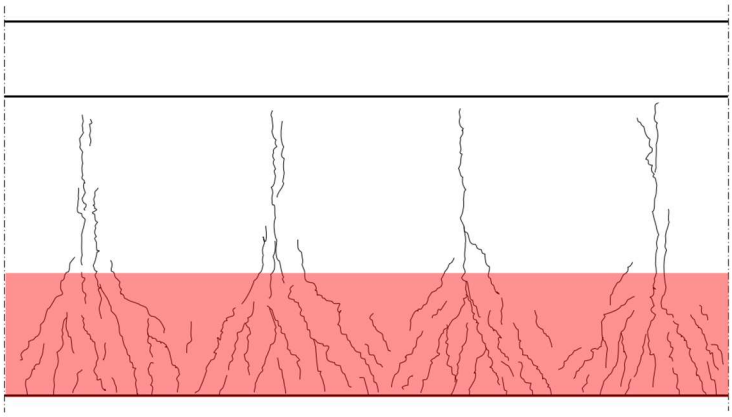

Appendix figure 73: effective area in which the reinforcement controls the crack width (Luković & van der Ham, 2020)

The height of this effective area can be calculated using the Eurocode (NEN, 2011):

$$h_{c,eff} = \min\{2.5(h-d); (h-x)/3\} \qquad \textit{Appendix eq. (31)}$$

Here, 'd' is the distance between the center of the reinforcement bars to the top of the beam, and 'x' is the height of the concrete compression zone. The height of the compression zone will be covered in the next subchapter. The parameters are illustrated in Appendix figure 74.

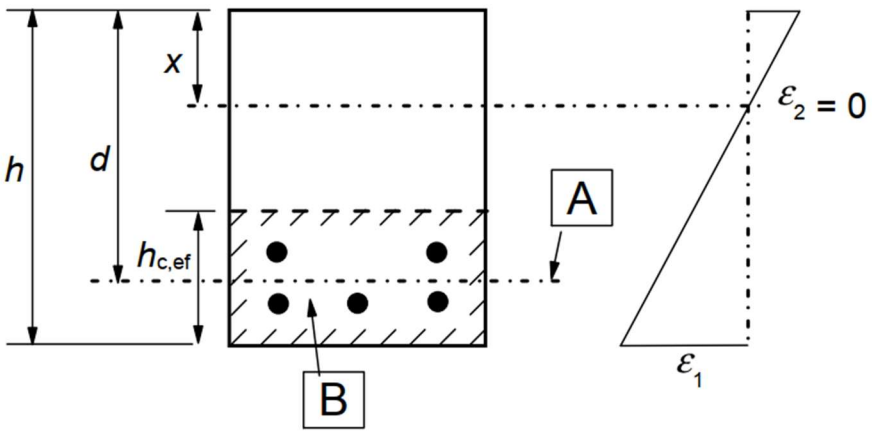

Appendix figure 74: determining the effective tension area for a beam loading in bending (NEN, 2011)

Using this information, the effective area becomes equal to:

$$A_{c,eff} = h_{c,eff} * b \qquad \textit{Appendix eq. (32)}$$

In which 'b' is the width. Now, the effective reinforcement ratio can be calculated, and is equal to:

$$\rho_{eff} = \frac{A_s}{A_{c,eff}} \qquad \textit{Appendix eq. (33)}$$

Here, 'A_s' is equal to the steel reinforcement area in the effective concrete area.

Steel rupture stress

The final parameter that needs explanation is the steel rupture stress 'σ_{sr}'. Immediately after the traditionally reinforced concrete beam cracks, it is assumed that the steel reinforcement bars take over all tensile forces. Although this is not necessarily what happens in the proposed MLM, it is assumed that it is the case. In the proposed MLM, the tensile stresses can also be taken by the concrete, depending on the tensile resistance that is used as input. The strain at the centerline of some of the layers of the MLM will still correspond to a stress that is not equal to zero (be it in the linear elastic stage, or in the softening regime), so some layers will provide some resistance. However, this means that the steel rupture stress calculated using the MLM will not be accurate, as not all tensile forces are taken by the steel reinforcement. In order to use the Eurocode expressions, the assumption needs to be made that the forces are only taken by the reinforcement. This leads to the situation shown in Appendix figure 75.

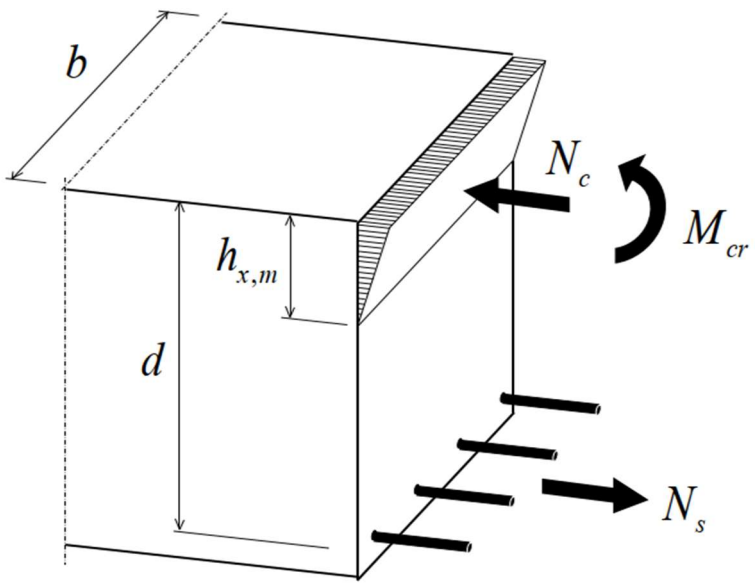

Appendix figure 75: the forces in steel & concrete right after cracking of the concrete (Luković & van der Ham, 2020)

The cracking moment 'M_{cr}' indicated in Appendix figure 75, divided by the lever arm 'z', which is the distance between 'N_c' and 'N_s', gives the force 'N_s' in the steel. Dividing that value by the area of the steel, the stress at rupture is found. The expression becomes:

$$\sigma_{sr} = \frac{M_{cr}}{zA_s} \qquad \textit{Appendix eq. (34)}$$

The moment 'M_{cr}' is the cracking moment which marks the end of the linear elastic stage, and 'A_s' is the total steel reinforcement area in the tension zone. The lever arm 'z' can be found using Appendix eq. (35):

$$z = d - \frac{1}{3}x \qquad \textit{Appendix eq. (35)}$$

The height of the compression zone can be found using Appendix eq. (36) (Luković & van der Ham, 2020):

$$x = d * \left(\sqrt{(\alpha_e\rho_l)^2 + 2\alpha_e\rho_l} - \alpha_e\rho_l\right) \qquad \textit{Appendix eq. (36)}$$

In this expression, 'α_e' is the ration between the Young's modulus of steel and concrete:

$$\alpha_e = \frac{E_s}{E_c} \qquad \textit{Appendix eq. (37)}$$

The 'ρ_l' parameter is now the reinforcement ratio, and **not** the effective reinforcement ratio. So in other words, it is equal to:

$$\rho_l = \frac{A_s}{A_c} \qquad \textit{Appendix eq. (38)}$$

Appendix H: longitudinal shear

In order to be able to determine the longitudinal shear, the relationship between longitudinal and vertical shear needs to be found. If a small piece of the beam in Appendix figure 76 is isolated, the relationship between the vertical and longitudinal shear becomes clear.

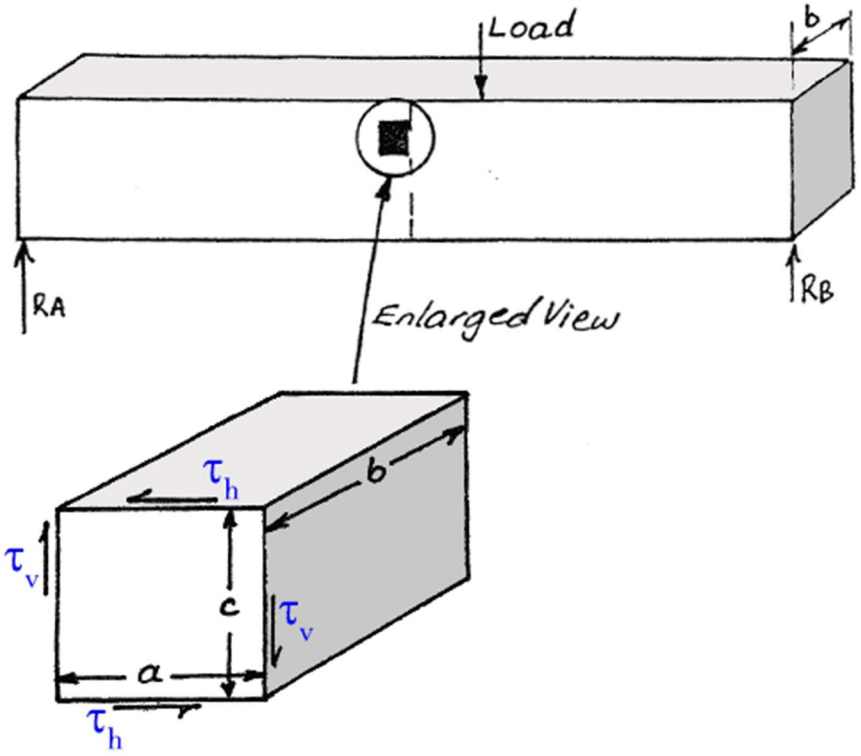

Appendix figure 76: relationship between vertical and longitudinal shear when a cut is made (Learneasy, 2020)

For any point, three equilibrium requirements need to be fulfilled. First, horizontal equilibrium is required. In the enlarged view in Appendix figure 76, 'τ_h' points both leftwards and rightwards. However, 'τ_h' is a stress. To translate it to a force, it is multiplied with the length over which it acts, which gives 'τ_h*a'. Formally, it also needs to be multiplied with the width 'b', but for now the calculation is made per unit width. There are no other forces, so the horizontal equilibrium requirement is satisfied. In the same way, vertical equilibrium is found. The vertical force is equal to 'τ_v*c'.

Finally, the moment equilibrium should be checked. As the vertical forces are equal to each other, and so are the horizontal forces, only one in each direction is needed for the moment calculation (because it forms a couple with the other equal force). If the anti-clockwise direction is taken as the positive direction, the moments become:

$$\tau_h * a * c - \tau_v * c * a = 0 \rightarrow \tau_h - \tau_v = 0 \rightarrow \boldsymbol{\tau_h = \tau_v} \qquad \textit{Appendix eq. (39)}$$

This final expression is what is searched for; the longitudinal shear stress is equal to the vertical shear stress.

List of figures

List of tables

TU Delft